# Effective actions from string and M-theory: compactifications on $G_2$-manifolds and dark matter in the KL moduli stabilization scenario

Dissertation
zur
Erlangung des Doktorgrades (Dr. rer. nat.)
der
Mathematisch-Naturwissenschaftlichen Fakultät
der
Rheinischen Friedrich-Wilhelms-Universität Bonn

von
Thaisa Carneiro da Cunha Guio
aus
Vitória, ES, Brasilien

Bonn, July 2018

Dieser Forschungsbericht wurde als Dissertation von der
Mathematisch-Naturwissenschaftlichen Fakultät der Universität Bonn angenommen und ist auf dem Hochschulschriftenserver der ULB Bonn
http://hss.ulb.uni-bonn.de/diss_online elektronisch publiziert.

| | |
|---|---|
| 1. Gutachter: | Prof. Dr. Albrecht Klemm |
| 2. Gutachter: | Priv. Doz. Dr. Stefan Förste |
| Tag der Promotion: | 21.09.2018 |
| Erscheinungsjahr: | 2018 |

*Dedicated to the loving memory of my grandmothers Aurora and Lêda,*
*who went to a better world while I was abroad.*

# Abstract

In this thesis we study the emergence of four-dimensional effective actions from compactifications of higher-dimensional string/M-theory and explore some of their phenomenological implications.

In order to compactify eleven-dimensional M-theory to a four-dimensional effective $\mathcal{N} = 1$ supergravity action, the relevant internal spaces turn out to be $G_2$-manifolds. Contrary to Calabi–Yau manifolds appearing in compactifications of string theory, the construction of $G_2$-manifolds is not directly obtained via standard techniques of complex algebraic geometry. For this reason, there were up to now only a few hundred examples of them. In the first part of this thesis, we find many novel examples of $G_2$-manifolds based on the so-called twisted connected sum construction. Furthermore, we identify a limit in which the $G_2$-metric is approximated in terms of the metrics of the constituents of this construction, allowing for the identification of universal moduli fields in the four-dimensional effective spectrum. A final expression for a (positive semi-definite) Kähler potential in terms of these moduli is obtained, together with interesting Abelian and non-Abelian enhanced supersymmetric ($\mathcal{N} = 2$ and $\mathcal{N} = 4$) gauge theory sectors including, for example, the Standard Model gauge group and possible grand unification scenarios.

In the second part we investigate the emergence of dark matter candidates from effective actions. Here we already start with a four-dimensional effective action motivated from F-theory/type IIB string theory on Calabi-Yau manifolds in the Kallosh–Linde (KL) moduli stabilization scenario. The non-positive vacuum in the KL scenario is uplifted by the Intriligator–Seiberg–Shih (ISS) sector, based on the free magnetic dual of $\mathcal{N} = 1$ supersymmetric QCD. We analyze interactions between the KL-ISS and the Minimal Supersymmetric Standard Model (MSSM) sectors in order to investigate the dynamics after the inflationary phase, obtaining constraints from late entropy production. Finally, we obtain neutralino dark matter candidates compatible with the observed dark matter relic density from both thermal and non-thermal production.

# Acknowledgements

First of all, I would like to thank my supervisor Albrecht Klemm for the opportunity to be a member of his research group. His friendly character provided a nice working atmosphere where we could discuss a manifold of topics on several occasions. I am profoundly grateful for his teachings on String Theory, and for his many valuable and inspiring ideas throughout these years, which I will carry along with me.

I am also indebtful to my second mentor and collaborator, Hans Jockers, with whom I had many discussions that helped me progress in my research.

I would like to thank Stefan Förste for being the second referee of this thesis. The opportunity to tutor in several of his lectures at the University, together with his patience and constant feedback, provided me with a valuable teaching experience, for which I am deeply grateful. I extend my thanks to Jochen Dingfelder and Matthias Lesch for also agreeing to be members of my PhD committee.

I also thank Hung-Yu Yeh and Ernany Rossi Schmitz for their collaboration in parts of the work presented here, as well as Manuel Drees for discussions that significantly improved the results of the second part of this thesis.

I am also thankful to the many colleagues I had throughout the years at the Bethe Center for Theoretical Physics. Many thanks to my current research group colleagues: Abhinav, Andreas, Cesar Alberto, Christoph, Fabian, Mahsa, Reza, Thorsten and Urmi. I had many interesting conversations with them during my PhD years on the most diverse topics and we shared many experiences together. In particular, I want to thank Cesar Alberto, Yeh, Iris, Jie and Paulina for their constant friendship and the many laughs we shared. Some helped me improving my Spanish and German, some are trying to make me learn Chinese. I also thank Cesar Alberto for increasing my list of books to read, and Iris for the nice football matches we played together and for her support when I had to go through knee surgery.

Special thanks to the amazing friends I made in Germany: Ernany Rossi Schmitz, Felipe Padilha Leitzke, Mariana Madruga de Brito and Rachel Werneck. We shared many invaluable experiences together, finding endless meanings for everything, through the difficulties and the good times we spent together in trying to reach the same goal of completing our PhDs. I could not have stayed strong without their constant support and friendship, which I am sure will last for our whole lives.

I would also like to thank my amazing friends back in Brazil, who supported me from all this distance during these years. You were always with me in my thoughts, and soon I will be there with you again.

I am thankful to the Bonn-Cologne Graduate school of Physics and Astronomy for selecting

me as a member of the honors branch program, which provided me with partial financial support for some PhD years, and helpful funding to attend conferences and workshops. I am indebted to the funding program *Ciências Sem Fronteiras* of the brazilian federal agency CNPq, which provided me with full financial support during my PhD. I hope I will be able to return this investment in contributing to the development of science in Brazil.

I am deeply thankful to my love, Gláuber Carvalho Dorsch. For his comprehension at even the most difficult times, when we worked in different places of the world in order to advance our scientific careers. For having stood by my side raising my mood at all times. For all the marvelous moments we are sharing everyday, and the many discussions regarding basically everything. I am more than certain that we are made for each other. *Eu te amo demais!*

Last but not least I would like to thank my parents Carmem and Vicente, and my brother Matheus, for so many reasons that it would be impossible to list them all here. I am extremely grateful for the environment they provided me with, allowing me to dedicate myself entirely to my studies. I am thankful for the invaluable education I gained from them, and for their incentive to always keep following my dreams and beliefs throughout my life. Without them, nothing would have been possible.

*Thank you all!*

# Contents

CHAPTER 1

# Introduction

## 1.1 The pillars of high energy physics and where they start to crack

The framework of Quantum Field Theory, arising from a reconciliation of quantum mechanics and special relativity for point-like particles, has been successfully applied to the description of three out of the four fundamental forces of Nature — the electromagnetic, the weak and the strong interactions —, culminating in the Standard Model of Particle Physics.

Crucially, the Standard Model leaves the gravitational interaction out of its scope. This is because every attempt to fit General Relativity into the framework of Quantum Field Theory ultimately leads to a non-renormalizable theory, where ultraviolet divergences reappear at every order in the perturbative expansion, thus requiring an infinite number of counter-terms and completely spoiling the predictive power of the theory.

At the root of this problem is the assumption that particles behave as point-like objects. Indeed, by relaxing this premise and writing a quantum theory of one-dimensional extended particles, i.e., of quantum strings, one finds that gravity not only can be accommodated in the formalism, but it emerges naturally out of it. Furthermore, the resulting theory is so constrained by self-consistency requirements that little room is left for *ad hoc* impositions from outside. In fact, the effective matter content of our world, their mutual interactions and even the four-dimensionality of spacetime cannot be taken for granted, and must be obtained *a posteriori*. This is, in broad terms, the subject of this thesis, and will be discussed at length in the next few hundreds of pages.

But for now, in order not to get ahead of ourselves, let us start with a short discussion of the main successes and the main open problems of the current standard models of high energy physics.

**The Standard Model of Cosmology**

Even though at small scales the Universe seems to be inhomogenous, with planets and stars concentrated in galaxies that are spread over a seemingly vast emptiness, at large scales of

$\mathcal{O}$(100 Mpc) the Universe is in fact highly homogeneous and isotropic. As it turns out, these conditions are enough to determine the spacetime metric of the Universe as the Friedmann-Lemaître-Robertson-Walker metric [1], depending only on the scale factor $R(t)$ and the curvature of the Universe. Plugging this metric into Einstein's equation of General Relativity, and assuming a Universe filled by matter and/or radiation, one finds that the Universe expands with a rate $H = \dot{R}/R$, the so-called Hubble parameter [2, 3, 4]. These are the basic assumptions constituting the Standard Model of Cosmology [5, 6, 7, 8].

In this paradigm, the Universe starts at the initial Big-Bang singularity and, as it expands and cools down, different types of particles decouple from the initial hot plasma at different times, leading to a thermal history of the Universe with distinct epochs. This framework is successful in explaining the correct abundance of light elements from the primordial nucleosynthesis — also called Big-Bang nucleosynthesis (BBN) [9, 10, 11, 12] — as well as the existence of the Cosmic Microwave Background radiation (CMB) with a blackbody spectrum at a temperature of $T \sim 2.7$ K as a relic of the time of decoupling of the photons [10, 11, 13, 14, 15, 16].

Despite these successes, the Standard Model of Cosmology cannot account for a series of observations, such as the approximate flatness of the Universe (the flatness problem), the homogeneity and isotropy of the CMB (the horizon problem), and the origin of large structures. A solution to these problems is provided by the framework of *inflation* [17]. This is an additional postulated early period in the history of the Universe, with an exponential accelerated expansion occurring before the radiation-dominated era. The inflationary paradigm also successfully predicts other observations, most notably the nearly-Gaussian anisotropies in the CMB power spectrum. However, despite many proposals [18, 19, 20, 21, 22], uncovering the exact mechanism driving inflation remains an open problem.

Another intriguing mystery of the Standard Model of Cosmology is that, in order to be aligned with the observations, we are forced to include a dark sector in the mass-energy content of the Universe. Observations of large redshift type IA supernovae, the CMB spectrum and the large scale structures indicate that 68.3% of the content of the Universe is dark energy [16, 23, 24, 25, 26], an exotic form of energy responsible for the accelerating expansion of the Universe. Moreover, successful BBN requires a 4.9% of ordinary baryonic matter, leaving the remaining 26.8% as an unknown form of non-baryonic matter, so-called *dark matter*. Its existence has been widely corroborated by a number of observational evidences, such as rotation curves of galaxies [27], gravitational lensing in galaxy clusters [28] and the observed angular power spectrum of the CMB [16]. If we assume that dark matter must be a new form of elementary particle, its existence also becomes a problem to be addressed within the Standard Model of Particle Physics, to which we now turn.

### The Standard Model of Particle Physics

The Standard Model of Particle Physics (SM) is a quantum field theory obeying a local gauge symmetry. Because of this symmetry, Noether's theorem guarantees that the fields carry a charge. The locality of the symmetry then requires the introduction of connection fields which act as the carriers of the interaction between these charges, called the gauge bosons. The first successful instance of a local gauge theory is Quantum Electrodynamics, a theory of the electromagnetic interaction based on the Abelian gauge group $\mathrm{U}(1)_{\mathrm{EM}}$, with the photon as

the gauge boson. This success was extended in the mid 1960s, when a unified description of the weak and electromagnetic interactions was achieved by enlarging the symmetry group to the non-Abelian $SU(2)_L \times U(1)_Y$ [29, 30, 31, 32]. Since the weak interaction is short-ranged, the corresponding mediators must be massive, which is not allowed by the gauge symmetry. The solution to this conundrum comes with the addition of a scalar particle, called the Higgs boson [33, 34, 35], which acquires a non-vanishing vacuum expectation value via the Higgs mechanism, spontaneously breaking the gauge group $SU(2)_L \times U(1)_Y$ down to $U(1)_{EM}$. This results in three massive weak gauge bosons, $W^+$, $W^-$ and $Z$, whereas the photon remains massless. Finally, Quantum Chromodynamics (QCD) was developed in the 1970s as a non-Abelian gauge theory based on the gauge group $SU(3)_C$ to describe the strong interaction mediated by massless gluons [36, 37].

The Standard Model of Particle Physics is, therefore, a unified perturbative framework of three interactions — electromagnetic, weak and strong — based on the gauge group $SU(3)_C \times SU(2)_L \times U(1)_Y$. As for the matter content, there are three generations of quarks and leptons which receive mass from Yukawa couplings to the Higgs. This model happens to be chiral since only left-handed fermions (and right-handed anti-fermions) interact weakly. The recent discovery [38] of its last missing piece, the Higgs boson, consolidated the Standard Model of Particle Physics as the most successful quantum field theory developed so far.

However, even though the Standard Model is very successful, it cannot be the final theory of Nature, both because of its theoretical problems as well as due to the many fundamental phenomena it cannot account for.

One of its biggest theoretical issues is the so-called *electroweak hierarchy problem*. In technical terms, the squared Higgs mass receives loop corrections which scale quadratically with the cutoff energy of the theory, which could be as large as the Planck mass $M_P \sim 10^{19}$ GeV if the Standard Model remains a good effective theory up to such high energies. Therefore, in order to bring the Higgs mass down to the electroweak scale, either some new physics must appear at the scale of a few TeV, or an enormous and unexplained amount of fine-tuning would be required. Moreover, the model does not explain the existence of three generations of matter or the origin of the 19 parameters entering its Lagrangian — these cannot be predicted theoretically, but have to be fixed by experimental data.

The Standard Model of Particle Physics also fails to account for a number of observed phenomena. It does not have a mechanism to dynamically generate the observed excess of matter over anti-matter, not only for lacking a source of sufficient deviation from thermodynamical equilibrium [39, 40], but also because of the insufficient amount of CP violation coming from the CKM matrix [41]. Moreover, in the Standard Model neutrinos are massless, in contradiction with the observed neutrino oscillations mixing flavour and mass eigenstates[1] [42, 43, 44, 45, 46]. The model also does not have candidates for dark matter, and its vacuum energy contribution to the cosmological constant is predicted to be 120 orders of magnitude larger than the observed value for the dark energy density of the Universe.

Finally, as already mentioned, the Standard Model does not take the gravitation interaction

[1] A very recent report by the MiniBooNE collaboration may give us a hint for the origin of their mass from sterile neutrinos, an hypothetical type of neutrinos that interact only gravitationally and not by the interactions in the Standard Model [47].

into account. Later we will see how string theory, in abandoning the notion of point-like particles, provides us with a consistent quantum description of gravity.

**Beyond the Standard Model: Supersymmetry, supergravity and grand unification**

An elegant solution to the aforementioned hierarchy problem is given by Supersymmetry (SUSY), an extension of the Poincaré algebra by half-integer spin generators, leading to a (global) symmetry between bosonic and fermionic particles. As a consequence, every particle has a superpartner, with their spin differing by a half-integer [48, 49, 50, 51, 52, 53, 54, 55]. Due to the relative negative sign between bosonic and fermionic loops, and the fact that supersymmetry enforces the couplings of superpartners to the Higgs to be the same, the would-be problematic quadratic divergences cancel out.

Supersymmetry is also attractive because it reconciles well with the idea of a grand unification of the electroweak and strong interactions in a Grand Unified Theory (GUT)[2] [56]. Indeed, the additional superpartners of the Minimal Supersymmetric Standard Model (MSSM) modify the running of the gauge couplings in such a way that they meet at $\Lambda_{\text{SUSY}} \sim 10^{16}$ GeV, pointing to a unique gauge coupling of an underlying simple gauge group.

Phenomenologically, an interesting feature of supersymmetric scenarios is the presence of various natural candidates for dark matter, such as sneutrinos, gravitinos and neutralinos [50, 53, 54]. If R-parity is conserved, the supersymmetric particles cannot decay into SM particles. This means that the lightest supersymmetric particles (LSPs) are guaranteed to be stable, which are typically the neutralinos [57, 58, 59, 60, 61].

It is important to notice that supersymmetry must be broken at high-energy scales $\gtrsim O(10\,\text{TeV})$. This is because we do not observe superpartners with the same mass as their corresponding partners, which would be the case if supersymmetry were exact. The precise mechanism of supersymmetry breaking is unknown, although many proposals do exist [62, 63].

Since fundamental symmetries of Nature are local, it is reasonable to propose gauging $\mathcal{N} = 1$ SUSY, turning it into a local symmetry. The resulting gauge group is an extension of the diffeomorphism group of General Relativity, so that the resulting theory is a supersymmetric version of the gravitational interaction, known as $\mathcal{N} = 1$ supergravity (SUGRA). The spin-2 graviton belongs to a gravity supermultiplet that also contains its superpartner, a spin-$3/2$ particle called the gravitino [64, 65, 66, 67, 68]. When it first appeared, supergravity was tought to provide a framework for the long-sought quantum description of the gravitational interaction. However, this initial first excitement was soon washed away. Since four-dimensional $\mathcal{N} = 1$ SUGRA turns out to be non-renormalizable [69] and the maximal eleven-dimensional supergravity theory is found to be plagued by gauge anomalies at the quantum level [70], supergravity theories can only be regarded as a low-energy effective theory of a more fundamental UV-completion.

[2] In these kind of theories, the SM gauge groups are unified into an enlarged simple gauge group, which should be at least of rank four and contain representations such as to accomodate the chiral spectrum of the SM. Typical examples are SU(5) and SO(10).

## 1.2 String theory and compactifications

String theory is so far the only framework that attempts to quantize the gravitational interaction while also achieving a unification of all known four interactions: the electromagnetic, the weak, the strong, and also the gravitational interaction [71, 72, 73, 74, 75].

The basic idea behind string theory is that it replaces the familiar notion of a worldline, traced by a point-like particle moving in spacetime, by a surface $\Sigma$ called the *worldsheet* which is swept out by a one-dimensional object, the string. The matter particles and gauge bosons that we observe arise from different vibrational modes of the strings, which can be open or closed. It is in this sense that string theory unifies all interactions in a quantum description, namely that the myriad of particles we observe arise from a single fundamental quantized object, the string with a length $l_s$. Therefore, there is only a single fundamental scale in string theory.

The dynamics of the string is governed by an action given by the area swept out by the worldsheet,

$$S = -T \int_{\Sigma} d\sigma d\tau \sqrt{-\det(\partial_\alpha X^\mu \partial_\beta X_\mu)} \,, \tag{1.1}$$

where $T \sim l_s^{-2}$ is the string tension, $\sigma$ and $\tau$ are coordinates on the worldsheet, and $X^\mu = X^\mu(\sigma, \tau)$ are coordinates on the *target space* obtained as maps from the worldsheet into spacetime. Perturbation theory is then performed as a sum over the worldsheet genus (the number of holes) and embeddings of the worldsheet into spacetime. This resembles the sum over loops of Feynman diagrams in quantum field theories. This also indicates a unique feature of string theory, namely that the free theory uniquely determines the structure of the allowed interactions. In particular, the value of the string coupling constant $g_s$ governing the string perturbation theory is generated dynamically from the vacuum expectation value of the so-called dilaton field.

An interesting feature of this framework is that divergences appearing in quantum field theories are softened by the extended nature of the string, which becomes manifest at very high-energy scales of the order of the string mass $M_s \sim 1/l_s$. This happens because interactions in string theory do not happen at specific points, but are rather delocalized. At low-energy scales $l_s \to 0$, the extended nature of the string becomes unreachable and the effective theory resembles the quantum field theories of point-like particles.

Moreover, at low-energy scales there emerges a spin-2 particle in the massless spectrum of the theory. Its low-energy effective action has the form of the Einstein-Hilbert action of General Relativity plus quantum corrections in terms of higher order derivatives. For this reason, this particle is associated with the graviton and, in this sense, string theory provides a consistent quantum theory of gravity.

#### Superstring theories

Bosonic string theory was the first string theory to be developed. It was plagued by several inconsistencies, such as the presence of tachyons inducing instabilities in the vacuum and the absence of fermions in its spectrum. Both of these problems were solved by supersymmetrizing the formalism, originating the so-called *superstring theories*.

There are five superstring theories, namely type I, type IIA, type IIB, and the two heterotic

theories with gauge groups SO(32) and $E_8 \times E_8$. The type I theory describes unoriented open and closed strings with $\mathcal{N} = 1$ supersymmetry. The types IIA and IIB describe oriented closed strings with $\mathcal{N} = 2$ supersymmetry. Finally, the heterotic theories describe oriented closed strings with $\mathcal{N} = 1$ supersymmetry and matter fields transforming in representations of SO(32) or $E_8 \times E_8$, these groups being singled out after imposing cancellation of quantum mechanical anomalies. At low-energies, the massive superstring states are extremely heavy, $\mathcal{O}(M_s)$, and can be integrated out. It can be shown, for each of these superstring theories, that the resulting effective theory for the massless states are supegravity theories.

Consistency of the superstring theories requires that they should live in a ten-dimensional spacetime. In order to make contact to our familiar four-dimensional world, and obtain an effective description that resembles the Standard Model (or some extension of it), the six non-observed extra dimensions should be compactified into a six-dimensional compact internal manifold[3]. We thus arrive at a four-dimensional effective action for the massless spectrum.

The geometry and topology — the size and shape — of the compact internal manifold are extremely relevant, for they determine the field content and the couplings of the resulting low-energy effective theory. The many parameters characterizing these internal manifolds receive the name of *moduli*. In the low-energy effective theories, they are represented by non-vanishing vacuum expectation values of massless scalars, thereby forming a manifold named as the *moduli space of vacua*. Since massless scalars have not been observed, these moduli must become massive via a mechanism called *moduli stabilization*. This would also ensure stability of the vacuum and thus of the extra dimensions.

There is a huge amount of possibilities for the compact internal manifolds and, therefore, of effective theories arising from the string framework. In order to better understand this *landscape*, it is important not to restrict oneself to only specific classes of manifolds, but to broaden the horizon of investigations in order to better assess the universal properties of these effective theories and their relation to the Standard Model of Particle Physics.

## 1.3 M-theory and $G_2$-manifolds

### Dualities and M-theory

A powerful aspect in the superstring framework is that the seemingly different types of theories are mutually related, in distinct regimes of the parameters $l_s$ and $g_s$, by so-called dualities.

The first one to be discovered was *T-duality* [79, 80]. This symmetry suggests that there are equivalent compactifications on two different geometries for the extra dimensions, one with small scales and the other with large scales. In its simplest example, it relates compactification on a circle of radius $R$ with the compactification on a circle of radius $l_s^2/R$. The two type II

[3] The idea for compactifications in string theory resembles the idea of Kaluza and Klein [76, 77, 78], who started with a metric in five dimensions and, by applying the same machinery of General Relativiy, performed a compactification on a curled up circle of a very small radius to four dimensions. The effective theory obtained in four dimensions is that of General Relativity coupled to electromagnetism, with an extra massless scalar accounting for the radius of the circle.

theories are related to the two heterotic theories, in the case when the first two are compactified on a circle of radius $R$ and the last two on a circle of radius $l_s^2/R$, and vice-versa.

In 1995, a different kind of duality named *S-duality* was discovered [81]. This symmetry relates a string theory at the string coupling $g_s$ to another string theory at the inverse string coupling $1/g_s$, thus relating strongly coupled theories to weakly coupled ones, and allowing us to obtain intrinsic non-perturbative results via well-known perturbative methods. These developments also led to the discovery of D$p$-branes [82, 83, 84], extended objects of $(p+1)$ spacetime dimensions on which open strings can end[4]. These objects become extremely heavy as $g_s \to 0$ and could not have been predicted in a perturbative analysis. Their discovery led to a rapid progress in understanding non-perturbative dualities.

For the five superstring theories, type I is S-dual to heterotic SO(32) at inverse string couplings, and type IIB is self-dual, i.e., it is related to itself at different string coupling regimes. Since only three out of the five superstring theories had their strong coupling regime well understood, the question remained as to what actually happens to type IIA and the heterotic $\mathrm{E}_8 \times \mathrm{E}_8$ at strong coupling. The answer was that, in both cases, there appears an extra eleventh dimension of size $R_{11} = l_s g_s$, giving rise to a strongly coupled quantum theory whose low-energy limit should be the unique eleven-dimensional supergravity [70]. By studying the tension of both D2- and D4-branes at strong coupling, we find that the fundamental objects of this yet unknown eleven-dimensional quantum gravity theory are three-dimensional *M2-branes* and six-dimensional *M5-branes* [85]. Furthermore it should also contain a three-form $C_3$, electrically coupled to M2-branes and magnetically coupled to M5-branes. This theory is called *M-theory* [86, 87, 88].

On the other hand, the self-dual property of type IIB superstring theory has prompted further studies into the details of its non-perturbative regime. A success has been achieved in interpreting the $\mathrm{SL}(2,\mathbb{Z})$ symmetry of the theory as the modular group of transformations of the so-called axio-dilaton $\tau = C_0 + i g_s^{-1}$, which in turn can be interpreted as a complex structure modulus of an auxiliary two-dimensional torus. Here $C_0$ is a scalar field appearing in type IIB. By varying the complex structure modulus we can therefore probe a non-perturbative regime of type IIB. The result is an auxiliary twelve-dimensional theory named F-theory. Notice that we do not imply that type IIB arises from compactifications of the twelve-dimensional theory on the two-torus. The two-torus only serves as a geometrization of the $\mathrm{SL}(2,\mathbb{Z})$ symmetry and is not physical. This is further hinted by the fact that there is no twelve-dimensional supergravity theory arising as a low-energy effective theory of F-theory. Moreover, there is no scalar field in ten dimensions corresponding to the volume modulus of the auxiliary torus.

Even though F-theory is a powerful tool for probing the non-perturbative regime of type IIB as well as for model building, it is M-theory that seems to be the fundamental theory. First recall that M-theory does have an eleven-dimensional supergravity description. Furthermore, compactifying M-theory on a circle of radius $R_{11}$ results in type IIA, which we can further compactify on another circle leading to a T-dual theory to type IIB. Therefore, in contrast to the F-theory perspective, here the two consecutive compactifications of M-theory gives the resulting two-torus a physical interpretation in the sense that ten-dimensional type IIB arises in the zero-size limit of this torus.

This intricate web of dualities [89, 90, 91, 92, 93, 94] relating the five superstring theories

[4] The string endpoints satisfy Dirichlet boundary conditions, from which D-branes receive their name.

indicates that they are nothing but perturbative limits of eleven-dimensional M-theory — see figure 1.1.

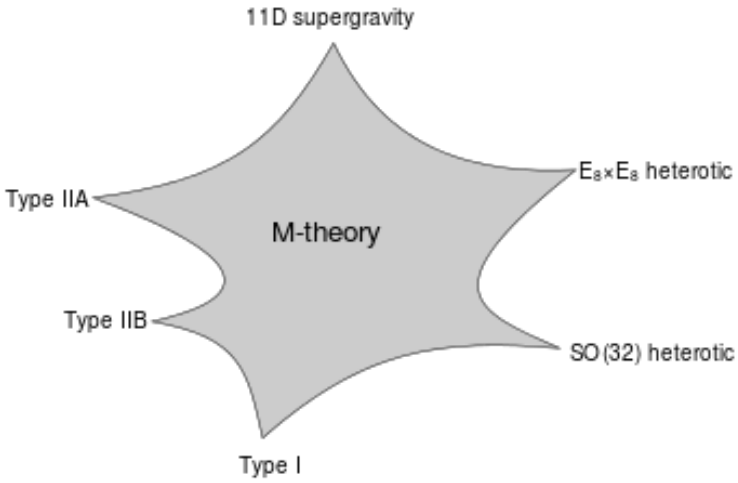


Figure 1.1: The web of dualities relating the fundamental eleven-dimensional M-theory to its eleven-dimensional SUGRA low-energy limit and to types I, II and heterotic string theories.

### Holonomy groups and $G_2$-manifolds

We have already mentioned that the properties of the compact internal manifolds determines the details of the four-dimensional effective theories. One important such property is the dimensionality of the section of the spinor bundle which remains invariant under parallel transport. In other words, the number of linearly independent covariantly constant spinors of the manifold [95]. This fixes the amount of supersymmetry to be preserved in four dimensions. To understand this property on the compact manifold $M$, we need to study its *holonomy group*[5].

Due to the classification by Berger [96], we know all possible holonomy groups for a simply-connected, irreducible and non-symmetric Riemannian manifold $M$ of dimension $d$ equipped with a Riemannian metric $g$. Let $N$ be the number of covariantly constant spinors on $M$. If $d$ is even, it can be decomposed in terms of the number of spinors with positive and negative chiralities, $N = N_+ + N_-$. For each dimension $d$, exactly one of the following cases must hold [97]

- $\mathrm{Hol}(g) = \mathrm{SO}(d)$.
- $d = 2n$, $n \geq 2$, and $\mathrm{Hol}(g) = \mathrm{U}(n) \subseteq \mathrm{SO}(2n)$.
- $d = 2n$, $n \geq 2$, and $\mathrm{Hol}(g) = \mathrm{SU}(n) \subseteq \mathrm{SO}(2n)$. Moreover, $N_+ = 2$ and $N_- = 0$ for even $n$, and $N_\pm = 1$ for odd $n$.

[5] In general, when we parallel transport a vector around a closed loop, it will not preserve its original orientation. The group of all possible transformations of a vector upon parallel transport along all possible closed loops starting and ending at $p$ on $M$ is called the *holonomy group* of $M$.

- $d = 4n$, $n \geq 2$, and $\mathrm{Hol}(g) = \mathrm{Sp}(n) \subseteq \mathrm{SO}(4n)$. Moreover, $N_+ = n + 1$ and $N_- = 0$.
- $d = 4n$, $n \geq 2$, and $\mathrm{Hol}(g) = \mathrm{Sp}(n)\mathrm{Sp}(1) \subseteq \mathrm{SO}(4n)$.
- $d = 7$ and $\mathrm{Hol}(g) = G_2 \subseteq \mathrm{SO}(7)$. Moreover, $N = 1$.
- $d = 8$, and $\mathrm{Hol}(g) = \mathrm{Spin}(7) \subseteq \mathrm{SO}(8)$. Moreover, $N_+ = 1$ and $N_- = 0$.

For the first two cases, these manifolds do not necessarily admit covariantly constant spinors, unless $d \geq 3$. $\mathrm{SO}(d)$ is the holonomy group of generic Riemannian metrics. Riemannian metrics with $\mathrm{Hol}(g) = \mathrm{U}(n) \subseteq \mathrm{SO}(2n)$ are called Kähler metrics. For $\mathrm{Hol}(g) = \mathrm{SU}(n) \subseteq \mathrm{SO}(2n)$, they are called Calabi–Yau metrics. Locally, Calabi–Yau metrics are Ricci-flat Kähler metrics, and the existence of these metrics on compact manifolds follows from the proof by Yau of the Calabi conjecture [98, 99, 100]. Riemannian metrics with $\mathrm{Hol}(g) = \mathrm{Sp}(n) \subseteq \mathrm{SO}(4n)$ are called hyper-Kähler metrics and, because $\mathrm{Sp}(n) \subseteq \mathrm{SU}(2n) \subset \mathrm{U}(n)$, they are Ricci-flat and Kähler. For $\mathrm{Hol}(g) = \mathrm{Sp}(n)\mathrm{Sp}(1) \subseteq \mathrm{SO}(4n)$, they are called quaternionic Kähler metrics. Finally, the holonomy groups $G_2$ and Spin(7) are called *exceptional holonomy groups* with metrics called $G_2$-metrics and Spin(7)-metrics.

We can group the holonomy groups apart from the generic $\mathrm{SO}(d)$ on Berger's list by their common nature. First of all, any Riemannian manifold with one of the following Kähler holonomy groups $\mathrm{U}(n)$, $\mathrm{SU}(n)$ and $\mathrm{Sp}(n)$, is a *Kähler manifold*, and thus a complex manifold. Because complex manifolds are locally trivial, they have the huge advantage that one can use complex algebraic geometry to understand many of their features [101]. The second class of holonomy groups are the Ricci-flat holonomy groups $\mathrm{SU}(n)$, $\mathrm{Sp}(n)$, $G_2$ and Spin(7). To find examples of metrics, and therefore the geometry associated to these holonomy groups, is a difficult task.

Most studies of compactifications of string theory and M-theory have been performed on the so-called *Calabi–Yau manifolds*. These are compact, complex, and Kähler manifolds with $\mathrm{SU}(n)$ holonomy. The so-called *K3 surfaces* are the lowest-dimensional examples of both Calabi–Yaus — with holonomy SU(2) — as well as compact hyper-Kähler manifolds — with holonomy Sp(1). Apart from some references already presented in this introduction, for a more thorough view on these spaces, we also refer the reader to [102, 103, 104, 105, 106, 107, 108, 109, 110, 111, 112, 113]. The most studied and interesting case so far has been on Calabi–Yau threefolds, manifolds with 3 complex dimensions. This is because compactifications of heterotic string theories on such manifolds provided the first semi-realistic models for particle phenomenology [114, 115, 116, 117, 118, 119, 120, 121, 122, 123], whereas compactifications of type II strings on such manifolds exhibit the amazing property called mirror symmetry, which in the string worldsheet perspective is associated with topological strings [124, 125, 126, 127, 128, 129, 130, 131].

To finish grouping the holonomy groups by their common nature, we have the exceptional holonomy groups $G_2$ and Spin(7). These groups are rather different from the others since we cannot use familiar methods from complex geometry to understand their global structure, but must rather approach them via their local nature.

Compactifications on non-Calabi–Yau manifolds are much less understood. Even less is known about compactifications of M-theory on seven-dimensional manifolds, especially those leading to the phenomenologically motivated $\mathcal{N} = 1$ supergravity in four dimensions. Since

the other string theories are obtained as certain limits of M-theory, it is necessary to perform a careful study of M-theory compactifications on non-Calabi–Yau manifolds in order to obtain a good general understanding of properties of the low-energy effective theories and the associated four-dimensional landscape. From the Berger classification of holonomy groups sketched above, it turns out that the relevant spaces for compactifications of eleven-dimensional M-theory to a four-dimensional $\mathcal{N} = 1$ low-energy supergravity effective theory, requiring $d = 7$ extra dimensions, are manifolds with holonomy group $G_2$. In part I of this thesis we delve into this particular class of manifolds, called *$G_2$-manifolds*.

Compactifications of eleven-dimensional M-theory on $G_2$-manifolds are difficult to be achieved.

First of all, this is due to our sparse knowledge regarding M-theory. We have seen that we are only familiar with its low-energy effective regime, given by eleven-dimensional supergravity. On the one hand, this means that Kaluza-Klein reductions of the eleven-dimensional supergravity action on compact $G_2$-manifolds already capture many physical properties of the associated M-theory compactifications [132, 133, 134, 135, 136, 137, 138]. However, the semi-classical four-dimensional effective action has to be further corrected by non-perturbative effects specific to M-theory, such as M2-branes and M5-branes wrapping cycles on the seven-dimensional compactification manifold.

Another difficulty arises from the very intricate nature of $G_2$-manifolds. For Calabi–Yau manifolds, the Calabi–Yau theorem guarantees the existence of a Ricci-flat metric on a compact, complex, Kähler manifold with a vanishing first Chern class. In other words, there is a necessary and sufficient topological criterion for the existence of Calabi–Yau manifolds. An analogue of such a theorem does not exist in the case of $G_2$-manifolds.

In addition to that, whereas standard techniques of complex algebraic geometry can provide immediately hundreds of thousands Calabi-Yau manifolds, these cannot be directly applied to $G_2$-manifolds. Therefore, for a long time there were only a few hundred examples of $G_2$-manifolds constructed by the resolution of special singularities in orbifolds of seven-dimensional tori $T^7$ [97, 139].

Yet another reason for the difficulty in dealing with these types of manifolds is that, to find torsion-free $G_2$-structures, thereby providing Ricci-flat $G_2$ metrics, one must solve a highly non-linear partial differential equation for the unknown three-form $\varphi$. For Kähler manifolds in general we have a similar type of differential equation for the $(1, 1)$-form $\omega$. However, due to the $\partial\bar{\partial}$-lemma for Kähler manifolds [71], this highly non-linear partial differential equation reduces to a partial differential equation for a single scalar function.

Finally, little is known about singularities on $G_2$, which are physically motivated as they give rise to non-Abelian gauge groups and chiral matter.

Despite all these difficulties, in the first part of this thesis we delve into the mathematical machinery behind general $G_2$-manifolds. We focus on a special type of them based on the so-called twisted connected sum construction [140], recently extended in references [141, 142]. This allows for building a large number of explicit examples of $G_2$-manifolds. We review in detail compactifications of the low-energy limit of M-theory on $G_2$-manifolds, and find many interesting new results when restricting to $G_2$-manifolds of the twisted connected sum type. In particular, we obtain a limit in which Ricci-flat $G_2$-metrics can be approximated by Ricci-flat Calabi–Yau metrics, thereby allowing us to geometrically obtain a four-dimensional

$\mathcal{N} = 1$ effective supergravity theory with a phenomenologically motivated Kähler potential. In addition to that, we identify two scales that also control the behaviour of M-theory corrections. Furthermore, the same limit allows for the accomodation of many singularities leading to Abelian and enhanced non-Abelian gauge symmetries — for example including the Standard Model gauge group and Grand Unification groups — as well as interesting matter in the adjoint, bi-fundamental and fundamental representations of the resulting gauge groups. Furthermore, we find evidences for transitions among classes of $\mathcal{N} = 1$ effective supergravity theories connecting topologically inequivalent $G_2$-manifolds. The findings of this part of the thesis have many interesting mathematical, physical and phenomenological consequences for a variety of different topics. We will detail them in the conclusions and outlook section of this thesis.

## 1.4 Dark matter in the KL moduli stabilization scenario

After compactifications of the extra dimensions, the low-energy effective theories emerging from superstring scenarios are typically very rich, with a myriad of new particles. This constitutes a fertile ground for phenomenological and cosmological investigations in attempts to tackle the current problems in high energy physics.

**Moduli stabilization and the KL scenario**

We have already seen that, in geometrical and topological terms, the moduli parametrize the size and shape of the internal manifold formed by the extra dimensions. For example, in type IIB compactifications on Calabi–Yau threefolds, three types of moduli appear. The first are the so-called Kähler moduli, which are massless scalar fields corresponding to deformations of Ricci-flat metrics on the internal manifold. The second are the so-called complex structure moduli, which are massless scalar fields corresponding to deformations of the complex structure of the internal manifold. And the third are additional massless scalar fields that arise from the dilaton as well as from expanding RR and NS-NS fluxes in basis of harmonic forms.

These moduli — together with stringy axions — are the only masless remnants in four-dimensional low-energy effective theories resulting from compactifications of the extra dimensions in string theories/M-theory. Their dynamics is extremely relevant for our understanding of the cosmological evolution of the universe both during and after inflation [143]. However, their existence can also pose serious problems for our four-dimensional world. In fact, one of the biggest tasks for string/M-theory cosmology is to solve the so-called moduli stabilization problem, giving them masses and thus stabilizing the extra dimensions. These masses are required to be quite large, $\mathcal{O}(30\ \text{TeV})$ or more, to avoid the late overproduction of entropy from its decays, which would dilute the Big-Bang nucleosynthesis products [144, 145, 146, 147, 148, 149]. This is known as the *moduli problem* in cosmology.

After supersymmetry breaking, one could give masses to these moduli by adding quantum perturbative corrections in $\alpha' \sim l_s^2$ and non-perturbative corrections in $g_s$ to the effective scalar potential [150, 151]. However, one encounters an issue. Indeed, consider a single modulus $\rho$ — for example the Kähler modulus that measures the volume of the internal manifold or $g_s^{-1}$ — controlling the weak-coupling expansion such that $\rho \to \infty$ leads to free classical effective theory.

In other words, the classical potential must dominate at $\rho \to \infty$. Any potential $V(\rho)$ given to the moduli due to perturbative or non-perturbative corrections to the effective description must vanish from below and from above as we approach $\rho \to \infty$. On the one hand, if $V(\rho)$ is positive for large $\rho$, its leading correction creates an instability that runaways the theory to $\rho \to \infty$. On the other hand, if $V(\rho)$ is negative for large $\rho$, its leading correction creates another instability driving the theory to small $\rho$ and, therefore, to its strongly-coupled regime. Therefore, from the leading order correction terms, we will always find unstable vacua. The inclusion of higher order terms in $\alpha'$ and $g_s$ could in principle help us to find stable vacua. However, this is complicated precisely because in most cases we only have knowledge on the leading order term in these corrections.

Many models of moduli stabilization have been constructed in the literature by analysing cases where higher order terms in the corrections are known. The two leading ones are the Large Volume Scenario (LVS) [152] and the Kachru–Kallosh–Linde–Trivedi (KKLT) scenario [153].

In the LVS scenario, one stabilizes the overall Kähler volume modulus $\mathcal{V}$ that governs $\alpha'$–corrections at large values such that one can neglect other unknown $\alpha'$ and $g_s$ corrections subleading in $\mathcal{V}$.

In KKLT, one adds a flux that allows for both the complex structure moduli and the dilaton to acquire large masses from the classical supersymmetric potential, such that they can be integrated out in the analysis. Moreover, non-perturbative effects such as gaugino condensation from stacks of D7-branes or instanton contributions from D3-branes, together with fine-tuning of the flux, are finally responsible for stabilizing the remaining Kähler volume modulus $\mathcal{V}$. Despite this success, this scenario leads to some phenomenological issues such as low-scale inflation and an extremely large gravitino mass of $\mathcal{O}(10^{10}$ GeV) and, therefore, an extension has been proposed by Kallosh and Linde in the so-called KL scenario [154].

In both scenarios, the moduli are stabilized in the sense that there are no instabilities and no flat directions in the scalar potential. In the LVS scenario moduli are stabilized in a non-supersymmetric vacuum, whereas in the KKLT/KL the vacuum is supersymmetric. Both of them lead to anti-de Sitter (AdS) (negative-valued vacuum) or Minkowski vacua (vanishing-valued vacuum), which are not realistic for cosmology since a positive de Sitter (dS) vacuum is required for describing inflation and dark energy.

**F-term supersymmetry breaking and de Sitter vacua**

Achieving realistic dS vacua from stabilized AdS/Minkowski vacua is known as *uplifting*. This mechanism requires the identification of a SUSY breaking sector that introduces a sufficient contribution to the potential, raising it to positive values. Still this uplifting has to be implemented without de-stabilizing the moduli.

In the original work of KL, a successful uplifting of its AdS/Minkowski vacuum was performed by explicit supersymmetric breaking with the inclusion of instanton contributions from several anti-D3-branes.

As for the case of spontaneous SUSY breaking, there have been attempts to uplift the vacuum via D-terms with, for example, the addition of fluxes from gauge fields within the D7-branes [155, 156, 157, 158, 159, 160, 161, 162]. For non-supersymmetric vacuum, uplifting with D-terms generically leads to a very heavy gravitino mass of the order of the Planck mass.

Moreover, a D-term cannot uplift a supersymmetric vacuum [163] and, therefore, cannot be applied to the KKLT/KL scenario.

Uplifting of supersymmetric vacua is possible via F-terms [164, 165, 166]. In association with strong gauge dynamics, these scenarios can also naturally incorporate an intermediate SUSY breaking scale TeV $\ll \Lambda_{\text{SUSY}} \ll M_P$ while at the same time accomodating a gravitino mass in the TeV range [167, 168]. This is due to the presence of a small dynamical scale, leading to a corresponding small mass parameter $M \ll M_{\text{P}}$.

Sufficient conditions for the occurrence of dynamical SUSY breaking were suggested in [169, 170, 171, 172]. Altough there have been some studies on dynamical SUSY breaking in a stable ground state, they turn out to be rather intricate and also pose various issues for phenomenology [173, 174, 175].

A simple class of dynamical supersymmetry breaking with metastable vacua is obtained from $\mathcal{N} = 1$ supersymmetric QCD (SQCD), called *ISS model* after the pionering work of Intriligator–Seiberg–Shih [176]. This model is also motivated from a superstring theory perspective, since it emerges as a low-energy effective theory on intersecting NS 5-branes and D-branes [177, 178, 179, 180, 181]. There is also an analogous M-theory version of this model, known as MQCD [182, 183, 184, 185, 186].

**Dark matter**

A combination of the KL scenario with the ISS model and the MSSM not only allows for the emergence of dS vacua from a string motivated framework, but its myriad of particles and interactions could also be exploited for finding possible dark matter candidates.

There are many prominent candidates for dark matter in the literature, such as axions [187, 188, 189, 190], general WIMPs and SIMPs [191, 192], complex scalars [193], heavy neutrinos [194], and supersymmetric particles such as sneutrinos, gravitinos and neutralinos [50, 53, 54].

In the second part of this thesis we give a detailed account on the viability of neutralinos as dark matter candidates in the KL-ISS-MSSM framework. On the one hand, we have already seen that the moduli problem can be catastrophic for BBN. On the other hand, if gravitinos are unstable and are copiously produced by decays of the ISS-MSSM fields, they could lead to a dark matter relic density much larger than allowed by observations. This is called the *gravitino problem*. For these reasons, we investigate whether the model can lead to a consistent thermal history of the Universe, avoiding these cosmological problems while also yielding an acceptable dark matter relic density.

## 1.5 Outline of this thesis

This thesis is divided into two parts, each starting with a prelude highlighting the most relevant new results presented in them.

Part I deals with the theoretical aspects of M-theory compactifications on $G_2$-manifolds, with some hints at their mathematical, physical and phenomenological applications. We give a brief overview of the mathematical aspects of $G_2$-manifolds in chapter 2, and in chapter 3 we perform

the compactification of the low-energy eleven-dimensional $\mathcal{N} = 1$ SUGRA limit of M-theory on these manifolds. A particular emphasis is laid on $G_2$-manifolds of the twisted connected sum type, where we identify a limit — called the Kovalev limit — in which the decomposition of the cohomology groups allows for the identification of universal chiral multiplets, relevant for the description of properties of the four-dimensional low-energy effective $\mathcal{N} = 1$ supergravity theory. Finally, in chapter 4, the orthogonal gluing method and the Kovalev limit are employed to find novel examples for twisted connected sum $G_2$-manifolds with interesting supersymmetric Abelian and non-Abelian gauge theory sectors.

In Part II, we move to a more phenomenological application of string theory compactifications. In chapter 5 we review the Kallosh–Linde (KL) moduli stabilization scenario within the low-energy $\mathcal{N} = 1$ supergravity theory from type IIB compactifications on orientifolded Calabi–Yaus — or from F-theory compactifications on elliptically fibered Calabi–Yaus. The non-positive KL vacuum structure is uplifted by the addition of an F-term dynamical supersymmetry breaking sector from the ISS model. In chapter 6 the dynamics after the inflationary phase of the universe is studied and constraints from both late entropy production and the dark matter relic density are imposed. We find neutralino dark matter candidates compatible with observations, either via their production from thermal gravitinos in the reheating phase of the inflaton or via decays of the ISS fields.

Our general conclusions and outlook are summarized in chapter 7.

The content of this thesis is based on the following publications by the author [195, 196]

• **Thaisa C. da C. Guio**, Hans Jockers, Albrecht Klemm and Hung-Yu Yeh, *Effective action from M-theory on twisted connected sum $G_2$-manifolds*, Commun. Math. Phys. 359 (2018) no.2, 535-601, [arXiv:1702.05435 [hep-th]];

• **Thaisa C. da C. Guio** and Ernany R. Schmitz, *Dark matter in the KL moduli stabilization scenario with SUSY breaking sector from $\mathcal{N} = 1$ SQCD*, submitted to Journal of High Energy Physics (JHEP), [arXiv:1805.01521 [hep-ph]].

# Part I

# M-theory compactifications on $G_2$-manifolds

# Prelude

In the introduction we argued that M-theory is expected to reside in an eleven-dimensional spacetime. In order to recover a four-dimensional theory, one then needs to compactify the extra dimensions on a compact seven-dimensional manifold, which according to Berger's classification must possess a $G_2$-holonomy. Therefore, in the first part of this thesis we are interested in compactifications of M-theory on $G_2$-manifolds.

We start by giving a detailed review on $G_2$-manifolds in chapter 2, introducing the relevant mathematical aspects behind these intricate spaces. We explain the twisted connected sum construction, a method for obtaining $G_2$-manifolds from a particular gluing of asymptotically cylindrical Calabi–Yau threefolds. We also introduce the so-called Kovalev limit, together with the decomposition of the cohomology groups in terms of this particular construction.

In chapter 3 we explicitly perform the compactification of the low-energy eleven-dimensional $\mathcal{N} = 1$ SUGRA limit of M-theory on $G_2$-manifolds. The four-dimensional spectrum of massless fields is obtained, as well as the resulting four-dimensional effective SUGRA action. For the twisted connected sum construction we use the Kovalev limit and the decomposition of the cohomology groups to identify universal chiral multiplets, relevant to describe properties of the four-dimensional low-energy effective $\mathcal{N} = 1$ SUGRA theory. We also find novel examples of twisted connected sum $G_2$-manifolds with interesting supersymmetric Abelian and non-Abelian gauge theory sectors in chapter 4.

The *novel results* presented in this part of the thesis are:

- the identification of the so-called Kovalev limit in which the $G_2$-metric is approximated in terms of metrics of the asymptotically cylindrical Calabi–Yau threefolds in the twisted connected sum construction;
- the derivation of the massless four-dimensional effective $\mathcal{N} = 1$ supergravity fermionic spectrum from compactifications of M-theory on $G_2$-manifolds and the corresponding (flux-induced) superpotential.

It is only due to the Kovalev limit that we are able to extract relevant information on the cohomology of twisted connected sum $G_2$-manifolds, allowing us to

- identify universal chiral multiplets in the four-dimensional effective $\mathcal{N} = 1$ SUGRA spectrum, making it possible to obtain an expression for the Kähler potential with interesting prospects for phenomenology and cosmology;
- find novel examples of twisted connected sum $G_2$-manifolds with interesting (Abelian and non-Abelian) extended supersymmetric $\mathcal{N} = 2$ and $\mathcal{N} = 4$ gauge theory sectors.

# CHAPTER 2

# $G_2$-manifolds

In this chapter we give a detailed overview of *$G_2$-manifolds*. These manifolds turn out to be relevant for compactifications of the low-energy limit of eleven-dimensional M-theory to four dimensions. We divide this chapter into two sections.

In section 2.1 we review the geometry and topology of general $G_2$-manifolds, and use the definitions presented here to delve into the topological structure of compact $G_2$-manifolds and the moduli space associated to them.

In section 2.2 we introduce the reader to a special type of $G_2$-manifolds, namely *twisted connected sum $G_2$-manifolds*. In section 2.2.1 we begin by reviewing the notion of *asymptotically cylindrical Calabi–Yau threefolds*, which are the constituent pieces in the construction of $G_2$-manifolds of the twisted connected sum type. We then give the details of the actual construction in section 2.2.2. The *first relevant contribution of this work* to the topic appears in section 2.2.3. Namely, we are able to identify a limit, which we call the *Kovalev limit*, in which a good approximation to the $G_2$-metric is found in terms of the metrics of its constituents. We then introduce the cohomology of twisted connected sum $G_2$-manifolds arising from the cohomology of the asymptotically cylindrical Calabi–Yau threefolds in section 2.2.4. In section 2.2.5 we show some examples of actual constructions of asymptotically cylindrical Calabi–Yau threefolds.

The content of section 2.1 is relevant for chapter 3, where we discuss the effective action from M-theory on $G_2$-manifolds. The content of section 2.2 is important as a basis for section 3.4 and chapter 4, where specific details of the twisted connected sum construction become relevant for the study of M-theory compactifications on twisted connected sum $G_2$-manifolds and for the extended supersymmetric gauge sectors appearing on them. It is only due to the Kovalev limit, and the decomposition of the cohomology groups in terms of the pieces of the twisted connected sum construction for $G_2$-manifolds, that we are able to obtain the four-dimensional low-energy effective theory from such compactifications.

## 2.1 Geometry and Topology of $G_2$-manifolds

In this section, we give definitions of the exceptional Lie group $G_2$, the $G_2$-structure and the $G_2$-manifold. Furthermore, we analyze the topology of compact $G_2$-manifolds and discuss the moduli space structure associated to them. The content is reviewed based on references [97, 197, 198].

### 2.1.1 The exceptional Lie group $G_2$ and the $G_2$-structure

Let $(x^1, \ldots, x^7)$ be coordinates on $\mathbb{R}^7$ and $\mathrm{d}x^{ij\ldots l} = \mathrm{d}x^i \wedge \mathrm{d}x^j \wedge \ldots \wedge \mathrm{d}x^l$ a differential form on $\mathbb{R}^7$. Define a three-form $\varphi_0$ on $\mathbb{R}^7$ by

$$\varphi_0 = \mathrm{d}x^{123} + \mathrm{d}x^{145} + \mathrm{d}x^{167} + \mathrm{d}x^{246} - \mathrm{d}x^{257} - \mathrm{d}x^{347} - \mathrm{d}x^{356} \,. \tag{2.1}$$

The *exceptional Lie group* $G_2$ is defined as the subgroup of the special orthogonal group SO(7) preserving a three-form $\varphi_0$ on $\mathbb{R}^7$. It is compact, connected, simply-connected, semi-simple and fourteen-dimensional. Furthermore, with the seven-dimensional Hodge star $*_7$, it also fixes a four-form

$$* \varphi_0 = \mathrm{d}x^{4567} + \mathrm{d}x^{2367} + \mathrm{d}x^{2345} + \mathrm{d}x^{1357} - \mathrm{d}x^{1346} - \mathrm{d}x^{1256} - \mathrm{d}x^{1247}, \tag{2.2}$$

as well as the Euclidean metric $g_0 = \mathrm{d}x_1^2 + \ldots \mathrm{d}x_7^2$ and the orientation on $\mathbb{R}^7$.

Any three-form $\varphi$ on $\mathbb{R}^7$ gives rise to a canonical symmetric bilinear form on $\mathbb{R}^7$

$$B_\varphi(u, v) = -\frac{1}{6}(u \lrcorner \varphi) \wedge (v \lrcorner \varphi) \wedge \varphi \tag{2.3}$$

with values in the one-dimensional space of seven-forms $\Lambda^7(\mathbb{R}^7)^*$. For a generic three-form $\varphi$, the bilinear form $B_\varphi$ yields a non-degenerate pairing of some signature $(p, q)$ with $p + q = 7$ and with respect to an oriented volume form on $\mathbb{R}^7$.

Let $Y$ be an oriented seven-dimensional manifold. For each point $p \in Y$, there is an open set $\dim \Lambda^3_+(\mathbb{R}^7)^*$ which is a subset of three-forms $\varphi \in \Lambda^3 T^*_p Y$ such that there exists an oriented isomorphism between the tangent space $T_pY$ and $\mathbb{R}^7$ identifying $\varphi$ with $\varphi_0$. This set is isomorphic to $\mathrm{GL}(7, \mathbb{R})/G_2$ since $\mathrm{GL}(7, \mathbb{R})$ acts on $\varphi$ and $G_2$ is its fourteen-dimensional stabilizer. Since $\dim \mathrm{GL}(7, \mathbb{R}) = 49$ and $\dim G_2 = 14$, the space $\mathrm{GL}(7, \mathbb{R})/G_2$ has dimension equal to $49-14 = 35$. Moreover, $\dim \Lambda^3(T^*_pY) = \binom{7}{3} = 35$, which shows that the subset $\dim \Lambda^3_+(\mathbb{R}^7)^*$ is in fact an open subset $\Lambda^3 T^*_p Y$. Due to the isomorphism between the tangent space $T_pY$ and $\mathbb{R}^7$, this subset is in the space of three-forms $\Lambda^3(\mathbb{R}^7)^*$ such that $B_\varphi$ is a positive definite bilinear form for $\varphi \in \Lambda^3_+(\mathbb{R}^7)^*$. In other words, the open set $\Lambda^3_+(\mathbb{R}^7)^*$ is given by $\mathrm{GL}(7, \mathbb{R})/G_2$, where $\mathrm{GL}(7, \mathbb{R})$ acts on $\varphi$ and $G_2$ is the fourteen-dimensional stabilizer subgroup of $\mathrm{GL}(7, \mathbb{R})$ that preserves the oriented volume form and the positive definite pairing $B_\varphi$. Since $G_2$ leaves the positive definite pairing $B_\varphi$ invariant, it is actually a subgroup of SO(7).

Furthermore, since this open set allows for the definition of a positive definite bilinear form for $\varphi$, one can define both a volume form on $T_pY$ and a Riemannian metric on $Y$ given by,

respectively,

$$\mathrm{vol}_\varphi(\partial_1|_p,\dots,\partial_7|_p)^9 \;=\; \det\left[B_\varphi(\partial_i|_p,\partial_j|_p)(\partial_1|_p,\dots,\partial_7|_p)\right]\,, \tag{2.4}$$

$$g_\varphi(X_p,Y_p) \;=\; \frac{B_\varphi(X_p,Y_p)(\partial_1|_p,\dots,\partial_7|_p)}{\mathrm{vol}_\varphi(\partial_1|_p,\dots,\partial_7|_p)}, \tag{2.5}$$

at any point $p$ on $Y$, for any basis $\partial_1|_p,\dots,\partial_7|_p$ at $T_pY$, and for vectors $X_p$ and $Y_p$ in the tangent space $T_pY$.

Since the Lie group $G_2$ is the stabilizer group of the described three-form, a compact seven-dimensional oriented manifold $Y$ together with the three-form $\varphi$ in $\Omega^3_+(Y)$ — which is the space of smooth three-forms oriented-isomorphic to $\Lambda^3 T^*_pY \simeq \Lambda^3_+(\mathbb{R}^7)^*$ for any $p \in Y$ — becomes a *$G_2$-structure manifold* and we call $\varphi$ a *$G_2$-structure* on $Y$.

### 2.1.2 The $G_2$-manifold

Let $\nabla$ be the Levi-Civita connection associated to the metric $g_\varphi$ defined in equation (2.5). The *torsion* of $\varphi$ is $\nabla\varphi$. If $\nabla\varphi = 0$, the pair $(\varphi, g_\varphi)$ is said to be *torsion-free* and we call $\varphi$ a *torsion-free $G_2$-structure*.

In this thesis, we refer to a *$G_2$-manifold $Y$* as a seven-dimensional manifold equipped with a torsion-free $G_2$-structure $\varphi$.

There is a remarkable and important proposition for the rest of the thesis, which we present in the following [97, 199, 200] — see Proposition 10.1.3 in [97].

**Proposition 2.1** Let $Y$ be a seven-dimensional manifold and $\varphi$ a $G_2$-structure on $Y$. The following are equivalent

(i) $(\varphi, g_\varphi)$ is torsion-free,

(ii) $\mathrm{Hol}(g_\varphi) \subseteq G_2$,

(iii) $\nabla\varphi = 0$ on $Y$,

(iv) $\mathrm{d}\varphi = \mathrm{d} *_{g_\varphi} \varphi = 0$ on $Y$, where $*_{g_\varphi}$ is the Hodge star of the metric $g_\varphi$.

Condition (iv) is called harmonicity condition and $\varphi$ is also called an *harmonic* three-form in $\Omega^3_+(Y)$. The condition that $\varphi$ is torsion-free is a highly non-linear partial differential equation of complicated form, due to relations (2.4) and (2.5) between the metric $g_\varphi$ and the $G_2$-structure $\varphi$. In fact, this can be seen easily by looking at condition (iv), where $\mathrm{d}*$ is explicitly dependent on the metric $g$, which itself depends on $\varphi$. This is one of the reasons why $G_2$-manifolds are more intricate than Calabi–Yau manifolds, e.g., Calabi–Yau threefolds appearing in compactifications of ten-dimensional superstring theories down to four dimensions. Whereas the Calabi conjecture proven by Yau gives necessary and sufficient conditions for a compact Kähler manifold to have a unique Ricci-flat Kähler metric [99], an analogous conjecture for $G_2$-manifolds, giving necessary and sufficient conditions for a $G_2$-structure manifold to admit a torsion-free $G_2$-structure[1] is not known. Therefore, $G_2$-manifolds must be analyzed case by case.

[1] We see later in proposition 2.2 that this is necessary for the existence of a Ricci-flat $G_2$-metric.

In general, differential $p$-forms on a manifold with $G$-structure fall into irreducible representations with respect to the structure group $G$. Specifically for a seven-dimensional manifold with $G_2$-structure, the spaces of differential $p$-forms $\Lambda^p T^*Y$ decompose according to — see Proposition 10.1.4 in [97],

$$\begin{aligned}
\Lambda^0 T^*Y &= \Lambda^0_{\mathbf{1}} \,, \\
\Lambda^1 T^*Y &= \Lambda^1_{\mathbf{7}} \,, \\
\Lambda^2 T^*Y &= \Lambda^2_{\mathbf{7}} \oplus \Lambda^2_{\mathbf{14}} \,, \\
\Lambda^3 T^*Y &= \Lambda^3_{\mathbf{1}} \oplus \Lambda^3_{\mathbf{7}} \oplus \Lambda^3_{\mathbf{27}} \,, \\
\Lambda^4 T^*Y &= \Lambda^4_{\mathbf{1}} \oplus \Lambda^4_{\mathbf{7}} \oplus \Lambda^4_{\mathbf{27}} \,, \\
\Lambda^5 T^*Y &= \Lambda^5_{\mathbf{7}} \oplus \Lambda^5_{\mathbf{14}} \,, \\
\Lambda^6 T^*Y &= \Lambda^6_{\mathbf{7}} \,, \\
\Lambda^7 T^*Y &= \Lambda^7_{\mathbf{1}} \,,
\end{aligned} \tag{2.6}$$

where the components $\Lambda^p_{\mathbf{q}}$ are spaces of $p$-forms transforming in the $q$-dimensional irreducible representations of the structure group $G_2$. As indicated in the arrangement of the spaces $\Lambda^p_{\mathbf{q}}$ in equation (2.6), the Hodge star $*$ provides for an isometry between $\Lambda^p_{\mathbf{q}}$ and $\Lambda^{7-p}_{\mathbf{q}}$. The differential $p$-form spaces $\Lambda^p_{\mathbf{7}}$ are isomorphic to each other for $p = 1, \ldots, 6$. Moreover, $\Lambda^3_{\mathbf{1}}$ and $\Lambda^4_{\mathbf{1}}$ are generated by $\varphi$ and $*\varphi$, respectively.

We now briefly discuss the conditions for obtaining spinors on seven-dimensional $G_2$-manifolds. This is relevant for the subsequent chapters in this thesis, where a careful analysis of the geometrical and topological structure of $G_2$-manifolds, in the context of M-theory compactifications, will single out the four-dimensional low-energy effective theories. In particular, the presence of a covariantly constant spinor on the $G_2$-manifold is relevant for the discussion of fermionic terms, and allows for some amount of supersymmetry to be preserved in the four-dimensional low-energy effective theory.

Since $G_2 \subset \mathrm{SO}(7)$ is simply-connected, any seven-dimensional manifold $Y$ with a $G_2$-structure is a *spin-manifold*. Lemma 11.8 in [200] and Proposition 10.1.6 in [97] hold, from which we have the following proposition.

**Proposition 2.2** Let $Y$ be a $G_2$-structure manifold. Then $Y$ is a spin-manifold with a preferred spin structure. Moreover, if $\mathrm{Hol}(g_\varphi) \subseteq G_2$, or equivalently $\varphi$ is torsion-free — i.e., if $Y$ is a $G_2$-manifold —, then the metric $g_\varphi$ is Ricci-flat and there exists a *covariantly constant spinor* $\eta$ on $Y$.

### 2.1.3 Topology of compact $G_2$-manifolds

For a compact $G_2$-manifold $Y$ equipped with a torsion-free $G_2$-structure, the de Rham cohomologies $H^p(Y, \mathbb{R})$ have a decomposition similar to the decomposition of the spaces of differential $p$-forms into irreducible representations with respect to the structure group $G_2$. That is, here we

have a decomposition of the *de Rham cohomologies*[2] $H^p(Y,\mathbb{R})$ into vector subspaces $H^p_{\mathbf{q}}(Y,\mathbb{R})$ of harmonic representatives — see Theorem 10.2.4 in [97],

$$\begin{aligned} H^2(Y,\mathbb{R}) &= H^2_{\mathbf{7}}(Y,\mathbb{R}) \oplus H^2_{\mathbf{14}}(Y,\mathbb{R}) \,, \\ H^3(Y,\mathbb{R}) &= H^3_{\mathbf{1}}(Y,\mathbb{R}) \oplus H^3_{\mathbf{7}}(Y,\mathbb{R}) \oplus H^3_{\mathbf{27}}(Y,\mathbb{R}) \,, \\ H^4(Y,\mathbb{R}) &= H^4_{\mathbf{1}}(Y,\mathbb{R}) \oplus H^4_{\mathbf{7}}(Y,\mathbb{R}) \oplus H^4_{\mathbf{27}}(Y,\mathbb{R}) \,, \\ H^5(Y,\mathbb{R}) &= H^5_{\mathbf{7}}(Y,\mathbb{R}) \oplus H^5_{\mathbf{14}}(Y,\mathbb{R}) \,. \end{aligned} \tag{2.7}$$

Notice that $H^3_{\mathbf{1}}(Y,\mathbb{R}) = \langle\!\langle [\varphi] \rangle\!\rangle$ and $H^4_{\mathbf{1}}(Y,\mathbb{R}) = \langle\!\langle [*\varphi] \rangle\!\rangle$, i.e., these subspaces are generated by representatives of the three- and the four-forms on $Y$, respectively. Moreover, the isomorphism $H^p_{\mathbf{q}}(Y,\mathbb{R}) \cong H^{7-p}_{\mathbf{q}}(Y,\mathbb{R})$ implies the following relations for the *Betti numbers*[3] on the $G_2$-manifold $Y$,

$$b^{\mathbf{q}}_p(Y) = b^{\mathbf{q}}_{7-p}(Y) \,, \tag{2.8}$$

$$b^{\mathbf{1}}_3(Y) = b^{\mathbf{1}}_4(Y) = 1 \,. \tag{2.9}$$

If the holonomy group is $G_2$ and not a subgroup thereof, we have in addition $H^p_{\mathbf{7}} = \{0\}$ for $p = 1, \ldots, 6$.

We now delve into relations of $G_2$-manifolds with SU(2) and SU(3) holonomy group manifolds. This is relevant because manifolds with such holonomy groups appear in section 2.2, when we focus on the recent construction due to Kovalev of compact $G_2$-manifolds of the twisted connected sum type, namely K3 surfaces with SU(2) holonomy group and Calabi–Yau manifolds with SU(3) holonomy groups, respectively. The content presented in the following is based on [139, 201, 202, 203].

Let $\{z^1, z^2, \ldots, z^n\}$ be holomorphic coordinates on $\mathbb{C}^n$. Then the *Kähler form*[4] $\omega_0$ and the standard holomorphic *volume form*[5] $\Omega_0$ are given by

[2] The $p$-th de Rham cohomology group $H^p(M)$ on a real manifold $M$ gives the set of cohomology classes, that is, the set of closed forms in $\Lambda^p T^*M$ modulo exact forms. In other words, it is the quotient of the vector space of closed $p$-forms on $M$ by the vector space of exact $p$-forms on $M$. For complex manifolds $M_{\mathbb{C}}$, one defines an analogous Dolbeault cohomology or $\bar\partial$-cohomology $H^{p,q}(M_{\mathbb{C}})$ as the quotient between $\bar\partial$-closed $(p,q)$-forms and $\bar\partial$-exact $(p,q)$-forms, where the operator $\bar\partial$ acts as $\bar\partial : \Lambda^{p,q}T^*M_{\mathbb{C}} \to \Lambda^{p,q+1}T^*M_{\mathbb{C}}$.

[3] The dimension of the $n$-th cohomology group is called the $n$-th Betti number for real manifolds. If the manifold has a metric, Betti numbers count the number of linearly independent harmonic $n$-forms on the manifold. Analogously, for complex manifolds, the Hodge number $h^{p,q}$ gives the dimension of the $(p,q)$-cohomology group $H^{p,q}$. If the manifold has a metric, Hodge numbers count the number of linearly independent harmonic $(p,q)$-forms on the manifold.

[4] Any complex manifold endowed with an hermitian metric and a $(1,1)$-closed form $\omega$ satisfying $\mathrm{d}\omega = 0$, called a Kähler form, is a Kähler manifold.

[5] A volume form on a differential $n$-dimensional manifold $M_D$ is a section of the line bundle $\Omega^n(M_D) = \Lambda^n T^*M_D$, where $\Lambda^n T^*M_D$ are vector bundles. For $n$-dimensional complex manifolds $M_{\mathbb{C}}$, a holomorphic line bundle over $M_{\mathbb{C}}$ is a holomorphic vector bundle with fiber $\mathbb{C}$. The canonical line bundle $K_{M_{\mathbb{C}}} = \Lambda^n T^{*1,0}M_{\mathbb{C}}$ has sections which are $(n,0)$-forms, where $\Lambda^n T^{*1,0}M_{\mathbb{C}}$ are holomorphic line bundles. The first Chern class is a topological invariant of the holomorphic line bundle over $M_{\mathbb{C}}$ lying in the cohomology $H^2(M_{\mathbb{C}},\mathbb{Z})$. Any compact Kähler manifold $M$ with vanishing first Chern class $c_1(M) = 0$ is flat, which implies that the canonical line bundle is topologically trivial. Consequently, there must exist a globally defined nowhere vanishing $n$-form on $M$. If the holonomy group of $M$ is such that $\mathcal{H} \subseteq \mathrm{SU}(n)$, there is a unique nowhere vanishing holomorphic section on

$$\omega_0 = \frac{i}{2}\left(dz^1 \wedge d\bar{z}^1 + \cdots dz^n \wedge d\bar{z}^n\right) ,$$
$$\Omega_0 = dz^1 \wedge dz^2 \wedge \cdots \wedge dz^n .$$

For any non-degenerate real two-form $\omega$ equivalent to $\omega_0$ and any complex $n$-form $\Omega$ equivalent to $\Omega_0$, the pair $(\omega, \Omega)$ satisfies

$$\omega \wedge \Omega = 0,$$
$$(-1)^{\frac{n(n-1)}{2}} \left(\frac{i}{2}\right)^n \Omega \wedge \overline{\Omega} = \frac{\omega^n}{n!}.$$

We start by considering the action of an SU(3)-structure on $\mathbb{R}^7 \simeq \mathbb{R} \times \mathbb{C}^3$. The action of SU(3) on $\mathbb{R}$ is the trivial one. Let $z^1 = x^2 + ix^3$, $z^2 = x^4 + ix^5$ and $z^3 = x^6 + ix^7$ be holomorphic coordinates on $\mathbb{C}^3$ with $\left\{x^1, \ldots, x^7\right\}$ being a normalized orthogonal basis on $\mathbb{R}^7 \simeq \mathbb{R} \times \mathbb{C}^3$. On the one hand, there exists a $G$-structure acting on $\mathbb{C}^3$ that preserves the forms

$$\omega_0 = \mathrm{d}x^{23} + \mathrm{d}x^{45} + \mathrm{d}x^{67}, \tag{2.10}$$
$$\mathrm{Re}\Omega_0 = \mathrm{d}x^{246} - \mathrm{d}x^{257} - \mathrm{d}x^{347} - \mathrm{d}x^{356}, \tag{2.11}$$
$$\mathrm{Im}\Omega_0 = -\mathrm{d}x^{247} - \mathrm{d}x^{256} - \mathrm{d}x^{346} + \mathrm{d}x^{357} . \tag{2.12}$$

This means that $G \subset \mathrm{SU}(3)$. On the other hand, an SU(3)-structure preserves a three-form $\varphi_0 = \mathrm{d}x^1 \wedge \omega_0 + \mathrm{Re}\Omega_0$. We conclude that $G$ is exactly equal to SU(3). Therefore, for SU(3)-structures on $\mathbb{C}^3$, the pair $(\omega, \Omega)$ induces a three-form $G_2$-structure $\varphi$ and an associated four-form $*\varphi$ on $\mathbb{R}^7$ given by, respectively,

$$\begin{aligned} \varphi &= \mathrm{d}t \wedge \omega + \mathrm{Re}\Omega , \\ *\varphi &= \frac{1}{2}\omega^2 - \mathrm{d}t \wedge \mathrm{Im}\Omega . \end{aligned} \tag{2.13}$$

Here we name $x^1 = t$ as will become clear in section 2.2. Hence, the stabilizer in $G_2$ of a non-trivial vector in $\mathbb{R}^7$ is isomorphic to SU(3).

We continue by considering the action of an SU(2)-structure on $\mathbb{R}^7 \simeq \mathbb{R}^3 \times \mathbb{C}^2$. The action of SU(2) on $\mathbb{R}^3$ is the trivial one. Let $z^1 = x^1 + ix^2$ and $z^2 = x^3 + ix^4$ be holomorphic coordinates on $\mathbb{C}^2$. On the one hand, there exists a $G$-structure acting on $\mathbb{C}^2$ that preserves the forms

$$\begin{aligned} \omega_0 &= \mathrm{d}x^{12} + \mathrm{d}x^{34} , \\ \mathrm{Re}\Omega_0 &= \mathrm{d}x^{13} + \mathrm{d}x^{14} , \\ \mathrm{Im}\Omega_0 &= \mathrm{d}x^{23} + \mathrm{d}x^{24} . \end{aligned} \tag{2.14}$$

This means that $G \subset \mathrm{SU}(2)$. On the other hand, an SU(2)-structure preserves a triplet of

the canonical bundle $K_M$, i.e., there exists a nowhere vanishing holomorphic $n$-form, the holomorphic volume $n$-form $\Omega$.

mutually orthogonal hyper-Kähler two-forms ($\omega_0^I \equiv \omega_0, \omega_0^J \equiv \mathrm{Re}\Omega_0, \omega_0^K \equiv \mathrm{Im}\Omega_0$) satisfying $\omega_0^I \wedge \omega_0^J = \omega_0^J \wedge \omega_0^K = \omega_0^K \wedge \omega_0^I = 0$ and $(\omega_0^I)^2 = (\omega_0^J)^2 = (\omega_0^K)^2 = 0$. We conclude that $G$ is exactly equal to SU(2). Therefore, for SU(2)-structures on $\mathbb{C}^2$, the pair $(\omega, \Omega)$ induces a Kähler two-form $\omega$ and a holomorphic volume two-form $\Omega$ on $\mathbb{C}^2$ given by, respectively,

$$\begin{aligned} \omega &= \omega^I \,, \\ \Omega &= \omega^J + i\omega^K \,. \end{aligned} \tag{2.15}$$

These, in turn, induce a three-form $G_2$-structure $\varphi$ and an associated four-form $*\varphi$ on $\mathbb{R}^7$ since SU(2) $\subset$ SU(3) as we see below.

The classification of Riemannian holonomy groups by Berger [96] implies a theorem on the existence of the following relation for holonomy groups,

$$\mathrm{SU}(2) \subset \mathrm{SU}(3) \subset G_2 \subset \mathrm{SO}(7) \,. \tag{2.16}$$

With this theorem, the only connected Lie subgroups of the exceptional group $G_2$ which can be the holonomy group of a Riemannian metric on a seven-dimensional manifold are, apart from the trivial identity group {1}, the groups SU(2), SU(3) and $G_2$, where SU(2) and SU(3) have been defined in the previous two paragraphs. Therefore, if $\varphi$ is a torsion-free $G_2$-structure on a seven-dimensional manifold, the holonomy groups for the associated Riemannian metric can only be the aforementioned groups. With this theorem, the following proposition holds — see Proposition 10.2.2 in [97].

**Proposition 2.3** Let $Y$ be a compact $G_2$-manifold. Then the holonomy group of the Riemannian metric associated to $Y$ is the exceptional group $G_2$, and not a subgroup thereof, if and only if the first fundamental group[6] $\pi_1(Y)$ is finite.

### 2.1.4 Moduli space of compact $G_2$-manifolds

In section 2.1.1, the set of oriented $G_2$-structures on a compact seven-dimensional oriented manifold $Y$ was identified with the set of positive three-forms $\varphi$ on $Y$. Let $\mathcal{X}$ be the set of positive three-forms corresponding to oriented and torsion-free $G_2$-structures, i.e.,

$$\mathcal{X} = \left\{ \varphi \in \Omega^3_+(Y) \mid \mathrm{d}\varphi = \mathrm{d}(*_{g_\varphi}\varphi) = 0 \right\} \,. \tag{2.17}$$

Furthermore, let $\mathcal{D}$ be the group of all diffeomorphisms of $Y$ isotopic to the identity.

The *moduli space* $\mathcal{M}$ of torsion-free $G_2$-structures on $Y$ is the quotient space $\mathcal{M} = \mathcal{X}/\mathcal{D}$. This moduli space is a non-singular, smooth manifold with dimension equal to $b_3(Y)$, according to the following theorem — see Theorem 10.4.4 in [97].

**Theorem 2.1** Let $Y$ be a compact seven-dimensional manifold, and $\mathcal{M}$ be the moduli space

[6] The fundamental group on a manifold $M$ gives a way to determine when two paths, starting and ending at a fixed base point $p$ on $M$, can be continuously deformed into each other. The first fundamental group is the set of all homotopy classes of loops with base point $p$.

of torsion-free $G_2$-structures on $Y$ as defined above. Then $\mathcal{M}$ is a smooth manifold of dimension $b_3(Y)$ with the projection $\mathcal{P} : \mathcal{M} \to H^3(Y, \mathbb{R})$ given by $\mathcal{P}(\varphi\mathcal{D}) = [\varphi]$.

In other words, this theorem says that a vicinity $U \subset \mathcal{M}$ of a given torsion-free $G_2$-structure $\varphi \in \mathcal{M}$ is locally diffeomorphic to the de Rham cohomology $H^3(Y, \mathbb{R})$. This translates to the fact that infinitesimal deformations of $\varphi$ are unobstructed to all orders, i.e., they can be extended order-by-order, thereby describing locally the moduli space $\mathcal{M}$ of $G_2$-manifolds. Notice that little information about the global structure of $\mathcal{M}$ can be inferred from this theorem. For example, we cannot say whether $\mathcal{M}$ is non-empty or not, whether it has only one connected component or many, whether the map $\mathcal{P}$ is injective or not, what the image of $\mathcal{P}$ is, and other related global issues.

## 2.2 Twisted connected sum $G_2$-manifolds

In the previous section, the geometrical and the topological aspects of general compact $G_2$-manifolds were introduced. In the present section we focus on the so-called twisted connected sum $G_2$-manifolds, which are based on a recent construction due to Kovalev [140], further developed by Corti and others [141, 142]. The $G_2$-manifolds in this construction are compact real seven-dimensional manifolds $Y$ obtained from the twisted connected sum of two compatible asymptotically cylindrical Calabi–Yau threefolds $X_L$ and $X_R$ times an additional circle $S^1$. They are constructed in a way that the $G_2$-structure $\varphi$ on $Y$ satisfies $\mathrm{d}\varphi = \mathrm{d}(*_{g_\varphi})\varphi = 0$ in an asymptotic limit. Therefore, propositions 2.1 and 2.2 as well as the decomposition of the de Rham cohomologies given in section 2.1.3 are satisfied. The validity of these is what allows us to deal with compactifications of M-theory on twisted connected sums later in this thesis.

We start this section with a brief introduction to asymptotically cylindrical Calabi–Yau threefolds and a review of the twisted connected sum construction. The first contribution of this thesis to the topic appears in section 2.2.3, namely the identification of the so-called Kovalev limit in which the Ricci-flat metric of the obtained $G_2$-manifold can be approximated by the metrics of the two Calabi–Yau summands. Then we study the moduli space of the constructed twisted connected sum $G_2$-manifold and its topology. We end this section with concrete examples of asymptotically cylindrical Calabi–Yau threefolds, and present the orthogonal gluing method to match two of these threefolds together in a twisted connected $G_2$-manifold. The content in this section, especially the Kovalev limit we have identified, turns out to be crucial in setting the stage for the derivation of the low-energy effective action for M-theory compactified on such $G_2$-manifolds in section 3.4, and of the interesting gauge sectors on them, which we analyze in chapter 4.

### 2.2.1 Asymptotically cylindrical Calabi–Yau threefold

Let us start with the definition of a Calabi–Yau cylinder, which enters into the definition of asymptotically cylindrical Calabi–Yau threefolds[7]. These are based on the references [140, 142,

[7] A Calabi–Yau $n$-fold is a compact Kähler manifold of dimension $n \geq 2$ with SU($n$) holonomy group. This is equivalent to defining it as a compact complex and Kähler manifold with vanishing first Chern class.

204]. We take a compact Calabi–Yau twofold to be a K3 surface[8] $S$ equipped with a Kähler form $\omega_S$ and a holomorphic two-form $\Omega_S$. A complex three-dimensional *Calabi–Yau cylinder* $X^\infty$ is defined as the product of a such compact Calabi–Yau twofold with the algebraic torus[9] $\mathbb{C}^*$. Let $z = \exp(t + i\theta^*)$ be the holomorphic coordinate on $\mathbb{C}^*$ and $\gamma^*$ the length of the cylinder $\Delta^{\text{cyl}}$ [140]. In this way[10], the Kähler form $\omega^\infty$ and the holomorphic three-form $\Omega^\infty$ of the Calabi–Yau cylinder $X^\infty$ read

$$\begin{aligned} \omega^\infty &= \gamma^{*2}\frac{i\mathrm{d}z\wedge\mathrm{d}\bar{z}}{2z\bar{z}} + \omega_S = \gamma^{*2}\,\mathrm{d}t\wedge\mathrm{d}\theta^* + \omega_S\,, \\ \Omega^\infty &= -\gamma^*\frac{i\mathrm{d}z}{z}\wedge\Omega_S = \gamma^*(\mathrm{d}\theta^* - i\mathrm{d}t)\wedge\Omega_S\,, \end{aligned} \tag{2.18}$$

with the metric $g_{X^\infty} = \gamma^{*2}\left(\mathrm{d}t^2 + \mathrm{d}\theta^{*2}\right) + g_S$ on the Calabi–Yau cylinder $X^\infty$ in terms of the metric $g_S$ on the K3 surface. Notice that the length scale $\gamma^*$ furnishes the radius of the cylindrical metric on $\Delta^{\text{cyl}}$, whereas the map $\xi : X^\infty \to \mathbb{R}^+$ with $\xi = \log|z|$ projects onto the longitudinal direction of the cylinder such that $\xi^{-1}(\mathbb{R}^+) = X^\infty$.

An *asymptotically cylindrical Calabi–Yau threefold* $X$ is a non-compact Calabi–Yau threefold with SU(3) holonomy and a complete[11] Calabi–Yau metric $g_X$ with the following properties. There exists a compact subspace $K \subset X$ such that the complement $X \setminus K$ is diffeomorphic to a three-dimensional Calabi–Yau cylinder $X^\infty$, and such that the Kähler and the holomorphic three-form of $X$ approach fast enough $\omega^\infty$ and $\Omega^\infty$ of the cylindrical Calabi–Yau threefold $X^\infty$, given in equations (2.18). More precisely, given the diffeomorphism $\eta : X^\infty \to X \setminus K$, we require that in the limit $\xi \to +\infty$ and for any positive integer $k$,

$$\begin{aligned} \eta^*\omega - \omega^\infty &= \mathrm{d}\mu \quad \text{with} \quad |\nabla^k\mu| = O(e^{-\lambda\gamma^*\xi})\,, \\ \eta^*\Omega - \Omega^\infty &= \mathrm{d}\nu \quad \text{with} \quad |\nabla^k\nu| = O(e^{-\lambda\gamma^*\xi})\,, \end{aligned} \tag{2.19}$$

for a one-form $\mu$ and a two-form $\nu$ with the norm $|\cdot|$ and the Levi-Civita connection $\nabla$ of the metric $g_{X^\infty}$. The scale $\lambda$ has inverse length dimension and is determined by the inverse length scale of the asymptotic region $X^\infty$. To be precise

$$\lambda = \min\left\{\tfrac{1}{\gamma^*}, \lambda_S\right\}\,, \tag{2.20}$$

where $\lambda_S$ is the square root of the smallest positive eigenvalue of the Laplacian of the K3 surface $S$ in the asymptotic Calabi–Yau cylinder $X^\infty$.

[8] A complex two-dimensional compact Kähler manifold with Hodge number $h^{1,0} = 0$ and trivial canonical bundle. They are the lowest dimensional example of a Calabi–Yau with holonomy SU(2) and of a hyperkähler manifold with holonomy Sp(1).

[9] The open cylinder $\Delta^{\text{cyl}}$ given as the complement of the unit disk in the complex plane $\mathbb{C}$, i.e., $\Delta^{\text{cyl}} = \{z \in \mathbb{C}\,|\,|z| > 1\}$.

[10] With the conventional mutual normalization $(-1)^{\frac{n(n-1)}{2}}\left(\frac{i}{2}\right)^n \Omega\wedge\bar{\Omega} = \frac{\omega^n}{n!}$ between the Kähler form $\omega$ and the holomorphic $n$-form $\Omega$ of Calabi–Yau $n$-folds, we note that — assuming this normalization for $\omega_S$ and $\Omega_S$ of the K3 surface $S$ — the Kähler form $\omega^\infty$ and the holomorphic three-form $\Omega^\infty$ of $X^\infty$ are conventionally normalized.

[11] A complete metric is a metric on a complete metric space, where every Cauchy sequence of points in the space has a limit that is also in the same space.

### 2.2.2 The twisted connected sum construction

In the following, we introduce the reader to the twisted connected sum construction of $G_2$-manifolds as put forward by Kovalev [140] and further developed by Corti and others [141, 142].

First of all, one notices that, from any Calabi–Yau threefold $X$ with SU(3) holonomy, it is always possible to construct the seven-dimensional manifold $X \times S^1$ with a torsion-free $G_2$-structure $\varphi_0$ and its dual four-form $*\varphi_0$ given by — recall section 2.1.3 —

$$\varphi_0 \;=\; \gamma\, \mathrm{d}\theta \wedge \omega + \mathrm{Re}\Omega\,, \qquad *\varphi_0 \;=\; \frac{1}{2}\omega^2 - \gamma\, \mathrm{d}\theta \wedge \mathrm{Im}\Omega\,. \tag{2.21}$$

Here $\omega$ is the Kähler form and $\Omega$ is the holomorphic three-form of the asymptotically cylindrical Calabi–Yau threefold $X$, whereas $\theta$ is the coordinate on the circle $S^1$ of radius $\gamma$. However, this resulting seven-dimensional manifold has only SU(3) holonomy, which is a subgroup of $G_2$, and not the whole group $G_2$.

In order to obtain a genuine seven-dimensional $G_2$-manifold with full holonomy group $G_2$, rather than only a subgroup thereof, the following three steps are necessary.

- *First step:* start with two asymptotically cylindrical Calabi–Yau threefolds — instead of only one —, which we call $X_L$ and $X_R$ or, for brevity, $X_{L/R}$.

- *Second step:* take a direct product of each asymptotically cylindrical Calabi–Yau threefold $X_L$ and $X_R$ with an extra circle $S^1_L$ and $S^1_R$, respectively. The circles have coordinates $\theta_L$ and $\theta_R$, with radius $\gamma_L$ and $\gamma_R$, respectively. In this way, one obtains two seven-dimensional manifolds $Y_{L/R}$ of SU(3) holonomy with torsion-free $G_2$-structures $\varphi_{0\,L/R}$ and associated dual four-forms $*\varphi_{0\,L/R}$, as explained above,

$$\varphi_{0L/R} = \gamma_{L/R} d\theta_{L/R} \wedge \omega_{L/R} + \mathrm{Re}\Omega_{L/R}\,, \tag{2.22}$$

$$*\varphi_{0L/R} = \frac{1}{2}\omega^2_{L/R} - \gamma_{L/R} d\theta_{L/R} \wedge \mathrm{Im}\Omega_{L/R}\,. \tag{2.23}$$

- *Third step:* obtain a genuine compact $G_2$-manifold $Y$. This is done after appropriately gluing together the asymptotic regions of type $Y^\infty_{L/R} = X^\infty_{L/R} \times S^1_{L/R}$ in such a way that the final obtained manifold $Y = Y_L \cup Y_R$ admits a torsion-free $G_2$-structure, resulting in an associated metric with holonomy group $G_2$ and not a subgroup thereof. We now give the details of this lengthy step.

  Due to proposition 2.3, to obtain the full $G_2$ holonomy it is necessary to glue together the infinite fundamental groups $\pi_1(Y_{L/R})$ into a finite fundamental group $\pi_1(Y)$. For suitable choices of $Y_{L/R}$ this can be achieved by the following *twisted connected sum construction*. Recall that the asymptotic regions of $Y_{L/R}$ are given by

$$Y^\infty_{L/R} \;=\; X^\infty_{L/R} \times S^1_{L/R} \;=\; S_{L/R} \times \Delta^{\mathrm{cyl}}_{L/R} \times S^1_{L/R}\,, \tag{2.24}$$

  with the K3 surfaces $S_{L/R}$ and the cylinders $\Delta^{\mathrm{cyl}}_{L/R}$ — cf. section 2.2.1. Now, let us denote by $\omega^I_{0L/R}, \omega^J_{0L/R}$ and $\omega^K_{0L/R}$ the triplet of mutually orthogonal hyper-Kähler two-forms,

satisfying the relations $(\omega^I_{0L/R})^2 = (\omega^J_{0L/R})^2 = (\omega^K_{0L/R})^2$ and $\omega^I_{0L/R} \wedge \omega^J_{0L/R} = \omega^J_{0L/R} \wedge \omega^K_{0L/R} = \omega^K_{0L/R} \wedge \omega^I_{0L/R} = 0$. From section 2.1.3, SU(2)-structures of K3 surfaces $S_{L/R}$ determine their Kähler two-forms $\omega^\infty_{S_{L/R}}$ and their holomorphic two-forms $\Omega^\infty_{S_{L/R}}$ according to

$$\omega^\infty_{S_{L/R}} = \omega^I_{L/R}\,, \qquad \Omega^\infty_{S_{L/R}} = \omega^J_{L/R} + i\,\omega^K_{L/R}\,. \tag{2.25}$$

These, together with equations (2.18) and (2.21), explicitly specify the asymptotic torsion-free $G_2$-structures

$$\begin{aligned}\varphi^\infty_{0\,L/R} =& \gamma_{L/R}\mathrm{d}\theta_{L/R} \wedge \left(\gamma^{*\,2}_{L/R}\mathrm{d}t_{L/R} \wedge \mathrm{d}\theta^*_{L/R} + \omega^\infty_{S_{L/R}}\right) \\ &+ \gamma^*_{L/R}\mathrm{d}\theta^*_{L/R} \wedge \mathrm{Re}\Omega^\infty_{S_{L/R}} + \gamma^*_{L/R}\mathrm{d}t_{L/R} \wedge \mathrm{Im}\Omega^\infty_{S_{L/R}}\,.\end{aligned} \tag{2.26}$$

Furthermore, one assumes that the asymptotically cylindrical Calabi–Yau threefolds $X_{L/R}$ are chosen such that the resulting K3 surfaces $S_{L/R}$ are mutually isometric with respect to a hyper-Kähler rotation $r : S_L \to S_R$ obeying[12]

$$r^*\omega^I_R = \omega^J_L\,, \quad r^*\omega^J_R = \omega^I_L\,, \quad r^*\omega^K_R = -\omega^K_L\,. \tag{2.27}$$

This requirement is such that there is a family of diffeomorphisms $F_\Lambda : Y^\infty_L \to Y^\infty_R$ with constant $\Lambda \in \mathbb{R}$ in terms of the local coordinates $(\theta^*_{L/R}, t_{L/R})$ of $\Delta^{\mathrm{cyl}}_{L/R}$, $u^\alpha_{L/R} = (\omega^I_{L/R}, \omega^J_{L/R}, \omega^K_{L/R})$ of $S_{L/R}$, and $\theta_{L/R}$ of $S^1_{L/R}$, given by

$$F_\Lambda :\ (\theta^*_L, t_L, u^\alpha_L, \theta_L) \mapsto (\theta^*_R, t_R, u^\alpha_R, \theta_R) = (\theta_L, \Lambda - t_L, r(u^\alpha_L), \theta^*_L)\,. \tag{2.28}$$

If and only if the radii of the extra circles $S^1_{L/R}$ are equal, i.e.,

$$\gamma \equiv \gamma_L = \gamma_R = \gamma^*_L = \gamma^*_R\,, \tag{2.29}$$

this asymptotic diffeomorphism is also an asymptotic isometry. This is true because it leaves the asymptotic $G_2$-structures $\varphi^\infty_{0\,L/R}$ — and hence the asymptotic metric — invariant, i.e.,

$$F^*_\Lambda\varphi^\infty_{0R} = \varphi^\infty_{0L}\,. \tag{2.30}$$

In fact, on the one hand, by computing $\varphi_{0L}$ with equations (2.25) and (2.26) we obtain

$$\varphi^\infty_{0L} = \gamma_L\mathrm{d}\theta_L \wedge \gamma^{*\,2}_L\mathrm{d}t_L \wedge \mathrm{d}\theta^*_L + \gamma_L\mathrm{d}\theta_L \wedge \omega^I_L + \gamma^*_L\mathrm{d}\theta^*_L \wedge \omega^J_L + \gamma^*_L\mathrm{d}t_L \wedge \omega^K_L\,. \tag{2.31}$$

[12] These conditions impose rather non-trivial constraints on the pair of asymptotically cylindrical Calabi–Yau threefolds $X_{L/R}$, which — at least for certain classes of pairs — have been studied systematically in reference [141]. In this section we assume that these conditions on $X_{L/R}$ are met, and we come back to this issue in section 2.2.5 where we give examples of asymptotically cylindrical Calabi–Yau threefolds $X_{L/R}$ fulfilling these constraints.

On the other hand, by computing $F_\Lambda^* \varphi_{0R}^\infty$ we obtain

$$\begin{aligned} F_\Lambda^* \varphi_{0R}^\infty &= \gamma_R \mathrm{d}\theta_L^* \wedge \gamma_R^{*2} \mathrm{d}(\Lambda - t_L) \wedge \mathrm{d}\theta_L + \gamma_R \mathrm{d}\theta_L^* \wedge \omega_R^I + \gamma_R^* \mathrm{d}\theta_L \wedge \omega_R^J + \gamma_R^* \mathrm{d}(\Lambda - t_L) \wedge \omega_R^K \\ &= \gamma_R \mathrm{d}\theta_L \wedge \gamma_R^{*2} \mathrm{d}t_L \wedge \mathrm{d}\theta_L^* + \gamma_R \mathrm{d}\theta_L^* \wedge \omega_L^J + \gamma_R^* \mathrm{d}\theta_L \wedge \omega_L^I + \gamma_R^* \mathrm{d}t_L \wedge \omega_L^K \,, \end{aligned} \tag{2.32}$$

where in the second equality we made use of equation (2.27). Therefore, these imply equation (2.29).

The $G_2$-manifold $Y$ is now obtained by gluing the asymptotic ends of $Y_{L/R}$ with the help of the diffeomorphism $F_\Lambda$. This is schematically depicted in figure 2.1. Let $X_{L/R}(T)$ and $Y_{L/R}(T)$ be truncated asymptotically cylindrical Calabi–Yau threefolds and truncated seven-dimensional manifolds, respectively, given by cutting off their asymptotic regions at $t_{L/R} = T + 1$ for some large $T$, i.e.,

$$X_{L/R}(T) \;=\; K_{L/R} \cup \eta_{L/R}(\mathbb{R}_{<T+1}) \,, \quad Y_{L/R}(T) \;=\; X_{L/R}(T) \times S^1_{L/R} \,. \tag{2.33}$$

Here the diffeomorphisms $\eta_{L/R}$ and the compact subspaces $K_{L/R}$ have been defined in section 2.2.1. Then, using the diffeomorphism $F_{2T+1}$ — which maps the coordinate $t_L \in (T, T+1)$ to $t_R = -t_L + 2T + 1 \in (T, T+1)$ — we glue the two seven-dimensional manifolds $Y_{L/R}(T)$ at the overlap $t_{L/R} \in (T, T+1)$ to arrive at the compact seven-dimensional manifold

$$Y \;=\; Y_L(T) \cup_{F_{2T+1}} Y_R(T) \,. \tag{2.34}$$

Finally, to construct a $G_2$-structure $\varphi$ on $Y$, we first introduce interpolating $G_2$-structures on the two pieces $Y_{L/R}(T)$. This is done with the help of a smooth interpolating function between 0 and 1 in the interval $(-1, 0)$, i.e., $\alpha : \mathbb{R} \to [0, 1]$ with $\alpha(s) = 0$ for $s \leq -1$ and $\alpha(s) = 1$ for $s \geq 0$. Then the truncated asymptotically cylindrical Calabi–Yau threefolds $X_{L/R}(T)$ are endowed with the forms

$$\begin{aligned} \widetilde{\omega}_{L/R}^T &= \omega_{L/R} - \mathrm{d}\left(\alpha(t - T)\mu_{L/R}\right) \,, \\ \widetilde{\Omega}_{L/R}^T &= \Omega_{L/R} - \mathrm{d}\left(\alpha(t - T)\nu_{L/R}\right) \,, \end{aligned} \tag{2.35}$$

in terms of the forms $\mu_{L/R}$ and $\nu_{L/R}$ of equations (2.19). By construction, the forms $\widetilde{\omega}_{L/R}^T$ and $\widetilde{\Omega}_{L/R}^T$ smoothly interpolate between the corresponding Calabi–Yau cylinder forms (2.18) and the asymptotically cylindrical Calabi–Yau forms (2.19). At the interpolating regions $t_{L/R} \in (T - 1, T)$, the symplectic forms $\omega_{L/R}^T$ fail to induce a Ricci-flat metric and the three-forms $\Omega_{L/R}^T$ cease to be holomorphic. Analogously to equation (2.21), the interpolating $G_2$-structures $\widetilde{\varphi}_{L/R}(\gamma, T)$ on $Y_{L/R}$ read

$$\widetilde{\varphi}_{L/R}(\gamma, T) \;=\; \gamma \, \mathrm{d}\theta \wedge \widetilde{\omega}_{L/R}^T + \mathrm{Re}\widetilde{\Omega}_{L/R}^T \,, \tag{2.36}$$

which according to equation (2.30) glue together to a well-defined $G_2$-structure $\widetilde{\varphi}(\gamma, T)$ on the seven-dimensional manifold $Y$.

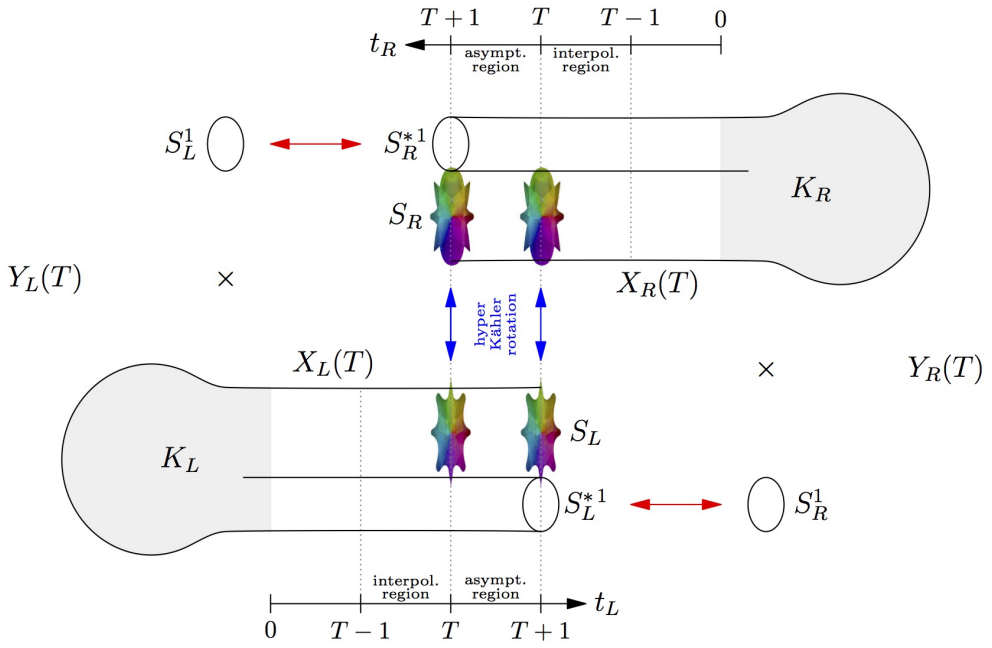


Figure 2.1: The twisted connected sum construction due to Kovalev to obtain the $G_2$-manifold $Y$. $X_{L/R}(T)$ are the truncated asymptotically cylindrical Calabi–Yau threefolds together with their compact subspaces $K_{L/R}$. Their Cartesian products with the circles $S^1_{L/R}$ yield the two seven-dimensional components $Y_{L/R}(T)$, which combine to form the $G_2$-manifold $Y$. There are three essential aspects in the construction. Firstly, two asymptotically cylindrical Calabi–Yau threefolds — each with SU(3) holonomy — are used if we require the resulting seven-dimensional manifold to have full $G_2$-holonomy after the gluing procedure. Secondly, as indicated by the red horizontal arrows, the circles $S^1_{L/R}$ are identified with the asymptotic circles of $X_{L/R}(T)$ here denoted by $S^{*1}_{R/L}$. Thirdly, as depicted by the blue vertical arrows, the asymptotic polarized K3 surfaces $S_{L/R}$ must be matched with a certain hyper-Kähler rotation. The diagram highlights the interpolating regions, $t_{L/R} \in (T-1, T]$, and the asymptotic gluing regions, $t_{L/R} \in (T, T+1)$, important for the construction of the $G_2$-structure $\varphi(\gamma, T)$ of $Y$.

Note that the constructed $G_2$-structure $\widetilde{\varphi}(\gamma, T)$ is closed by construction, i.e., $\mathrm{d}\widetilde{\varphi}(\gamma, T) = 0$, because $\omega^T_{L/R}$ and $\Omega^T_{L/R}$ are closed. However, it is not torsion-free. In fact, the torsion of $\varphi(\gamma, T)$ is measured by $\mathrm{d}{*}\widetilde{\varphi}(\gamma, T)$ and this is only non-vanishing at the interpolating regions $t_{L/R} \in (T-1, T)$. Indeed, the non-torsion term is of order $O(e^{-\gamma\lambda T})$ due to equation (2.19).[13]

Therefore, it is plausible that we view $\widetilde{\varphi}(\gamma, T)$ as an order $O(e^{-\gamma\lambda T})$ approximation to a torsion-free $G_2$-structure $\varphi(\gamma, T)$, which equips the seven-dimensional manifold $Y$ with a Ricci-flat metric. Indeed, in Lemma 4.25 of Kovalev's work [140], it is shown that, for sufficiently large $T$, there exists a torsion-free $G_2$-structure $\varphi(\gamma, T)$ in the same three-form cohomology class of $\widetilde{\varphi}(\gamma, T)$ such that, for any positive integer $k$,

$$\varphi(\gamma, T) = \widetilde{\varphi}(\gamma, T) + \mathrm{d}\rho(\gamma, T) \quad \text{with} \quad \left|\nabla^k \rho(\gamma, T)\right| = O(e^{-\gamma\lambda T}) \,, \tag{2.37}$$

[13] Note that, due to relation (2.29) and the hyper-Kähler isometry (2.30), we have the identifications $\lambda = \lambda_L = \lambda_R$ among inverse length scales.

in terms of the norm $|\cdot|$ and the Levi–Civita connection $\nabla$ of the metric induced from the asymptotic $G_2$-structure $\tilde{\varphi}(\gamma, T)$.

Furthermore, from the Van Kampen theorem [205], there is a relationship $\pi_1(Y) \cong \pi_1(X_L) \times \pi_1(X_R)$ among the fundamental groups in the twisted connected sum. Since each of the factors $\pi_1(X_L)$ and $\pi_1(X_R)$ is finite, this implies that the torsion-free $G_2$-structure $\varphi(\gamma, T)$ indeed gives rise to a genuine $G_2$-manifold $Y$ with metric of $G_2$-holonomy and not a subgroup thereof.

This summarizes the main result of reference [140] — clarified and further developed in references [141, 142, 204] —, namely the proof that the $G_2$-structure $\widetilde{\varphi}(\gamma, T)$ in Kovalev's twisted connected sum construction in terms of the two asymptotically cylindrical Calabi–Yau threefolds furnishes an approximation to the torsion-free $G_2$-structure $\varphi(\gamma, T)$ in the same three-form cohomology class that gives rise to a compact seven-dimensional Ricci-flat Riemannian manifold $Y$ with $G_2$-holonomy.

### 2.2.3 The Kovalev limit

As discussed in the last section, the torsion-free $G_2$-structure $\varphi(\gamma, T)$ in Kovalev's twisted connected sum is approximated, via equation (2.21), in terms of the Kähler forms $\omega_{L/R}$ and the holomorphic forms $\Omega_{L/R}$ of the asymptotically cylindrical Calabi–Yau threefolds $X_{L/R}$. According to equations (2.19) and (2.37) this approximation is of order $O(e^{-\gamma\lambda T})$.

In this section we discuss the torsion-free $G_2$-structure $\varphi(\gamma, T)$ as a function of the parameters $\gamma$ and $T$ in order to obtain a well-defined limit in which we can make sense of a four-dimensional effective action from eleven-dimensional M-theory compactifications on twisted connected sum $G_2$-manifolds.

Except for the overall volume modulus $R$ of each of the asymptotically cylindrical Calabi–Yau threefolds $X_{L/R}$, we keep all other moduli fixed. In other words, we consider the moduli dependence of the two metrics $g_{L/R}$ of $X_{L/R}$ as

$$g_{L/R}(z_{L/R}, t_{L/R}) \;=\; \gamma_0^2\, R^2\, \tilde{g}(z_{L/R}, \tilde{t}_{L/R})\,, \tag{2.38}$$

where $z_{L/R}$ and $t_{L/R}$ are the (dimensionless) complex structure moduli and the Kähler moduli[14] of $X_{L/R}$, respectively. The constant $\gamma_0$ has dimension of length such that the metrics $\tilde{g}_{L/R}$ become dimensionless. We split the Kähler moduli $t_{L/R}$ further into the overall volume modulus $R$ and the remaining Kähler moduli $\tilde{t}_{L/R}$ — measuring ratios of volumes of subvarieties in $X_{L/R}$ — such that[15]

$$t_{L/R}^n \;=\; \begin{cases} R^2 & n = 1\,, \\ R^2\, \tilde{t}_{L/R}^n & n \neq 1\,. \end{cases} \tag{2.39}$$

[14] For a Calabi–Yau manifold, the deformations $\delta g = \delta g_{ij} dz^i \wedge dz^j + \delta g_{i\bar{j}} dz^i \wedge dz^{\bar{j}}$ of the metric $g$ that still mantain a vanishing Ricci tensor are called the complex structure and the Kähler moduli. Indeed, $\delta g_{ij} dz^i \wedge dz^j = \Omega_{ijk} g^{k\bar{k}} \delta_{\bar{k}\bar{l}} dz^i \wedge dz^i \wedge d\bar{z}^{\bar{l}}$ are associated to elements of $H^{2,1}_{\bar{\partial}}$ and called complex structure moduli, whereas $\delta g_{i\bar{j}} dz^i \wedge dz^{\bar{j}}$ are associated to elements $H^{1,1}_{\bar{\partial}}$ and called Kähler moduli.

[15] For an asymptotically cylindrical Calabi–Yau threefold with a single Kähler modulus $t$, the volume modulus $R$ relates to this Kähler modulus as $R^2 = t$ without the presence of any further moduli.

When obtaining the $G_2$-manifold $Y$ from the seven-dimensional building blocks $Y_{L/R}$, the hyper-Kähler compatibility condition (2.27) constrains the explicit values of the moduli $z_{L/R}$ and $\tilde{t}_{L/R}$. Furthermore, the required identification (2.29) of the radii of all circles in the asymptotic region of $Y_{L/R}$ determines the volume modulus $R$ as the dimensionless ratio

$$R = \frac{\gamma}{\gamma_0} \,. \tag{2.40}$$

This justifies the introduction of a mutual volume modulus $R$ for both threefolds $X_{L/R}$.

In the context of eleven-dimensional M-theory compactifications on the seven-dimensional $G_2$-manifold $Y$ — see details in chapter 3 —, the volume $V_Y$ of the resulting $G_2$-manifold $Y$ determines the four-dimensional Planck constant $\kappa_4$. Indeed, let $G_N$ and $\hat{G}_N$ be the four- and eleven-dimensional Newton's constants, respectively. Furthermore, $l_{\mathrm{P}}$ and $M_{\mathrm{P}}$ are the four-dimensional Planck length and Planck mass constants, whereas $\hat{l}_{\mathrm{P}}$ and $\hat{M}_{\mathrm{P}}$ are their eleven-dimensional counterparts. With $\lambda_0$ being a dimensionless volume factor, and $V_{Y_0}$ a dimensionful reference volume that we specify in a moment, we have

$$\kappa_4^2 = \frac{\kappa_{11}^2}{V_{Y_0}} \,, \tag{2.41}$$

with

$$\begin{aligned} \kappa_4^2 &= 8\pi G_N = 8\pi \ell_{\mathrm{P}}^2 = \frac{8\pi}{M_{\mathrm{P}}^2} \,, \\ \kappa_{11}^2 &= 8\pi \hat{G}_N = \frac{(2\pi)^8 \hat{l}_{\mathrm{P}}^9}{2} = \frac{(2\pi)^8}{2\hat{M}_{\mathrm{P}}^9} \,, \\ \lambda_0 &= \frac{V_Y}{V_{Y_0}} = \frac{1}{7}\int_Y \varphi \wedge *_{g_\varphi}\varphi \,. \end{aligned} \tag{2.42}$$

The fact that the four-dimensional Planck constant $\kappa_4$ must be a constant allows us to define the so-called *Kovalev limit*. This limit is an approximation in which the four-dimensional Planck constant $\kappa_4$ — and hence the volume $V_Y$ — remains constant, while exponential correction terms due to equation (2.37) become sufficiently small. Therefore, let us study in detail the volume of the constructed $G_2$-manifold $Y$ in the Kovalev limit.

The resulting volume should sum up contributions from all the pieces of the twisted connected sum construction and, therefore, it should depend on the moduli $R$ and $T$ and the remaining moduli of the $G_2$-manifold $Y$ — collectively denoted by $\tilde{S}$.

The volumes $V_{Y_{L/R}(T)}$ of the truncated building blocks $Y_{L/R}(T)$ are calculated with the metrics of the (truncated) asymptotically cylindrical Calabi–Yau threefolds $X_{L/R}(T)$ using expression (2.18) and the volume formula

$$V_{Y_{L/R}(T)} = \frac{\gamma_0^7}{7}\int_{Y_{L/R}(T)} \varphi_{L/R} \wedge *\varphi_{L/R} \,, \tag{2.43}$$

where the dimensionful reference volume is given by $V_{Y_0} = \gamma_0^7$.

If we sum contributions from both $V_{Y_L(T)}$ and $V_{Y_R(T)}$, the volume of the overlapping region $V_{Y_L(T)\cap Y_R(T)}$ will be counted twice. Therefore, we need to subtract this contribution again once. This is given by the product of the volumes of the overlapping interval, the asymptotic two-torus $S^1_L \times S^{*1}_L \equiv S^1_R \times S^{*1}_R$, and the asymptotic K3-surface $S_L \equiv S_R \equiv S$ according to

$$V_{Y_L(T)\cap Y_R(T)} \;=\; (2\pi)^2\gamma_0^3 R^3 V_S(\tilde{\rho}_S, R) \;=\; (2\pi)^2\gamma_0^7 R^7 V_S^{\tilde{g}}(\tilde{\rho}_S)\,. \tag{2.44}$$

Here we single out those moduli fields $\tilde{\rho}_S$ deforming the K3 surface $S$ from the set $\tilde{S}$. In the last equality, the volume of the K3-surface $S$ is expressed in terms of the dimensionless (asymptotic) metric $\tilde{g}$. Due to approximation (2.19) of the metrics of the building blocks $Y_{L/R}(T)$ by the limiting metrics of $Y^\infty_{L/R}(T)$ in the interpolation region $t_{L/R} \in (T-1, T)$, and due to the overall correction (2.37) to the torsion-free $G_2$-structure $\varphi(\gamma, T)$, the computed volume of the $G_2$-manifold $Y$ receives exponentially suppressed corrections in $\tilde{\lambda}RT$ for large $RT$, where $\tilde{\lambda} = \lambda\gamma_0$ is a dimensionless constant — recall equation (2.20).

Note that, up to exponentially correction terms suppressed for large $RT$, the volume (2.44) is entirely determined by the (relative) periods[16] and the Kähler forms of the asympotically cylindrical Calabi–Yau threefolds $X_{L/R}$. However, due to non-compactness of $X_{L/R}$, the relative periods and the Kähler volumes of non-compact cycles diverge linearly in $T$. Therefore, in order to obtain the finite periods and finite volumes of the truncated asymptotically cylindrical Calabi–Yau threefolds $X_{L/R}(T)$, a suitable regularization scheme must be employed to extract the required geometric data from the diverging periods and infinite volumes. This analysis is beyond the scope of this thesis. Hence, instead of deriving the entire moduli dependence of the volume of the $G_2$-manifold $Y$, we focus on the moduli dependence of the two fields $R$ and $T$, and view the remaining moduli fields $\tilde{S}$ as fixed parameters.

In this way, we compute the volumes $V_{Y_{L/R}(T)}$ of each truncated piece. They are given by

$$\begin{aligned} V_{Y_{L/R}(T)} \;&=\; \frac{\gamma_0^7}{7}\int_{Y_{L/R}(T)} \varphi_{L/R}\wedge *\varphi_{L/R} \\ &=\; \frac{\gamma_0^7}{7}\int_{Y_{L/R}(T)\setminus K_{L/R}} \varphi^\infty_{L/R}\wedge *\varphi^\infty_{L/R} + V_{K_{L/R}} + (2\pi)^2\gamma_0^7 R^7\Delta_{L/R}(\tilde{S}, T) \\ &=\; (2\pi)^2\gamma_0^7 R^7\left[V_S^{\tilde{g}}(\tilde{\rho}_S)\Big((T+1) + D_{L/R}(\tilde{S})\Big) + \Delta_{L/R}(\tilde{S}, T)\right]\,. \end{aligned} \tag{2.45}$$

The integration was performed by splitting the integral over the compact parts $K_{L/R}$ and the asymptotic regions $Y_{L/R}(T)\setminus K_{L/R}$. The former part factors into the volume of the K3 surface $S$ and a contribution $D_{L/R}(\tilde{S})$ to be discussed in a moment. The latter part is evaluated with respect to the asymptotic $G_2$-structure $\varphi^\infty_{L/R}$. This contributes with the correction terms

$$\Delta_{L/R}(\tilde{S}, T) \;=\; R\int_0^{T+1} \mathrm{d}t\, f_{L/R}(\tilde{S}, Rt)e^{-\tilde{\lambda}Rt} \;=\; C_{L/R}(\tilde{S}) + \mathcal{O}(e^{-\tilde{\lambda}RT})\,, \tag{2.46}$$

[16] Elements of the $n$-th homology group of a manifold $M$ are equivalence classes of cycles $z_n \sim z_n + \partial a_{n+1}$, called homology classes and denoted by $[z_n]$, where $\partial a_{n+1}$ is a boundary of a $n$-chain $a_n$. Elements of the $n$-th cohomology group of a manifold $M$ are equivalence classes of closed forms $\omega_n \sim \omega_n + \alpha_{n+1}$, called cohomology classes and denoted by $[\omega_n]$, where $\mathrm{d}\alpha_{n-1}$ is an exact $n$-form. A period is the inner product $\pi(z_n, \omega_n) = \int_{z_n}\omega_n$.

in terms of the function $f_{L/R}(\tilde{S}, Rt)$ determined by equation (2.19). Thus, taking the correction terms $\Delta_{L/R}$ into account, we obtain

$$\begin{aligned} V_Y(\tilde{S}, R, T) \; &: = \; V_{Y_{L}(T)}(z_L, t_L) + V_{Y_R(T)}(z_R, t_R) - V_{Y_{L}(T)\cap Y_R(T)} \\ &= \; (2\pi)^2 \gamma_0^7 R^7 V_S^{\tilde{g}}(\tilde{\rho}_S) \left(2T + \alpha(\tilde{S})\right) + O(e^{-\tilde{\lambda}RT}) \,, \end{aligned} \tag{2.47}$$

with

$$\alpha(\tilde{S}) = \left(D_L(\tilde{S}) + C_L(\tilde{S})\right) + \left(D_R(\tilde{S}) + C_R(\tilde{S})\right) + 1 \,. \tag{2.48}$$

As discussed, the moduli-dependent contributions $D_{L/R}(\tilde{S}) + C_{L/R}(\tilde{S})$ — and hence the moduli dependent function $\alpha(\tilde{S})$ — are in principle computable from the (relative) periods and the Kähler forms of the asymptotically cylindrical Calabi–Yau threefolds $X_{L/R}$.

Now we analyse when the volume in equation (2.47) stays constant in order to keep the four-dimensional Planck constant $\kappa_4$ really a constant. For fixed moduli $\tilde{S}$, we require that the dimensionless quantity $\chi$, given by

$$\chi^7 \; = \; R^7(2T + \alpha) \,, \tag{2.49}$$

remains constant. Therefore, requiring that the four-dimensional Planck constant is indeed a constant yields the functional dependence for the modulus $R$,

$$R(T) \; = \; \frac{\chi}{\sqrt[7]{2T + \alpha}} \,. \tag{2.50}$$

This implies that corrections terms should scale as

$$O(e^{-\tilde{\lambda}RT}) \; = \; O(e^{-\frac{\tilde{\lambda}\chi T}{\sqrt[7]{2T+\alpha}}}) \,. \tag{2.51}$$

Thus, for large $T$, with $R = R(T)$ — as in equation (2.50) — the corrections for the volume $V_Y$ in equation (2.47) are exponentially suppressed. Furthermore, for $T \gg \tilde{\lambda}\chi$ — loosely also referred to as the Kovalev limit — the torsion-free $G_2$-structure of $Y$ is well approximated in terms of the geometric data of the asymptotically cylindrical Calabi–Yau threefolds $X_{L/R}$ for a given four-dimensional Planck constant $\kappa_4$. However, taking literally the limit $T \to \infty$ with $R = R(T)$ does not yield a limiting Riemannian manifold, but instead yields only a Hausdorff limit in the sense of Gromov–Hausdorff convergence of compact metric spaces[17].

In the context of M-theory compactifications on twisted connected sum $G_2$-manifolds — for more details see chapter 3.4 —, the Kovalev limit will then imply that, for large $T$ with $R = R(T)$, the Ricci-flat $G_2$-metric gets more and more accurately approximated in terms of the Ricci-flat Calabi–Yau metrics of $X_{L/R}$. These allow us to compute the resulting four-dimensional effective action explicitly in terms of Ricci-flat Calabi–Yau metrics of $X_{L/R}$. This is already a huge advantage compared to previous situation, where we could not even guarantee the existence of a

[17] A Gromov–Hausdorff distance measures how far two compact metric spaces are from being isometric. Therefore, it turns the set of all isometries of compact metric spaces into a metric space, called Gromov–Hausdorff space. This defines a notion of convergence for sequences of compact metric spaces, called Gromov–Hausdorff convergence. If such a sequence converges to a compact metric space, this is called its Hausdorff limit.

Ricci-flat $G_2$-metric — recall our discussion after proposition 2.1 regarding the non-existence of an analogue of the Calabi conjecture for the case of $G_2$-manifolds.

However, notice that, while for large $T$ with $R = R(T)$ the Ricci-flat $G_2$-metric gets more and more accurately approximated in terms of the Ricci-flat Calabi–Yau metrics of $X_{L/R}$, the semi-classical dimensional reduction on the $G_2$-manifold $Y$ in terms of the Kaluza–Klein zero modes will become less accurate due to the emergence of both light Kaluza–Klein modes as well as substantial non-perturbative and instanton corrections from M2- and M5-branes.

### 2.2.4 Cohomology of twisted connected sum $G_2$-manifolds

In this section we analyze the de Rham cohomology of $Y$ as arising from the cohomology of the asymptotically cylindrical Calabi–Yau summands. A primary contribution has already been given in Kovalev's paper [140]. Corti *et al* have presented a systematic analysis of the cohomology of $Y$ [141], which we summarize and use in the following section 2.2.5 when discussing concrete examples of asymptotically cylindrical Calabi–Yaus. Furthermore, the analysis presented here is relevant to deduce the four-dimensional $\mathcal{N} = 1$ supersymmetric spectrum of M-theory compactified on a $G_2$-manifold of the twisted connected sum type, as well as to investigate gauge sectors on these type of manifolds — see chapters 3 and 4.

First of all, we start by recalling some needed background material on lattices for K3 surfaces — see e.g. [206, 207, 208]. For a given K3 surface $S$, since its second Betti number is $b_2(S) = 22$, the integral second cohomology $H^2(S, \mathbb{Z})$ has the structure of a lattice[18]. Indeed, we refer to $H^2(S, \mathbb{Z})$ with its intersection pairing as the *K3 lattice L*. Let $E_8$ be the unique, even, unimodular, and positive definite lattice of rank 8. Moreover, let $H = \begin{pmatrix} 0 & 1 \\ 1 & 0 \end{pmatrix}$ be the standard hyperbolic plane lattice. The lattice $L$ is a marked K3 surface, since it is isomorphic to the unique, unimodular, even lattice of signature $(3, 19)$, i.e.,

$$L = H^2(S, \mathbb{Z}) \cong -E_8 \oplus -E_8 \oplus H \oplus H \oplus H \, . \tag{2.52}$$

The Picard group or *Picard lattice N* of a K3 surface is defined as

$$\mathrm{Pic}(S) = H^2(S, \mathbb{Z}) \cap H^{1,1}(S) \, , \tag{2.53}$$

and $\rho$ is defined as the rank of the Picard lattice, called the *Picard number*. The signature of the Picard lattice is $(1, \rho - 1)$ whenever it admits an embedding into a projective space. A sublattice $L'$ of a lattice $L$ is said to be *primitive* if the quotient group $L/L'$ is torsion-free. A lattice $L'$ is said to be *primitively embedded* into a lattice $L$ if it is isometric to a primitive sublattice of $L$. Notice that the Picard lattice $N$ embeds primitively into the K3 lattice $L$ via $\mathrm{Pic}(S) \hookrightarrow H^2(S, \mathbb{Z})$. A *transcendental lattice T* of the K3 surface $S$ is a lattice orthogonal to the Picard lattice.

[18] A lattice $L$ is defined as a free abelian group of finite rank together with a symmetric intersection pairing $\langle \cdot, \cdot \rangle : L \times L \to \mathbb{Z}$, which we assume to be non-degenerate. The determinant of the intersection matrix with respect to an arbitrary integer basis is called det. The signature of a lattice is $(n_+, n_-)$, where $n_\pm$ is the number of $\pm 1$ on its diagonal, and its index is $\tau(L) \equiv n_+ - n_-$. A lattice is called even if $x^2 \equiv x.x \in 2\mathbb{Z} \; \forall \; x \in L$. Otherwise, it is odd. A lattice is called unimodular (or self-dual) when its determinant is $\pm 1$. A lattice is called positive definite when $n_- = 0$ and negative definite when $n_+ = 0$. A lattice is unique if $n_\pm > 0$.

Following references [140, 141, 142], let us now introduce the notion of a building block $(Z, S)$, which allows us to construct an asymptotically cylindrical Calabi–Yau threefold $X$. Denote the inclusion $\rho : S \hookrightarrow X$ inducing the map $\rho^* : H^2(X, \mathbb{Z}) \to L$, with kernel $k := \ker \rho^*$ and image $N := \mathrm{Im}\, \rho^*$.

A *building block* $(Z, S)$ is a pair consisting of a non-singular threefold $Z$ together with a smooth K3 fiber $S = \pi^{-1}(p)$ for some point $p \in \mathbb{P}^1$ and smooth K3 fibration $\pi : Z \to \mathbb{P}^1$. The building block is required to satisfy the following conditions,

- the anti-canonical class $-K_Z \in H^2(Z, \mathbb{Z})$ is primitive and $S$ is linearly equivalent to it, i.e., $S \sim -K_Z$;
- the integral two-form cohomology $H^2(X, \mathbb{Z})$ embeds primitively into the K3 lattice $L \simeq H^2(S, \mathbb{Z})$ via the pullback map of the inclusion $\rho : S \hookrightarrow X$, which is well-defined up to homotopy;
- the inclusion $N \hookrightarrow L$ is primitive and, thus, $L/N$ is torsion-free;
- $H^3(Z, \mathbb{Z})$ is torsion-free — and thus also $H^4(Z, \mathbb{Z})$.

Due to the fibrational structure, the self-intersection of $S$ is trivial, which implies that the manifold $X = Z \setminus S$ has the topology of an asymptotically cylindrical Calabi–Yau threefold that admits a Ricci-flat Kähler metric[19]. It is in this sense that building blocks give rise to the useful asymptotically cylindrical Calabi–Yau threefolds necessary for the twisted sum construction.

Recall that the non-compact seven-dimensional manifolds $Y_{L/R}$ were defined by equation (2.33) in terms of the asymptotically cylindrical Calabi–Yau threefolds $X_{L/R}$. Notice that $Y_R \cap Y_L$ deformation retracts to $T^2 \times S$, where $T^2$ is a two-torus and $S$ is the K3 fiber. This is because $Y_R \cap Y_L \cong S^1 \times S^1 \times S \cong T^2 \times S$.

We define the standard restriction $r_{L/R} : Y_{L/R} \to Y$ and inclusion $\iota_{L/R} : T^2 \times S \hookrightarrow Y_{L/R}$. In this way, the *Mayer–Vietoris sequence* for the $n$-th de Rham cohomology applied to the union given in equation (2.34) of the overlapping non-compact seven-dimensional manifolds $Y_{L/R}$ reads

$$\cdots \to H^{n-1}(Y_L \cap Y_R) \xrightarrow{\delta} H^n(Y) \xrightarrow{r^*} H^n(Y_L) \oplus H^n(Y_R) \xrightarrow{\iota^*} H^n(Y_L \cap Y_R) \to \cdots , \tag{2.54}$$

in terms of $r^*$ and $\iota^*$ and the coboundary map $\delta : H^{n-1}(Y_L \cap Y_R) \to H^n(Y = Y_L \cup Y_R)$. Using arguments of torsion-freeness of $H^n(Y_{L/R})$, the *Künneth formula* of decomposition of $H^n(Y_{L/R})$ and of $H^n(Y_L \cap Y_R)$, and the *van Kampen theorem*, the two- and three-form cohomologies

[19] This can be understood in the following sense. The trivial normal bundle of $S$ in $X$ defines a tubular neighborhood $T_\epsilon(S) \subset X$ and, by construction, $T^*_\epsilon(S) \equiv T_\epsilon(S) \setminus S$ is homeomorphic to $\Delta^{\mathrm{cyl}} \times S$. Therefore, this has the topology of a three-dimensional Calabi–Yau cylinder $X^\infty$, which can be viewed as the asymptotic region of the asymptotically cylindrical Calabi–Yau threefold $X$ as discussed in section 2.2.1.

$H^2(Y,\mathbb{Z})$ and $H^3(Y,\mathbb{Z})$ turn out to be written as

$$\begin{aligned} H^2(Y,\mathbb{Z}) &= \ker\left(H^2(Y_L,\mathbb{Z})\oplus H^2(Y_R,\mathbb{Z}) \xrightarrow{(\iota_L^*,-\iota_R^*)} H^2(T^2\times S,\mathbb{Z})\right) , \\ H^3(Y,\mathbb{Z}) &= \ker\left(H^3(Y_L,\mathbb{Z})\oplus H^3(Y_R,\mathbb{Z}) \xrightarrow{(\iota_L^*,-\iota_R^*)} H^3(T^2\times S,\mathbb{Z})\right) \\ &\quad \oplus \operatorname{coker}\left(H^2(Y_L,\mathbb{Z})\oplus H^2(Y_R,\mathbb{Z}) \xrightarrow{(\iota_L^*,-\iota_R^*)} H^2(T^2\times S,\mathbb{Z})\right) . \end{aligned} \tag{2.55}$$

Now consider a pair of building blocks $(Z_{L/R}, S_{L/R})$ such that the K3 surfaces $S_{L/R}$ are isometric and fulfill the hyper-Kähler matching condition $r : S_L \to S_R$. From the asymptotically cylindrical Calabi–Yau threefolds $X_{L/R} = Z_{L/R} \setminus S_{L/R}$ a $G_2$-manifold $Y$ is now constructed from Kovalev's twisted connected sum construction, as detailed in section 2.2.2. The cohomology of the $G_2$-manifold $Y$ is now derived from the cohomology of the building blocks $(Z_{L/R}, S_{L/R})$ [141],

$$\begin{aligned} \pi_1(Y) &= H^1(Y,\mathbb{Z}) = 0 , \\ H^2(Y,\mathbb{Z}) &\simeq (k_L\oplus k_R)\oplus(N_L\cap N_R) , \\ H^3(Y,\mathbb{Z}) &\simeq H^3(Z_L,\mathbb{Z})\oplus H^3(Z_R,\mathbb{Z})\oplus k_L\oplus k_R\oplus N_L\cap T_R \,\oplus\, N_R\cap T_L \\ &\quad \oplus \mathbb{Z}[S]\oplus L/\left(N_L+N_R\right) . \end{aligned} \tag{2.56}$$

Here $L$ denotes the K3 lattice $L \simeq H^2(S_L,\mathbb{Z}) \simeq H^2(S_R,\mathbb{Z})$. The inclusion maps

$$\rho_{L/R} : S_{L/R} \hookrightarrow X_{L/R} \tag{2.57}$$

induce the pullback maps

$$\rho_{L/R}^* : H^2(X_{L/R},\mathbb{Z}) \to L . \tag{2.58}$$

These define the kernels and images, respectively,

$$\begin{aligned} k_{L/R} &:= \ker\rho_{L/R}^* , \\ N_{L/R} &:= \operatorname{Im}\rho_{L/R}^* , \end{aligned} \tag{2.59}$$

as well as the so-called transcendental lattices

$$T_{L/R} = N_{L/R}^{\perp} = \{l\in L \,\big|\, \langle l, N_{L/R}\rangle = 0\} . \tag{2.60}$$

Furthremore, $[S]$ is the Poincaré dual three-form of the K3 fiber $S$ in the building blocks $(Z_{L/R}, S_{L/R})$.

Note that, by the assumptions imposed on the cohomological properties of the buildings blocks, the images $N_{L/R}$ are primitive sublattices of the K3 lattice $L$. Therefore, $N_{L/R}$ inherit the structure of a lattice from the K3 lattice $L$. We also call $N_{L/R}$ by *polarizing K3 lattices*, since the K3 surfaces $S_{L/R}$ are *polarized* with respect to the complex structures of the asymptotically cylindrical Calabi–Yau threefolds $X_{L/R}$. We further assume that the sum $N_L + N_R$ embeds primitively into the K3 lattice $L$. As a consequence, the quotient $L/(N_L+N_R)$ is torsion-free, and

— due to the assumed torsion-freeness of $H^3(Z_{L/R}, \mathbb{Z})$ — all the integral cohomology groups in equation (2.56) are torsion-free as well.

We refer the reader to Theorem 4.9 in reference [141] for a very detailed proof of both equations 2.55 and 2.56.

### 2.2.5 Examples of asymptotically cylindrical Calabi–Yau threefolds

A rich class of building blocks $(Z, S)$, which give rise to asymptotically cylindrical Calabi–Yau threefolds as discussed in the previous section, is obtained from toric weak Fano threefolds $P$ [142].

Let us explain what is meant by toric weak Fano threefolds. First of all, notice that projective varieties are examples of toric varieties[20]. A smooth projective variety $P$ is *Fano* if its anti-canonical divisor is ample, i.e., $-K_P \cdot C > 0$ for any algebraic curve $C$ in $P$. A projective smooth threefold $P$ is *weak Fano* if its anti-canonical divisor $-K_P$ is nef (numerically effective) and big, which means that the intersections obey $-K_P \cdot C \geq 0$ for any algebraic curve $C$ in $P$ and $(-K_P)^3 > 0$, respectively.

Now, let us obtain a building block $(Z, S)$ from such toric weak Fano threefolds. We start by assuming that two global sections $s_0$ and $s_1$ of the anti-canonical divisor $-K_P$ of the toric weak Fano threefold $P$ intersect transversely in a smooth reduced curve $C = \{s_0 = 0\} \cap \{s_1 = 0\} \subset P$. Furthermore, let $S = \{\alpha_0 s_0 + \alpha_1 s_1 = 0\} \subset P$ be a smooth K3 surface for some choice of homogeneous coordinates $[\alpha_0 : \alpha_1] \in \mathbb{P}^1$. A building block $(Z, S)$ is obtained from the *blow-up* $\pi_C : Z \to P$ along $C$, i.e.,

$$Z = \mathrm{Bl}_C P = \left\{ (x, z) \in P \times \mathbb{P}^1 \,\middle|\, z_0 s_0 + z_1 s_1 = 0 \right\} , \tag{2.61}$$

together with the proper transform $S$ of the smooth anti-canonical divisor $S$ on $P$ [142]. For ease of notation, in the following we use the same $S$ for both the K3 surface in the toric weak Fano threefold $P$ and its proper transform in the blow-up $Z$. The K3 fibration $\pi : Z \to \mathbb{P}^1$ becomes

$$\pi : Z \to \mathbb{P}^1, \, (x, z) \mapsto z \, , \tag{2.62}$$

and $S = \pi^{-1}([\alpha_0, \alpha_1])$ is the K3 surface of the building block $(Z, S)$.

Denoting by $g(C)$ the genus of the curve $C$, the three-form Betti number $b_3(Z)$ of the blown-up threefold $Z$ from this description is given by

$$b_3(Z) = b_3(P) + 2g(C) = b_3(P) + (-K_P)^3 + 2 \, , \tag{2.63}$$

where in the last equality we use the *adjunction formula*

$$g(C) = \frac{1}{2} C \cdot C + 1 \, . \tag{2.64}$$

As remarked several times, it is essential to find a pair of asymptotically cylindrical Calabi–Yau threefolds fulfilling the matching condition given by equation (2.27) in order to build

[20] We refer the reader to references [209, 210] for an extended account on toric varieties.

twisted connected sum $G_2$-manifolds.

A common strategy is to first focus only on the moduli spaces of the polarized $K3$ surfaces $S_{L/R}$ and ignore their origin from the building blocks $(Z_{L/R}, S_{L/R})$ [141, 142, 211]. Once a matching pair of polarized $K3$ surfaces $S_{L/R}$ is found, we check if these particular $K3$ surfaces $S_{L/R}$ arise as zero sections of anti-canonical divisors in $Z_{L/R}$. A theorem due to Beauville [212] guarantees that, indeed, any general $K3$ surface polarized by the anti-canonical divisor of a Fano threefold can be realized as the zero locus of a global anti-canonical section for a suitable choice of the Fano threefold in its moduli space. Therefore it suffices to construct a matching pair of polarized $K3$ surfaces $S_{L/R}$ to ensure the existence of a pair of matching building blocks $(Z_{L/R}, S_{L/R})$ obtained from Fano threefolds in their moduli spaces.

For building blocks $(Z_{L/R}, S_{L/R})$ obtained from weak Fano threefolds, this procedure of simply matching their polarized $K3$ surfaces $S_{L/R}$ may not be sufficient. In other words, in the more general setting of building blocks from weak Fano threefolds, rather than from Fano threefolds, the entire moduli space of the polarized $K3$ surfaces cannot necessarily be obtained from a global anti-canonical section within the associated family of weak Fano threefolds. Therefore, Corti *et al* introduce the notion of *semi-Fano threefolds*. These comprise a subclass of weak Fano threefolds for which Beauville's theorem is still applicable [141, 142]. We are not interested in the rather technical definition of generic semi-Fano threefolds — which is given in definition 6.14 of reference [141] or, alternatively, in definition 4.11 of reference [142] — but we are interested only in the toric setup of semi-Fano threefolds.

We present the details of the toric setup for general Fano threefolds. First of all, let us define the notion of reflexive polyhedra. Let $\Gamma \cong \mathbb{Z}$ be a lattice, $\Gamma^*$ its dual lattice, and $\Gamma_{\mathbb{R}} = \mathbb{R} \otimes \Gamma$ its extension. A pairing is given by

$$\langle \cdot, \cdot \rangle : \Gamma \times \Gamma^* \to \mathbb{Z} \,. \tag{2.65}$$

A $d$-dimensional lattice polyhedron $\Delta_d$ is given as the bounded polyhedron or the convex hull of points $\{v^{(i)}\} \in \Gamma$ such that the origin is contained in this set of points and this set spans $\Gamma_{\mathbb{R}}$. The dual polyhedron $\Delta_d^*$ is defined by

$$\Delta_d^* = \{y \in \Gamma_{\mathbb{R}}^* | \langle y, x \rangle \geq -1, \forall x \in \Delta_d\} \,. \tag{2.66}$$

We call a pair of polyhedra $(\Delta_d, \Delta_d^*)$ *reflexive* if both are lattice polyhedra.

Toric Fano threefolds $P_\Sigma$ are described in terms of a three-dimensional toric fan $\Sigma$. On its turn, the toric fan $\Sigma$ of a toric Fano threefold $P_\Sigma$ is described in terms of a three-dimensional reflexive lattice polyhedron $\Delta$ spanned by the one-dimensional cones of $\Sigma$ — which are identified with divisors $D_i$— together with a triangulation encoding the higher-dimensional cones of the fan $\Sigma$. Due to the work of Batyrev [213] and the classification of Kreuzer and Skarke [214, 215], there are 4319 three-dimensional reflexive polyhedra, which often admit several triangulations, typically of the order of ten to a few hundred. To give the reader an idea for the toric setup, we show in figure 2.2 the sixteen reflexive polyhedra in two dimensions.

We now focus on the class of toric semi-Fano threefolds $P_\Sigma$ in order to follow the outlined recipe to construct explicit matching pairs for twisted connected sum $G_2$-manifolds. They are characterized by those three-dimensional reflexive polyhedra $\Delta_3$ that do not have any interior points inside codimension one faces. Therefore, there are now 'only' 899 three-dimensional

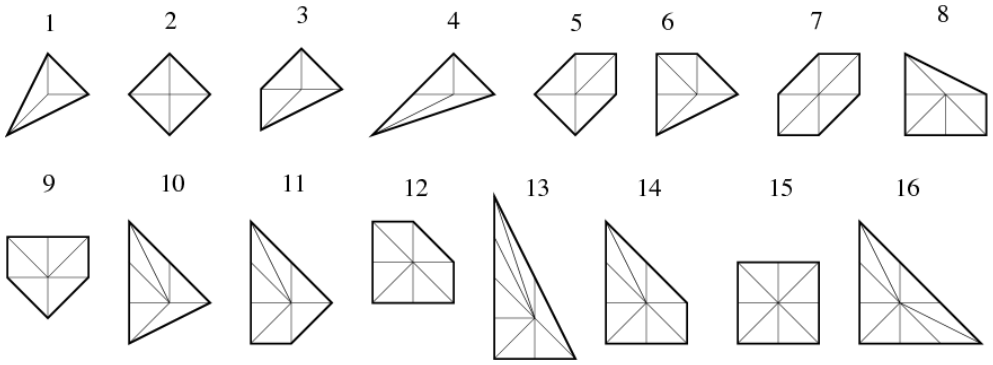


Figure 2.2: The sixteen reflexive polyhedra in the two-dimensional case, which build eleven dual pairs $(\Delta_2, \Delta_2^*)$. Polyhedron $n$ is dual to polyhedron $17 - n$ for $n = 1, \ldots, 5$ and polyhedra $n = 6, \ldots, 11$ are self-dual. Figure from reference [216].

reflexive polyhedra of the semi-Fano type [142]. For brevity, we call $\Delta_3 \equiv \Delta$ as the relevant toric semi-Fanos in this thesis are always threefolds.

The toric approach to semi-Fano threefolds provides a powerful combinatorial machinery to explicitly carry out computations. For instance, a general global section $s_\Delta$ of the anti-canonical line bundle $-K_{P_\Sigma}$ is readily described by

$$s_\Delta = \sum_{\nu^{(i)} \in \Delta} s_i \prod_{\nu^{*(j)} \in \Delta^*} x_j^{\langle \nu^{(i)}, \nu^{*(j)} \rangle + 1} , \tag{2.67}$$

with the points $\nu^{(i)}$ and $\nu^{*(j)}$ of the lattice polyhedron $\Delta$ and its dual lattice polyhedron $\Delta^*$. Moreover, $x_j$ are toric homogenous coordinates — whose vanishing define the divisors $D_i$ such that the anti-canonical divisor is $-K_{P_\Sigma} = \sum_i D_i$ —, and $s_i$ are coordinates on the space of global anti-canonical sections. Furthermore, for the discussed three-dimensional semi-Fano lattice polyhedron, a choice of generic sections $s_0$ and $s_1$ yields a smooth reduced curve $C = \{s_0 = 0\} \cap \{s_1 = 0\} \subset P_\Sigma$. This curve has a smooth K3 surface $S = \{\alpha_0 s_0 + \alpha_1 s_1 = 0\} \subset P_\Sigma$ such that the blow-up given in equation (2.61), together with the proper transform $S$, yield in fact a well-defined building block $(Z, S)$. We refer to it as the toric semi-Fano building block $(Z, S)$. They do satisfy all the requirements from section 2.2.4 — see also [142].

### 2.2.6 The orthogonal gluing method

In order to construct explicit examples of twisted connected sum $G_2$-manifolds, Corti *et al* introduce the method of *orthogonal gluing* in reference [141]. This is a particular recipe to fulfill the matching condition — given by equation (2.27) — for a pair of asymptotically cylindrical Calabi–Yau threefolds $X_{L/R}$ obtained from suitable pairs of building blocks $(Z_{L/R}, S_{L/R})$.

In this section, we review the method of orthogonal gluing to a pair of building blocks $(Z_{L/R}, S_{L/R})$ of two semi-Fano threefolds $P_{L/R}$, which consists of the following three-step algorithm [141].

- *Construction of the orthogonal pushout lattice $W$*: First of all, choose a negative definite

lattice $R$ embedded primitively into both Picard lattices $N_{L/R}$ of the polarized K3 surfaces $S_{L/R}$. Then the *orthogonal pushout lattice* $W$ is constructed as

$$W = N_L + N_R\,, \qquad R = N_L \cap N_R\,, \tag{2.68}$$

such that

$$N_L^\perp \subset N_R\,, \qquad N_R^\perp \subset N_L\,, \tag{2.69}$$

with the orthogonal lattices (transcendental) $N_{L/R}^\perp$ defined in equation (2.60). The lattice $W$ is called the orthogonal pushout of $N_{L/R}$ with respect to $R$, and is also denoted by [141]

$$W = N_L \perp_R N_R\,. \tag{2.70}$$

Note that the pushout lattice $W$ is unique but in general does not need to exist, because the non-degenerate lattice pairing $\langle\cdot,\cdot\rangle_W : W \times W \to \mathbb{Z}$ induced from the pairings $\langle\cdot,\cdot\rangle_{N_{L/R}} : N_{L/R} \times N_{L/R} \to \mathbb{Z}$ is not necessarily well-defined. To see this, let $e_{L/R}, f_{L/R} \in N_{L/R}$ and $(e_L + e_R, f_L + f_R) \in W$. The induced pairing

$$\langle e_L + e_R, f_L + f_R\rangle_W = \langle e_L, f_L\rangle_{N_L} + \langle e_R, f_R\rangle_{N_R} \tag{2.71}$$

must be integral for any pair of lattice points $(e_L + e_R, f_L + f_R) \in W$. Therefore, since $(e_L + e_R, f_L + f_R) \in W$ is not necessarily uniquely represented by $e_{L/R}, f_{L/R} \in N_{L/R}$, the non-degenerate lattice pairing $\langle\cdot,\cdot\rangle_W$ may not be well-defined.

Furthermore, we also require that the constructed orthogonal pushout lattice $W$ has non-empty intersections $W_{L/R} = N_{L/R} \cap T_{R/L}$ with the (generic) *Kähler cones*[21] $\mathcal{K}(P_{L/R})$ of (deformation families of) $P_{L/R}$, i.e.,

$$\mathcal{K}(P_{L/R}) \cap W_{L/R} \neq \emptyset\,. \tag{2.72}$$

- *Construction of primitive embedding of pushout lattice $W$ into the K3 lattice $L$*: The existence of such an embedding can be deduced from results by Nikulin [218]. In particular, such a primitive embedding is guaranteed to exist if the following rank condition is fulfilled [141],

  $$\operatorname{rk} N_L + \operatorname{rk} N_R \;\leq\; 11\,. \tag{2.73}$$

  The existence of this primitive embedding is necessary to achieve the matching condition for a suitable pair of polarized K3 surfaces $S_{L/R}$ in their moduli spaces.

- *Lift matching condition for K3 surfaces $S_{L/R}$ to building blocks $(Z_{L/R}, S_{L/R})$*: Finally, we must ensure that the matching condition for the polarized K3 surfaces $S_{L/R}$ can be lifted to the moduli space of the building blocks $(Z_{L/R}, S_{L/R})$.

  This is indeed the case, as has been shown in proposition 6.18 by Corti *et al* [141]. The imposed assumptions on the orthogonal pushout $W$ — namely that $(Z_{L/R}, S_{L/R})$ are building

[21] For a compact Kähler manifold $M$, the Kähler cone is the set of Kähler classes $[\omega] \in H^{1,1} \cap H^2(M, \mathbb{R})$ of the Kähler form $\omega$. For Fanos, these cones are rational polyhedral, i.e., there is a matrix $A$ such that the cone is spanned by a finite number of rays $C = \{x \in \mathbb{R}^n | Ax \geq 0\}$ [217].

blocks of semi-Fano threefolds, that the lattice $R$ is negative definite, that the intersections (2.72) are non-empty, and that $W$ embeds primitively into the K3 lattice $L$ — are sufficient to ensure that the matching condition of the polarized K3 surfaces $S_{L/R}$, given by equation (2.27), can indeed be lifted to the moduli spaces of the building blocks $(Z_{L/R}, S_{L/R})$.

We now determine the Betti numbers from the cohomology groups given in equation (2.56) of the $G_2$-manifolds $Y$ with the use of the orthogonal gluing method. First of all, we observe that $\mathrm{rk}\, N_L \cap T_R = \mathrm{rk}\, W_L$ and $\mathrm{rk}\, N_R \cap T_L = \mathrm{rk}\, W_R$. Furthermore, $N_L + N_R$ becomes the orthogonal pushout $W$ with $\mathrm{rk}\, W = \mathrm{rk}\, W_L + \mathrm{rk}\, W_R + \mathrm{rk}\, R$. Therefore, we deduce that the Betti numbers $b_2(Y) = \dim H^2(Y)$ and $b_3(Y) = \dim H^3(Y)$ of twisted connected sum $G_2$-manifolds $Y$ from the method of orthogonal gluing are given by

$$\begin{aligned} b_2(Y) &= \mathrm{rk}\, R + \dim k_L + \dim k_R \,, \\ b_3(Y) &= b_3(Z_L) + b_3(Z_R) + \dim k_L + \dim k_R - \mathrm{rk}\, R + 23 \,. \end{aligned} \tag{2.74}$$

Here $b_3(Z_{L/R})$ are the three-form Betti numbers of the threefolds $Z_{L/R}$, and $\dim k_{L/R}$ are the dimensions of the kernels $k_{L/R}$ defined below equation (2.56).

The motivation to study this method is to algorithmically find novel twisted connected sum $G_2$-manifolds and work out the gauge theory sectors that appear in this construction from Fano and toric semi-Fano building blocks, which we perform in chapter 4 after discussing M-theory compactifications on generic $G_2$-manifolds in chapter 3.

CHAPTER 3

# Effective action from M-theory on $G_2$-manifolds

In this chapter we perform compactifications of the eleven-dimensional low-energy limit of M-theory on $G_2$-manifolds. We begin in section 3.1 by summarizing the four-dimensional effective $\mathcal{N} = 1$ supergravity massless spectrum from the Kaluza-Klein reduction. In section 3.2 we are able to bring the four-dimensional bosonic action into the conventional form of four-dimensional $\mathcal{N} = 1$ supergravity, i.e., we write a Kähler potential $K(\phi, \bar{\phi})$ and a gauge kinetic coupling function $f_{IJ}(\phi)$ for complex scalar fields $\phi$. In section 3.3 we derive the superpotential induced by internal four-form fluxes and single out the relevant fermionic term for the gravitino mass.

In section 3.4 we investigate compactifications of M-theory on twisted connected sum $G_2$-manifolds. We employ both the Kovalev limit, as well as the cohomology in terms of the building blocks of the construction to obtain the four-dimensional low-energy effective theory. The *second* and *third relevant contributions* of this thesis to the topic appear in section 3.4.2. Firstly, we identify the relevant moduli fields characterizing the effective four-dimensional $\mathcal{N} = 1$ supergravity spectrum as well as their geometrical interpretation. We use them to describe phenomenological properties of the associated Kähler potential. Secondly, we use the Kovalev limit to identify abelian gauge sectors exhibiting extended supersymmetries on the local geometries of the twisted connected sum $G_2$-manifolds. These will impose severe constraints on non-Abelian gauge sectors and charged matter fields of the effective theory, as we will see in chapter 4.

## 3.1 The Kaluza-Klein reduction on $G_2$-manifolds

The geometry of the low-energy effective action of M-theory is given by an eleven-dimensional Lorentz manifold $M^{1,10}$ together with a four-form flux $G$ of an anti-symmetric three-form tensor field $\hat{C}$. Firstly, due to fermionic degrees of freedom in M-theory, the Lorentz manifold $M^{1,10}$ must be spin. This condition implies that the first Pontryagin class $p_1(M^{1,10})$ must be divisible

by two, i.e.,

$$\lambda = \frac{p_1(M^{1,10})}{2} \,. \tag{3.1}$$

Notice that the class $\lambda$ is integral since the first Pontryagin class $p_1$ is even for seven-dimensional spin manifolds.

Secondly, consistency of the effective action at one-loop, imposes the cohomological flux quantization condition [219]

$$\frac{G}{2\pi} - \frac{\lambda}{2} \in H^4(M^{1,10}, \mathbb{Z}) \,. \tag{3.2}$$

For compactifications of the low-energy eleven-dimensional $\mathcal{N} = 1$ supergravity limit of M-theory on smooth $G_2$-manifolds to four-dimensional Minkowski space $\mathbb{R}^{1,3}$ with $\mathcal{N} = 1$ supersymmetry, we consider the following *Ansatz* for the eleven-dimensional Lorentz manifold $M^{1,10}$

$$M^{1,10} = \mathbb{R}^{1,3} \times Y \,. \tag{3.3}$$

Here $Y$ is the seven-dimensional compact smooth manifold. In the absence of background fluxes, such a four-dimensional $\mathcal{N} = 1$ Minkowski vacuum implies that the compact internal space $Y$ must be a $G_2$-manifold [132, 220, 221].

Eleven-dimensional $\mathcal{N} = 1$ supergravity compactified[1] on a seven-dimensional manifold $Y$ without four-form background fluxes to four-dimensional supergravity has been first discussed in reference [132]. The structure of the massless four-dimensional $\mathcal{N} = 1$ multiplets that arise from such compactification possesses $b_2(Y)$ abelian U(1) vector fields and $b_3(Y)$ neutral chiral fields $\Phi^i$ [220, 221]. The inclusion of background fluxes $G$, generating a superpotential $W$ for the neutral chiral fields $\Phi^i$, thereby generically breaks supersymmetry [134, 135].

We now review the *Kaluza-Klein reduction* of eleven-dimensional $\mathcal{N} = 1$ supergravity, which furnishes the low-energy effective description of M-theory. The massless spectrum of this maximally supersymmetric supergravity theory is very simple and consists only of the eleven-dimensional gravity multiplet. Its bosonic massless field content is given by the eleven-dimensional spacetime metric tensor $\hat{g}_{MN}$, the three-form tensor $\hat{C}_{[MNP]}$, whereas the fermionic massless field content is given by the eleven-dimensional gravitino $\hat{\Psi}^{\alpha}_{M}$, where upper-case latin letters are used for eleven-dimensional indices ($M, N = 0, \ldots, 10$). The degrees of freedom of the massless component fields in the gravity multiplet transform in the following irreducible representations of the little group SO(9):

- The metric $\hat{g}_{MN}$ in the traceless symmetric representation **44**.
- The three-form $\hat{C}_{[MNP]}$ in the anti-symmetric three-tensor representation **84**.
- The gravitino $\hat{\Psi}^{\alpha}_{M}$ in the spinorial representation $\mathbf{128}_s$.

[1] A possible warp factor in this compactification has been considered in reference [133], where it was shown that the warping breaks four-dimensional $\mathcal{N} = 1$ supersymmetry. While these authors give the criteria for the compactification manifold $Y$ to yield four-dimensional $\mathcal{N} = 1$ supergravity, they do not refer to the $G_2$-manifolds in Berger's classification of special holonomy manifolds [96], likely because compact examples of $G_2$-manifolds were only found much later in reference [139].

Let $x^\mu$ and $y^m$ furnish (local) coordinates of the four-dimensional Minkowski space $\mathbb{R}^{1,3}$ with the flat spacetime metric $\eta_{\mu\nu}$ and the seven-dimensional $G_2$-manifold $Y$ with the Ricci-flat Riemannian metric $g_{mn}$, respectively. The notation is such that we use lower-case latin letters for seven-dimensional indices ($m, n = 4, \ldots, 7$), and greek letters for four-dimensional indices ($\mu, \nu = 0, \ldots, 4$). With the use of the compactification *Ansatz* (3.3), to solve Einstein's equations in the absence of background fluxes, we consider the block diagonal metric[2]

$$\hat{g}(x, y) = \eta_{\mu\nu} dx^\mu dx^\nu + g_{mn}(y) dy^m dy^n \,, \tag{3.4}$$

**The dimensional reduction of the metric $\hat{g}_{MN}$**

The first task is to deduce the massless spectrum of the effective four-dimensional low-energy theory. We start with the gravitational degrees of freedom, which infinitesimally describe the fluctuations of the metric background (3.4), i.e., $\hat{g} \to \hat{g} + \delta\hat{g}$. Firstly, we obtain the four-dimensional metric fluctuations $\delta g_{\mu\nu}$, which correspond to the gravitational degrees of the four-dimensional low-energy effective theory. Secondly, since the fundamental group of $G_2$-manifolds is finite, there are no massless gravitational Kaluza–Klein vectors. Finally, we determine the gravitational Kaluza–Klein scalars $S^i$, which furnish coordinates on the moduli space $\mathcal{M}$ of $G_2$-metrics. At a given point $S^i$ in the moduli space, we fix a reference metric and consider its infinitesimal deformation under $\delta S^i$, i.e.,

$$g_{mn}(S^i) dy^m dy^n \to g_{mn}(S^i) dy^m dy^n + \sum_i \delta S^i \rho^{\text{sym}}_{i,(mn)}(S^i) dy^m dy^n \,. \tag{3.5}$$

By solving Einstein's equations to linear order in the *symmetric metric fluctuations* $\rho^{\text{sym}}_{i,(mn)}$, we obtain

$$\text{Ric}\left(g + \sum \delta S^i \rho^{\text{sym}}_i\right) = 0 \quad \Rightarrow \quad \Delta_L \rho^{\text{sym}}_i = 0 \,, \tag{3.6}$$

where $\Delta_L$ is the Lichnerowicz Laplacian for the symmetric tensor fields. Notice that we can use the $G_2$-structure $\varphi$ on $Y$ to construct the anti-symmetric three-form tensors as

$$\rho^{(3)}_{i,[mnp]} = g^{rs} \rho^{\text{sym}}_{i,r[m} \varphi_{np]s} \,. \tag{3.7}$$

On $G_2$-manifolds, the symmetric tensor $\rho^{\text{sym}}_i$ is a zero mode of the Lichnerowicz Laplacian operator if and only if the above constructed three-form $\rho^{(3)}_i$ is harmonic [222], namely

$$\Delta_L \rho^{\text{sym}}_i = 0 \quad \Leftrightarrow \quad \Delta \rho^{(3)}_i = 0 \,. \tag{3.8}$$

Therefore, the massless gravitational Kaluza–Klein scalars $S^i$ arise from harmonic three-forms $\rho^{(3)}_i$, which represent a basis for the vector space $H^3(Y)$ of dimension $b_3(Y)$. According to condition (iv) in proposition 2.1, the harmonic three-forms $\rho^{(3)}_i$ are the first order deformations

[2] In the presence of background fluxes in the internal space $Y$, the ansatz for the metric is generalized to a warped product $\hat{g}(x, y) = e^{2A(y)} \eta_{\mu\nu} dx^\mu dx^\nu + e^{-2A(y)} g_{mn} dy^m dy^n$ in terms of the function $A(y)$ on $Y$ called the warped factor [133, 134].

to the torsion-free $G_2$-structure

$$\varphi(S^i) \to \varphi(S^i) + \sum_i \delta S^i \rho_i^{(3)}(S) \,. \tag{3.9}$$

Furthermore, since $Y$ has holonomy group $G_2$ and not a subgroup thereof, recall from section 2.1.3 that, at a given point $S^i$ in moduli space, the harmonic three-forms $\rho_i^{(3)}$ of $Y$ will then fall into representations of the structure group $G_2$, and $H^3(Y)$ splits as [139]

$$H^3(Y) = H^3_{\mathbf{1}}(Y) \oplus H^3_{\mathbf{27}}(Y) \,, \quad \dim H^3_{\mathbf{1}}(Y) = 1 \,, \quad \dim H^3_{\mathbf{27}}(y) = b_3(Y) - 1 \,. \tag{3.10}$$

The harmonic torsion-free $G_2$-structure $\varphi$ corresponds to the unique singlet, and the associated deformation simply rescales the volume of the $G_2$-manifold $Y$. The remaining harmonic forms in the representation **27** infinitesimally deform the torsion-free $G_2$-structure such that the volume of $Y$ remains constant at first order approximation. Analogously, the symmetric tensors $\rho_i^{\text{sym}}$ solving the Lichnerowicz Laplacian $\Delta_L$ split into a unique singlet — given by the metric tensor $g$ — and $b_3(Y) - 1$ traceless symmetric tensors in the representation **27** of the $G_2$-structure group.

We have seen that the infinitesimal deformations to the torsion-free $G_2$-structure $\varphi$ can be identified with harmonic three-forms. According to theorem 4.1 in section 2.1.4, these infinitesimal deformations are actually unobstructed to all orders. In other words, the vicinity $U_{\varphi(S^i)} \subset \mathcal{M}$ of a given torsion-free $G_2$-structure $\varphi(S^i) \in \mathcal{M}$ — at a given point $S^i$, $i = 1, \ldots, b_3(Y)$, in the moduli space — is locally diffeomorphic to the de Rham cohomology $H^3(Y)$,[3] i.e.,

$$\mathcal{P}_{\varphi(S^i)} : U_{\varphi(S^i)} \subset \mathcal{M} \to H^3(Y) \,, \; \varphi \mapsto [\varphi] \,. \tag{3.11}$$

Hence, the Betti number $b_3(Y)$ is indeed the dimension of $\mathcal{M}$, and the scalar fields $S^i$ furnish local coordinates on $\mathcal{M}$ with infinitesimal deformations $\delta S^i$ spanning the tangent space $T_{S^i}\mathcal{M}$. This local structure implies that the massless infinitesimally metric deformations $\rho_i^{\text{sym}}$ — or alternatively the first order deformations $\rho_i^{(3)}$ to the torsion-free $G_2$-structure — extend order-by-order to unobstructed finite deformations, which therefore describe locally the moduli space $\mathcal{M}$ of $G_2$-manifolds. While the harmonic three-forms $\rho_i^{(3)}$ themselves depend (non-linearly) on the moduli space coordinates $S^i$, we can – due to equation (3.11) – locally expand the cohomology class $[\varphi]$ of the torsion-free $G_2$-structure $\varphi$ as

$$[\varphi(S^i)] \;=\; \sum_i S^i \, [\rho_i^{(3)}] \,, \tag{3.12}$$

which is a useful local description of the moduli space of $Y$.[4]

[3] We assume that the scalars $S^i$ describe a generic point in $\mathcal{M}$. First of all, the associated $G_2$-manifold $Y$ should be smooth. Furthermore, it should not be a special symmetric point corresponding to an orbifold singularity in $\mathcal{M}$.

[4] Note, however, that a given cohomology class $[\varphi(S^i)]$ is not necessarily represented by a unique torsion-free $G_2$-structure $\varphi(S^i)$. Recall from section 2.1.4 that, mathematically, not much is known about the global structure of the moduli space $\mathcal{M}$ and, in particular, about the global map $\mathcal{P} : \mathcal{M} \to H^3(Y)$.

### The dimensional reduction of the three-form $\hat{C}_{[MNP]}$

We now move on to determine the massless four-dimensional modes arising from the coefficients in the decomposition of the eleven-dimensional anti-symmetric three-form tensor $\hat{C}$ as

$$\hat{C}(x,y) \;=\; \sum_I A^I(x) \wedge \omega_I^{(2)}(y) + \sum_i P^i(x) \wedge \rho_i^{(3)}(y)\,. \tag{3.13}$$

Here $\omega_I^{(2)}$ are harmonic two-forms and $\rho_i^{(3)}$ are three-forms $\rho_i^{(3)}$, identified with non-trivial cohomology representatives of $H^2(Y)$ and $H^3(Y)$ of dimension $b_2(Y)$ and $b_3(Y)$, respectively. Since there are no dynamical degrees of freedom in four-dimensional anti-symmetric three-form tensor fields, and due to the absence of harmonic one-forms on the internal $G_2$-manifolds since $b_1(Y) = 0$, the four-dimensional vectors $A^I$, $I = 1, \ldots, b_2(Y)$, and the four-dimensional scalars $P^i$, $i = 1, \ldots, b_3(Y)$, are the only massless modes obtained from the dimensional reduction of the eleven-dimensional anti-symmetric three-form tensor field $\hat{C}$.

### The dimensional reduction of the gravitino $\hat{\Psi}^{\alpha}_{M}$

Let us now turn to the dimensional reduction of the eleven-dimensional gravitino $\hat{\Psi}$, which geometrically is a section of $T^*M^{1,10} \otimes S\,M^{1,10}$, where $S\,M^{1,10}$ denotes a spin bundle of $M^{1,10}$. Upon dimensional reduction, we will show that the gravitino $\hat{\Psi}$ enjoys the expansion

$$\hat{\Psi}(x,y) \;=\; \left(\psi_\mu(x)dx^\mu + \psi_\mu^*(x)dx^\mu\right)\zeta(y) + \left(\chi(x) + \chi^*(x)\right)\zeta_n^{(1)}(y)dy^n\,. \tag{3.14}$$

Here $(\psi_\mu, \psi_\mu^*)$ and $(\chi, \chi^*)$ are four-dimensional Rarita-Schwinger and four-dimensional spinor fields of both chiralities in $\mathbb{R}^{1,3}$.[5] Furthermore, $\zeta$ is a section of the (real) spin bundle $S\,Y$ of the compact $G_2$-manifold[6] $Y$ whereas $\zeta^{(1)}$ is a section of the (real) Rarita–Schwinger bundle $T^*Y \otimes S\,Y$, which locally takes the form $\theta^{(1)} \otimes \tilde{\zeta}$ in terms of the local one-form $\theta^{(1)}$ and the spinorial section $\tilde{\zeta}$. Let us see how this expansion is justified.

The massless four-dimensional fermionic spectrum must arise from the zero modes of the seven-dimensional Dirac operator $\not{D}$ and Rarita-Schwinger operator $\not{D}^{\mathrm{RS}}$, i.e,

$$\not{D}\zeta \;=\; 0\,, \qquad \not{D}^{\mathrm{RS}}\zeta^{(1)} \;=\; 0\,. \tag{3.15}$$

First of all, due to the existence of a covariantly constant (Majorana) spinor $\eta$ on $S\,Y$, the Rarita-Schwinger bundle $T^*Y \otimes S\,Y$ on the $G_2$-manifold $Y$ becomes reducible, namely

$$T^*Y \otimes S\,Y \cong T^*Y \otimes (T^*Y \oplus \mathbb{R})\,. \tag{3.16}$$

[5] In our conventions the fermionic fields $\psi_\mu, \chi$ and $\psi_\mu^*, \chi^*$ are chiral and anti-chiral, respectively, such that $\psi_\mu + \psi_\mu^*$ and $\chi + \chi^*$ become Majorana fermions.

[6] As the $G_2$-structure group of $Y$ — a subgroup of SO(7) — is simply connected, it defines a canonical spin structure on $Y$.

Accordingly, the section $\zeta$ decomposes as

$$\zeta = \sum_m a_m(y)\gamma^m\eta + b(y)\eta \,. \tag{3.17}$$

Here $\gamma^m$ are seven-dimensional gamma matrices. For definitions and useful relations among higher dimensional gamma matrices appearing in this chapter, we refer the reader to appendix A.

With this decomposition, we arrive at the following equation for the zero modes

$$\not{D}\zeta \;=\; (\nabla_n a_m)\gamma^n\gamma^m\eta + (\partial_n b)\gamma^n\eta \;=\; \nabla_{[n}a_{m]}\gamma^{nm}\eta + (\nabla^n a_n)\eta + (\partial_n b)\gamma^n\eta \;=\; 0 \,. \tag{3.18}$$

Due to the linear independence of $\eta$, $\gamma^n\eta$, and $\gamma^{nm}\eta$, this yields, for the coefficient one-form $a(y) = a_n(y)dy^n$ and the function $b(y)$, together with equations (3.27)

$$da(y) \;=\; 0 \,, \qquad d^\dagger a(y) \;=\; 0 \,, \qquad db(y) \;=\; 0 \,. \tag{3.19}$$

The first two equations imply that $a(y)$ must be a harmonic one-form, whereas the last equation determines the function $b(y)$ to be constant. As there are no harmonic one-forms on the $G_2$-manifold $Y$ because $b_1(Y) = 0$, the covariantly constant spinor $\eta$ furnishes the only zero mode in the spin bundle $SY$. Therefore, this zero mode gives rise to the massless four-dimensional gravitino field $\psi_\mu$ and its conjugate $\psi_\mu^*$ of the four-dimensional massless $\mathcal{N} = 1$ gravity multiplet as given in expansion (3.14), and we list them in table 3.1.

Furthermore, (3.16) allows us to make the following identification

$$\begin{aligned} T^*Y \otimes SY &\cong T^*Y \otimes (T^*Y \oplus \mathbb{R}) \\ &= (T^*Y \otimes T^*Y) \oplus T^*Y \\ &= \mathrm{Sym}^2(T^*Y) \oplus \Lambda^2 T^*Y \oplus T^*Y \,, \end{aligned} \tag{3.20}$$

where $\mathrm{Sym}^2(T^*Y)$ is the space of symmetric two-tensors on $Y$ and $\Lambda^2 T^*Y$ is the space of two-forms. It is known that $\mathrm{Sym}^2(T^*Y) \cong \Lambda^3_{\mathbf{1}} \oplus \Lambda^3_{\mathbf{27}}$ [223]. Since the spaces $\Lambda^2_{\mathbf{7}}$ and $\Lambda^3_{\mathbf{7}}$ are isomorphic to the cotangent bundle $\Lambda^1_{\mathbf{7}}$ — recall equation (2.6) and text below it —, we arrive at

$$T^*Y \otimes SY \cong \Lambda^3_{\mathbf{1}} \oplus \Lambda^3_{\mathbf{27}} \oplus \Lambda^2_{\mathbf{14}} \oplus \Lambda^1_{\mathbf{7}} \,. \tag{3.21}$$

Therefore, this decomposition of the Rarita-Schwinger $G_2$-bundle justifies the following *Ansatz* for the global Rarita-Schwinger section $\zeta^{(1)}$,

$$\zeta^{(1)} \;=\; \sum_{n,m} a^{28}_{(nm)}(y)dy^n \otimes \gamma^m\eta + \sum_{n,m} a^{14}_{[nm]}(y)dy^n \otimes \gamma^m\eta + \sum_n b^7_n(y)dy^n \otimes \eta \,. \tag{3.22}$$

The superscripts in the symmetric tensor $a^{28}_{(nm)}(y)$, the anti-symmetric tensor $a^{14}_{[nm]}(y)$, and the vector $b^7_n(y)$ indicate the dimension of their respective representations with respect to the structure group $G_2$. While the anti-symmetric tensor $a^{14}_{[nm]}(y)$ and the vector $b^7_n(y)$ transform in the irreducible representations **14** and **7**, the symmetric tensor $a^{28}_{(nm)}(y)$ further decomposes into the trace and the traceless symmetric part, which respectively correspond to the irreducible

representations **1** and **27**.

Following conventions given in reference [138], the $G_2$-structure $\varphi$ fulfills the following contraction relations

$$\varphi_{mnp}\varphi^{npq} \;=\; 6\,\delta_n^q\,, \qquad \varphi_{mnp}\varphi^{pqr} \;=\; \Phi_{mn}{}^{qr} + \delta_m^q\delta_n^r - \delta_m^r\delta_n^q\,, \tag{3.23}$$

with the Hodge dual form $\Phi = *\varphi$, and the Fierz identity

$$\gamma^{mn}\eta \;=\; -i\varphi^{mnp}\gamma_p\eta\,. \tag{3.24}$$

By acting with the Rarita–Schwinger operator $\not{D}^{\mathrm{RS}}$ on the *Ansatz* (3.22) for $\zeta^{(1)}$, and using equations (3.23), (3.24) and (A.7), we arrive at

$$\begin{aligned}\not{D}^{\mathrm{RS}}\zeta^{(1)} \;=\; &(\nabla_{[n}b^7_{m]})\gamma^{mnp}dy_p\otimes\eta - \left(\nabla^n a^{14}_{nm}\right)dy^m\otimes\eta + \frac{3}{2}\left(\nabla_{[n}a^{14}_{pq]}\right)\gamma^{mnpq}dy_m\otimes\eta\\ &- \frac{3i}{2}\left(\nabla^n a^{28}_{npq}\right)dy^p\otimes\gamma^q\eta + \frac{i}{3}\left(\nabla_{[m}a^{28}_{npq]}\right)\gamma^{mnpqr}dy_r\otimes\eta\\ &- \frac{1}{2}\partial_p(\mathrm{tr}_g\, a^{28}_{(mn)})dy_q\otimes\gamma^{pq}\eta\,,\end{aligned} \tag{3.25}$$

in terms of the three-form $a_{[nmp]}$ and the singlet $\mathrm{tr}_g\, a^{28}_{(mn)} = a^{28}_{nm}g^{nm}$

$$a^{28}_{[mnp]} \;=\; g^{rs}a^{28}_{r[m}\varphi_{np]s}\,, \qquad a^{28}_{(nm)} \;=\; \frac{3}{4}a^{28}_{[npq]}\varphi^{pqr}g_{rm} - \frac{1}{12}g_{nm}a^{28}_{[pqr]}\varphi^{pqr}\,. \tag{3.26}$$

Let us now analyze the zero modes of the Rarita–Schwinger section $\zeta^{(1)}$ from equation (3.25). The one-form $b(y) = b_n(y)dy^n$ does not contribute any zero modes as we have already seen and, due to equations (3.27), such a zero mode must be a closed one-form $db(y) = 0$. Furthermore, due to $b_1(Y) = 0$ it also must be exact $b(y) = df(y)$. However, an exact one-form $df(y)$ furnishes no physical degrees of freedom as it can be removed by a gauge transformation of the Rarita–Schwinger section, i.e., $\zeta^{(1)} \to \zeta^{(1)} - \nabla(f(y)\otimes\eta)$.

For any $p$-form $\alpha$, the Levi–Civita connection $\nabla$, the exterior derivative $d$ and its adjoint $d^\dagger$ fulfill the relations

$$\begin{aligned}(d\alpha)_{\mu_1\ldots\mu_{p+1}} &= (p+1)\nabla_{[\mu_1}\alpha_{\mu_2\ldots\mu_{p+1}]}\,,\\ (d^\dagger\alpha)_{\mu_1\ldots\mu_{p-1}} &= -\nabla^\nu\alpha_{\nu\mu_1\ldots\mu_{p-1}}\,.\end{aligned} \tag{3.27}$$

Therefore, for the remaining tensors we find that the zero modes of the Rarita–Schwinger operator $\not{D}^{\mathrm{RS}}$ are

$$\begin{aligned}da^{14}(y) \;&=\; 0\,, \qquad & d^\dagger a^{14}(y) \;&=\; 0\,,\\ da^{28}(y) \;&=\; 0\,, \qquad & d^\dagger a^{28}(y) \;&=\; 0\,,\end{aligned} \tag{3.28}$$

in terms of the two-form $a^{14}(y) = \frac{1}{2}a^{14}_{nm}(y)dy^n\wedge dy^m$ and the three-form $a^{28}(y) = \frac{1}{6}a^{28}_{nmp}(y)dy^n\wedge dy^m\wedge dy^p$. Thus, the zero modes are in one-to-one correspondence with harmonic two-forms $a^{14}(y)$ and three-forms $a^{28}(y)$ on the $G_2$-manifolds $Y$, where the harmonic property of $a^{28}(y)$ implies that the symmetric tensor $a^{28}_{(nm)}$ must be solutions to the Lichnerowicz Laplacian as well,

cf. equation (3.8), i.e.,

$$\Delta_L a^{28}(y) = 0\,, \qquad \Delta a^{14}(y) = 0\,. \tag{3.29}$$

The zero modes of the Lichnerowicz Laplacian on $G_2$-manifolds are again identified with harmonic three-forms according to equations (3.7) and (3.8) — with a single zero mode and $b_3(Y) - 1$ traceless symmetric zero modes transforming in the $G_2$-representations **1** and **27**, respectively. Therefore, the zero modes of the Rarita–Schwinger bundle on $Y$ are in one-to-one correspondence with non-trivial cohomology elements[7] of both $H^3(Y)$ and $H^2(Y)$. In terms of the bases of zero modes $\rho_i^{\text{sym}}$ of the Lichnerowicz Laplacian and of the harmonic two-forms $\omega_I^{(2)}$, we therefore arrive at the expansion of the four-dimensional chiral fermions given in equation (3.14)

$$\chi(x)\zeta^{(1)}(y) = \sum_{i=1}^{b_3(Y)} \chi^i(x)\rho^{\text{sym}}_{i,(nm)} dy^n \otimes \gamma^m \eta + \sum_{I=1}^{b_2(Y)} \lambda^I \omega^{(2)}_{I[nm]} dy^n \otimes \gamma^m \eta\,. \tag{3.30}$$

Now, we can spell out the massless four-dimensional spectrum in terms of $\mathcal{N} = 1$ supergravity multiplets as obtained from the dimensional reduction of M-theory on the $G_2$-manifolds $Y$. It consists of the four-dimensional supergravity multiplet, $b_3(Y)$ (neutral) chiral multiplets $\Phi^i$, and $b_2(Y)$ (Abelian) vector multiplets $V^I$, as summarized in detail in table 3.1.

| Multiplicity | Massless 4d component fields | | Massless 4d |
|---|---|---|---|
| | bosonic fields | fermionic fields | $\mathcal{N} = 1$ multiplets |
| 1 | metric $g_{\mu\nu}$ | gravitino $\psi_\mu, \psi_\mu^*$ | gravity multiplet |
| $i = 1, \ldots, b_3(Y)$ | scalars $(S^i, P^i)$ | spinors $\chi^i, \chi^{*i}$ | chiral multiplets $\Phi^i$ |
| $I = 1, \ldots, b_2(Y)$ | vectors $A_\mu^I$ | gauginos $\lambda_\alpha^I$ | vector multiplets $V^I$ |

Table 3.1: The massless four-dimensional low-energy effective $\mathcal{N} = 1$ supergravity spectrum obtained from the dimensional reduction of M-theory — or rather of eleven-dimensional supergravity — on a smooth $G_2$-manifold $Y$.

In order to specify the four-dimensional low-energy effective $\mathcal{N} = 1$ supergravity action for the determined spectrum of the massless fields, we must insert the mode expansions for the metric (3.5), the anti-symmetric three-form tensor (3.13), and the gravitino (3.14) into the eleven-dimensional supergravity action [70]. This action, in terms of the eleven-dimensional

[7] A priori, the constructed zero modes furnish elements of $H^3_{\mathbf{1}}(Y)$, $H^3_{\mathbf{27}}(Y)$ and $H^2_{\mathbf{14}}(Y)$ that transform in the specified representations of the $G_2$-structure group. However, on $G_2$-manifolds all non-trivial three- and two-form cohomology elements can respectively be represented in the representations **1**, **27**, and **14**, which justifies the identification of zero modes with $H^3(Y)$ and $H^2(Y)$ [139].

Hodge star $*_{11}$ and the eleven-dimensional gamma matrices $\hat{\Gamma}^M$, reads

$$\begin{aligned} S_{11\mathrm{d}} \;=\; \frac{1}{2\kappa_{11}^2}\int\Big(*_{11}\hat{R}_S - \frac{1}{2}d\hat{C}\wedge *_{11}d\hat{C} - *_{11}i\,\bar{\hat{\Psi}}_M\hat{\Gamma}^{MNP}\hat{D}_N\hat{\Psi}_P\Big) \\ - \frac{1}{192\kappa_{11}^2}\int *_{11}\bar{\hat{\Psi}}_M\hat{\Gamma}^{MNPQRS}\hat{\Psi}_N(d\hat{C})_{[PQRS]} - \frac{1}{2\kappa_{11}^2}\int d\hat{C}\wedge *_{11}\hat{F} \\ - \frac{1}{12\kappa_{11}^2}\int d\hat{C}\wedge d\hat{C}\wedge\hat{C} + \dots\,. \end{aligned} \tag{3.31}$$

Here we denote $\hat{F}_{[MNPQ]} = 3\bar{\hat{\Psi}}_{[M}\hat{\Gamma}_{NP}\hat{\Psi}_{Q]}$. The first line contains the kinetic terms of the eleven-dimensional supergravity multiplet, i.e., the Einstein–Hilbert term in terms of the Ricci scalar $\hat{R}_S$, the kinetic term for the anti-symmetric three-form tensor $\hat{C}$, and the Rarita–Schwinger kinetic term for the gravitino $\hat{\Psi}$. The second line comprises the interaction terms. The third line is the Chern–Simons term of the eleven-dimensional supergravity action since it contains the Chern Simons three-form in eleven dimensions and is only topological. There are additional four-fermion interactions denoted by '…' [70]. The coupling constant $\kappa_{11}$ relates to the eleven-dimensional Newton constant $\hat{G}_N$, the eleven-dimensional Planck length $\hat{\ell}_P$ and Planck mass $\hat{M}_P$ according to

$$\kappa_{11}^2 \;=\; 8\pi\hat{G}_N \;=\; \frac{(2\pi)^8\,\hat{\ell}_P^9}{2} \;=\; \frac{(2\pi)^8}{2\,\hat{M}_P^9}\,. \tag{3.32}$$

To perform the Kaluza–Klein reduction we introduce the moduli-dependent volume $V_Y(S^i)$ of the $G_2$-manifold $Y$

$$V_Y(S^i) \;=\; \int_Y d^7y\,\sqrt{\det g(S^i)_{mn}}\,. \tag{3.33}$$

Furthermore, we introduce a reference $G_2$-manifold $Y_0$ with respect to some background expectation values $S^i_0 = \langle S^i\rangle$, upon which we carry out the dimensional reduction. This allows us to introduce the dimensionless (but yet moduli-dependent) volume factor

$$\lambda_0(S^i) \;=\; \frac{V_Y(S^i)}{V_{Y_0}} \;=\; \frac{1}{7}\int_Y \varphi\wedge *_{g_\varphi}\varphi\,, \tag{3.34}$$

in terms of the reference volume $V_{Y_0} = V_Y(S^i_0)$, where $*_{g_\varphi}$ is the seven-dimensional Hodge star explicitly showing its non-linear dependence on $\varphi$ — recall proposition 5.1 and the text below it. Here the choice of $Y_0$ fixes via the resulting volume factor $V_{Y_0}$ the normalization of the three-form $\varphi$ and consequently also the normalization of $g_{mn}$. Furthermore, due to equation (3.9), the normalization of the three-form $\varphi$ also affects the normalization of $\rho_i^{(3)}$. We choose a normalization for $\varphi$ such that only the dimensionless volume factor $\lambda_0$ appears in the resulting low-energy effective action.

In the following sections 3.2 and 3.3, we determine the bosonic and the fermionic pieces of the four-dimensional low-energy effective $\mathcal{N} = 1$ supergravity action for the above determined spectrum of massless fields.

## 3.2 The bosonic action

In this section, we explicitly perform the computation of the bosonic piece of the four-dimensional low-energy effective $\mathcal{N} = 1$ supergravity action after dimensional reduction of the corresponding higher dimensional terms in eleven dimensions. This means we focus on a subset of terms from the eleven-dimensional action given by (3.31), namely

$$S_{11\text{d}}^{\text{bos.}} = \frac{1}{2\kappa_{11}^2}\int\left(*_{11}\hat{R}_S - \frac{1}{2}d\hat{C}\wedge *_{11}d\hat{C} - \frac{1}{6}d\hat{C}\wedge d\hat{C}\wedge\hat{C}\right). \tag{3.35}$$

Again, the first term is the Einstein-Hilbert term in terms of the eleven-dimensional Ricci scalar $\hat{R}_S$. The second term is the kinetic term for the anti-symmetric three-form tensor $\hat{C}$ and the third term is the Chern-Simons term of the eleven-dimensional supergravity action.

In order to have the convenient four-dimensional normalization of the Ricci scalar term, we must perform the Weyl rescaling of the four-dimensional metric according to

$$g_{\mu\nu} \to \frac{g_{\mu\nu}}{\lambda_0(S^i)}, \qquad \sqrt{-\text{det}g_{\mu\nu}} \to \frac{\sqrt{\text{det}g_{\mu\nu}}}{\lambda_0^2(S^i)}. \tag{3.36}$$

This is such that the four-dimensional coupling constant $\kappa_4$ — relating the four-dimensional Newton constant $G_N$, the four-dimensional Planck length $\ell_P$ and the Planck mass $M_P$ — becomes

$$\kappa_4^2 = \frac{\kappa_{11}^2}{V_{Y_0}}, \qquad \kappa_4^2 = 8\pi G_N = 8\pi\ell_P^2 = \frac{8\pi}{M_P^2}. \tag{3.37}$$

**The Ricci scalar term**

We start by looking at the dimensional reduction of the Ricci scalar term. The eleven-dimensional Ricci scalar $\hat{R}_S$ has the following decomposition in terms of the four-dimensional Ricci scalar $R_S$,

$$\hat{R}_S = R_S + g^{\mu\nu}R^m{}_{\mu m\nu} + g^{mn}R^\mu{}_{m\mu n}. \tag{3.38}$$

With the use of $*_{11} = d^7y d^4x\sqrt{-\text{det}g_{\mu\nu}}\sqrt{\text{det}g_{mn}}$, the four-dimensional Hodge dual $*_4$, and equation (3.33), we obtain

$$\frac{1}{2\kappa_{11}^2}\int *_{11}\hat{R}_S = \frac{1}{2\kappa_4^2}\int_{\mathbb{R}^{1,3}} *_4 R_S\,\lambda_0 + \frac{1}{2\kappa_4^2}\int_{\mathbb{R}^{1,3}}\lambda_0\sqrt{-\text{det}g_{\mu\nu}}(g^{\mu\nu}R^m{}_{\mu m\nu} + g^{mn}R^\mu{}_{m\mu n}). \tag{3.39}$$

We now perform the Weyl rescaling with equation (3.36), which gives $R_S \to \lambda_0 R_S$ and $g^{\mu\nu}R^m{}_{\mu m\nu} + g^{mn}R^\mu{}_{m\mu n} \to \lambda_0(g^{\mu\nu}R^m{}_{\mu m\nu} + g^{mn}R^\mu{}_{m\mu n})$, such that we obtain

$$\frac{1}{2\kappa_{11}^2}\int *_{11}\hat{R}_S = \frac{1}{2\kappa_4^2}\int_{\mathbb{R}^{1,3}} *_4 R_S + \frac{1}{2\kappa_4^2}\int_{\mathbb{R}^{1,3}}\sqrt{-\text{det}g_{\mu\nu}}(g^{\mu\nu}R^m{}_{\mu m\nu} + g^{mn}R^\mu{}_{m\mu n}). \tag{3.40}$$

In this expression the Ricci tensors must be computed with the Weyl rescaled four-dimensional

metric. They are given in terms of the Christoffel symbols appearing in — here $\lambda$ runs over four- and seven-dimensional indices,

$$\begin{aligned} R^{m}{}_{\mu m\nu} &= \partial_m \Gamma^m_{\nu\mu} - \partial_\nu \Gamma^m_{m\mu} + \Gamma^m_{m\lambda}\Gamma^\lambda_{\nu\mu} - \Gamma^m_{\nu\lambda}\Gamma^\lambda_{m\mu} \,, \\ R^{\mu}{}_{m\mu n} &= \partial_\mu \Gamma^\mu_{nm} - \partial_n \Gamma^\mu_{\mu m} + \Gamma^\mu_{\mu\lambda}\Gamma^\lambda_{nm} - \Gamma^\mu_{n\lambda}\Gamma^\lambda_{\mu m} \,. \end{aligned} \tag{3.41}$$

Furthermore, in computing the non-vanishing Christoffel symbols, we make use of the relation

$$\partial_\mu \sqrt{\det g_{mn}} = \frac{1}{2}\sqrt{\det g_{mn}}(g^{mn}\partial_\mu g_{mn}) \,. \tag{3.42}$$

When inserting the dependence of the seven-dimensional metric on the moduli $S^i$, there appears a term $\mathrm{d}S^i \wedge *_4 \mathrm{d}S^j$ which should be further Weyl rescaled. Taking these into account, we obtain the resulting dimensional reduction of the eleven-dimensional Ricci scalar to be

$$\frac{1}{2\kappa_{11}^2}\int *_{11}\hat{R}_S = \frac{1}{2\kappa_4^2}\int_{\mathbb{R}^{1,3}} *_4 R_S - \frac{1}{2\kappa_4^2}\int_{\mathbb{R}^{1,3}} \frac{1}{2\lambda_0} dP^i \wedge *_4 dP^j \int_Y \rho_i^{(3)} \wedge *_{g_\varphi}\rho_j^{(3)} \,, \tag{3.43}$$

where the first term is the usual Einstein-Hilbert term in four dimensions.

**The kinetic term for $\hat{C}$**

Now we move on to the kinetic term for the three-form $\hat{C}$. First of all, from (3.13), we have

$$d\hat{C}(x,y) = \sum_I dA^I(x)\wedge\omega_I^{(2)}(y) + \sum_i dP^i(x)\wedge\rho_i^{(3)}(y) \,, \tag{3.44}$$

since $\omega_I^{(2)}$ and $\rho_i^{(3)}$ are harmonic forms, i.e., $d\omega_I^{(2)} = 0$ and $d\rho_i^{(3)} = 0$. We define

$$F^I(x) \equiv dA^I(x) \,. \tag{3.45}$$

Moreover, we make use of the following relations

$$\begin{aligned} *_{11}(F^J \wedge \omega_J^{(2)}) &= *_4 F^J \wedge *_{g_\varphi}\omega_J^{(2)} \,, \\ *_{11}(dP^j \wedge \rho_j^{(3)}) &= -*_4 dP^j \wedge *_{g_\varphi}\rho_j^{(3)} \,, \end{aligned} \tag{3.46}$$

in terms of the four- and seven-dimensional Hodge duals $*_4$ and $*_{g_\varphi}$. Therefore, the non-vanishing contributions to the second term in equation (3.35) are

$$\begin{aligned} -\frac{1}{2\kappa_{11}^2}\int \frac{1}{2} d\hat{C}\wedge *_{11} d\hat{C} = -\frac{1}{2\kappa_{11}^2}\int \frac{1}{2}[&(F^I\wedge\omega_I^{(2)})\wedge(*_4F^J\wedge *_{g_\varphi}\omega_J^{(2)}) \\ &- (dP^i\wedge\rho_i^{(3)})\wedge(*_4 dP^j\wedge *_{g_\varphi}\rho_i^{(3)})] \,. \end{aligned} \tag{3.47}$$

Rearranging the terms, we obtain

$$\begin{aligned} -\frac{1}{2\kappa_{11}^2}\int \frac{1}{2} d\hat{C}\wedge *_{11} d\hat{C} = -\frac{1}{2\kappa_{11}^2}\int \frac{1}{2}[&(F^I\wedge *_4 F^J)\wedge(\omega_I^{(2)}\wedge *_{g_\varphi}\omega_J^{(2)}) \\ &+ (dP^i\wedge *_4 dP^j)\wedge(\rho_i^{(3)}\wedge *_{g_\varphi}\rho_i^{(3)})] \,. \end{aligned} \tag{3.48}$$

Because harmonic two-forms transform in the $H^2_{\mathbf{14}}(Y)$, then $*_{g_\varphi}\omega^{(2)}_J = -\varphi \wedge \omega^{(2)}_J$ [224]. This, together with equations (3.5), (3.9) and (3.37) as well as a convenient normalization for $\varphi$, allow us to obtain the final expression for the kinetic term for $\hat{C}$

$$\begin{aligned}-\frac{1}{2\kappa_{11}^2}\int \frac{1}{2}d\hat{C}\wedge *_{11}d\hat{C} = &+\frac{1}{2\kappa_4^2}\int_{\mathbb{R}^{1,3}}\frac{1}{2}S^k F^I\wedge *_4 F^J\int_Y \omega^{(2)}_I\wedge\omega^{(2)}_J\wedge\rho^{(3)}_k\\ &-\frac{1}{2\kappa_4^2}\int_{\mathbb{R}^{1,3}}\frac{1}{2\lambda_0}dP^i\wedge *_4 dP^j\int_Y \rho^{(3)}_i\wedge *_{g_\varphi}\rho^{(3)}_j\,.\end{aligned} \tag{3.49}$$

### The Chern-Simons term

Now we present the dimensional reduction of the Chern-Simons term, i.e., the third term in (3.35). Using equation (3.44), the non-vanishing contributions to the third term in equation (3.35) are

$$\begin{aligned}\frac{1}{2\kappa_{11}^2}\int\frac{1}{6}d\hat{C}\wedge d\hat{C}\wedge\hat{C} = -\frac{1}{12\kappa_{11}^2}\int(&F^I\wedge\omega^{(2)}_I\wedge dP^j\wedge\rho^{(3)}_j\wedge A^K\wedge\omega^{(2)}_K\\ &+F^I\wedge\omega^{(2)}_I\wedge F^J\wedge\omega^{(2)}_J\wedge P^k\wedge\rho^{(3)}_k\\ &+dP^i\wedge\rho^{(3)}_i\wedge F^J\wedge\omega^{(2)}_J\wedge A^K\wedge\omega^{(2)}_K)\end{aligned} \tag{3.50}$$

Rearranging the terms, we obtain

$$\begin{aligned}\frac{1}{2\kappa_{11}^2}\int\frac{1}{6}d\hat{C}\wedge d\hat{C}\wedge\hat{C} = -\frac{1}{12\kappa_{11}^2}\int(&F^I\wedge A^K\wedge dP^j\wedge\omega^{(2)}_I\wedge\omega^{(2)}_K\wedge\rho^{(3)}_j\\ &+F^I\wedge F^J\wedge P^k\wedge\omega^{(2)}_I\wedge\omega^{(2)}_J\wedge\rho^{(3)}_k\\ &+F^J\wedge A^K\wedge dP^i\wedge\omega^{(2)}_J\wedge\omega^{(2)}_K\wedge\rho^{(3)}_i)\end{aligned} \tag{3.51}$$

Now we make use of relation $d(A^K\wedge P^j) = dA^K\wedge P^j - A^K\wedge dP^j$ and assume $d(A^K\wedge P^j)=0$ after integration. This leads to $A^K\wedge dP^j = F^K\wedge P^j$ and, therefore,

$$\frac{1}{2\kappa_{11}^2}\int\frac{1}{6}d\hat{C}\wedge d\hat{C}\wedge\hat{C} = -\frac{1}{4\kappa_{11}^2}\int_{\mathbb{R}^{1,3}}F^I\wedge F^J\wedge P^k\int_Y\omega^{(2)}_I\wedge\omega^{(2)}_J\wedge\rho^{(3)}_k. \tag{3.52}$$

With the use of equation (3.37) and the normalization of $\varphi$, the third term in equation (3.35) is written as

$$\frac{1}{2\kappa_{11}^2}\int\frac{1}{6}d\hat{C}\wedge d\hat{C}\wedge\hat{C} = -\frac{1}{2\kappa_4^2}\int_{\mathbb{R}^{1,3}}\frac{1}{2}F^I\wedge F^J\wedge P^k\int_Y\omega^{(2)}_I\wedge\omega^{(2)}_J\wedge\rho^{(3)}_k\,. \tag{3.53}$$

Putting together equations (3.43), (3.49) and (3.53), the dimensional reduction yields the

four-dimensional bosonic action

$$S_{4d}^{\text{bos}} = \frac{1}{2\kappa_4^2}\int_{\mathbb{R}^{1,3}}\Big[ *_4 R_S + \frac{1}{2}\int_Y \omega_I^{(2)}\wedge\omega_J^{(2)}\wedge\rho_k^{(3)}\left(S^k F^I\wedge *_4 F^J - P^k F^I\wedge F^J\right) - \frac{1}{2\lambda_0}\int_Y \rho_i^{(3)}\wedge *_{g_\varphi}\rho_j^{(3)}\left(dP^i\wedge *_4 dP^j + dS^i\wedge *_4 dS^j\right)\Big] . \tag{3.54}$$

in terms of the four-dimensional Hodge star $*_4$, the Ricci scalar $R_S$ with respect to the metric $g_{\mu\nu}$, the dimensionless volume factor $\lambda_0$, and the seven-dimensional Hodge star $*_{g_\varphi}$.

### 3.2.1 The Kähler potential and the gauge kinetic coupling function

The bosonic part of the four-dimensional effective supergravity action at second-order derivative is specified by a Kähler target space for massless chiral scalars $\phi^i$ with Kähler potential $K(\phi,\bar\phi)$, a holomorphic gauge kinetic function $f_{IJ}(\phi)$, and a holomorphic superpotential $W(\phi)$. The expected bosonic four-dimensional effective action takes the following form

$$\begin{aligned} S_{4d}^{\text{bos}} =& \frac{1}{2\kappa_4^2}\int_{\mathbb{R}^{1,3}} *_4 R_S \\ &+ \frac{1}{2\kappa_4^2}\int_{\mathbb{R}^{1,3}} d^4x\,\sqrt{-g_{\mu\nu}}\left(-\frac{1}{2}\text{Re}f_{IJ}F^I_{\mu\nu}F^{\mu\nu,J} + \frac{1}{4}\text{Im}f_{IJ}F^I_{\mu\nu}\epsilon^{\mu\nu\rho\sigma}F^J_{\rho\sigma}\right) \\ &- \frac{1}{\kappa_4^2}\int_{\mathbb{R}^{1,3}} d^4x\,\sqrt{-g_{\mu\nu}}\left(K_{i\bar\jmath}\partial_\mu\phi^i\partial^\mu\bar\phi^{\bar\jmath} + V\right) , \end{aligned} \tag{3.55}$$

where $V$ is the scalar potential

$$V = e^K(K^{i\bar\jmath}D_iW\overline{D}_{\bar\jmath}\overline{W} - 3|W|^2) , \tag{3.56}$$

in terms of the covariant derivative of the superpotential $D_iW = \partial_iW + (\partial_iK)W$ and the moduli space metric $K_{i\bar\jmath} = \partial_i\partial_{\bar\jmath}K$.

We can now bring the (bosonic) action (3.54) into this conventional form of four-dimensional $\mathcal{N}=1$ supergravity [225].[8] To identify the chiral multiplets — that is to say, to identify the complex structure of the Kähler target space — we observe that — at least to the leading order — the action of the membrane instantons generating non-perturbative superpotential interactions is given by [228]

$$\phi^i = -P^i + iS^i . \tag{3.57}$$

Hence, due to holomorphy of the $\mathcal{N}=1$ superpotential, the complex fields $\phi^i$ furnish complex coordinates of the Kähler target space and thus represent the complex scalar fields in the $\mathcal{N}=1$ chiral multiplets $\Phi^i$ in table 3.1. This allows us to quickly read off from the action (3.54) the

[8] The structure of the four-dimensional effective $\mathcal{N}=1$ action from type II and M-theory dimensional reduction including Kaluza–Klein massive modes— which we do not consider here — has recently been discussed in references [226, 227].

Kähler potential and the gauge kinetic coupling functions [135, 136]

$$K(\phi,\bar{\phi}) \;=\; -3\log\left(\frac{1}{7}\int_Y \varphi\wedge *_{g_\varphi}\varphi\right)\,, \tag{3.58}$$

$$f_{IJ}(\phi) \;=\; \frac{i}{2}\sum_k \phi^k \int_Y \omega_I^{(2)}\wedge\omega_J^{(2)}\wedge\rho_k^{(3)} \;=\; \frac{i}{2}\sum_k \kappa_{IJk}\phi^k. \tag{3.59}$$

Note that the holomorphy of the gauge kinetic coupling functions is in accordance with the complex chiral coordinates (3.57). The moduli space metric is then given by

$$K_{i\bar{j}} = \partial_i\partial_{\bar{j}}K = \frac{1}{4\lambda_0}\int_Y \rho_i^{(3)}\wedge *_{g_\varphi}\rho_j^{(3)}\,. \tag{3.60}$$

Thus, we see that in the physical theory the real scalar fields $S^i$ and $P^i$ combine to the complex chiral scalars $\phi^i$ according to equation (3.57). These complex scalar fields parametrize locally the (semi-classical) M-theory moduli space $\mathcal{M}_{\mathbb{C}}$ of the $G_2$-compactification on $Y$ of complex dimension $b_3(Y)$, where the real subspace $\mathrm{Re}(\phi^i) = 0$ of real dimension $b_3(Y)$ is the geometric moduli space $\mathcal{M}$ of $G_2$-metrics on $Y$.[9] Note, however, that the derived moduli space $\mathcal{M}_{\mathbb{C}}$ merely arises from the semi-classical dimensional reduction of eleven-dimensional supergravity on the $G_2$-manifold $Y$. For the resulting four-dimensional $\mathcal{N} = 1$ supersymmetric theory, one expects on general grounds that the flat directions of $\mathcal{M}_{\mathbb{C}}$ are lifted at the quantum level due to non-perturbative effects in M-theory [228] — even in the absence of background fluxes.

Finally, let us remark that the presence of non-trivial four-form background fluxes $G$ of anti-symmetric three-form tensor fields $\hat{C}$ supported on the $G_2$-manifold $Y$ generates a flux-induced superpotential [134, 135, 138]. While the superpotential enters quadratically in the bosonic action, it appears linearly in the fermionic action generating a gravitino mass term $M_\psi$ [225]

$$M_\psi \;=\; \frac{1}{2\kappa_4^2}e^{K/2}\left(\bar{W}(\bar{\phi})\,\psi_\mu^T\gamma^{\mu\nu}\psi_\nu + W(\phi)\,\bar{\psi}_\mu\gamma^{\mu\nu}\psi_\nu^*\right)\,. \tag{3.61}$$

This linear dependence on $W$ allows us to directly derive the superpotential from the dimensional reduction of the gravitino terms, which we investigate in the following.

## 3.3 The fermionic action

Due to expansion (3.14) for the gravitino $\hat{\Psi}$ and relation (A.6), the dimensional reduction of the Rarita–Schwinger kinetic term for the gravitino $\hat{\Psi}$, given by the third term of the first line in

[9] For corrections to the semi-classical moduli space $\mathcal{M}_{\mathbb{C}}$ see reference [229].

(3.31), is

$$
\begin{aligned}
-\frac{1}{2\kappa_{11}^2}\int *_{11} i\,\bar{\hat{\Psi}}_M\hat{\Gamma}^{MNP}\hat{\nabla}_N\hat{\Psi}_P = &-\frac{i}{2\kappa_{11}^2}\int_{\mathbb{M}^{1,3}} *_4\bar{\psi}_\mu\gamma^{\mu\nu\rho}\nabla_\nu\psi^*_\rho\int_Y *_{g_\varphi}\bar{\zeta}\zeta\\
&-\frac{i}{2\kappa_{11}^2}\int_{\mathbb{M}^{1,3}} *_4\bar{\psi}_\mu\gamma^{\mu-\rho}\psi^*_\rho\int_Y *_{g_\varphi}\bar{\zeta}\gamma^n\nabla_n\zeta\\
&-\frac{i}{2\kappa_{11}^2}\int_{\mathbb{M}^{1,3}} *_4\frac{1}{3}\bar{\chi}\gamma^\nu\nabla_\nu\chi^*\int_Y *_{g_\varphi}\bar{\zeta}^{(1)}_m\gamma^{pm}\zeta^{(1)}_p\\
&-\frac{i}{2\kappa_{11}^2}\int_{\mathbb{M}^{1,3}} *_4\bar{\chi}\gamma\chi^*\int_Y *_{g_\varphi}\bar{\zeta}^{(1)}_m\gamma^{mnp}\nabla_n\zeta^{(1)}_p\\
&+\text{c.c.}\,.
\end{aligned}
\tag{3.62}
$$

The resulting terms comprise the kinetic and mass terms for both the four-dimensional gravitinos $\psi_\mu$ — the first and second line on the right hand side of equation (3.62), respectively — and the four-dimensional fermions $\chi$ — the third and fourth line on the right hand side of equation (3.62), respectively. It also gives rise to mixed terms between $\psi$ and $\chi$. However, since such mixed terms are not present in standard four-dimensional supergravity theories, they have been neglected in this analysis.[10]

### 3.3.1 The holomorphic superpotential

Let us now determine the holomorphic superpotential generated by a cohomologically non-trivial four-form background flux $G$ on the $G_2$-manifold $Y$, which is locally given by $d\hat{C}$. The superpotential can be read off from the four-dimensional gravitino mass term (3.61). Such a term arises from the dimensional reduction of the fourth term in the eleven-dimensional action (3.31). That is to say, we find

$$
\begin{aligned}
-\frac{1}{192\kappa_{11}^2}\int *_{11}\bar{\hat{\Psi}}_M\hat{\Gamma}^{MNPQRS}\hat{\Psi}_N(d\hat{C})_{[PQRS]} \;\supset\; &-\frac{1}{192\kappa_{11}^2}\int *_{11}\bar{\hat{\Psi}}_\mu\hat{\Gamma}^{\mu\nu pqrs}\hat{\Psi}_\nu(d\hat{C})_{[pqrs]}\\
= &-\frac{1}{192\kappa_{11}^2}\int *_{11}(\bar{\psi}_\mu+\bar{\psi}^*_\mu)\bar{\zeta}\gamma^{\mu\nu}\gamma^{pqrs}(\psi_\nu+\psi^*_\nu)\zeta(d\hat{C})_{[pqrs]}\,.
\end{aligned}
\tag{3.63}
$$

Since there are no harmonic one-forms on the $G_2$-manifold $Y$, we can identify the spinorial section $\zeta$ with the unique covariant constant spinor $\eta$ on the $G_2$-manifold $Y$, cf. section 3.1. Furthermore, we notice that the covariantly constant three-form $\varphi$ and its Hodge dual four-form $\Phi = *_{g_\varphi}\varphi$ are bilinear in $\eta$, namely $\varphi_{mnp} = i\bar{\eta}\gamma_{mnp}\eta$ and $\Phi_{[mnpq]} = (*_{g_\varphi}\varphi)_{[mnpq]} = -\bar{\eta}\gamma_{mnpq}\eta$, such

[10] Actually, one should perform a redefinition of $\Psi_\mu$ with $\Psi_\mu \to \Psi'_\mu = \Psi_\mu + \hat{\Gamma}_\mu\hat{\Gamma}^m\Psi_m$ in order for such terms to cancel out. However, we do not consider this field redefinition as such a shift does not affect the gravitino mass [138, 230].

that

$$-\frac{1}{192\kappa_{11}^2}\int *_{11}\bar{\hat{\Psi}}_M\hat{\Gamma}^{MNPQRS}\hat{\Psi}_N(d\hat{C})_{[PQRS]} \supset \frac{1}{192\kappa_{11}^2}\int *_{11}\bar{\psi}_\mu\gamma^{\mu\nu}\psi_\nu^*\Phi_{[pqrs]}(d\hat{C})^{[pqrs]} + \text{c.c.} \quad (3.64)$$

We must employ the following Weyl rescalings

$$g_{\mu\nu}\to\frac{g_{\mu\nu}}{\lambda_0(S^i)}\,,\qquad \gamma^\mu\to\sqrt{\lambda_0(S^i)}\gamma^\mu\,,\qquad \psi_\mu\to\frac{\psi_\mu}{(\lambda_0(S^i))^{1/4}}\,. \quad (3.65)$$

Furthermore, we use the following replacement

$$\int_Y *_{g_\varphi}\Phi_{[pqrs]}(d\hat{C})^{[pqrs]} = -4!\int_Y\Phi\wedge *_{g_\varphi}\mathrm{d}\hat{C} = +4!\int_Y\mathrm{d}\hat{C}\wedge *_{g_\varphi}\varphi\,. \quad (3.66)$$

Therefore, (3.64) is given by

$$-\frac{1}{192\kappa_{11}^2}\int *_{11}\bar{\hat{\Psi}}_M\hat{\Gamma}^{MNPQRS}\hat{\Psi}_N(d\hat{C})_{[PQRS]} \supset \frac{1}{8\lambda_0^{7/2}\kappa_4^2}\int_Y G\wedge\varphi\int_{\mathbb{R}^{1,3}} *_4\bar{\psi}_\mu\gamma^{\mu\nu}\psi_\nu^* + \text{c.c.} \quad (3.67)$$

We should compare this result with the corresponding fermionic term in the four-dimensional $\mathcal{N}=1$ supergravity action,

$$S_{4d}^{\text{ferm}} \supset \frac{1}{2\kappa_4^2}\int_{\mathbb{R}^{1,3}} *_4\mathcal{L}_{4d}^{M_\psi} = \frac{1}{2\kappa_4^2}e^{K/2}\left(\bar{W}(\bar{\phi})\,\psi_\mu^T\gamma^{\mu\nu}\psi_\nu + W(\phi)\,\bar{\psi}_\mu\gamma^{\mu\nu}\psi_\nu^*\right)\,. \quad (3.68)$$

Since the Kähler potential is $K=-3\log\lambda_0$ — derived in section (3.58) —, with the Weyl rescaled four-dimensional metric $g_{\mu\nu}$, we arrive at the following superpotential contribution

$$W(\phi)\supset\frac{1}{4}\int_Y G\wedge\varphi\,. \quad (3.69)$$

Note that the derived term is not holomorphic in the four-dimensional chiral coordinates since it couples to the three-form $\varphi$ and not its complexification. To arrive at the full superpotential we must render the moduli dependence holomorphic in terms of the replacement $\varphi\to\varphi+i\hat{C}$, which is in accordance with the deduced chiral coordinates (3.57). This proposed replacement is in agreement with the domain wall tensions interpolating between distinct flux vacua [231, 232]. As explained in reference [135], this is also required in order to obtain the chiral combination $-\delta\hat{C}+i\delta\varphi$ in the variation $\delta W$ of the superpotential $W$ and, therefore, it is necessary to introduce a

relative factor $\frac{1}{2}$ between $\hat{C}$ and $\varphi$. Thus, altogether we arrive at the flux-induced superpotential[11]

$$W(\phi^i) = \frac{1}{4}\int_Y G \wedge \left(-\frac{1}{2}\hat{C} + i\varphi\right) . \tag{3.70}$$

Our result yields the flux-induced superpotential in references [134, 135, 138, 229].

Note that — both in the presence and in the absence of background fluxes $G$ — we expect generically additional non-perturbative superpotential contributions arising from membrane instanton effects [221, 228].

## 3.4 M-theory on twisted connected sum $G_2$-manifolds

Having dealt with the more general setup of compactifications of M-theory on $G_2$-manifolds, we now turn to specific details resulting from the twisted connected sum construction. In section 3.4.1 we obtain a reduced form for the four-dimensional $\mathcal{N} = 1$ supergravity Kähler potential by a brute force calculation in terms of the constituents of this construction. Furthermore, we present the second and third contributions of this thesis to the topic. Firstly, the identification of the relevant four-dimensional universal chiral multiplets, allowing for the specification of the four-dimensional spectrum as well as its geometrical interpretation, and the final form of its associated Kähler potential. Secondly, we identify abelian gauge sectors exhibiting extended supersymmetries on the local geometries of the twisted connected sum $G_2$-manifolds in the Kovalev limit.

### 3.4.1 The Kähler potential: a reduced form

In this section we obtain a reduced form for the four-dimensional Kähler potential from equation (3.58) in terms of the constituents of Kovalev's twisted connected sum construction.

[11] Non-vanishing four-form fluxes induce a gravitational back-reaction to the eleven-dimensional metric. This requires a warped metric *Ansatz* that breaks supersymmetry [133, 134]. As the presented derivation neglects such back-reactions, the resulting effective action becomes more accurate the smaller the effect of warping. Similarly as argued in reference [138] this is the case for a small number of four-form flux quanta.

Due to the twisted connected sum construction in section 2.2, the Kähler potential splits into

$$\begin{aligned} K =& -3\log\left(\frac{1}{7}\int\limits_{Y_r=Y_L\cup Y_R}\varphi\wedge*\varphi\right)\\ =& -3\log\Bigg(\frac{1}{7}\int\limits_{[K_L\cup(0,T-1]\times S^{1*}_L\times S_L]\times S^1_L}\varphi_L\wedge*\varphi_L+\frac{1}{7}\int\limits_{[K_R\cup(0,T-1]\times S^{1*}_R\times S_R]\times S^1_R}\varphi_R\wedge*\varphi_R\\ &+\frac{1}{7}\int\limits_{X^\infty_L|_{(T-1,T]}\times S^1_L}\varphi_L\wedge*\varphi_L+\frac{1}{7}\int\limits_{X^\infty_R|_{(T-1,T]}\times S^1_R}\varphi_R\wedge*\varphi_R\\ &+\frac{1}{14}\int\limits_{X^\infty_L|_{(T,T+1]}\times S^1_L}\varphi_L\wedge*\varphi_L+\frac{1}{14}\int\limits_{X^\infty_L|_{(T,T+1]}\times S^1_R}\varphi_R\wedge*\varphi_R\Bigg)\,. \end{aligned} \tag{3.71}$$

The second line gives the contribution from the compact subspaces $K_{L/R}\subset X_{L/R}$ of the non-compact asymptotically cylindrical Calabi–Yaus $X_{L/R}$ times an $S^1_{L/R}$ and from the Calabi–Yau cylinder region in the interval $(0,T-1]$. The third line gives the contribution from the Calabi–Yau cylinder region in the interval $(T-1,T]$. The last line gives the contribution from the asymptotical ends of the Calabi–Yau cylinders in the interval $(T,T+1]$. The extra factor of $1/2$ in the last line guarantees that we are not overcounting contributions from the left- and right-sides as they are glued together in this region.

In the following, we perform the computation for the left-side of the construction only. We present the final expression for the Kähler potential (3.71) after taking into account analagous terms for the right-side of the construction.

### Region $[K_L\cup(0,T-1]\times S^{1*}_L\times S_L]\times S^1_L$

In this region we are interested in the contribution from the compact subspaces $K_{L/R}$ times an $S^1_{L/R}$ and from the Calabi–Yau cylinder region in $(0,T-1]$. In the compact region, the three-form $\varphi_L$ and four-form $*\varphi_L$ are given by

$$\varphi_L=\gamma_L d\theta_L\wedge\omega_L|_{K_L}+\mathrm{Re}\Omega_L|_{K_L}\,, \tag{3.72}$$

$$*\varphi_L=\tfrac{1}{2}(\omega_L|_{K_L})^2-\gamma_L d\theta_L\wedge\mathrm{Im}\Omega_L|_{K_L}\,, \tag{3.73}$$

where $\omega_L|_{K_L}$ and $\Omega_L|_{K_L}$ are the restrictions of the three-form and four-form of $X_L$ to the compact subspace $K_L$.

Therefore, the contribution from the compact subspace $K_L$ is

$$\begin{aligned}\int\limits_{K_L\times S^1_L} \varphi_L\wedge *\varphi_L &= \int\limits_{K_L}\int\limits_0^{2\pi}\left(\frac{1}{2}\omega_L|^3_{K_L}\wedge\gamma_L d\theta_L + \mathrm{Re}\Omega_L|_{K_L}\wedge\mathrm{Im}\Omega_L|_{K_L}\wedge\gamma_L d\theta_L\right)\\ &= \pi\gamma_L\int\limits_{K_L}\omega_L|^3_{K_L} + 2\pi\gamma_L\int\limits_{K_L}\mathrm{Re}\Omega_L|_{K_L}\wedge\mathrm{Im}\Omega_L|_{K_L}\,.\end{aligned} \tag{3.74}$$

Notice that here we have neglected contributions at $t=0$. When analysing the Calabi–Yau cylinder region in $(0,T-1]$ below, there will also appear contributions at $t=0$ due to continuity of the twisted connected sum construction — recall figure 2.1. These allow us to neglect the contributions at $t=0$ for the compact region. We make this point more clear in the following.

In the Calabi–Yau cylinder region in $(0,T-1]$, the forms $\omega_L^T$ and $\Omega_L^T$ are given by

$$\begin{aligned}\omega_L^T &= \omega_L^\infty + d\mu_L := (\gamma_L^*)^2 dt\wedge d\theta_L^* + \omega_L^S + +d\mu_L\,,\\ \Omega_L^T &= \Omega_L^\infty + d\nu_L := \gamma_L^* d\theta_L^*\wedge\Omega_L^S - i\gamma_L^* dt\wedge\Omega_L^S + d\nu_L\,.\end{aligned} \tag{3.75}$$

Furthermore, the three-form $\varphi_L$ and four-form $*\varphi_L$ are given by, respectively,

$$\varphi_L = \gamma_L d\theta_L\wedge\omega_L^T + \mathrm{Re}\Omega_L^T\,, \tag{3.76}$$

$$*\varphi_L = \tfrac{1}{2}(\omega_L^T)^2 - \gamma_L d\theta_L\wedge\mathrm{Im}\Omega_L^T\,. \tag{3.77}$$

The contribution from this Calabi–Yau cylinder region in $(0,T-1]$ is then rewritten as

$$\begin{aligned}\int\limits_{(0,T-1]\times S^{1*}_L\times S_L\times S^1_L}\varphi_L\wedge*\varphi_L = &\int\limits_{(0,T-1]\times S^{1*}_L\times S_L\times S^1_L}(\gamma_L d\theta_L\wedge\omega_L^\infty + \mathrm{Re}\Omega_L^\infty)\\ &\wedge\left[\frac{1}{2}(\omega_L^\infty)^2 - \gamma_L d\theta_L\wedge\mathrm{Im}\Omega_L^\infty\right]\\ &+\int\limits_{(0,T-1]\times S^{1*}_L\times S_L\times S^1_L}F(d\mu_L,d\nu_L)\,,\end{aligned} \tag{3.78}$$

where $F(d\mu_L,d\nu_L)$ is a correction term given by

$$\begin{aligned}F(d\mu_L,d\nu_L) = &(\gamma_L d\theta_L\wedge\omega_L^\infty + \mathrm{Re}\Omega_L^\infty)\wedge\left[\omega_L^\infty\wedge d\mu_L + \frac{1}{2}(d\mu_L)^2 - \gamma_L d\theta_L\wedge\mathrm{Im}d\nu_L\right]\\ &+(\gamma_L d\theta_L\wedge d\mu_L + \mathrm{Re}d\nu_L)\wedge\left[\frac{1}{2}(\omega_L^\infty + d\mu_L)^2 - \gamma_L d\theta_L\wedge\mathrm{Im}\Omega_L^\infty - \gamma_L d\theta_L\wedge\mathrm{Im}d\nu_L\right].\end{aligned} \tag{3.79}$$

After inserting the contributions for $\omega_L^\infty$ and $\Omega_L^\infty$ given by equation (3.75), the first integral in

equation (3.78) is reduced to

$$\begin{aligned}\int\limits_{(0,T-1]\times S^{1*}_L\times S_L\times S^1_L} &(\gamma_L d\theta_L\wedge\omega_L^\infty+\mathrm{Re}\Omega_L^\infty)\wedge\left[\frac{1}{2}(\omega_L^\infty)^2-\gamma_L d\theta_L\wedge\mathrm{Im}\Omega_L^\infty\right]=\\ &=\int_0^{T-1}\int_0^{2\pi}\int_{S_L}\int_0^{2\pi}\Big[\frac{3}{2}(\gamma_L^*)^2dt\wedge d\theta_L^*\wedge(\omega_L^S)^2\wedge\gamma_L d\theta_L\\ &\qquad+(\gamma_L^*)^2dt\wedge d\theta_L^*\wedge(\mathrm{Re}\Omega_L^S)^2\wedge\gamma_L d\theta_L\\ &\qquad+(\gamma_L^*)^2dt\wedge d\theta_L^*\wedge(\mathrm{Im}\Omega_L^S)^2\wedge\gamma_L d\theta_L\Big]\\ &=4\pi^2(T-1)(\gamma_L^*)^2\gamma_L\int_{S_L}\left[\frac{3}{2}(\omega_L^S)^2+(\mathrm{Re}\Omega_L^S)^2+(\mathrm{Im}\Omega_L^S)^2\right]\end{aligned}\tag{3.80}$$

The second integral in equation (3.78) is given by the contribution from the correction term $F(d\mu_L, d\nu_L)$, explicitly written in equation (3.79). With $(d\mu_L)^2=(d\mu_L)^3=(d\nu_L)^2=0$ and, by degree counting, the surviving terms are

$$\begin{aligned}\int\limits_{(0,T-1]\times S^{1*}_L\times S_L\times S^1_L} F(d\mu_L,d\nu_L)=\int_0^{T-1}\int_0^{2\pi}\int_{S_L}\int_0^{2\pi}\Big[&\frac{3}{2}(\omega_L^\infty)^2\wedge d\mu_L\wedge\gamma_L d\theta_L\\ &+\mathrm{Re}d\nu_L\wedge\mathrm{Im}\Omega_L^\infty\wedge\gamma_L d\theta_L-\mathrm{Im}d\nu_L\wedge\mathrm{Re}\Omega_L^\infty\wedge\gamma_L d\theta_L\\ &+\mathrm{Re}d\nu_L\wedge\mathrm{Im}d\nu_L\wedge\gamma_L d\theta_L\Big]\end{aligned}\tag{3.81}$$

Plugging $\omega_L^\infty$ and $\Omega_L^\infty$ from equation (3.75), we evaluate the first integral in equation (3.81) with Stokes's theorem, closedness of $\omega_L^S$ and the fact that the algebraic K3 $S_L$ has no boundary. Therefore, we obtain

$$\begin{aligned}&\int\limits_{(0,T-1]\times S^{1*}_L\times S_L\times S^1_L}(\omega_L^\infty)^2\wedge d\mu_L\wedge\gamma_L d\theta_L\\ &\qquad=2\pi\gamma_L\int\limits_{(0,T-1]\times S^{1*}_L\times S_L}[2(\gamma_L^*)^2dt\wedge d\theta_L^*\wedge\omega_L^S\wedge d\mu_L+(\omega_L^S)^2\wedge d\mu_L]\\ &\qquad=2\pi\gamma_L\int\limits_{S^{1*}_L\times S_L}(\mu_{L|t=T-1}-\underline{\mu_{L|t=0}})\wedge(\omega_L^S)^2\end{aligned}\tag{3.82}$$

Due to continuity of the entire twisted connected sum construction, we highlight the underlined terms that must vanish with part of the contribution from the compact region $K_L$ as we have already mentioned.

Now, notice that, for any smooth complex function $f = f_1 + if_2$, we have $\mathrm{Re}(df) = d(\mathrm{Re}f)$ and $\mathrm{Im}(df) = d(\mathrm{Im}f)$. Therefore, we can write

$$\int \mathrm{Re}dv_L \wedge \mathrm{Im}\Omega_L^\infty \wedge d\theta_L = \int d(\mathrm{Re}v_L) \wedge \mathrm{Im}\Omega_L^\infty \wedge d\theta_L \,, \tag{3.83}$$

$$\int \mathrm{Im}dv_L \wedge \mathrm{Re}\Omega_L^\infty \wedge d\theta_L = \int d(\mathrm{Im}v_L) \wedge \mathrm{Re}\Omega_L^\infty \wedge d\theta_L \,, \tag{3.84}$$

$$\int \mathrm{Re}dv_L \wedge \mathrm{Im}dv_L \wedge d\theta_L = \int d(\mathrm{Re}v_L) \wedge d(\mathrm{Im}v_L) \wedge d\theta_L \,. \tag{3.85}$$

With these expressions at hand, we reduce the second integral in equation (3.83) using Stokes's theorem several times, closedness of $\Omega_L^S$ and the fact that the algebraic K3 $S_L$ and the circle $S_L^{1*}$ have no boundaries.

$$\begin{aligned}
\int_0^{T-1}\int_0^{2\pi}\int_{S_L}\int_0^{2\pi} \mathrm{Re}dv_L \wedge \mathrm{Im}\Omega_L^\infty \wedge \gamma_L d\theta_L &= \int_0^{T-1}\int_0^{2\pi}\int_{S_L}\int_0^{2\pi} d(\mathrm{Re}v_L) \wedge \mathrm{Im}\Omega_L^\infty \wedge \gamma_L d\theta_L \\
&= \int_0^{T-1}\int_0^{2\pi}\int_{S_L}\int_0^{2\pi} \Big[ d(\mathrm{Re}v_L) \wedge \gamma_L^* d\theta_L^* \wedge \mathrm{Im}\Omega_L^S \wedge \gamma_L d\theta_L \\
&\qquad\qquad - d(\mathrm{Re}v_L) \wedge \gamma_L^* dt \wedge \mathrm{Re}\Omega_L^S \wedge \gamma_L d\theta_L \Big] \\
&= 2\pi\gamma_L^*\gamma_L \int_0^{2\pi}\int_{S_L} (\mathrm{Re}v_{L|t=T-1} - \underline{\mathrm{Re}v_{L|t=0}}) \wedge d\theta_L^* \wedge \mathrm{Im}\Omega_L^S
\end{aligned} \tag{3.86}$$

Again, due to continuity of the twisted connected sum construction, we underline another term that must vanish with part of the contribution from the compact region $K_L$. In a similar way, we also obtain the following

$$\int_0^{T-1}\int_0^{2\pi}\int_{S_L}\int_0^{2\pi} \mathrm{Im}dv_L \wedge \mathrm{Re}\Omega_L^\infty \wedge \gamma_L d\theta_L = 2\pi\gamma_L^*\gamma_L \int_0^{2\pi}\int_{S_L} (\mathrm{Im}v_{L|t=T-1} - \underline{\mathrm{Im}v_{L|t=0}}) \wedge d\theta_L^* \wedge \mathrm{Im}\Omega_L^S \tag{3.87}$$

$$\int_0^{T-1}\int_0^{2\pi}\int_{S_L}\int_0^{2\pi} \mathrm{Re}dv_L \wedge \mathrm{Im}dv_L \wedge \gamma_L d\theta_L = 0 \tag{3.88}$$

Summing up the contributions from the Calabi–Yay cylinder region in $(0, T-1]$, we obtain

$$\begin{aligned}\int\limits_{S_L^{1*}\times S_L\times(0,T-1]\times S_L^1} \varphi_L\wedge *\varphi_L &= 4\pi^2(T-1)(\gamma_L^*)^2\gamma_L\int\limits_{S_L}\left[\frac{3}{2}(\omega_L^S)^2+(\mathrm{Re}\Omega_L^S)^2+(\mathrm{Im}\Omega_L^S)^2\right]\\ &+2\pi\gamma_L\int\limits_{S_L^{1*}\times S_L}(\mu_{L|t=T-1}-\underline{\mu_{L|t=0}})\wedge(\omega_L^S)^2\\ &+2\pi\gamma_L^*\gamma_L\int\limits_0^{2\pi}\int\limits_{S_L}(\mathrm{Re}\nu_{L|t=T-1}-\underline{\mathrm{Re}\mu_{L|t=0}})\wedge d\theta_L^*\wedge\mathrm{Im}\Omega_L^S\\ &+2\pi\gamma_L^*\gamma_L\int\limits_0^{2\pi}\int\limits_{S_L}(\mathrm{Im}\nu_{L|t=T-1}-\underline{\mathrm{Im}\mu_{L|t=0}})\wedge d\theta_L^*\wedge\mathrm{Im}\Omega_L^S\end{aligned}\tag{3.89}$$

Finally, summing up these contributions from the Calabi–Yau cylinder region in $(0, T-1]$ together with contributions from the compact subspace $K_L$ and neglecting the underlined terms due to continuity, as already mentioned, we obtain

$$\begin{aligned}\int\limits_{[K_L\cup S_L^{1*}\times S_L\times(0,T-1]]\times S_L^1}\varphi\wedge*\varphi &= \pi\gamma_L\int\limits_{K_L\setminus(t=0)}\omega_L|_{K_L}^3+2\pi\gamma_L\int\limits_{K_L\setminus(t=0)}\mathrm{Re}\Omega_L|_{K_L}\wedge\mathrm{Im}\Omega_L|_{K_L}\\ &+4\pi^2(T-1)(\gamma_L^*)^2\gamma_L\int\limits_{S_L}\left[\frac{3}{2}(\omega_L^S)^2+(\mathrm{Re}\Omega_L^S)^2+(\mathrm{Im}\Omega_L^S)^2\right]\\ &+2\pi\gamma_L\int\limits_{S_L^{1*}\times S_L}\mu_{L|t=T-1}\wedge(\omega_L^S)^2\\ &+2\pi\gamma_L^*\gamma_L\int\limits_0^{2\pi}\int\limits_{S_L}\mathrm{Re}\nu_{L|t=T-1}\wedge d\theta_L^*\wedge\mathrm{Im}\Omega_L^S\\ &+2\pi\gamma_L^*\gamma_L\int\limits_0^{2\pi}\int\limits_{S_L}\mathrm{Im}\nu_{L|t=T-1}\wedge d\theta_L^*\wedge\mathrm{Im}\Omega_L^S\end{aligned}\tag{3.90}$$

### Region $X_L^\infty|_{(T-1,T]}\times S_L^1$

We now turn to the region $(T-1, T]$ where the contributions come from the Calabi–Yau cylinder regions only. In this region, the forms $\omega_L^T$ and $\Omega_L^T$ interpolate between $\omega_L^T=\omega_L^\infty+d\mu_L$ when $t=T-1$, and $\omega_L^T=\omega_L^\infty$ when $t=T$ — due to the interpolating function used in equation (2.35). We recall

$$\begin{aligned}\omega_L^T &= \omega_L^\infty+d\tilde{\mu}_L := (\gamma_L^*)^2dt\wedge d\theta_L^*+\omega_L^S+d[1-\alpha(t-T+1)]\mu_L\,,\\ \Omega_L^T &= \Omega_L^\infty+d\tilde{\nu}_L := \gamma_L^*d\theta_L^*\wedge\Omega_L^S-i\gamma_L^*dt\wedge\Omega_L^S+d[1-\alpha(t-T+1)]\nu_L\,.\end{aligned}\tag{3.91}$$

Furthermore, the three-form $\varphi_L$ and four-forms $*\varphi_L$ are given by, respectively,

$$\varphi_L = \gamma_L d\theta_L \wedge \omega_L^T + \mathrm{Re}\Omega_L^T \,, \tag{3.92}$$
$$*\varphi_L = \tfrac{1}{2}(\omega_L^T)^2 - \gamma_L d\theta_L \wedge \mathrm{Im}\Omega_L^T \,. \tag{3.93}$$

Notice that this contribution to the Kähler potential is almost the same as the one performed in the region $[K_L \cup (0, T-1] \times S^{1^*}_L \times S_L] \times S^1_L$. The first difference is that now we have $F := F(d\tilde{\mu}_L, d\tilde{\nu}_L)$ and the region is in $(T-1, T]$ instead of in $(0, T-1]$. Therefore, we only state the result here with the modifications we have just mentioned. The contribution from the Calabi–Yau cylinder region in $(T-1, T]$ is given by

$$\begin{aligned}\int_{S^{1^*}_L \times S_L \times (T-1,T] \times S^1_L} \varphi_L \wedge *\varphi_L &= 4\pi^2 (\gamma_L^*)^2 \gamma_L \int_{S_L} \left[\frac{3}{2}(\omega_L^S)^2 + (\mathrm{Re}\Omega_L^S)^2 + (\mathrm{Im}\Omega_L^S)^2\right] \\ &+ 2\pi\gamma_L \int_{S^{1^*}_L \times S_L} (\tilde{\mu}_{L|t=T} \xrightarrow{0} \tilde{\mu}_{L|t=T-1}) \wedge (\omega_L^S)^2 \\ &+ 2\pi\gamma_L^* \gamma_L \int_0^{2\pi} \int_{S_L} (\mathrm{Re}\tilde{\nu}_{L|t=T} \xrightarrow{0} \mathrm{Re}\tilde{\nu}_{L|t=T-1}) \wedge d\theta_L^* \wedge \mathrm{Im}\Omega_L^S \\ &+ 2\pi\gamma_L^* \gamma_L \int_0^{2\pi} \int_{S_L} (\mathrm{Im}\tilde{\nu}_{L|t=T} \xrightarrow{0} \mathrm{Im}\tilde{\nu}_{L|t=T-1}) \wedge d\theta_L^* \wedge \mathrm{Im}\Omega_L^S\end{aligned} \tag{3.94}$$

The crossed terms do vanish because $\tilde{\mu}_L = \tilde{\nu}_L = 0$ at $t = T$.

### Region $X_L^\infty|_{(T,T+1]} \times S^1_L$

Finally we analyse the gluing region $(T, T+1]$. In this region, we have

$$\begin{aligned}\omega_L^T &= \omega_L^\infty = (\gamma_L^*)^2 dt \wedge d\theta_L^* + \omega_L^S \,, \\ \Omega_L^T &= \Omega_L^\infty = \gamma_L^* d\theta_L^* \wedge \Omega_L^S - i\gamma_L^* dt \wedge \Omega_L^S \,.\end{aligned} \tag{3.95}$$

Furthermore, the three-form $\varphi_L$ and four-forms $*\varphi_L$ are given by, respectively,

$$\varphi_L = \gamma_L d\theta_L \wedge \omega_L^T + \mathrm{Re}\Omega_L^T \,, \tag{3.96}$$
$$*\varphi_L = \tfrac{1}{2}(\omega_L^T)^2 - \gamma_L d\theta_L \wedge \mathrm{Im}\Omega_L^T + *\tilde{\varphi}_L^T \,. \tag{3.97}$$

Notice that the extra term $*\tilde{\varphi}_L^T$ in $\varphi_L$ is due to the cutting of the left side at $t = T+1$, which modifies the metric in the Hodge star $*$ and therefore induces the correction of order $O(e^{-\lambda\gamma_L^* T})$ for any $\lambda > 0$, as introduced in (2.19).

Following the same procedure adopted to reduce the integrals in the previous two regions, we

use equations (3.95), (3.96) and (3.97) to obtain

$$\begin{aligned}\int\limits_{X_L^\infty|_{(T,T+1]}\times S^1_L} \varphi_L \wedge *\varphi_L =&(\gamma_L^*)^2\gamma_L \int\limits_0^{2\pi}\int\limits_{S_L}\int\limits_0^{2\pi}\int\limits_T^{T+1}\Big[\frac{3}{2}d\theta_L^*\wedge(\omega_L^S)^2\wedge d\theta_L\wedge dt \\ &+ d\theta_L^*\wedge(\mathrm{Re}\Omega_L^S)^2\wedge d\theta_L\wedge dt + d\theta_L^*\wedge(\mathrm{Im}\Omega_L^S)^2\wedge d\theta_L\wedge dt\Big] \\ &+\int\limits_0^{2\pi}\int\limits_{S_L}\int\limits_0^{2\pi}\int\limits_T^{T+1}\varphi_L\wedge*\tilde{\varphi}_L \\ =&\,4\pi^2(\gamma_L^*)^2\gamma_L\int\limits_{S_L}\left[\frac{3}{2}(\omega_L^S)^2+(\mathrm{Re}\Omega_L^S)^2+(\mathrm{Im}\Omega_L^S)^2\right] \\ &+O(e^{-\lambda\gamma_L^* T})\,.\end{aligned} \tag{3.98}$$

The final expression for the Kähler potential — defined in equation (3.71) — in terms of the constituents of the twisted connected sum adds the contributions from all the pieces given by equations (3.90), (3.94) and (3.98) — together with similar contributions from the right-side of the construction. Notice that $\tilde{\mu}=\mu$ and $\tilde{\nu}=\nu$ at $t=T-1$. Furthermore, we use the identification of the radii by equation (2.29). Therefore, the Kähler potential can be written as

$$\begin{aligned}K =&-3\log\left(\frac{1}{7}\int\limits_{Y_r=Y_L\cup Y_R}\varphi\wedge*\varphi\right) \\ =&-3\log\Bigg[\frac{1}{7}\Bigg(\pi\gamma\int\limits_{K_L}\omega_L|^3_{K_L}+2\pi\gamma\int\limits_{K_L}\mathrm{Re}\Omega_L|_{K_L}\wedge\mathrm{Im}\Omega_L|_{K_L} \\ &4\pi^2(T+1)\gamma^3\int\limits_{S_L}\left[\frac{3}{2}(\omega_L^S)^2+(\mathrm{Re}\Omega_L^S)^2+(\mathrm{Im}\Omega_L^S)^2\right]+O(e^{-\lambda\gamma T})\Bigg)\Bigg] \\ &+(\text{right-side})\,.\end{aligned} \tag{3.99}$$

The so-called *Hitchin functional* $H(\varphi)$ on a real seven-dimensional manifold $Y$ is defined as the total volume of $Y$ with respect to the metric and orientation determined by $\varphi$ on $Y$ [198, 233]. In other words, it is given by

$$H(\varphi) := \frac{1}{7}\int_Y \varphi\wedge *_{g_\varphi}\varphi\,. \tag{3.100}$$

Therefore we notice that the Hitchin functional determines the Kähler potential. Furthermore, Hitchin proved that a closed stable three-form $\varphi$ is a critical point of $H(\varphi)$ in its cohomology class if and only if $\varphi$ is co-closed, i.e. $\mathrm{d}(*_{g_\varphi}\varphi)=0$ [198]. In other words, when restricted

to a closed $G_2$-structure $\varphi$ in a fixed cohomology class, the torsion-free $G_2$-structures are the critical points of $\Phi$. As $T$ approaches $\infty$ in the Kovalev limit, the $G_2$-structure $\tilde{\varphi}(\gamma, T)$ becomes torsion-free — recall chapter 3. Therefore, this is a critical point of the Hitchin functional. On the one hand, due to appearance of the term $4\pi^2(T+1)\gamma^3$, the Hitchin functional mainly depends on the volume of the K3 surface glued together since this diverges as $T \to \infty$. On the other hand, because of lack of further information about the compact subspaces $K_{L/R} \subset X_{L/R}$, there is no definite method to determine the integration over $K_{L/R}$.

In the next section we analyse the spectrum of the four-dimensional low-energy effective theory and see how this helps to obtain a final expression for the Kähler potential (and Hitchin functional).

### 3.4.2 The four-dimensional $\mathcal{N} = 1$ effective supergravity spectrum

In section 2.2.4, the properties of the building blocks $(Z_{L/R}, S_{L/R})$ determined the cohomology equations (2.56). After discussing the generalities of M-theory compactifications on $G_2$-manifolds, we are now ready to investigate M-theory compactifications on the specific case of twisted connected sum $G_2$-manifolds. Therefore, we are interested in determining how the four-dimensional $\mathcal{N} = 1$ effective supersymmetric spectrum of M-theory compactifications on $G_2$-manifolds according to table 3.1 is now specified for the case of twisted connected sum $G_2$-manifolds. More precisely, let us determine the dependence of the spectrum in table 3.1 on the building blocks $(Z_{L/R}, S_{L/R})$ of the twisted connected sum construction by delving into the three- and two-form cohomology $H^3(Y,\mathbb{Z})$ and $H^2(Y,\mathbb{Z})$, respectively. Furthermore, we find the emergence of interesting extended supersymmetric gauge sectors on the twisted connected sum constituents.

#### Three-form cohomology $H^3(Y,\mathbb{Z})$

Let us first focus on the four-dimensional neutral $\mathcal{N} = 1$ chiral moduli multiplets $\Phi^i$, which are associated with the three-form cohomology $H^3(Y,\mathbb{Z})$. Recall that the three-form cohomology $H^3(Y,\mathbb{Z})$ is given by

$$\begin{aligned} H^3(Y,\mathbb{Z}) \;=\; & \ker\Big(H^3(Y_L,\mathbb{Z}) \oplus H^3(Y_R,\mathbb{Z}) \xrightarrow{(\iota_L^*,-\iota_R^*)} H^3(T^2\times S,\mathbb{Z})\Big) \\ & \oplus \operatorname{coker}\Big(H^2(Y_L,\mathbb{Z}) \oplus H^2(Y_R,\mathbb{Z}) \xrightarrow{(\iota_L^*,-\iota_R^*)} H^2(T^2\times S,\mathbb{Z})\Big)\,, \end{aligned} \tag{3.101}$$

and the two summands ker and coker are specified in terms of the building blocks $(Z_{L/R}, S_{L/R})$ as

$$\begin{aligned} &\ker\Big(H^3(Y_L,\mathbb{Z}) \oplus H^3(Y_R,\mathbb{Z}) \to H^3(T^2\times S,\mathbb{Z})\Big) \\ &\qquad = H^3(Z_L,\mathbb{Z}) \oplus H^3(Z_R,\mathbb{Z}) \oplus k_L \oplus k_R \oplus N_L \cap T_R \,\oplus\, N_R \cap T_L\,, \\ &\operatorname{coker}\Big(H^2(Y_L,\mathbb{Z}) \oplus H^2(Y_R,\mathbb{Z}) \to H^2(T^2\times S,\mathbb{Z})\Big) \;=\; \mathbb{Z}[S\,] \oplus L/\,(N_L + N_R)\;. \end{aligned} \tag{3.102}$$

Moreover, recall that $\rho^*_{L/R} : H^2(X_{L/R},\mathbb{Z}) \to L$ defines $k_{L/R} := \ker\rho^*_{L/R}$ and $N_{L/R} := \operatorname{Im}\rho^*_{L/R}$,

where $L$ is the K3 lattice $L \simeq H^2(S_L, \mathbb{Z}) \simeq H^2(S_R, \mathbb{Z})$. Furthermore, $T_{L/R} = N_{L/R}^{\perp}$.

According to equation (3.102), we can decompose $H^3(Y, \mathbb{Z})$ in terms of the corresponding orderly three-form cohomology representatives

$$\langle\!\langle \Theta_A \rangle\!\rangle \;=\; \langle\!\langle \theta_l^L \rangle\!\rangle \oplus \langle\!\langle \theta_r^R \rangle\!\rangle \oplus \langle\!\langle \omega_{a_l}^L \rangle\!\rangle \oplus \langle\!\langle \omega_{a_r}^R \rangle\!\rangle \oplus \langle\!\langle \tau_{i_l}^L \rangle\!\rangle \oplus \langle\!\langle \tau_{i_r}^R \rangle\!\rangle \oplus \langle\!\langle V^{K3} \rangle\!\rangle \oplus \langle\!\langle \tau_j^{L\cup R} \rangle\!\rangle \,. \tag{3.103}$$

If we now expand the torsion-free $G_2$-structure $\varphi$ of $Y$ similarly as in equation (3.12) in terms of the basis $\langle\!\langle \Theta_A \rangle\!\rangle$, the individual elements will have the following interpretations

- $\theta_l^L$ are Poincaré duals to four-cycles $S_L^1 \times \gamma_l^L \in H_4(Y_L) = H_4(S_L^1 \times \gamma_l^L)$, with a basis of homology three-cycles $\gamma_l^L \in H_3(X_L)$,
- $[\omega_{a_l}^L] = [\Gamma_{a_l}^L]$ with basis $[\Gamma_{a_l}^L]$ of Poincaré dual homology four-cycles in $H_4(X_L)$,
- $\tau_{i_l}^L$ in $Y_L = S^1_{\text{diag}} \times X_L$ are Poincaré duals to $C_{i_l}^L \in H_4(X_L, \partial X_L)$, where $\partial C_{i_l}^L = S^1_{\text{diag}} \times \mathcal{T}_{i_l}^L \neq 0$ in terms of $\mathcal{T}_{i_l}^L$, which are transcendental two-cycles with respect to the K3 surface $S_L$ and Picard two-cycles with respect to the K3 surface $S_R$,
- $V^{K3}$ is Poincaré dual to four-cycles $\mathcal{V}^{K3}$ with $\partial \mathcal{V}^{K3} = S_L \simeq S_R$ ,
- $\tau_j^{L\cup R}$ are Poincaré duals to four-cycles $C_j^{L\cup R}$ that give rise to boundary three-cycles $\mathcal{T}_j^{L\cup R}$, where the boundary is $\partial \mathcal{T}_j^{L\cup R} = S^1_{\text{diag}} \times \mathcal{T}_j^{L\cup R}$ in terms of transcendental two-cycles $\mathcal{T}_j^{L\cup R}$, with respect to both K3 surfaces $S_L$ and $S_R$.

In an analogous way, we define the elements $\theta_r^R$, $[\omega_{a_r}^R]$ and $\tau_{i_r}^R$.

In the Kovalev limit, the coefficients of these individual cohomology elements capture particular geometric moduli of the twisted connected sum and their summands as we further detail in the following.

- *Kernel contributions*

  First of all, the kernel contributions in equation (3.102) describe the moduli of the asymptotically cylindrical Calabi–Yau manifolds $X_{L/R}$. The coefficients of $H^3(Z_{L/R})$ and $k_{L/R}$ realize the complex structure moduli and the Kähler moduli of the asymptotically cylindrical Calabi–Yau manifolds $X_{L/R}$, respectively. Moreover, $N_L \cap T_R$ captures mutual Kähler moduli of $X_L$ and complex structure moduli of $X_R$, which are interlinked in this way due to the non-trivial gluing with the hyper-Kähler rotation given in equation (2.27) that exchanges $X_L$ and $X_R$. The intersection $N_R \cap T_L$ follows an analog interpretation.

- *Cokernel contributions*

  Second of all, we analyze the cokernel contribution in equation (3.102). To get a better geometric picture for these moduli, let us explain why we can view the resulting $G_2$-manifold $Y$ as a topological K3 fibration. Due to the K3 fibrations $Z_{L/R} \to \mathbb{P}^1$, the

Calabi–Yau threefolds $X_{L/R}$ are K3 fibrations over a disk $D_{L/R}$. As a result, both $Y_{L/R}$ become K3 fibrations over solid tori $T_{L/R} \equiv S^1_{L/R} \times D_{L/R}$, i.e.,

$$\begin{array}{ccc} S_{L/R} & \longrightarrow & Y_{L/R} \\ & & \big\downarrow \pi \\ & & T_{L/R} \, . \end{array} \tag{3.104}$$

The gluing diffeomorphism given in equation (2.28) of the twisted connected sum construction identifies the boundary of the disk $D_L$ with the circle $S^1_R$ and the circle $S^1_L$ with the boundary of the disk $D_R$. Therefore, the two solid tori $T_{L/R}$ are glued together to a three-sphere $S^3$. It is in this sense that the resulting $G_2$-manifold $Y$ is a *topological K3 fibration*[12]

$$\begin{array}{ccc} S & \longrightarrow & Y \\ & & \big\downarrow \pi \\ & & S^3 \, . \end{array} \tag{3.105}$$

The cohomology three-forms of the cokernel in equation (3.102) describe moduli of the asymptotic boundary of $\partial Y_L \simeq \partial Y_R \simeq T^2 \times S$. Their dual homology three-cycles restrict to relative three-cycles in the summands $Y_L$ and $Y_R$, and hence the associated moduli are sensitive to the overlapping gluing regions $Y_{L/R}(T) \setminus K_{L/R}$ — recall figure 2.1. In particular, the three-form generator $[S]$ is Poincaré dual to a K3 fiber $S$, and hence its dual homology three-cycle is interpreted as the base $S^3$ of the K3 fibration of the diagram (3.105). As a consequence, the modulus associated to $[S]$ measures the volume of the base $S^3$. Similarly, the remaining cokernel moduli measure volumes of three-cycles that project under the map $\pi : Y \to S^3$ to paths in the base $S^3$ connecting the disjoint compact subsets $\pi(K_L)$ and $\pi(K_R)$ of $S^3$. Note that $2T + 1$ is the distance between these two compact subsets in terms of the parameter $T$ introduced in section 2.2.3. Therefore, it now follows that — in the Kovalev limit — all cokernel moduli depend linearly on the parameter $T$. Hence, $T$ enjoys the geometric interpretation of a *squashing parameter* for the base $S^3$ of the K3 fibration of diagram (3.105).

- *The two universal geometric moduli: the volume and the squashing parameter*

  It is interesting to comment on some distinctions encountered in the spectrum of general $G_2$-manifolds and the twisted connected sum $G_2$-manifolds. The split into two types of moduli fields in equation (3.102) motivates the introduction of *two universal geometric moduli* $v$ and $b$. For any $G_2$-manifold, there is a universal *volume modulus* $v$, associated to the singlet $H^3_{\mathbf{1}}(Y, \mathbb{Z})$ of the three-form cohomology as we have already seen. This modulus simply rescales the torsion-free $G_2$-structure $\varphi$. In the twisted connected sum, we additionally identify the squashing modulus $b$ of the base $S^3$ in the fibration of the diagram (3.105). Note that $b \to +\infty$ describes the Kovalev limit discussed in section 2.2.3. According to equation (3.12), we write the torsion-free $G_2$-structure $\varphi$ depending on these

[12] See also reference [234] for a recent account on the topological K3 fibration in the context of the twisted connected sum construction.

two moduli as

$$\varphi(v, b, \tilde{S}) \;=\; v\left[\left(\rho_0^{\text{ker}} + \sum_{\hat{\imath}} \tilde{S}^{\hat{\imath}}\rho_{\hat{\imath}}^{\text{ker}}\right) + b\left([S] + \sum_{\tilde{\imath}} \tilde{S}^{\tilde{\imath}}\rho_{\tilde{\imath}}^{\text{coker}}\right)\right] . \tag{3.106}$$

Here $[S]$ is the harmonic three-form that is Poincaré dual to the K3 fiber $S$. Furthermore, from now on we generically call $(\rho_0^{\text{ker}}, \rho_{\hat{\imath}}^{\text{ker}})$ and $\rho_{\tilde{\imath}}^{\text{coker}}$ as basis of harmonic three-forms arising from the kernel contributions and the cokernel part $L/\,(N_L + N_R)$ in (3.102), respectively, with $\tilde{S}^{\hat{\imath}}$ and $\tilde{S}^{\tilde{\imath}}$ their respective associated geometric real moduli fields.[13]

- *The Kovalevton: a four-dimensional $\mathcal{N} = 1$ neutral chiral multiplet*

  The description of the torsion-free $G_2$-structure $\varphi(v, b, \tilde{S})$ therefore gives rise to two universal $\mathcal{N} = 1$ neutral chiral moduli multiplets $\nu$ and $\varkappa$ in the effective four-dimensional theory, which are given by

$$\text{Re}(\nu) \;=\; v\,, \qquad \text{Re}(\varkappa) \;=\; vb\,. \tag{3.107}$$

  In particular, we refer to the chiral multiplet $\varkappa$ as the *Kovalevton* since it describes the Kovalev limit discussed in section 2.2.3 in the limit $\text{Re}(\varkappa) \to +\infty$ — while $\text{Re}(\nu)$ is kept constant.

  The remaining real moduli fields $\tilde{S}^{\hat{\imath}}$ and $\tilde{S}^{\tilde{\imath}}$ are not universal and relate to the non-universal neutral chiral multiplets $\phi^{\hat{\imath}}$ and $\phi^{\tilde{\imath}}$ in the following way

$$\text{Re}(\phi^{\hat{\imath}}) \;=\; v\tilde{S}^{\hat{\imath}}\,, \qquad \text{Re}(\phi^{\tilde{\imath}}) \;=\; vb\tilde{S}^{\tilde{\imath}}\,. \tag{3.108}$$

  These depend on the topological details of the building blocks $(Z_{L/R}, S_{L/R})$ and the choice of the gluing diffeomorphism in equation (2.28).

### Two-form cohomology $H^2(Y, \mathbb{Z})$

Let us now analyze the two-form cohomology $H^2(Y, \mathbb{Z})$ for (smooth) $G_2$-manifolds, which yields four-dimensional massless abelian $\mathcal{N} = 1$ vector multiplets, cf. table 3.1. In Kovalev's twisted connected sum, we get two types of abelian $\mathcal{N} = 1$ vector multiplets according to equation (2.56). To see this, first of all recall that the two-form cohomology $H^2(Y, \mathbb{Z})$ is given by

$$H^2(Y, \mathbb{Z}) \;\simeq\; (k_L \oplus k_R) \oplus (N_L \cap N_R)\;. \tag{3.109}$$

- *Kernel contributions*

  Firstly, the kernel contributions $k_L$ and $k_R$ associate to zero modes of the two summands $Y_L$ and $Y_R$. Hence $Y_{L/R}$ can be viewed as the local geometries governing these gauge theory degrees of freedom. As the individual summands $Y_{L/R} = S^1_{L/R} \times X_{L/R}$ have SU(3) holonomy in the Kovalev limit, we expect that the two gauge theory sectors of the kernels

[13] Note that the kernel contribution in equation (3.102) is at least one-dimensional. In this way we can always choose a basis element $\rho_0^{ker}$ [141].

$k_L$ and $k_R$ exhibit $\mathcal{N} = 2$ supersymmetry. In fact, in addition to the abelian $\mathcal{N} = 1$ vector multiplet, notice that the kernels $k_{L/R}$ of the local geometries $Y_{L/R}$ also contribute to the three-form cohomology $H^3(Y, \mathbb{Z})$ resulting in $\mathcal{N} = 1$ neutral chiral multiplets. Thus, the abelian $\mathcal{N} = 1$ vector and the neutral $\mathcal{N} = 1$ chiral multiplets associated to $k_{L/R}$ combine into *four-dimensional* $\mathcal{N} = 2$ *vector multiplets*.

- $N_L \cap N_R$ *contributions*

  Secondly, the abelian $\mathcal{N} = 1$ vector multiplets obtained from the intersection $N_L \cap N_R$ can be attributed to the local geometry of the asymptotic region $Y_L(T) \cap Y_R(T) \simeq T^2 \times S \times (0, 1)$, which has SU(2) holonomy in the Kovalev limit. Thus, we expect that these $\mathcal{N} = 1$ vector multiplets give rise to a *four-dimensional abelian* $\mathcal{N} = 4$ *gauge theory sector*, which can be seen as follows.

  To any two-form $\omega^{(2)}$ in $N_L \cap N_R$ of the K3 surface $S$, we attribute the three-forms

  $$\omega^{(2)} \wedge h(t) d\theta_L \,, \qquad \omega^{(2)} \wedge h(t) d\theta_R \,, \qquad \omega^{(2)} \wedge h(t) dt \,, \tag{3.110}$$

  in terms of the coordinates $\theta_{L/R}$ of the circles $S^1_L$ or $S^1_R$ such that $S^1_L \times S^1_R \simeq T^2$ and the smooth bump function $h(t)$ in the coordinate $t$ of the interval $(0, 1)$.[14] These three-forms yield geometrically non-trivial cohomology elements of compact support in $H^3_c(T^2 \times S \times (0, 1), \mathbb{Z})$ , which give rise to normalizable scalar fields. In a combination with three scalar deformations of the hyper-Kähler metric of the K3 surface $S$ to three complex scalar moduli fields, these furnish three four-dimensional neutral $\mathcal{N} = 1$ chiral multiplets. These three $\mathcal{N} = 1$ chiral multiplets combine with the $\mathcal{N} = 1$ vector multiplet of $\omega^{(2)}$ to one $\mathcal{N} = 4$ *vector multiplet*.[15]

  Note that the three-forms in equation (3.110) canonically extend to Kovalev's $G_2$-manifold $Y$. However, they become trivial in cohomology because $N_L \cap N_R$ is not an element of $H^3(Y, \mathbb{Z})$ according to equation (3.101). Nevertheless, we can Fourier expand any of these three-forms into eigenforms with respect to the three-form Laplacian $\Delta$ of the $G_2$-manifold $Y$. By a simple scaling argument we find that the eigenvalues of these three-form Fourier modes scale with $T^{-1}$, i.e., they are inversely proportional to the parameter $T$ realizing the Kovalev limit. Therefore, we argue that the normalizable zero modes associated to the three-forms in equation (3.110) acquire a mass term $m^2 \simeq \mathcal{O}(T^{-1})$, which vanishes in the Kovalev limit. Furthermore, we expect that the scalar fields associated to the hyper-Kähler metric deformations are generically obstructed at first order by a mass term that also vanishes in the Kovalev limit. As a consequence, the massless four-dimensional abelian $\mathcal{N} = 4$ vector multiplets of the asymptotic region decomposes into a massless

[14] The bump function $h(t)$ is given by a smooth non-negative function $h(t) : (0, 1) \to \mathbb{R}$ with compact support, which is normalized such that $\int_0^1 h(t) dt = 1$.

[15] Alternatively, we can consider the five-dimensional theory obtained from M-theory on $T^2 \times S$ with SU(2) holonomy. Then the two-form cohomology element $\omega^{(2)}$ is accompanied by the two three-form cohomology elements $\omega^{(2)} \wedge d\theta_{L/R}$. Combined with the mentioned three hyper-Kähler metric deformations, these cohomology elements provide the zero modes of five scalar fields, which — together with the vector field and the superpartners — assemble into a five-dimensional $\mathcal{N} = 2$ vector multiplet for each harmonic two-form $\omega^{(2)}$. Upon dimensional reduction to four dimensions, we arrive at four-dimensional $\mathcal{N} = 4$ vector multiplets.

four-dimensional abelian $\mathcal{N} = 1$ vector multiplet and three massive four-dimensional $\mathcal{N} = 1$ chiral multiplets with masses of order $\mathcal{O}(T^{-1/2})$. Therefore, we expect that the four-dimensional $\mathcal{N} = 4$ gauge theory sector is only realized in the strict Kovalev limit $T \to +\infty$.

We summarize the discussed local abelian gauge theory sectors in table 3.2. In particular, we find that in the Kovalev limit — at least in the absence of background four-form fluxes and for smooth $G_2$-manifolds $Y$ — the spectrum of all abelian gauge theory sectors exhibit extended supersymmetry. The observed extended supersymmetries of the local geometries appearing in Kovalev's twisted connected sum become relevant in sections 4.1 and 4.2 because they impose strong constraints on the possibility of non-Abelian gauge theory sectors with charged matter fields, which are ingredients of the Standard Model.

| local geometry | multiplicity of $\mathcal{N} = 1$ multiplets | | $U(1)$ vector multiplets | |
|---|---|---|---|---|
| (Kovalev limit) | $U(1)$ vectors | chirals | multiplicity | supersym. |
| $Y_L = S^1_L \times X_L$ SU(3) holonomy | $\dim k_L$ | $\dim k_L$ | $\dim k_L$ | $\mathcal{N} = 2$ |
| $Y_R = S^1_R \times X_R$ SU(3) holonomy | $\dim k_R$ | $\dim k_R$ | $\dim k_R$ | $\mathcal{N} = 2$ |
| $T^2 \times S \times (0,1)$ SU(2) holonomy | $\dim N_L \cap N_R$ | $3 \cdot \dim N_L \cap N_R$ | $\dim N_L \cap N_R$ | $\mathcal{N} = 4$ |

Table 3.2: The abelian gauge theory sectors of the local geometries appearing in twisted connected sum $G_2$-manifolds in the Kovalev limit $T \to +\infty$. The left column specifies the Ricci-flat local geometries with their associated holonomy groups. The middle column lists the four-dimensional $\mathcal{N} = 1$ neutral chiral multiplets that assemble in the right column to four-dimensional vector multiplets of extended supersymmetry ($\mathcal{N} = 2$ and $\mathcal{N} = 4$).

### 3.4.3 The final Kähler potential and its phenomenological properties

The aim of this section is to describe the universal properties of the four-dimensional low-energy effective action in terms of the universal chiral multiplets $\nu$ and $\varkappa$ identified in the previous section. More precisely, we find a final expression for the Kähler potential for the universal chiral multiplets $\nu$ and $\varkappa$ in the Kovalev limit.

First of all, while keeping the ratio $\mathrm{Re}(\nu)/\mathrm{Re}(\varkappa)$ constant, the chiral multiplet $\nu$ directly relates to the (dimensionless) overall volume modulus $R$ of section 2.2.3 via

$$\mathrm{Re}(\nu) \;=\; R^3 \;. \tag{3.111}$$

This relation occurs because the $\mathrm{Re}(\nu)$ measures (dimensionless) volumes of three-cycles while $R = \gamma/\gamma_0$ measures (dimensionless) length scales in the $G_2$-manifold $Y$. Apart from the overall

volume dependence, the Kovalevton $\varkappa$ measures the squashed volume of the $S^3$ base. Therefore, from expression (2.47) of the volume $V_Y(\tilde{S}, R, T)$ we obtain the relation

$$\mathrm{Re}(\varkappa) \;=\; (2\pi)^2 R^3 (2T + \alpha(\tilde{S}))\,, \tag{3.112}$$

where $\tilde{S}$ denotes collectively the remaining geometric moduli fields $\tilde{S}^{\tilde{\imath}}$ and $\tilde{S}^{\hat{\imath}}$.

The obtained Kähler potential for general $G_2$-manifolds, in terms of the volume $V_Y(\tilde{S}, R, T)$, is

$$K = -3\log\left(\frac{1}{7}\int_Y \varphi \wedge *_{g_\varphi}\varphi\right) = -3\log\left(\frac{1}{\gamma_0^7} V_Y(\tilde{S}, R, T)\right)\,. \tag{3.113}$$

With the help of equation (2.47), in the Kovalev limit, we therefore obtain

$$\begin{aligned} K(\nu, \bar{\nu}, \varkappa, \bar{\varkappa}) &= -3\log\Big[(2\pi)^2 R^7 V_S^{\tilde{g}}(\tilde{\rho}_S)\left(2T + \alpha(\tilde{S})\right)\Big] \\ &= -3\log(R^4) - 3\log\Big[(2\pi)^2 R^3\left(2T + \alpha(\tilde{S})\right)\Big] - 3\log(V_S^{\tilde{g}}) \\ &= -4\log(R^3) - 3\log\Big[(2\pi)^2 R^3\left(2T + \alpha(\tilde{S})\right)\Big] - 3\log(V_S^{\tilde{g}})\,. \end{aligned} \tag{3.114}$$

Therefore, with the identifications of the universal chiral multiplets in equations (3.111) and (3.112), the universal structure of the four-dimensional low-energy effective $\mathcal{N} = 1$ supergravity action is governed by the Kähler potential

$$K(\nu, \bar{\nu}, \varkappa, \bar{\varkappa}) \;=\; -4\log(\nu + \bar{\nu}) - 3\log(\varkappa + \bar{\varkappa}) - 3\log\left(V_S^{\tilde{g}}(\tilde{S})\right)\,. \tag{3.115}$$

**Regime of validity and phenomenological/cosmological properties**

Let us now discuss some basic properties of the derived Kähler potential. First of all, the structure of the Kähler potential is reminiscent of the Kovalev limit, in which the volume of the $G_2$-manifold is dominated by the cylindrical region $S \times T^2 \times I$ in terms of the interval $I$ of size $2T + 1$. In other words, in this limit the individual summands in equation (3.115) reflect the volume of the K3 surface $S$, the squashed volume of the $S^3$ base dominated by $T^2 \times I$, and the moduli dependence of the K3 fiber $S$ on the non-universal moduli $\tilde{S}$. As long as we treat the non-universal moduli fields $\tilde{S}$ as constants, the Kähler geometry for the universal Kähler moduli $\nu$ and $\varkappa$ factorizes into two (complex) one-dimensional parts with a block diagonal Kähler metric. However, this block structure in the Kähler metric vanishes as soon as we treat the non-universal moduli fields $\tilde{S}$ dynamically, because relation (3.108) implies that the real geometric moduli $\tilde{S}$ also depend non-trivially on the chiral fields $\nu$ and $\varkappa$ as

$$\tilde{S}^{\hat{\imath}} = \frac{\phi^{\hat{\imath}} + \bar{\phi}^{\hat{\imath}}}{\nu + \bar{\nu}}\,, \qquad \tilde{S}^{\tilde{\imath}} = \frac{\phi^{\tilde{\imath}} + \bar{\phi}^{\tilde{\imath}}}{\varkappa + \bar{\varkappa}}\,. \tag{3.116}$$

Furthermore, note that this Kähler potential is only a valid approximation both in the large volume regime and in the Kovalev regime, where quantum corrections and metric corrections of

the asymptotically cylindrical Calab–Yau threefolds are suppressed. The semi-classical large volume limit arises when both $\mathrm{Re}(\nu)$ and $\mathrm{Re}(\varkappa)$ are taken sufficiently large, and when $\mathrm{Re}(\varkappa)$ is (parametrically) larger than $\mathrm{Re}(\nu)$ — cf. the discussion at the end of section 2.2.3 — while the corrections to the $G_2$-metric in the twisted connected sum are suppressed.

Observe that, in terms of the inverse Kähler metric $K^{i\bar{\jmath}}$, the Kähler potential (3.115) with the non-universal moduli fields $\tilde{S}$ treated as constants satisfies

$$K^{i\bar{\jmath}}\partial_i K \partial_{\bar{\jmath}} K - 3 \;=\; 4 \;\geq\; 0\,, \qquad i \in \{\nu, \varkappa\},\ \bar{\jmath} \in \{\bar{\nu}, \bar{\varkappa}\}\,. \tag{3.117}$$

This implies that the *no-scale inequality* $K^{i\bar{\jmath}}\partial_i K \partial_{\bar{\jmath}} K - 3 \geq 0$ is fulfilled (but not saturated). The no-scale inequality is a property of the Kähler potential only, and it guarantees that the scalar potential of the described four-dimensional $\mathcal{N} = 1$ supergravity theory is positive semi-definite for any non-vanishing superpotential [235]. As a consequence, the analyzed Kähler potential (of the two chiral fields $\nu$ and $\varkappa$ only) does not admit a negative cosmological constant and hence no (supersymmetric) anti-de-Sitter vacua.

According to equation (2.47), if we include the leading order correction to the Kovalev limit, the Kähler potential will have the form

$$K = -\log\left[\left(V_S^{\tilde{g}}(\tilde{S})\right)^3 (\nu+\bar{\nu})^4(\varkappa+\bar{\varkappa})^3 + A(\tilde{S}, \nu+\bar{\nu}, \varkappa+\bar{\varkappa})\,\exp\left(-\lambda\frac{\varkappa+\bar{\varkappa}}{(\nu+\bar{\nu})^{1/3}}\right)\right]\,, \tag{3.118}$$

where the coefficient $A(\tilde{S}, \nu+\bar{\nu}, \varkappa+\bar{\varkappa})$ of the exponentially suppressed correction is expected to generically depend on both universal and non-universal geometric moduli fields. Once we better understand such corrections, a detailed analysis of this class of Kähler potential may also exhibit interesting phenomenological properties.

CHAPTER 4

# Gauge sectors on twisted connected sum $G_2$-manifolds

In the previous chapters we have introduced the mathematical aspects of generic $G_2$-manifolds and, particularly, of the twisted connected sum construction of $G_2$-manifolds. After reviewing the four-dimensional effective low-energy spectrum of M-theory compactifications on generic $G_2$-manifolds and carefully performing the same compactification on $G_2$-manifolds of the twisted connected sum type, the identification of the Kovalev limit allowed us to obtain universal chiral multiplets and predict gauge theory sectors of extended supersymmetry for the latter case. In this chapter, all the work presented so far culminates in the appearance of many novel examples of $G_2$-manifolds and into several interesting mathematical, physical and phenomenological application emerging from the careful study of their gauge theory sectors.

We apply the orthogonal gluing method from section 2.2.6 to Fano and toric semi-Fano building blocks to algorithmically find the novel twisted connected sum $G_2$-manifolds, and we also explain the emergence of the extended $\mathcal{N} = 4$ and $\mathcal{N} = 2$ supersymmetric gauge sectors.

We focus on building blocks $(Z_{L/R}, S_{L/R})$ of polarized K3 surfaces $S_{L/R}$ with Picard lattices of small rank, and generate a list of new examples in order to get an impression of the multitude of possibilities to realize twisted connected sum $G_2$-manifolds in terms of orthogonal gluing. In order to specify a particular semi-Fano threefold, in the following we use the Mori–Mukai classification for Fano threefolds [236] and the Kasprzyk classification for reflexive polytopes with terminal singularities for certain toric semi-Fano threefolds [237, 238]. We label the corresponding semi-Fano threefolds by their respective reference numbers MM#$_\rho$ or/and K# in these classifications, where the subscript $\rho$ in the Mori–Mukai list denotes the Picard number.

## 4.1 Abelian $\mathcal{N} = 4$ gauge theory sectors

Recall from sections 2.2.6 and 3.4.2 as well as table 3.2 that, in the Kovalev limit, the kernels $k_{L/R}$ describe the $\mathcal{N} = 2$ gauge theory sectors. Furthermore, the rank of the intersection lattice $R = N_L \cap N_R$ in the orthogonal pushout $W$ coincides with the rank of the gauge group of the $\mathcal{N} = 4$ gauge theory sector — cf. table 3.2. A particular simple choice of orthogonal gluing is

achieved if the intersection lattice $R$ has rank zero, i.e., $N_L \cap N_R = \{0\}$. We refer to this special case of orthogonal gluing as *perpendicular gluing*, with its trivial orthogonal pushout $W$ denoted by [141]

$$W = N_L \perp N_R \,. \tag{4.1}$$

As a consequence, if the twisted connected $G_2$-manifold is obtained via perpendicular gluing, there is no $\mathcal{N} = 4$ gauge theory sector in the Kovalev limit. Therefore, in this section we study concrete examples of twisted connected sum $G_2$-manifolds obtained via orthogonal gluing with non-trivial intersection lattices $R$ in the orthogonal pushout $W$. We postpone the analysis of the $\mathcal{N} = 2$ sectors to the next section, and in this section we focus on the $\mathcal{N} = 4$ gauge theory sectors.

Enhancement to a non-Abelian gauge group $G$ of rank $r$ would occur if the intersection lattice $R = N_L \cap N_R$ had a sublattice $G(-1)$ of rank $r$, with the pairing given by minus the Cartan matrix of the Lie algebra of $G$ [86]. Then we could *blow-down* the mutual $r$ rational curves of both polarized K3 surfaces $S_{L/R}$ because — by the definition of the intersection lattice $R$ — $G(-1)$ resides in the intersection of both Picard lattices $N_{L/R}$. In this way we would arrive at singular polarized K3 surfaces $S_{L/R}$ resulting in the enhanced $\mathcal{N} = 4$ gauge theory sector with non-Abelian gauge group $G \times \mathrm{U}(1)^{\mathrm{rk}\,R-r}$. However, when using the method of orthogonal gluing, such a gauge theory enhancement is not possible. This happens because the orthogonal complement to $R$ in the polarized K3 surfaces $S_{L/R}$ is required to contain an ample class, which — due to the ampleness — would always have a non-zero intersection with any rational curve, thereby invalidating the requirement in equation (2.72). As a result, we therefore always arrive at four-dimensional Abelian $\mathcal{N} = 4$ gauge theory sectors with gauge group $\mathrm{U}(1)^{\mathrm{rk}\,R}$ in the Kovalev limit using the orthogonal gluing method.

In the following we study some concrete examples of twisted connected sum $G_2$-manifolds via orthogonal gluing with non-trivial intersection lattice $R$ of rank 1, for building blocks from rank two, three and four semi-Fanos. For orthogonal gluing along an intersection lattice of rank 2 we refer the reader to the full publication [195]. Notice that, for all these cases, if we are able to construct the orthogonal pushout lattice $W$, as required in the first step of the orthogonal gluing method, we guarantee that the building blocks can indeed be constructed, i.e., that steps 2 and 3 of the orthogonal gluing method are satisfied. This is because $\mathrm{rk}N_L + \mathrm{rk}N_R \leq 11$ is always satisfied for the small rank of Picard lattices we study and, therefore, step 3 is also realized.

**Orthogonal gluing of rank two semi-Fano threefolds**

In the first version of reference [211], Crowley and Nordström classify, for rank two Fano threefold building blocks, all possible non-trivial orthogonal gluings to twisted connected sum $G_2$-manifolds except for one missing pair. According to table 4 in the first version of [211], the orthogonal gluing between the building blocks $\mathrm{MM5}_2$ and $\mathrm{MM25}_2$ of table 2 was missing. We have worked out this gluing and, after our suggestion, the authors of [211] included it in table 5 of the recent updated version of their work, thereby enumerating nineteen instead of eighteen pairs of twisted connected sum $G_2$-manifolds in their theorem 6.5. As a warm-up, here we present the example of orthogonal gluing of these two rank two Fano threefolds. Furthermore, there is a unique toric semi-Fano threefold with Picard number 2 which is not Fano, given by

the projective bundle — example 4.15 in reference [142],

$$\mathbb{P}(\mathcal{O} \oplus \mathcal{O}(-1) \oplus \mathcal{O}(-1)) \to \mathbb{P}^1 \,, \tag{4.2}$$

where $\mathcal{O}(d)$ stands for $\mathcal{O}_{\mathbb{P}^1}(d)$. The toric realization $P_\Sigma$ of this threefold $P$ arises from the reflexive lattice polytope $\Delta$ and its dual reflexive polytope $\Delta^*$, spanned by the following lattice points $\nu_1, \ldots, \nu_5$ and the dual lattice points $\nu_1^*, \ldots, \nu_5^*$,

$$\begin{array}{lll} \Delta: & \nu_1 = (-1,-1,\ 0) & \Delta^*: \quad \nu_1^* = (-1,-1,\ 1) \\ & \nu_2 = (\ 1,\ 0,\ 0) & \qquad\ \ \nu_2^* = (-1,\ 2,-2) \\ & \nu_3 = (\ 0,\ 1,\ 0) & \qquad\ \ \nu_3^* = (-1,\ 2,\ 1) \\ & \nu_4 = (\ 1,\ 1,\ 1) & \qquad\ \ \nu_4^* = (\ 2,-1,-2) \\ & \nu_5 = (\ 0,\ 0,-1) & \qquad\ \ \nu_5^* = (\ 2,-1,\ 1) \end{array} \tag{4.3}$$

The reflexive lattice polytope $\Delta$ appears as entry K32 in the Kasprzyk classification [237, 238]. In the following we also consider possible orthogonal gluings of this toric semi-Fano of Picard number 2 with the rank two Fano threefolds $\mathrm{MM5}_2$ and $\mathrm{MM25}_2$. Let us first understand this unique toric semi-Fano of Picard number 2 below.

The reflexive lattice polytope $\Delta$ admits two triangulations, both of them realizing the projective bundle (4.2). For one of these triangulations[1] we obtain the Mori cone spanned by the curves $C_B \simeq \mathbb{P}^1$ and the curve $C_F \simeq \mathbb{P}^1 \subset \mathbb{P}^2_F$ in a projective fiber $\mathbb{P}^2_F$. These curves have the following intersection numbers with the toric divisors $D_i$ associated to the vertices $\nu_i$

| | $D_1$ | $D_2$ | $D_3$ | $D_4$ | $D_5$ |
|---|---|---|---|---|---|
| $C_F$: | 1 | 1 | 1 | 0 | 0 |
| $C_B$: | 0 | −1 | −1 | 1 | 1 |

(4.4)

Since the columns in (4.4) contain the linear equivalences between the divisors, we find $D_2 \sim D_3$, $D_4 \sim D_5$, $D_2 \sim D_1 - D_4$. Therefore, the Kähler cone $\mathcal{K}(P_\Sigma)$ is spanned by

$$\mathcal{K}(P_\Sigma) \,=\, \langle\!\langle D_1, D_4 \rangle\!\rangle \,. \tag{4.5}$$

The intersection matrix $\kappa_{P_\Sigma}$ of the generators $D_1$ and $D_4$ with the anti-canonical divisor $-K_{P_\Sigma}$ reads

$$\kappa_{P_\Sigma} \,=\, \begin{pmatrix} 6 & 3 \\ 3 & 0 \end{pmatrix} \,, \tag{4.6}$$

and has discriminant $\Delta^\kappa = -9$. This intersection matrix $\kappa_{P_\Sigma}$ furnishes the intersection pairing of

[1] For the other triangulation the Mori cone takes the form

| | $D_1$ | $D_2$ | $D_3$ | $D_4$ | $D_5$ |
|---|---|---|---|---|---|
| $C_F$: | 1 | 0 | 0 | 1 | 1 |
| $C_B$: | 0 | 1 | 1 | −1 | −1 |

the Picard lattice of the K3 surface in $P_\Sigma$. Furthermore, notice that

$$-K_{P_\Sigma} = \sum_i D_i = D_1 + D_2 + D_3 + D_4 + D_5 \sim D_1 + (D_1 - D_4) + D_2 + (D_1 - D_2) = 3D_1 \quad (4.7)$$

with the triple intersection of the anti-canonical divisor $-K^3_{P_\Sigma} = 54$.

According to the described algorithm of orthogonal gluing given in section 2.2.6 — more precisely due to equation (2.72) —, a pair of Picard lattices $(N_L, N_R)$ of rank two yields a non-trivial orthogonal pushout $W = N_L + N_R$ if the rank one sublattices $W_{L/R} = N_{L/R} \cap T_{R/L}$ are generated by ample classes in the Kähler cone $\mathcal{K}(P_{L/R})$. Therefore, we need to construct two ample classes $A_{L/R}$ and orthogonal lattice vectors $e_{L/R}$ in $N_{L/R}$ with $e_L^2 = e_R^2$, such that indeed $e_{L/R}$ generate the rank one intersection lattice $R$. Crowley and Nordström show that the induced lattice pairing $\langle \cdot, \cdot \rangle_W$ is a well-defined integral lattice pairing if and only if [211]

$$\frac{\Delta_L^\kappa \Delta_R^\kappa}{A_L^2 A_R^2} = k^2 \,, \quad \text{for } k \in \mathbb{Z} \,, \quad (4.8)$$

where $\Delta^\kappa_{L/R}$ are the discriminants of $N_{L/R}$. Moreover, in order to fulfill the matching condition of a rank two semi-Fano threefold $P_{L/R}$ with a rank two Fano threefold $P_{R/L}$, Crowley and Nordström deduce an upper bound for the semi-Fanos $P_{L/R}$ [211]

$$\left| \frac{\Delta^\kappa_{L/R}}{A^2_{L/R}} \right| \leq \frac{8}{5} \,. \quad (4.9)$$

In the above case of the toric semi-Fano of Picard number 2 with toric realization given by the entry K32 in the Kasprzyk classification, equation (4.5) implies that the ample class must be given by $A = nD_1 + mD_4$, where the intersection matrix $\kappa_{P_\Sigma}$ leads to $A^2 = 6n(n+m)$. Therefore, in order to be in accordance with the inequality in equation (4.9), we notice that the only possible ample class is $A = D_1 + D_4$ with $A^2 = D_1^2 + 2D_1D_4 = 12$. For this class, the orthogonal complement $R$ is generated by $e = -D_1 + 3D_4$ with $e^2 = -12$ since $A.e = 0$.

In table 4.1, we give the data of this toric semi-Fano threefold together with the corresponding data for the building blocks of rank two Fano threefolds, giving rise to compatible rank one intersection lattices, i.e., the rank two Fano threefolds with ample classes generated by vectors of length square $-12$. For $\mathrm{MM5}_2$ and $\mathrm{MM25}_2$, the entries are taken from the Crowley–Nordström classification [211].

We recall from section 2.2.6 the expressions for the Betti numbers of twisted connected sum $G_2$-manifolds obtained from the method of orthogonal gluing,

$$\begin{aligned} b_2(Y) &= \mathrm{rk}\, R + \dim k_L + \dim k_R \,, \\ b_3(Y) &= b_3(Z_L) + b_3(Z_R) + \dim k_L + \dim k_R - \mathrm{rk}\, R + 23 \,. \end{aligned} \quad (4.10)$$

Denote $Y^{\cdots}_{\cdots}$ as the twisted connected $G_2$-manifolds obtained from the orthogonal pushout $W^{\cdots}_{\cdots}$ with their Betti numbers computed with equation (4.10). For the entries in table 4.1, condition

| No. | $-K^3$ | $\kappa$ | $\Delta^\kappa$ | $A$ | $e$ | $A^2$ | $e^2$ | $b_3(Z)$ |
|---|---|---|---|---|---|---|---|---|
| K32 (semi-Fano) | 54 | $\begin{pmatrix} 6 & 3 \\ 3 & 0 \end{pmatrix}$ | $-9$ | $\begin{pmatrix} 1 \\ 1 \end{pmatrix}$ | $\begin{pmatrix} -1 \\ 3 \end{pmatrix}$ | 12 | $-12$ | 56 |
| $\mathrm{MM5}_2$ (Fano) | 12 | $\begin{pmatrix} 0 & 3 \\ 3 & 6 \end{pmatrix}$ | $-9$ | $\begin{pmatrix} 1 \\ 1 \end{pmatrix}$ | $\begin{pmatrix} 3 \\ -1 \end{pmatrix}$ | 12 | $-12$ | 26 |
| $\mathrm{MM25}_2$ (Fano) | 32 | $\begin{pmatrix} 0 & 4 \\ 4 & 4 \end{pmatrix}$ | $-16$ | $\begin{pmatrix} 1 \\ 1 \end{pmatrix}$ | $\begin{pmatrix} 2 \\ -1 \end{pmatrix}$ | 12 | $-12$ | 36 |

Table 4.1: The unique rank two $\rho = 2$ toric semi-Fano threefold and the rank two Fano threefolds that admit an intersection lattice $R$ generated by a vector of length square $-12$. The columns show the reference numbers $\mathrm{MM}\#_\rho$ in the Mori–Mukai classification [236] or K# in the Kasprzyk classification [238], the triple intersection of the anti-canonical divisor $-K$, the intersection matrix $\kappa$ of the Picard lattice of the K3 surface, the discriminant $\Delta^\kappa$ of the intersection matrix $\kappa$, the chosen ample class $A$ in the basis of the intersection matrix $\kappa$, the orthogonal complement $e$ to the ample class $A$, the length squares of the classes $A$ and $e$, and the three-form Betti number $b_3(Z)$ of the associated building block $Z$.

(4.8) implies that the two possible gluings with rank one intersection lattices are given by

$$\begin{aligned} W^{\mathrm{K32}}_{\mathrm{MM25}_2} &= N_{\mathrm{K32}} \perp_e N_{\mathrm{MM25}_2} : \quad b_2(Y^{\mathrm{K32}}_{\mathrm{MM25}_2}) = 1 \,, \quad b_3(Y^{\mathrm{K32}}_{\mathrm{MM25}_2}) = 114 \,, \\ W^{\mathrm{MM5}_2}_{\mathrm{MM25}_2} &= N_{\mathrm{MM5}_2} \perp_e N_{\mathrm{MM25}_2} : \quad b_2(Y^{\mathrm{MM5}_2}_{\mathrm{MM25}_2}) = 1 \,, \quad b_3(Y^{\mathrm{MM5}_2}_{\mathrm{MM25}_2}) = 84 \,. \end{aligned} \tag{4.11}$$

Here $b_2(Y) = 1$ is inherited from the rank of the intersection lattice and the trivial kernels in the first equation in (4.10). Furthermore, the third Betti numbers are computed via the second equation in (4.10) with trivial kernels, namely $b_3(Y^{\mathrm{K32}}_{\mathrm{MM25}_2}) = 56 + 36 - 1 + 23 = 114$ and $b_3(Y^{\mathrm{MM5}_2}_{\mathrm{MM25}_2}) = 26 + 36 - 1 + 23 = 84$. The first $G_2$-manifold realizes the only possible combination with the rank two toric semi-Fano threefold K32, whereas the second $G_2$-manifold realizes the non-trivial orthogonal gluing among the rank two Fano threefolds that has been overseen in the first version of reference [211].

### Orthogonal gluing of higher rank semi-Fano threefolds

We now increase the rank of the semi-Fano threefolds and consider the illustrative example of orthogonal gluings along a rank one intersection lattice with the rank three Fano threefold $P_L = \mathbb{P}^1 \times \mathbb{P}^1 \times \mathbb{P}^1$, which has the reference numbers $\mathrm{MM27}_3$ and K62 in the Mori–Mukai and Kasprzyk classifications, respectively [236, 237, 238].

Let $H_i$, $i = 1, 2, 3$, be the hyperplane classes of the respective $\mathbb{P}^1$ factors of this Fano threefold, which generate the three-dimensional Kähler cone

$$\mathcal{K}(P_\Sigma) = \langle\!\langle H_1, H_2, H_3 \rangle\!\rangle \,. \tag{4.12}$$

This is such that the ample anti-canonical divisor becomes $-K_{P_L} = 2H_1 + 2H_2 + 2H_3$, and its

intersection matrix $\kappa_{P_L}$ with the Kähler cone generators reads

$$\kappa_{P_L} = \begin{pmatrix} 0 & 2 & 2 \\ 2 & 0 & 2 \\ 2 & 2 & 0 \end{pmatrix} . \tag{4.13}$$

This intersection matrix $\kappa_{P_L}$ furnishes the intersection pairing of the Picard lattice of the K3 surface in $P_\Sigma$, which corresponds to the ternary quadratic form $q(x, y, z) = 4(xy + yz + zx)$. We focus on orthogonal gluing with the rank one intersection lattice $R$ generated by a vector $e$ of length square[2] $e^2 = -4$. Up to trivial permutations of the Kähler cone generators $H_1$, $H_2$, $H_3$, we use the ternary quadratic form $q(x, y, z) = 4(xy + yz + zx)$ to parametrize all vectors $e$ with $e^2 = -4$ with the help of reference [239]. Therefore, we write

$$e = (d_1 - k)H_1 + (d_2 - k)H_2 + kH_3 , \tag{4.14}$$

where the integers $k, d_1, d_2$ obey

$$k^2 - d_1 d_2 = 1 , \qquad 0 \leq d_1 < k \leq d_2 . \tag{4.15}$$

According to equation (4.12), the ample class is $A = a_1H_1 + a_2H_2 + a_3H_3$, given in terms of positive integers $a_1$, $a_2$, $a_3$. Similarly to the first example, in order to fulfill condition (2.72), we require $A.e = 0$ to find the $k$, $d_1$ and $d_2$. Requiring $A.e = 0$ implies that

$$A.e = 0 \leftrightarrow a_1 d_2 + a_2 d_1 + a_3(d_1 + d_2 - 2k) = 0 . \tag{4.16}$$

Now, noticing that the sum of the first two terms in equation (4.16) is always positive due to positivity of $a_1$, $a_2$, $d_1$ and $d_2$, the orthogonality condition is met only if

$$d_1 + d_2 < 2k \leftrightarrow (d_1 + d_2)^2 < 4k^2 . \tag{4.17}$$

Replacing $k^2$ as given in equation (4.15) on the right-hand side of this inequality, we obtain

$$(d_1 + d_2)^2 < 4k^2 \leftrightarrow (d_2 - d_1)^2 < 4 . \tag{4.18}$$

Since $d_1$ and $d_2$ are positive integers, this condition implies that $d_2 = d_1 + 1$. Therefore, with $0 \leq d_1 < k \leq d_2$, we obtain $k = 1, d_1 = 0, d_2 = 1$. This leads to the following orthogonal lattice vector $e$, generating the rank one intersection lattice $R$,

$$e = -H_1 + H_3 . \tag{4.19}$$

For this vector $e$, the ample class $A = H_1 + H_2 + H_3$ is indeed orthogonal. Therefore, this vector, with $e^2 = -4$, is the only one that generates a rank one intersection lattice $R$ for a left building block $(Z_L, S_L)$ of the Fano threefold $\mathbb{P}^1 \times \mathbb{P}^1 \times \mathbb{P}^1$ — up to trivial relabelling of the Kähler cone

[2] This length square realizes the maximal negative value. We take this because the pairing $\kappa_{P_L}$ is even and vectors with length square $e^2 = -2$ are associated to curves with positive intersection number with any ample class $A$, thereby violating the orthogonal gluing requirement of equation (2.72).

generators.

With $w_1 = H_1 + H_3$ and $w_2 = H_2$, the Picard lattice $N_L$ in terms of $(w_1, w_2, e)$ reads

$$N_L \;=\; \mathbb{Z}\,w_1 + \mathbb{Z}\,w_2 + \mathbb{Z}\,e + \frac{1}{2}\mathbb{Z}\,(w_1 + e)\;. \tag{4.20}$$

To orthogonally glue this left Picard lattice $N_L$ along $e$ with a Picard lattice $N_R$ of a right rank two Fano building block $(Z_R, S_R)$, we find in the Crowley–Nordström classification [211] that the rank two Fano threefolds with Mori–Mukai reference numbers $\mathrm{MM6}_2$, $\mathrm{MM12}_2$, $\mathrm{MM21}_2$, and $\mathrm{MM32}_2$ give rise to compatible intersection lattices. For convenience, these particular building blocks together with some geometric data are summarized in table 4.2. For all these examples, the rank two Picard lattices $N_R$ are generated in the orthogonal basis $(A, e)$ by

$$N_R \;=\; \mathbb{Z}\,A + \mathbb{Z}\,e + \frac{1}{2}\mathbb{Z}\,(A + e)\;, \tag{4.21}$$

with $e^2 = -4$ and the length square of the ample class $A$ as listed in table 4.2.

| No. | $-K^3$ | $\kappa$ | $\Delta^\kappa$ | $A$ | $e$ | $A^2$ | $e^2$ | $b_3(Z)$ |
|---|---|---|---|---|---|---|---|---|
| $\mathrm{MM6}_2$ | 12 | $\begin{pmatrix}2&4\\4&2\end{pmatrix}$ | $-12$ | $\begin{pmatrix}1\\1\end{pmatrix}$ | $\begin{pmatrix}1\\-1\end{pmatrix}$ | 12 | $-4$ | 32 |
| $\mathrm{MM12}_2$ | 20 | $\begin{pmatrix}4&6\\6&4\end{pmatrix}$ | $-20$ | $\begin{pmatrix}1\\1\end{pmatrix}$ | $\begin{pmatrix}1\\-1\end{pmatrix}$ | 20 | $-4$ | 28 |
| $\mathrm{MM21}_2$ | 28 | $\begin{pmatrix}6&8\\8&6\end{pmatrix}$ | $-28$ | $\begin{pmatrix}1\\1\end{pmatrix}$ | $\begin{pmatrix}1\\-1\end{pmatrix}$ | 28 | $-4$ | 30 |
| $\mathrm{MM32}_2$ | 48 | $\begin{pmatrix}2&4\\4&2\end{pmatrix}$ | $-12$ | $\begin{pmatrix}1\\1\end{pmatrix}$ | $\begin{pmatrix}1\\-1\end{pmatrix}$ | 12 | $-4$ | 50 |

Table 4.2: The rank two Fano threefolds admitting an intersection lattice $R$ generated by a vector of length square $-4$. The columns show the reference number in the Mori–Mukai classification, the triple intersection of the anti-canonical divisor $-K$, the intersection matrix $\kappa$ of the Picard lattice of the K3 surface, the discriminant $\Delta^\kappa$ of the intersection matrix $\kappa$, the chosen ample class $A$ in the basis of the intersection matrix $\kappa$, the orthogonal complement $e$ to the ample class $A$, the length squares of the classes $A$ and $e$, and the three-form Betti number $b_3(Z)$ of the associated building block $Z$.

The orthogonal pushout $W = N_L \perp_e N_R$ in the basis $(w_1, w_2, e, A)$ therefore takes the following form

$$W \;=\; \mathbb{Z}\,w_1 + \mathbb{Z}\,w_2 + \mathbb{Z}\,e + \mathbb{Z}\,A + \frac{1}{2}\mathbb{Z}\,(w_1 + e) + \frac{1}{2}\mathbb{Z}\,(A + e)\;, \tag{4.22}$$

where, for the integral generators $(\frac{1}{2}(w_1 + e), w_2, \frac{1}{2}(A + e), e)$, the intersection pairing $\kappa_W$ of the pushout $W$ becomes

$$\kappa_W \;=\; \begin{pmatrix} 0 & 2 & -1 & -2 \\ 2 & 0 & 0 & 0 \\ -1 & 0 & \frac{1}{4}A^2 - 1 & -2 \\ -2 & 0 & -2 & -4 \end{pmatrix}, \qquad \det \kappa_W \;=\; 4A^2\;. \tag{4.23}$$

Notice that the entry $\frac{1}{4}A^2 - 1$ is integral and even according to table 4.2.

For the orthogonal pushouts $W$ of the rank three Fano threefold $\mathbb{P}^1 \times \mathbb{P}^1 \times \mathbb{P}^1$ with reference number $\mathrm{MM27}_3$ and the rank two Fano threefolds listed in table 4.2, we therefore obtain the twisted connected sum $G_2$-manifolds $Y^{\mathrm{MM27}_3}_{\cdots}$, with their corresponding two- and three-form Betti numbers

$$\begin{aligned}
W^{\mathrm{MM27}_3}_{\mathrm{MM6}_2} &= N_{\mathrm{MM27}_3} \perp_e N_{\mathrm{MM6}_2} : \quad b_2(Y^{\mathrm{MM27}_3}_{\mathrm{MM6}_2}) = 1\,, \quad b_3(Y^{\mathrm{MM27}_3}_{\mathrm{MM6}_2}) = 104\,,\\
W^{\mathrm{MM27}_3}_{\mathrm{MM12}_2} &= N_{\mathrm{MM27}_3} \perp_e N_{\mathrm{MM12}_2} : \quad b_2(Y^{\mathrm{MM27}_3}_{\mathrm{MM12}_2}) = 1\,, \quad b_3(Y^{\mathrm{MM27}_3}_{\mathrm{MM12}_2}) = 100\,,\\
W^{\mathrm{MM27}_3}_{\mathrm{MM21}_2} &= N_{\mathrm{MM27}_3} \perp_e N_{\mathrm{MM21}_2} : \quad b_2(Y^{\mathrm{MM27}_3}_{\mathrm{MM21}_2}) = 1\,, \quad b_3(Y^{\mathrm{MM27}_3}_{\mathrm{MM21}_2}) = 102\,,\\
W^{\mathrm{MM27}_3}_{\mathrm{MM32}_2} &= N_{\mathrm{MM27}_3} \perp_e N_{\mathrm{MM32}_2} : \quad b_2(Y^{\mathrm{MM27}_3}_{\mathrm{MM32}_2}) = 1\,, \quad b_3(Y^{\mathrm{MM27}_3}_{\mathrm{MM32}_2}) = 122\,.
\end{aligned} \tag{4.24}$$

Analogously, we can construct twisted connected sum $G_2$-manifolds via orthogonal gluing along rank one intersection lattices for semi-Fano threefolds with higher rank Picard lattices. In table 4.3 we collect all (resolved) toric terminal Fano threefolds of Picard rank three and four that allow for a rank one intersection lattice generated by a vector $e$ of length square $e^2 = -4$. The geometries of these threefolds are again specified by their reference number $\mathrm{MM\#}_\rho$ and/or K# as arising in the Mori–Mukai and/or Kasprzyk classifications [236, 237, 238]. Notice that the resulting twisted connected sum $G_2$-manifolds $Y^{\cdots}_{\cdots}$ obtained from orthogonal gluing along the rank one intersection lattice $R$ all have the two-form Betti number $b_2(Y^{\cdots}_{\cdots}) = 1$ and, therefore, in table 4.4 we list only their three-form Betti numbers $b_3(Y^{\cdots}_{\cdots})$. These Betti numbers are easily calculated with relations (4.10).

For example, for the first pair between $\mathrm{MM27}_3$ and $\mathrm{MM6}_2$, the third Betti number is computed as $b_3(Y^{\mathrm{MM27}_3}_{\mathrm{MM6}_2}) = 50 + 32 - 1 + 23 = 104$, where the dimensions of the kernels are trivial. Here the 50 comes from the third Betti number of the blown-up threefold $\mathrm{MM27}_3$ from $P_L = \mathbb{P}^1 \times \mathbb{P}^1 \times \mathbb{P}^1$, which is computed to be $b_3(\mathrm{MM27}_3) = b_3(P_L) + (-K_{P_L})^3 + 2 = 0 + 48 + 2 = 50$ with the help of equation (2.63). This Betti number is also given in table 4.3.

| No. | rk $N$ | $-K^3$ | $\kappa$ | $e$ | $e^2$ | $b_3(Z)$ |
|---|---|---|---|---|---|---|
| MM27$_3$, K62 (Fano) | 3 | 48 | $\begin{pmatrix} 0 & 2 & 2 \\ 2 & 0 & 2 \\ 2 & 2 & 0 \end{pmatrix}$ | $\begin{pmatrix} 1 \\ 0 \\ -1 \end{pmatrix}$ | $-4$ | 50 |
| MM25$_3$, K68 (Fano) | 3 | 44 | $\begin{pmatrix} 0 & 2 & 1 \\ 2 & 0 & 3 \\ 1 & 3 & -2 \end{pmatrix}$ | $\begin{pmatrix} -1 \\ 1 \\ 0 \end{pmatrix}$ | $-4$ | 46 |
| MM31$_3$, K105 (Fano) | 3 | 52 | $\begin{pmatrix} 0 & 2 & 1 \\ 2 & 0 & 3 \\ 1 & 3 & -2 \end{pmatrix}$ | $\begin{pmatrix} -1 \\ 1 \\ 0 \end{pmatrix}$ | $-4$ | 54 |
| K124 (semi-Fano) | 3 | 48 | $\begin{pmatrix} 2 & 4 & 2 \\ 4 & 2 & 2 \\ 2 & 2 & 0 \end{pmatrix}$ | $\begin{pmatrix} -1 \\ 1 \\ 0 \end{pmatrix}$ | $-4$ | 50 |
| MM12$_4$, K218 (Fano) | 4 | 46 | $\begin{pmatrix} 2 & 4 & 2 & 0 \\ 4 & 2 & 2 & 2 \\ 2 & 2 & 0 & 1 \\ 0 & 2 & 1 & -2 \end{pmatrix}$ | $\begin{pmatrix} 1 \\ -1 \\ 0 \\ 0 \end{pmatrix}$ | $-4$ | 48 |
| MM10$_4$, K266 (Fano) | 4 | 42 | $\begin{pmatrix} 0 & 2 & 2 & 0 \\ 2 & 0 & 2 & 0 \\ 2 & 2 & 0 & 1 \\ 0 & 0 & 1 & -2 \end{pmatrix}$ | $\begin{pmatrix} 1 \\ -1 \\ 0 \\ 0 \end{pmatrix}$ | $-4$ | 44 |
| K221 (semi-Fano) | 4 | 38 | $\begin{pmatrix} -2 & 2 & 0 & 0 \\ 2 & 2 & 1 & 1 \\ 0 & 1 & -2 & 1 \\ 0 & 1 & 1 & -2 \end{pmatrix}$ | $\begin{pmatrix} 0 \\ -1 \\ 1 \\ 1 \end{pmatrix}$ | $-4$ | 40 |
| K232 (semi-Fano) | 4 | 40 | $\begin{pmatrix} 0 & 2 & 2 & 0 \\ 2 & 0 & 2 & 0 \\ 2 & 2 & 0 & 0 \\ 0 & 0 & 0 & -2 \end{pmatrix}$ | $\begin{pmatrix} -1 \\ 0 \\ 1 \\ 0 \end{pmatrix}$ | $-4$ | 42 |
| K233 (semi-Fano) | 4 | 38 | $\begin{pmatrix} -2 & 0 & 1 & 0 \\ 0 & -2 & 1 & 2 \\ 1 & 1 & 0 & 2 \\ 0 & 2 & 2 & -2 \end{pmatrix}$ | $\begin{pmatrix} -1 \\ 1 \\ 0 \\ 0 \end{pmatrix}$ | $-4$ | 40 |
| K247 (semi-Fano) | 4 | 44 | $\begin{pmatrix} 4 & 3 & 3 & 2 \\ 3 & 0 & 2 & 0 \\ 3 & 2 & 0 & 0 \\ 2 & 0 & 0 & -2 \end{pmatrix}$ | $\begin{pmatrix} 0 \\ -1 \\ 1 \\ 0 \end{pmatrix}$ | $-4$ | 46 |
| K257 (semi-Fano) | 4 | 46 | $\begin{pmatrix} 0 & 2 & 0 & 3 \\ 2 & 0 & 0 & 3 \\ 0 & 0 & -2 & 1 \\ 3 & 3 & 1 & 6 \end{pmatrix}$ | $\begin{pmatrix} -1 \\ 1 \\ 0 \\ 0 \end{pmatrix}$ | $-4$ | 48 |

Table 4.3: The rank three and four (resolved) toric terminal Fano threefolds for an intersection lattice $R$ generated by a vector of length square $-4$. The columns show the reference number in the Mori–Mukai [236] and/or Kasprzyk [238] classification, the rank of the Picard lattice (note that in the semi-Fano cases this rank as reported in [238] is smaller, since it refers to a singular variety), the triple intersection of the anti-canonical divisor $-K$, the intersection matrix $\kappa$ of the Picard lattice of the K3 surface, the generator $e$ of the lattice $R$ and its length square, and the three-form Betti number $b_3(Z)$ of the associated building block $Z$.

| $b_3(Y^{\cdots}_{\cdots})$ | $\mathrm{MM27}_3$ | $\mathrm{MM25}_3$ | $\mathrm{MM31}_3$ | K124 | $\mathrm{MM12}_4$ | $\mathrm{MM10}_4$ | K221 | K232 | K233 | K247 | K257 |
|---|---|---|---|---|---|---|---|---|---|---|---|
| $\mathrm{MM27}_3$ | 122 | 118 | 126 | 122 | 120 | 116 | 112 | 114 | 112 | 118 | 120 |
| $\mathrm{MM25}_3$ | 118 | 114 | 122 | 118 | 116 | 112 | 108 | 110 | 108 | 114 | 116 |
| $\mathrm{MM31}_3$ | 126 | 122 | 130 | 126 | 124 | 120 | 116 | 118 | 116 | 122 | 124 |
| K124 | 122 | 118 | 126 | 122 | 120 | 116 | 112 | 114 | 112 | 118 | 120 |
| $\mathrm{MM12}_4$ | 120 | 116 | 124 | 120 | 118 | 114 | 110 | 112 | 110 | 116 | 118 |
| $\mathrm{MM10}_4$ | 116 | 112 | 120 | 116 | 114 | 110 | 106 | 108 | 106 | 112 | 114 |
| K221 | 112 | 108 | 116 | 112 | 110 | 106 | 102 | 104 | 102 | 108 | 110 |
| K232 | 114 | 110 | 118 | 114 | 112 | 108 | 104 | 106 | 104 | 110 | 112 |
| K233 | 112 | 108 | 116 | 112 | 110 | 106 | 102 | 104 | 102 | 108 | 110 |
| K247 | 118 | 114 | 122 | 118 | 116 | 112 | 108 | 110 | 108 | 114 | 116 |
| K257 | 120 | 116 | 124 | 120 | 118 | 114 | 110 | 112 | 110 | 116 | 118 |

Table 4.4: The three-form Betti numbers $b_3(Y^{\cdots}_{\cdots})$ of the twisted connected sum $G_2$-manifolds $Y^{\cdots}_{\cdots}$ arising from the orthogonal pushout $N_{\cdots} \perp_e N_{\cdots}$ along the rank one intersection lattice with $e^2 = -4$ from all pairs of building blocks collected in table 4.3. By construction of gluing along a rank one intersection lattice, all these examples have the two-form Betti numbers $b_2(Y^{\cdots}_{\cdots}) = 1$. The reference numbers $\mathrm{MM}\#_\rho$ or K# for the rows and columns label the building blocks, and the lines in the table divide between the examples with rank three and rank four Picard lattices.

## 4.2 $\mathcal{N} = 2$ gauge theory sectors

We now turn to a careful study of the $\mathcal{N} = 2$ gauge theory sectors, which turn out to be much richer than the Abelian $\mathcal{N} = 4$ gauge theory sectors studied in the previous section. This happens because the building blocks $(Z_{L/R}, S_{L/R})$ of the twisted connected sum $G_2$-manifolds now admit enhancement to $\mathcal{N} = 2$ non-Abelian gauge theory sectors, whereas we have seen at the beginning of the previous section that, due to the condition required in equation (2.72), enhancement to $\mathcal{N} = 4$ non-Abelian gauge theory sectors is not possible.

Different points in the Calabi–Yau moduli space associated to a smooth Calabi–Yau threefold can be connected via deformations of the complex and Kähler structures on the Calabi–Yau threefold. The boundary points of this moduli space correspond to singular Calabi–Yau threefolds obtained from some of these deformations. Therefore, we can roll on the moduli space from one of these degenerate Calabi–Yaus to another with a possibly different topology. These geometrical transitions relating boundary points are called extremal transitions for Calabi–Yaus threefolds. In this section we see how the $\mathcal{N} = 2$ non-Abelian gauge theory sectors possess an interesting branch structure geometrically accessible in terms of extremal transitions in the asymptotically cylindrical Calabi–Yau threefolds $X_{L/R}$.

We recall from [240] that there is a simple hierarchy of singularities in $G_2$-manifolds in real codimension four, six and seven, which respectively lead to non-Abelian gauge groups, non-trivial matter representations, and chirality of the charged $\mathcal{N} = 1$ matter spectrum. While our setup admits non-Abelian gauge groups with non-trivial matter representations, we should not expect singularities inducing chirality, as the trivial $S^1$ fibration in the non-compact seven-dimensional manifolds $Y_{L/R}$ prevents the appearance of codimension seven singularities. In order to see what kind of features we can expect by degenerating the building blocks $(Z_{L/R}, S_{L/R})$ in the twisted connected sum construction of $G_2$-manifolds, let us first recall the picture proposed in [240] which leads to the singularities mentioned in the previous paragraph.

The picture in [240] uses the heterotic/M-theory duality [86], the Strominger–Yau–Zaslow fibration of Calabi–Yau manifolds [241], and the fact that $G_2$-manifolds can be locally constructed as degenerating $S^1$ fibrations[3] over Calabi–Yau threefolds [243, 244].

Namely, it starts by considering the heterotic string compactification on the Calabi–Yau threefold $W$, which is assumed to admit a geometric mirror[4] threefold such that it has a Strominger–Yau–Zaslow Lagrangian $T^3$ fibration over a (real) three-dimensional Lagrangian cycle $Q$. In the limit where the volume of the base $Q$ is large compared to the volume of the Lagrangian fibers $T^3$, the essential idea is to adiabatically extend the duality[5] between the heterotic string on $T^3$ and M-theory on K3 over the entire base $Q$. The M-theory geometries defined in this way realize the same fibration structure as appearing in the twisted connected sum $G_2$-manifolds, namely in the diagram (3.105). In this way, whenever the heterotic string has a non-Abelian ADE type gauge group $G$, the dual K3 fibers develop the corresponding ADE singularity extending over the entire real three-dimensional base $Q$. In the context of twisted connected sum $G_2$-manifolds a possibility to arrive at non-Abelian ADE type gauge theories has been contemplated in reference [249].

Even though the K3 fibration described in reference [240] is in accordance with the K3 fibration of diagram (3.105) of the twisted connected sum construction, the non-Abelian gauge theory enhancement we encounter arises from singularities along a three-cycle $S^1 \times C$, where the curve $C$ of genus $g$ resides in K3 fibers along a circle $S^1$ in the base $Q$. Hence, the non-Abelian gauge group still emerges from a real codimension four singularity as in reference [240], but here it is such that they arise along different types of three-cycles. In the Kovalev limit, the three-cycle $S^1 \times C$ appears in one of the seven-dimensional manifolds $Y_{L/R} = X_{L/R} \times S^1_{L/R}$, such that the curve $C$ realizes an ADE singularity in one of the asymptotically cylindrical Calabi–Yau threefolds $X_{L/R}$. Therefore, the non-Abelian gauge theory enhancement discussed here relates to non-Abelian gauge groups from curves of ADE singularities in Calabi–Yau threefolds in the context of type IIA strings [250, 251]. More specifically, in this setting, an ADE singularity along a curve $C$ yields a four-dimensional $\mathcal{N} = 2$ gauge theory, with the associated gauge group $G$ together with $g$ hypermultiplets in the adjoint representation. More general matter representations occur at points along the curve $C$ where the ADE singularity further enhances, i.e., along real codimension six singularities. For example, at the intersection point of two curves $C$ and $C'$ with ADE singularities we encounter matter in the bi-fundamental representation of the two associated gauge groups $G$ and $G'$ [252].

In this section we find that the described $\mathcal{N} = 2$ gauge theory spectra of the previous paragraph can indeed be realized within the $\mathcal{N} = 2$ gauge theory sectors of the building blocks $(Z_{L/R}, S_{L/R})$. Remarkably, even the phase structure of the four-dimensional $\mathcal{N} = 2$ gauge theory sectors, which connects topologically distinct Calabi–Yau threefolds via extremal transitions, carries over to the four-dimensional $\mathcal{N} = 1$ M-theory compactifications on twisted connected sum $G_2$-manifolds. In the picture of $\mathcal{N} = 1$ M-theory compactifications on twisted connected sum

[3] The $S^1$ can be identified in a hyper-Kähler quotient construction starting in eight dimensions [240, 242].

[4] Further suggestions on the role of mirror symmetry in the context of $G_2$-manifolds have been proposed in references [245, 246].

[5] The proposed construction can be viewed as an $\mathcal{N} = 1$ version of the $\mathcal{N} = 2$ heterotic/type II duality between the heterotic string on $K3 \times T^2$ and type IIA string on the dual K3 fibered Calabi–Yau threefolds, as proposed in references [247, 248].

$G_2$-manifolds, the gauge theory branches relate topologically distinct $G_2$-manifolds.

For completeness, the picture presented in references [86, 253] would explain chirality of non-Abelian matter as a local effect occurring in codimension seven. However, since the twisted connected sum breaks supersymmetry from $\mathcal{N} = 2$ to $\mathcal{N} = 1$ non-locally via the twisted gluing recipe, it is much more subtle to realize chiral charged matter. We briefly discuss some ideas that could help us achieve chiral charged matter, as phenomenologically required by the Standard Model of Particle Physics.

### 4.2.1 Phases of $\mathcal{N} = 2$ Abelian gauge theory sectors

Let us focus on twisted connected sum $G_2$-manifolds with non-trivial $\mathcal{N} = 2$ gauge theory sectors in the Kovalev limit. According to table 3.2, we have to construct building blocks with $(Z_{L/R}, S_{L/R})$ with non-trivial kernels $k_{L/R}$ as defined in equation (2.59). This is achieved with the proposal by Kovalev and Lee [207] that generalizes the construction of asymptotically cylindrical Calabi–Yau threefolds outlined in section 2.2.5. An example on how to realize $\mathcal{N} = 2$ Abelian gauge theory from this generalized construction appeared in reference [254].

Let us see how this generalization comes about. Consider the semi-Fano threefold $P$ with two global sections $s_0$ and $s_1$ of its anti-canonical divisor $-K_P$. Instead of choosing a generic section $s_0$, we now assume that the global section $s_0$ factors into a product

$$s_0 \;=\; s_{0,1} \cdots s_{0,n} \;, \tag{4.25}$$

where $s_{0,i}$ are global sections of line bundles $\mathcal{L}_i$ with $-K_P = \mathcal{L}_1 \otimes \ldots \otimes \mathcal{L}_n$. In consequence of this factorization, the curve $C_{\text{sing}} = \{s_0 = 0\} \cap \{s_1 = 0\}$ becomes reducible in terms of individually smooth and reduced curves $C_i$ such that

$$C_{\text{sing}} \;=\; \sum_{i=1}^{n} C_i \;, \qquad C_i = \{s_{0,i} = 0\} \cap \{s_1 = 0\} \;. \tag{4.26}$$

Following Kovalev and Lee [207], the building block $(Z^\sharp, S)$ associated to $P$ are now constructed by the sequence of blow-ups $\pi_{\{C_1,\ldots,C_n\}} : Z^\sharp \to P$ along the individual curves $C_i$ according to

$$Z^\sharp \;=\; \text{Bl}_{\{C_1,\ldots,C_n\}} P \;=\; \text{Bl}_{C_n} \text{Bl}_{C_{n-1}} \cdots \text{Bl}_{C_1} P \;. \tag{4.27}$$

Since the curves $C_i$ and the semi-Fano threefold $P$ are smooth, the blow-up $Z^\sharp$ is smooth as well. As before, the K3 surface $S$ arises as the proper transform of a smooth anti-canonical divisor $S^\sharp = \{\alpha_0 s_0 + \alpha_1 s_1 = 0\} \subset P$ for some coordinates $[\alpha_0 : \alpha_1] \in \mathbb{P}^1$. By blowing up a semi-Fano threefold $P$, the resulting dimension of the kernel $k$ in equation (2.59) is given by [142]

$$\dim k \;=\; n - 1 \;. \tag{4.28}$$

Let $b_3(P)$ be the three-form Betti number of the semi-Fano threefold $P$, and $g(C_i)$ the genera of the smooth curve components $C_i$. The three-form Betti number $b_3(Z^\sharp)$ of the blown-up threefold

$Z^\sharp$ becomes

$$b_3(Z^\sharp) \;=\; b_3(P) + 2\sum_{i=1}^{n} g(C_i)\;. \tag{4.29}$$

Let $C_i.C_i$ be the self-intersections of the curves $C_i$ in the K3 fiber $S$. Since all these curves $C_i$ lie in $S$, the genus $g(C_i)$ is readily computed by the *adjunction formula*

$$g(C_i) \;=\; \frac{1}{2}C_i.C_i + 1\;. \tag{4.30}$$

For a building block $(Z^\sharp, S^\sharp)$ constructed following the recipe above, the orthogonal gluing method of section 2.2.6 can still be carried out in the same way [141, 142].

An observation proves to be very fruitful. From a single semi-Fano threefold $P$, several building blocks can often be constructed depending on the properties of the curve $C = \{s_0 = 0\} \cap \{s_1 = 0\}$. For smooth irreducible curves $C^\flat$, we obtain a smooth building block $(Z^\flat, S^\flat)$ with vanishing kernel $k$. For reducible curves $C_{\text{sing}}$ with smooth components $C_i$ we arrive, after the sequence of blow-ups (4.27), at a smooth building block $(Z^\sharp, S^\sharp)$ with non-vanishing kernel $k$. The former building block does not contribute with any vector multiplets to the $\mathcal{N} = 2$ gauge theory sector, while the latter building block contributes with Abelian vector multiplets to the $\mathcal{N} = 2$ gauge theory sector. In the sequel we argue that these different possibilities realize *distinct branches of the $\mathcal{N} = 2$ gauge theory sectors*.

To arrive at this gauge theory interpretation, let us consider a semi-Fano threefold $P$ with a curve $C_{\text{sing}}$ of the reducible type (4.26) with the factorized global anti-canonical section (4.25). Performing a blow-up along this reducible curve yields the fibration $\pi : Z_{\text{sing}} \to \mathbb{P}^1$ with

$$Z_{\text{sing}} \;=\; \text{Bl}_{C_{\text{sing}}}P \;=\; \Big\{(x,z) \in P \times \mathbb{P}^1 \;\Big|\; z_0 s_{0,1} \cdots s_{0,n} + z_1 s_1 = 0\Big\}\;. \tag{4.31}$$

In the patch of the affine coordinate $t = \frac{z_1}{z_0}$ we get

$$s_{0,1} \cdots s_{0,n} + t s_1 = 0\;. \tag{4.32}$$

Therefore, the threefold $Z_{\text{sing}}$ becomes singular in the vicinity of the fiber $\pi^{-1}([1,0])$. By assuming transverse intersections among the smooth curves $C_i$, at the discrete intersection loci $\mathcal{I}_{ij} \;=\; \{t = 0\} \cap \{s_1 = 0\} \cap \{s_{0,i} = 0\} \cap \{s_{0,j} = 0\}$ for $1 \le i \le j \le n$ with $\chi_{ij} = |\mathcal{I}_{ij}|$ intersection points, *conifold singularities* will appear. The number of intersection points is given by

$$\chi_{ij} \;=\; C_i.C_j\;, \tag{4.33}$$

in terms of the intersection numbers of the reduced curves $C_i$ and $C_j$ within the K3 surface $S$. Notice that this singularity structure prevails in the asymptotically cylindrical Calabi–Yau threefold $X_{\text{sing}} = Z_{\text{sing}} \setminus S$ since, for $\alpha_1 \neq 0$, the asymptotic fiber $S \;=\; \pi^{-1}([\alpha_0, \alpha_1])$ is disjoint from the singular fiber $\pi^{-1}([1,0])$.

In the vicinity of the singular fiber $\pi^{-1}([1,0]) \subset X_{\text{sing}}$, we interpret the dimensional reduction of M-theory on the local seven-dimensional singular space $S^1 \times X_{\text{sing}}$ as the dimensional reduction of type IIA string theory on the asymptotically cylindrical Calabi–Yau threefold $X_{\text{sing}}$, where the $S^1$ factor corresponds to the M-theory circle of type IIA string theory. In this type IIA picture,

the conifold singularities given by equation (4.32) yield an Abelian $\mathcal{N} = 2$ gauge theory with charged matter multiplets [255, 256].[6] Namely, to each curve $C_i$ we assign an Abelian group factor $\mathrm{U}(1)_i$ such that the total Abelian gauge group of rank $(n-1)$ becomes

$$\mathrm{U}(1)^{n-1} \simeq \frac{\mathrm{U}(1)_1 \times \ldots \times \mathrm{U}(1)_n}{\mathrm{U}(1)_{\mathrm{Diag}}}\,, \tag{4.34}$$

where $\mathrm{U}(1)_{\mathrm{Diag}}$ is the diagonal subgroup of $\mathrm{U}(1)_1 \times \ldots \times \mathrm{U}(1)_n$.

Therefore, in the low-energy four-dimensional effective theory, we obtain $(n-1)$ four-dimensional $\mathcal{N} = 2$ U(1) vector multiplets, which decomposes into $(n-1)$ four-dimensional $\mathcal{N} = 1$ U(1) vector multiplets and $(n-1)$ four-dimensional $\mathcal{N} = 1$ neutral chiral multiplets. Furthermore, to each intersection point in $\mathcal{I}_{ij}$ one assigns a four-dimensional $\mathcal{N} = 2$ hypermultiplet of charge $(+1,+1)$ with respect to the $\mathrm{U}(1)_i \times \mathrm{U}(1)_j$ group factor. Then each of these $\mathcal{N} = 2$ hypermultiplet of charge $(+1,+1)$ decomposes into two four-dimensional $\mathcal{N} = 1$ chiral multiplets of charge $(+1,+1)$ and $(-1,-1)$, respectively. The resulting Abelian $\mathcal{N} = 2$ gauge theory spectrum[7] is summarized in table 4.5.

| Multiplicity | $\mathcal{N} = 2$ multiplets | | $\mathcal{N} = 1$ multiplets | |
|---|---|---|---|---|
| | $\mathrm{U}(1)^{n-1}$ charges | multiplet | $\mathrm{U}(1)^{n-1}$ charges | multiplet |
| $n-1$ | $(0,0,\ldots,0)$ | vector | $(0,\ldots,0)$ | vector |
| | | | $(0,\ldots,0)$ | chiral |
| $\chi_{ij}$ | $(0,\ldots,+1_i,\ldots,+1_j,\ldots,0)$ | hyper | $(0,\ldots,+1_i,\ldots,+1_j,\ldots,0)$ | chiral |
| $1 \le i < j < n$ | | | $(0,\ldots,-1_i,\ldots,-1_j,\ldots,0)$ | chiral |
| $\chi_{in}$ | $(0,\ldots,+1_i,\ldots,0)$ | hyper | $(0,\ldots,+1_i,\ldots,0)$ | chiral |
| $1 \le i < n$ | | | $(0,\ldots,-1_i,\ldots,0)$ | chiral |

Table 4.5: The spectrum of the Abelian $\mathcal{N} = 2$ gauge theory sector arising from the conifold singularities in the building block $(Z_{\mathrm{sing}}, S)$. Listed are the four-dimensional $\mathcal{N} = 2$ multiplets and their decomposition into the four-dimensional $\mathcal{N} = 1$ multiplets together with their multiplicities $\chi_{ij}$. The subscripts of the entries of the U(1) charges indicate their position in the charged vector.

[6] Starting from the Fano threefold $\mathbb{P}^3$, it has also been proposed that the singular building block $(Z_{\mathrm{sing}}, S)$ with conifold singularities realizes an Abelian gauge theory with charged matter [254].

[7] In an alternative picture, by dimensionally reducing M-theory on the local Calabi–Yau fourfold $T^2 \times X_{\mathrm{sing}}$ to three space-time dimensions, the conifold points in $X_{\mathrm{sing}}$ become genus one curves of conifold singularities [257]. The three-dimensional $\mathcal{N} = 4$ gauge theory sectors appearing in this picture agree with the four-dimensional $\mathcal{N} = 2$ spectrum in table 4.5 upon further dimensional reduction on a circle $S^1$. This further justifies that the local dimensional reduction of type IIA theory on $X_{\mathrm{sing}}$ correctly describes the gauge theory of M-theory on $S^1 \times X_{\mathrm{sing}}$ without requiring that the $S^1$ factor realizes the M-theory circle for the dual type IIA description.

### The Higgs and the Coulomb branches

The described four-dimensional $\mathcal{N} = 2$ Abelian gauge theory now predicts a *Higgs branch* $H^\flat$ and a *Coulomb branch* $C^\sharp$. In the following, we analyse these branches within our context.

- *The gauge theory perspective*

  On the one hand, generic non-vanishing vacuum expectation values of the charged $\mathcal{N} = 2$ hypermultiplets break the $\mathrm{U}(1)^{n-1}$ gauge theory entirely and parametrize the Higgs branch $H^\flat$ of the gauge theory. As a consequence $(n-1)$ charged $\mathcal{N} = 2$ hypermultiplets play the role of $\mathcal{N} = 2$ Goldstone multiplets, which combine with the $(n-1)$ short massless $\mathcal{N} = 2$ vector multiplets giving rise to $(n-1)$ long massive $\mathcal{N} = 2$ vector multiplets. According to the spectrum in table 4.5, we arrive at the Higgs branch $H^\flat$ of complex dimension $h^\flat$ [256]

  $$h^\flat \;=\; \dim_{\mathbb{C}} H^\flat \;=\; 2\left(\sum_{1\leq i<j\leq n} \chi_{ij}\right) - 2(n-1)\;. \tag{4.35}$$

  Here the factor two takes into account that each hypermultiplet contains two complex scalar fields. This complex dimension readily describes the Higgs branch as parametrized by the *non-vanishing vacuum expectation values of the corresponding charged* $\mathcal{N} = 1$ *chiral multiplets*.

  On the other hand, the non-vanishing vacuum expectation values of the neutral complex scalar fields in the $\mathcal{N} = 2$ vector multiplets furnish the coordinates on the Coulomb branch $C^\sharp$ such that its complex dimension $c^\sharp$ reads

  $$c^\sharp \;=\; \dim_{\mathbb{C}} C^\sharp \;=\; n-1\;. \tag{4.36}$$

  In the $\mathcal{N} = 1$ language, the Coulomb branch moduli space is parametrized by the *non-vanishing vacuum expectation value of neutral* $\mathcal{N} = 1$ *chiral multiplets*.

- *The geometrical perspective*

  From the geometrical perspective, the Higgs branch $H^\flat$ arises from *deforming the conifold singularities* in $X_{\text{sing}}$ to the deformed asymptotically cylindrical Calabi–Yau threefold $X^\flat$ [256]. On the level of the semi-Fano threefold $P$, this amounts to *deforming the reducible curve* $C_{\text{sing}}$ in equation (4.26) to the smooth irreducible curve $C^\flat$ such that the building block $(Z_{\text{sing}}, S)$ deforms to the building block $(Z^\flat, S^\flat)$ of vanishing kernel. According to equations (4.28), (4.29) and (4.30), this yields for the kernel $k^\flat$ and the three-form Betti number $b_3(Z^\flat)$

  $$\dim k^\flat \;=\; 0\;, \qquad b_3(Z^\flat) \;=\; b_3(P) + C^\flat.C^\flat + 2\;. \tag{4.37}$$

  Furtheremore, the Coulomb branch $C^\sharp$ arises from the *resolution of the conifold singularities* in $X_{\text{sing}}$ [256]. On the level of the semi-Fano threefold $P$, this amounts to the *sequential blow-ups* in equation (4.27) along the components $C_i$ of $C_{\text{sing}}$ to the building block $(Z^\sharp, S^\sharp)$

of non-vanishing kernel.[8] According to equations (4.28) and (4.29), this yields for the kernel $k^\sharp$ and the three-form Betti number $b_3(Z^\sharp)$

$$\dim k^\sharp \;=\; n-1\;, \qquad b_3(Z^\sharp) \;=\; b_3(P) + 2n + \sum_{i=1}^{n} C_i.C_i\;. \tag{4.38}$$

**The twisted connected sum $G_2$-manifolds**

Let us now consider two twisted connected sum $G_2$-manifolds $Y^\flat$ and $Y^\sharp$ respectively constructed via orthogonal gluing of the left building blocks $(Z^\flat, S^\flat)$ and $(Z^\sharp, S^\sharp)$ with another right building block $(Z_R, S_R)$.

- *The geometrical perspective*

  From equations (4.37) and (4.38), we use (4.10) to obtain the general expressions for the two- and three-form Betti numbers

$$b_2(Y^\flat) \;=\; \delta_R^{(2)}\;, \quad b_3(Y^\flat) \;=\; b_3(P) + C^\flat.C^\flat + 25 + \delta_R^{(3)}\;, \tag{4.39}$$

$$b_2(Y^\sharp) \;=\; (n-1) + \delta_R^{(2)}\;, \quad b_3(Y^\sharp) \;=\; b_3(P) + \left(\sum_{i=1}^{n} C_i.C_i\right) + 3n + 22 + \delta_R^{(3)}\;, \tag{4.40}$$

  with the contributions from the right building block $(Z_R, S_R)$

$$\delta_R^{(2)} \;=\; \dim k_R + \mathrm{rk}\, R\;, \qquad \delta_R^{(3)} \;=\; b_3(Z_R) + \dim k_R - \mathrm{rk}\, R\;. \tag{4.41}$$

  These relations allow us to further define what we call the reduced Betti numbers $b_\ell^\flat$ and $b_\ell^\sharp$, $\ell = 2, 3$, given by

$$b_\ell^\flat \;=\; b_\ell(Y^\flat) - \delta_R^{(\ell)}\;, \qquad b_\ell^\sharp \;=\; b_\ell(Y^\sharp) - \delta_R^{(\ell)}\;, \qquad \ell = 2, 3\;. \tag{4.42}$$

  Furthermore, using the equivalence $C^\flat \sim C_1 + \ldots + C_n$ on the semi-Fano threefold $P$ and the definition given in equation (4.33) of the multiplicities $\chi_{ij}$, we finally arrive at the relations

$$\begin{aligned} b_2(Y^\flat) \;&=\; b_2(Y^\sharp) - (n-1)\;, \\ b_3(Y^\flat) \;&=\; b_3(Y^\sharp) + 2\left(\sum_{1\leq i<j\leq n} \chi_{ij}\right) - 3(n-1)\;. \end{aligned} \tag{4.43}$$

[8] The sequential resolution in equation (4.27) in the Coulomb branch depends on the order of the performed blow-ups. Changing the order geometrically realizes bi-rational transformations among the resulting asymptotically cylindrical Calabi–Yau threefolds $X^\sharp$ [254].

- *The correspondence between the gauge theory and the geometrical perspectives*

  The non-trivial result is now that the derived change in Betti numbers (4.43) between the twisted connected sum $G_2$-manifolds is in perfect agreement with the phase structure of the proposed $\mathrm{U}(1)^{n-1}$ gauge theory. The change in the Betti number $b_2$ geometrically realizes the *difference of massless four-dimensional* $\mathcal{N} = 1$ *vector multiplets*, whereas the change of the Betti number $b_3$ geometrically realizes the *difference of four-dimensional* $\mathcal{N} = 1$ *chiral multiplets*. This is in agreement with the gauge theory expectation. In fact, passing from the Coulomb branch $C^\sharp$ to the Higgs branch $H^\flat$ via the Higgs mechanism reduces the vector bosons by the rank $(n-1)$ of the Abelian gauge group. Furthermore, the difference in the four-dimensional $\mathcal{N} = 1$ chiral multiplets agrees with the change in the dimension of the moduli space[9] of these Abelian gauge theory phases, i.e.,

$$b_3(Y^\flat) - b_3(Y^\sharp) \;=\; b_3^\flat - b_3^\sharp \;=\; h^\flat - c^\sharp \,. \tag{4.44}$$

  In a similar fashion, we can also establish the correspondence between the phase structure of the gauge theory and the geometry for mixed Higgs–Coulomb branches, where the gauge group $\mathrm{U}(1)^{n-1}$ is broken to a subgroup $\mathrm{U}(1)^{k-1}$ with $1 < k < n$. The geometries of such mixed phases are obtained by partially resolving and partially deforming the conifold singularities in the asymptotically cylindrical Calabi–Yau threefold $X_{\text{sing}}$. In section 4.2.3, we illustrate the analysis of mixed Higgs–Coulomb branches with an explicit example.

### 4.2.2 Phases of $\mathcal{N} = 2$ non-Abelian gauge theory sectors

Let us now turn to the enhancement to non-Abelian $\mathcal{N} = 2$ gauge theory sectors in the context of twisted connected sum $G_2$-manifolds, indicated as a possibility in reference [249]. Let us assume that the anti-canonical line bundle $-K_P$ of the semi-Fano threefold $P$ factors as

$$-K_P \;=\; \tilde{\mathcal{L}}_1^{\otimes k_1} \otimes \ldots \otimes \tilde{\mathcal{L}}_s^{\otimes k_s} \quad \text{with} \quad n = k_1 + \ldots + k_s \,, \tag{4.45}$$

where $\tilde{\mathcal{L}}_i$ are line bundles with global sections $\tilde{s}_{0,i}$. The global section $s_0$ of $-K_P$ can further degenerate to $s_0 = \tilde{s}_{0,1}^{k_1} \cdots \tilde{s}_{0,s}^{k_s}$ and the singular building block (4.31) reads

$$Z_{\text{sing}} \;=\; \left\{ (x,z) \in P \times \mathbb{P}^1 \,\middle|\, z_0 \tilde{s}_{0,1}^{k_1} \cdots \tilde{s}_{0,s}^{k_s} + z_1 s_1 = 0 \right\} \,, \tag{4.46}$$

with the singular equation in the affine coordinate $t = \frac{z_1}{z_0}$ given by

$$\tilde{s}_{0,1}^{k_1} \cdots \tilde{s}_{0,s}^{k_s} + t s_1 = 0 \,. \tag{4.47}$$

In a similar way as performed in the study of Abelian phases of $\mathcal{N} = 2$ gauge theories, we assume that all curves $\tilde{C}_i = \{\tilde{s}_{0,i} = 0\} \cap \{s_1 = 0\}$ are smooth. In the vicinity of the singular fiber

[9] Recall from chapter 2 that the dimension of the moduli space for a $G_2$-manifold $Y$ is given by the three-form Betti number $b_3(Y)$.

$\pi^{-1}([1,0]) \subset Z_{\text{sing}}$, the singular building block $(Z_{\text{sing}}, S)$ develops $A_{k_i-1}$ singularities along those curves $\tilde{C}_i$ with $k_i > 1$.

To arrive at the gauge theory description, we again analyze the local M-theory geometry on $S^1 \times X_{\text{sing}}$ in terms of its dual type IIA picture on the asymptotically cylindrical Calabi–Yau threefold $X_{\text{sing}}$. Type IIA string theory on Calabi–Yau threefolds with a genus $g$ curve of $A_{k-1}$ singularities develops an $\mathcal{N} = 2$ SU($k$) gauge theory with $g$ four-dimensional $\mathcal{N} = 2$ hypermultiplets in the adjoint representation of SU($N$) [250, 251]. Furthermore, each intersection point of two such curves of $A_{k_1-1}$ and $A_{k_2-1}$ singularities contributes with a four-dimensional $\mathcal{N} = 2$ hypermultiplet in the bi-fundamental representation $(\mathbf{k_1}, \mathbf{k_2})$ of SU($k_1$) × SU($k_2$) [252].

Putting all these ingredients together and including the U(1) gauge theory factors of the previously discussed Abelian gauge theory sectors, we propose the following non-Abelian gauge theory description for M-theory on the local singular seven-dimensional space $S^1 \times X_{\text{sing}}$.

- The singularities along the curves $\tilde{C}_i$ determine the gauge group

$$G = \text{SU}(k_1) \times \ldots \times \text{SU}(k_s) \times \text{U}(1)^{s-1} \simeq \frac{\text{U}(k_1) \times \ldots \times \text{U}(k_s)}{\text{U}(1)_{\text{Diag}}} , \tag{4.48}$$

  where any SU(1) factors must be dropped out and $\text{U}(1)_{\text{Diag}}$ is the diagonal subgroup of $\text{U}(k_1) \times \ldots \times \text{U}(k_s)$.

- For any $i$ with $k_i > 0$, there are $g(\tilde{C}_i)$ four-dimensional $\mathcal{N} = 2$ hypermultiplets in the adjoint representation of SU($k_i$).

- There are $\tilde{\chi}_{ij}$ four-dimensional $\mathcal{N} = 2$ hypermultiplets in the bi-fundamental representation $(\mathbf{k_i}, \mathbf{k_j})_{(+1_i,+1_j)}$ of the gauge group factors SU($k_i$) × SU($k_j$), where the subscripts indicate the U(1) charges with respect to the diagonal $\text{U}(1)_i$ and $\text{U}(1)_j$ subgroups of the respective unitary groups U($k_i$) and U($k_j$) in relation (4.48). The multiplicities $\tilde{\chi}_{ij}$ are again determined by the intersection numbers of the curves $\tilde{C}_i$ and $\tilde{C}_j$ in the K3 fiber $S$.

The resulting non-Abelian $\mathcal{N} = 2$ gauge theory spectrum is summarized in table 4.6.

**The Higgs and the Coulomb branches**

From the described spectrum and the results of [251], we are now ready to analyze the branches of these $\mathcal{N} = 2$ gauge theory sectors. First, we determine the complex dimension $h^\flat$ of the Higgs branch

$$h^\flat = \dim_{\mathbb{C}} H^\flat = 2\left(\sum_{i=1}^{s}(g(\tilde{C}_i) - 1)(k_i^2 - 1)\right) + 2\left(\sum_{1\leq i<j\leq s} \tilde{\chi}_{ij} k_i k_j\right) - 2(s-1) . \tag{4.49}$$

Here, the first term captures the $2(k_i^2 - 1)$ complex degrees of freedom of the four-dimensional $\mathcal{N} = 2$ hypermultiplets in the corresponding adjoint representations of the SU($k_i$) gauge group factors — reduced by one adjoint $\mathcal{N} = 2$ Goldstone hypermultiplet rendering the four-dimensional $\mathcal{N} = 2$ SU($k_i$) vector multiplet massive. The second term realizes the complex

| Multiplicity | $\mathcal{N} = 2$ multiplets | | $\mathcal{N} = 1$ multiplets | |
|---|---|---|---|---|
| | $G$ reps. | multiplet | $G$ reps. | multiplet |
| $s - 1$ | $\mathbf{1}$ | U(1) vector | $\mathbf{1}$ | U(1) vector |
| | | | $\mathbf{1}$ | chiral |
| $i = 1, \ldots, s$ | $\mathbf{adj}_{\mathrm{SU}(k_i)}$ | SU($k_i$) vector | $\mathbf{adj}_{\mathrm{SU}(k_i)}$ | SU($k_i$) vector |
| | | | $\mathbf{adj}_{\mathrm{SU}(k_i)}$ | chiral |
| $g(\tilde{C}_i)$ | $\mathbf{adj}_{\mathrm{SU}(k_i)}$ | hyper | $\mathbf{adj}_{\mathrm{SU}(k_i)}$ | chiral |
| $1 \leq i \leq s$ | | | $\mathbf{adj}_{\mathrm{SU}(k_i)}$ | chiral |
| $\tilde{\chi}_{ij}$ | $(\mathbf{k_i}, \mathbf{k_j})_{(+1_i,+1_j)}$ | hyper | $(\mathbf{k_i}, \mathbf{k_j})_{(+1_i,+1_j)}$ | chiral |
| $1 \leq i < j \leq s$ | | | $(\bar{\mathbf{k}}_\mathbf{i}, \bar{\mathbf{k}}_\mathbf{j})_{(-1_i,-1_j)}$ | chiral |
| $\tilde{\chi}_{is}$ | $(\mathbf{k_i}, \mathbf{k_s})_{(+1_i)}$ | hyper | $(\mathbf{k_i}, \mathbf{k_s})_{(+1_i)}$ | chiral |
| $1 \leq i < s$ | | | $(\bar{\mathbf{k}}_\mathbf{i}, \bar{\mathbf{k}}_\mathbf{s})_{(-1_i)}$ | chiral |

Table 4.6: The spectrum of the $\mathcal{N} = 2$ gauge theory sector with gauge group $G = \mathrm{SU}(k_1) \times \ldots \times \mathrm{SU}(k_s) \times \mathrm{U}(1)^{s-1}$ as arising from the non-Abelian building blocks $(Z_{\mathrm{sing}}, S)$. Here both the four-dimensional $\mathcal{N} = 2$ and the four-dimensional $\mathcal{N} = 1$ multiplet structures are given. The adjoint matter is determined by the genus $g(\tilde{C}_i)$ of the curves $\tilde{C}_i$, whereas the bi-fundamental matter is determined by their intersection numbers $\tilde{\chi}_{ij}$ within the K3 surface $S$.

degrees of freedom of the four-dimensional $\mathcal{N} = 2$ matter hypermultiplets in the bi-fundamental representations of the associated special unitary gauge groups and charged with respect to the appropriate U(1) factors. The last term subtracts from the second term the $\mathcal{N} = 2$ Goldstone hypermultiplets for higgsing the $(s - 1)$ four-dimensional $\mathcal{N} = 2$ U(1) vector multiplets.

Next, we derive the complex dimension of the Coulomb branch $C^\flat$, in which the maximal Abelian subgroup $\mathrm{U}(1)^{n-1}$ remains unbroken. It is parametrized by the expectation value of all four-dimensional $\mathcal{N} = 2$ hypermultiplet components that are neutral with respect to this unbroken maximal Abelian subgroup. Therefore, the complex dimension $c^\sharp$ of the Coulomb branch becomes

$$c^\sharp \;=\; \dim_{\mathbb{C}} C^\sharp \;=\; 2\left(\sum_{i=1}^{s} g(\tilde{C}_i)(k_i - 1)\right) + (n - 1)\,. \tag{4.50}$$

The first term counts the traceless neutral diagonal degrees of freedom of the four-dimensional $\mathcal{N} = 2$ matter hypermultiplets in the adjoint representation, while the second term adds the contributions of the complex scalar fields in the four-dimensional unbroken Abelian $\mathcal{N} = 2$ vector multiplets.

### The twisted connected sum $G_2$-manifolds

The next task is to compute the Betti numbers of the twisted connected sum $G_2$-manifolds $Y^\flat$ and $Y^\sharp$, which geometrically realize the Higgs and Coulomb branches by orthogonal gluing of the building blocks $(Z^\flat, S^\flat)$ and $(Z^\sharp, S^\sharp)$ to a common right building block $(Z_R, S_R)$.

- *The geometrical perspective*

  We construct the building block $(Z^\flat, S^\flat)$ by blowing-up the semi-Fano threefold $P$ along the smooth irreducible curve $C^\flat$, which — as in the Higgs branch of the Abelian gauge theories — arises from a generic *deformation* of the section $s_0$ of the anti-canonical line bundle $-K_P$. Then, relations (4.39) determine again the two-form and three-form Betti numbers of the $G_2$-manifold $Y^\flat$. The smooth Coulomb branch building block $(Z^\sharp, S^\sharp)$ results from the sequence of $n = k_1 + \ldots + k_s$ *blow-ups*

$$Z^\sharp \;=\; \mathrm{Bl}_{\{\tilde{C}_1^{k_1},\ldots,\tilde{C}_s^{k_s}\}} P \,, \tag{4.51}$$

  where each individual curve $\tilde{C}_i$ is resolved $k_i$ times such that $\dim k^\sharp = n - 1$. Therefore, using equations (4.10), (4.29) and (4.30), we arrive at the two-form and the three-form Betti numbers for the smooth $G_2$-manifold $Y^\sharp$

$$b_2(Y^\sharp) \;=\; (n-1) + \delta_R^{(2)} \,, \quad b_3(Y^\sharp) \;=\; b_3(P) + \left(\sum_{i=1}^{s} k_i\, \tilde{C}_i.\tilde{C}_i\right) + 3n + 22 + \delta_R^{(3)} \,, \tag{4.52}$$

  with the definitions as in (4.41). Using the equivalence relation $C^\flat \sim k_1\tilde{C}_1 + \ldots + k_s\tilde{C}_s$, the changes of the Betti numbers are given by

$$\begin{aligned} b_2(Y^\flat) \;&=\; b_2(Y^\sharp) - (n-1) \,, \\ b_3(Y^\flat) \;&=\; b_3(Y^\sharp) + \left(\sum_{i=1}^{s} \tilde{\chi}_{ii} k_i (k_i - 1)\right) + 2\left(\sum_{1\leq i<j\leq s} \tilde{\chi}_{ij} k_i k_j\right) - 3(n-1) \end{aligned} \tag{4.53}$$

  in terms of the intersection numbers $\tilde{\chi}_{ij} = \tilde{C}_i.\tilde{C}_j$ on the K3 surface $S$.

- *The correspondence between the gauge theory and the geometrical perspectives*

  The computed change of Betti numbers is also in accordance with the phase structure of the proposed non-Abelian gauge theory description. Namely, the change of the two-form Betti number conforms with the *difference of the four-dimensional $\mathcal{N} = 1$ vector multiplets in the Higgs and Coulomb branches*, given by the rank of the non-Abelian gauge group (4.48). The *difference of four-dimensional $\mathcal{N} = 1$ chiral multiplets* is accurately predicted by the complex dimensions of the Higgs and Coulomb branches. In other words, with equations (4.30), (4.49) and (4.50), we find for the discussed non-Abelian gauge theories

$$b_3(Y^\flat) - b_3(Y^\sharp) \;=\; b_3^\flat - b_3^\sharp \;=\; \dim_{\mathbb{C}} H^\flat - \dim_{\mathbb{C}} C^\sharp \,. \tag{4.54}$$

The established correspondence between $G_2$-manifolds and non-Abelian Higgs and Coulomb branches carries over to mixed Higgs–Coulomb branches as well, which we illustrate with an explicit example in section 4.2.3. The fact that the performed analysis of the non-Abelian gauge theory sectors closely parallels the study of the Abelian gauge theories does not come as a surprise, because the Abelian gauge group (4.34) arises from partially higgsing the non-Abelian gauge group (4.48) to its maximal Abelian subgroup. As a result, the topological data of the $G_2$-manifolds for the Higgs, Coulomb and mixed Higgs–Coulomb phases resulting from a given semi-Fano threefold $P$ are the same for both the discussed Abelian and non-Abelian gauge theory sectors.

### 4.2.3 Examples of $G_2$-manifolds with $\mathcal{N} = 2$ gauge theory sectors

Following the general discussion of $\mathcal{N} = 2$ gauge theory sectors in sections 4.2.1 and 4.2.2, we now illustrate the emergence of $\mathcal{N} = 2$ gauge theory sectors in twisted connected sum $G_2$-manifolds with a few explicit examples. Two examples will be described step by step. Since the reasoning for the remaining examples is similar, we comment on their extra ingredients and present mainly the results.

**SU(4) gauge theory with adjoint matter from the Fano threefold $\mathbb{P}^3$**

Consider the Fano threefold $\mathbb{P}^3$ with the anti-canonical divisor $-K_{\mathbb{P}^3} = 4H$ in terms of the hyperplane class $H$. Let $\tilde{s}_{0,1}$ be a generic global section of $H$ and $s_1$ be generic global section of $-K_{\mathbb{P}^3}$. With the affine coordinate $t$ of the factor $\mathbb{P}^1$ of the resolved building block $Z_{\text{sing}} \subset \mathbb{P}^3 \times \mathbb{P}^1$, equation (4.46) leads to the hypersurface equation

$$\tilde{s}_{0,1}^4 + t s_1 \;=\; 0\,. \tag{4.55}$$

Therefore, there is only $k_1 = 4$ in equation (4.47). This implies that we are specializing to the case where there is a curve $\tilde{C}_1 = \{\tilde{s}_{0,1} = 0\} \cap \{s_1 = 0\} \cap \{t = 0\}$ exhibiting an $A_3$ singularity. In particular, this yields a $\mathcal{N} = 2$ gauge theory sector[10] with gauge group $\mathrm{SU}(k_1) = \mathrm{SU}(4)$.

First of all, notice that, due to equation (4.30), the curves $C^{(k)} = (-K_{\mathbb{P}^3}) \cap (kH)$ have the following intersection numbers on the K3 surface $S$ and genera

$$C^{(k)} \cdot C^{(l)} \;=\; 4kl\,, \qquad g(C^{(k)}) \;=\; \frac{1}{2} C^{(k)} \cdot C^{(k)} + 1 \;=\; 2k^2 + 1\,. \tag{4.56}$$

Furthermore, the equivalence $\tilde{C}_1 \sim C^{(1)}$ leads to $g(\tilde{C}_1) = 3$ four-dimensional $\mathcal{N} = 2$ hypermultiplets in the adjoint representation of SU(4).

- *The gauge theory perspective*: The first task is to compute the predictions for the Higgs and Coulomb branches arising from this spectrum. Since we have only a single curve in this example, the second term in parenthesis of equation (4.49) vanishes and, therefore,

[10] Note that for this particular example the deformed phases of the non-enhanced $\mathcal{N} = 2$ Abelian gauge theory sector have also been discussed in reference [254].

we obtain for the Higgs branch

$$\dim_{\mathbb{C}} H^\flat = 2 \times [(3-1) \times (4^2-1)] - 2 \times (1-1) = 60 \,. \tag{4.57}$$

Since $n = k_1 = 4$, with the help of equation (4.50), we obtain for the Coulomb branch

$$\dim_{\mathbb{C}} C^\sharp = 2 \times [3 \times (4-1)] + (4-1) = 21 \,. \tag{4.58}$$

Therefore, we obtain

$$\dim_{\mathbb{C}} H^\flat - \dim_{\mathbb{C}} C^\sharp \;=\; 39 \,. \tag{4.59}$$

- *The geometrical perspective*: The next task is to compute the Betti numbers of the twisted connected sum $G_2$-manifolds $Y^\flat$ and $Y^\sharp$, which geometrically realize the Higgs and Coulomb branches by orthogonal gluing of the building blocks $(Z^\flat, S^\flat)$ and $(Z^\sharp, S^\sharp)$ to a common right building block $(Z_R, S_R)$.

  As proposed in section 4.2.2, in order to determine the building block $(Z^\flat, S^\flat)$ of the Higgs branch $H^\flat$, we deform the hypersurface equation (4.55) to $s_0 + ts_1 = 0$ with generic sections $s_0$ and $s_1$ of $-K_{\mathbb{P}^3}$. This allows for the blow-up of $\mathbb{P}^3$ along the irreducible smooth curve with $C^\flat \sim C^{(4)}$. For this curve, we use equation (4.56) to obtain

$$C^{(4)} \cdot C^{(4)} = 4 \times 4 \times 4 = 64 \,, \qquad g(C^{(4)}) \;=\; \frac{1}{2} C^{(4)} \cdot C^{(4)} + 1 \;=\; (2 \times 4^2) + 1 = 33 \,. \tag{4.60}$$

  Therefore, since $b_3(\mathbb{P}^3) = 0$, from equation (4.37), the building block $(Z^\flat, S^\flat)$ has

$$\dim k^\flat \;=\; 0 \,, \qquad b_3(Z^\flat) \;=\; 2g(C^\flat) \;=\; 66 \,. \tag{4.61}$$

  Again, as proposed in section 4.2.2, in order to determine the building block $(Z^\sharp, S^\sharp)$ of the Coulomb branch $C^\sharp$, we sequentially perform $n = 4$ blow-ups of $\mathbb{P}^3$ along the curve $\tilde{C}_1$. For this curve, we use equation (4.56) to obtain

$$\tilde{C}_1 \cdot \tilde{C}_1 = 4 \times 1 \times 1 = 4 \,, \qquad g(\tilde{C}_1) \;=\; \frac{1}{2} \tilde{C}_1 \cdot \tilde{C}_1 + 1 \;=\; (2 \times 1^2) + 1 = 3 \,. \tag{4.62}$$

  Therefore, since $b_3(\mathbb{P}^3) = 0$ and all the blow-ups occurs along the same curve $\tilde{C}_1$, from equation (4.38), the building block $(Z^\sharp, S^\sharp)$ has

$$\dim k^\sharp \;=\; 4-1 = 3 \,, \qquad b_3(Z^\sharp) \;=\; (2\times 4) + \sum_{i=1}^{4} C_i \cdot C_i = 8 + (4 \times \tilde{C}_1 \cdot \tilde{C}_1) = 8 + (4 \times 4) = \; 24 \,. \tag{4.63}$$

  Finally, we orthogonally glue the building blocks $(Z^\flat, S^\flat)$ and $(Z^\sharp, S^\sharp)$ to a suitable right building block $(Z_R, S_R)$. We use equations (4.39), (4.52) and the definition of the reduced

Betti numbers given in equation (4.42) to find

$$\begin{aligned} b_2^\flat &= b_2(Y^\flat) - \delta_R^{(2)} = 0 \,, \\ b_3^\flat &= b_3(Y^\flat) - \delta_R^{(3)} = b_3(\mathbb{P}^3) + C^\flat \cdot C^\flat + 25 = 64 + 25 = 89 \,, \\ b_2^\sharp &= b_2(Y^\sharp) - \delta_R^{(2)} = (n-1) = (4-1) = 3 \,, \\ b_3^\sharp &= b_3(\mathbb{P}^3) + 4\tilde{C}_1 \cdot \tilde{C}_1 + 3n + 22 = (4\times 4) + (3\times 4) + 22 = 16 + 12 + 22 = 50 \,. \end{aligned} \tag{4.64}$$

- *The correspondence*: This is in accordance with the anticipated gauge theory description established in section 4.2.2. Indeed, observe that the differences $b_2^\sharp - b_2^\flat = 3$ and $b_3^\flat - b_3^\sharp = 39$ agree with the rank of the gauge group SU(4) and the change in the dimensionality of the Higgs and Coulomb branches in equation (4.59), respectively.

By partially deforming the first term $\tilde{s}_{0,1}^4$ in the hypersurface equation (4.55), we can realize hypersurface singularities describing various Abelian and non-Abelian subgroups of SU(4). Such partial deformations geometrically realize mixed Higgs–Coulomb branches of the SU(4) gauge theory. We collect the geometry and phase structure of these mixed Higgs–Coulomb branches in table 4.7, where the entries of this table are determined by equations (4.28), (4.29), (4.49), (4.50), and (4.56). Note that — depending on the breaking pattern of SU(4) arising from partially higgsing — the dimensions of Higgs and Coulomb branches vary because only the charged matter spectrum of the unbroken gauge group plays a role for the Higgs and Coulomb branches in this gauge theory sector. For all entries in table 4.7 we indeed find that

$$b_3^\flat - b_3^\sharp = h^\flat - c^\sharp \,, \qquad \dim k^\sharp = \mathrm{rk}\, G \,. \tag{4.65}$$

This agreement confirms nicely the correspondence between gauge theory branches and phases of twisted connected sum $G_2$-manifolds.

### SU(2) × SU(2) × U(1) gauge theory from the Fano threefold MM48$_2$

In the following we quickly present an example where both adjoint and bi-fundamental matter appear in the spectrum. This examples comes from the rank two Fano threefold $W_6$ with reference number MM48$_2$. This threefold is a hypersurface of bidegree $(1,1)$ in $\mathbb{P}^2 \times \mathbb{P}^2$ with $b_3(W_6) = 0$ [236]. Let $H_1$ and $H_2$ be the hyperplane classes of $\mathbb{P}^2 \times \mathbb{P}^2$. By the adjunction formula, the anti-canonical divisor of $W_6$ reads $-K_{W_6} = 2H_1 + 2H_2$. Furthermore, the self-intersection numbers of the curves $C^{(k,l)} = (-K_{W_6}) \cap (kH_1 + lH_2)$ in the anti-canonical divisor $-K_{W_6}$ and hence their genera are given by

$$C^{(k_1,l_1)} \cdot C^{(k_2,l_2)} = 2(k_1k_2 + l_1l_2 + 2k_1l_2 + 2l_1k_2) \,, \qquad g(C^{(k,l)}) = k^2 + l^2 + 4kl + 1 \,. \tag{4.66}$$

With generic global sections $\tilde{s}_{0,1}$, $\tilde{s}_{0,2}$ and $s_1$ of $H_1$, $H_2$ and $-K_{W_6}$, the equation for the singular building block $Z_{\mathrm{sing}} \subset W_6 \times \mathbb{P}^1$ becomes, with the affine coordinate $t$ of $\mathbb{P}^1$,

$$\tilde{s}_{0,1}^2 \tilde{s}_{0,2}^2 + t s_1 = 0 \,. \tag{4.67}$$

| $s_0$ factors | Gauge Group | $\mathcal{N}=2$ Hypermultiplet spectrum | $h^\flat$ | $c^\sharp$ | $b_3^\flat$ | $b_3^\sharp$ | $k^\sharp$ |
|---|---|---|---|---|---|---|---|
| $1^4$ | SU(4) | $3\times\mathbf{adj}$ | 60 | 21 | 89 | 50 | 3 |
| $1^3\cdot 1$ | $\mathrm{SU}(3)\times\mathrm{U}(1)$ | $3\times\mathbf{adj};4\times\mathbf{3}_{+1}$ | 54 | 15 | 89 | 50 | 3 |
| $1^2\cdot 1^2$ | $\mathrm{SU}(2)^2\times\mathrm{U}(1)$ | $3\times(\mathbf{adj},\mathbf{1});3\times(\mathbf{1},\mathbf{adj});4\times(\mathbf{2},\mathbf{2})_{+1}$ | 54 | 15 | 89 | 50 | 3 |
| $1^2\cdot 1\cdot 1$ | $\mathrm{SU}(2)\times\mathrm{U}(1)^2$ | $3\times\mathbf{adj};4\times\mathbf{2}_{(+1,+1)};4\times\mathbf{2}_{(+1,0)};4\times\mathbf{2}_{(0,+1)}$ | 48 | 9 | 89 | 50 | 3 |
| $1\cdot 1\cdot 1\cdot 1$ | $\mathrm{U}(1)^3$ | $4\times(+1,+1,0);4\times(+1,0,+1);4\times(0,+1,+1);$ $4\times(+1,0,0);4\times(0,+1,0);4\times(0,0,+1)$ | 42 | 3 | 89 | 50 | 3 |
| $2\cdot 1^2$ | $\mathrm{SU}(2)\times\mathrm{U}(1)$ | $3\times\mathbf{adj};8\times\mathbf{2}_{+1}$ | 42 | 8 | 89 | 55 | 2 |
| $2\cdot 1\cdot 1$ | $\mathrm{U}(1)^2$ | $4\times(+1,+1);8\times(+1,0);8\times(0,+1)$ | 36 | 2 | 89 | 55 | 2 |
| $2^2$ | SU(2) | $9\times\mathbf{adj}$ | 48 | 19 | 89 | 60 | 1 |
| $2\cdot 2$ | U(1) | $16\times(+1)$ | 30 | 1 | 89 | 60 | 1 |
| $3\cdot 1$ | U(1) | $12\times(+1)$ | 22 | 1 | 89 | 68 | 1 |

Table 4.7: The gauge theory branches of the SU(4) gauge theory of the building blocks associated to the rank one Fano threefold $\mathbb{P}^3$. The columns list the factorization of the anti-canonical section $s_0$ with degrees and multiplicities, the gauge group of the gauge theory branch, the matter spectrum of $\mathcal{N}=2$ hypermultiplets with their non-Abelian representations together with the Abelian U(1) charges, the complex dimensions $h^\flat$ and $c^\sharp$ of the Higgs and Coulomb branches, the reduced three-form Betti numbers $b_3^\flat$ and $b_3^\sharp$ of the twisted connected sum $G_2$-manifolds $Y^\flat$ and $Y^\sharp$, and the kernel $k^\sharp$ of the Coulomb phase building block $(Z^\sharp, S^\sharp)$.

Thus, since $k_1 = k_2 = 2$, we find $A_1$ singularities along the two curves $\tilde{C}_i = \{\tilde{s}_{0,i} = 0\} \cap \{s_1 = 0\} \cap \{t = 0\}$ with $i = 1, 2$.

- First of all, with equation (4.48) in section 4.2.2, we therefore find a $\mathrm{SU}(2)\times\mathrm{SU}(2)\times\mathrm{U}(1)$ gauge theory both with adjoint matter and with bi-fundamental matter from the intersection points $\tilde{C}_1\cap\tilde{C}_2$. Due to equation (4.48), we have the correspondence $\mathrm{SU}(2)\times\mathrm{SU}(2)\times\mathrm{U}(1) \simeq \mathrm{U}(2)\times\mathrm{U}(2)/\mathrm{U}(1)_{\mathrm{Diag}}$.

- Secondly, there are $g(\tilde{C}_i)$ four-dimensional $\mathcal{N}=2$ hypermultiplets in the adjoint of SU(2) for each $i = 1, 2$. Due to the equivalences $\tilde{C}_1 \sim C^{(1,0)}$ and $\tilde{C}_2 \sim C^{(0,1)}$ and relations (4.66), we find $g(\tilde{C}_1) = g(\tilde{C}_2) = 2$.

- Thirdly, since $C^{(1,0)}\cdot C^{(0,1)} = 4$, we have 4 four-dimensional $\mathcal{N}=2$ hypermultiplets in the bi-fundamental $(\mathbf{2},\mathbf{2})_{+1}$ where +1 is the U(1) charge with respect to the diagonal U(1) subgroup of the respective unitary group U(2) in the correspondence $\mathrm{SU}(2)\times\mathrm{SU}(2)\times\mathrm{U}(1) \simeq \mathrm{U}(2)\times\mathrm{U}(2)/\mathrm{U}(1)_{\mathrm{Diag}}$.

  In summary, we arrive at the following four-dimensional $\mathcal{N}=2$ hypermultiplet matter spectrum

$$2\times(\mathbf{adj},\mathbf{1})\ ;\quad 2\times(\mathbf{1},\mathbf{adj})\ ;\quad 4\times(\mathbf{2},\mathbf{2})_{+1}\ . \tag{4.68}$$

- *The gauge theory perspective*: The first task is to compute the predictions for the Higgs and Coulomb branches arising from this spectrum. Notice that this example has two curves and not a single one as in the previous example. Using equation (4.49) leads, for the Higgs branch,

$$\begin{aligned}\dim_{\mathbb{C}} H^\flat &= 2 \times [2 \times (2^2 - 1)] + 2 \times (\tilde{\chi}_{12} k_1 k_2) - 2 \times (2 - 1) \\ &= 12 + (2 \times 4 \times 2 \times 2) - 2 \\ &= 42 \, .\end{aligned} \tag{4.69}$$

  Furthermore, using equation (4.50) leads, for the Coulomb branch,

$$\begin{aligned}\dim_{\mathbb{C}} C^\sharp &= 2 \times [2 \times 2 \times (2 - 1)] + 3 \\ &= 11 \, .\end{aligned} \tag{4.70}$$

  Therefore, we obtain

$$\dim_{\mathbb{C}} H^\flat - \dim_{\mathbb{C}} C^\sharp = 31 \, . \tag{4.71}$$

- *The geometrical perspective*: The next task is to compute the Betti numbers of the twisted connected sum $G_2$-manifolds $Y^\flat$ and $Y^\sharp$.

  For the Higgs branch, we deform the hypersurface equation such that it allows for the blow-up of $\mathbb{P}^2 \times \mathbb{P}^2$ along the irreducible smooth curve $C^\flat \sim C^{(2,2)}$. For this curve, we use equation (4.66) to obtain $C^{(2,2)} \cdot C^{(2,2)} = 48$ and the genus $g(C^{(2,2)}) = 25$. Therefore, the building block $(Z^\flat, S^\flat)$ has

$$\dim k^\flat \; = \; 0 \, , \qquad b_3(Z^\flat) \; = \; 2g(C^\flat) \; = \; 50 \, . \tag{4.72}$$

  For the Coulomb branch, we sequentially perform $n = 4$ blow-ups of $\mathbb{P}^2 \times \mathbb{P}^2$ along the curves $\tilde{C}_1$ and $\tilde{C}_2$ (two blow-ups along each). For these curves, we find

$$\begin{aligned}\tilde{C}_1 \cdot \tilde{C}_1 &= 2 \, , \\ \tilde{C}_2 \cdot \tilde{C}_2 &= 2 \; .\end{aligned} \tag{4.73}$$

  Therefore, since $b_3(W_6) = 0$, the building block $(Z^\sharp, S^\sharp)$ has

$$\begin{aligned}&\dim k^\sharp \; = \; 4 - 1 = 3 \, , \\ &b_3(Z^\sharp) \; = \; (2 \times 4) \; + \; \sum_{i=1}^{2} k_i \tilde{C}_i \cdot \tilde{C}_i = 8 + 2\tilde{C}_1 \cdot \tilde{C}_1 + 2\tilde{C}_2 \cdot \tilde{C}_2 = 8 + 4 + 4 = 16 \, .\end{aligned} \tag{4.74}$$

  Finally, we orthogonally glue the building blocks $(Z^\flat, S^\flat)$ and $(Z^\sharp, S^\sharp)$ to a suitable right

building block $(Z_R, S_R)$. We use equations (4.39) and (4.52) to find

$$\begin{aligned} b_2^\flat &= b_2(Y^\flat) - \delta_R^{(2)} = 0 \,, \\ b_3^\flat &= b_3(Y^\flat) - \delta_R^{(3)} = b_3(\mathbb{P}^3) + C^\flat \cdot C^\flat + 25 = 48 + 25 = 73 \,, \\ b_2^\sharp &= b_2(Y^\sharp) - \delta_R^{(2)} = (n-1) = (4-1) = 3 \,, \\ b_3^\sharp &= b_3(W_6) + 2\tilde{C}_1 \cdot \tilde{C}_1 + 2\tilde{C}_2 \cdot \tilde{C}_2 + 3n + 22 = (2\times 2) + (2\times 2) + (3\times 4) + 22 = 42 \,. \end{aligned} \tag{4.75}$$

- *The correspondence*: This is in accordance with the gauge theory description. Indeed, the differences are $b_2^\sharp - b_2^\flat = 3$ and $b_3^\sharp - b_3^\flat = 73 - 42 = 31$.

The resulting correspondence between the gauge theory branches and the phase structure of the twisted connected sum $G_2$-manifolds is summarized in table 4.8, where the entries are computed with the formulas (4.28), (4.29), (4.49), (4.50), and (4.66) — similarly as the explicit computations for the first example in this section.

| $s_0$ factors | Gauge Group | $\mathcal{N}=2$ Hypermultiplet spectrum | $h^\flat$ | $c^\sharp$ | $b_3^\flat$ | $b_3^\sharp$ | $k^\sharp$ |
|---|---|---|---|---|---|---|---|
| $(1,0)^2(0,1)^2$ | $\mathrm{SU}(2)\times\mathrm{SU}(2)\times\mathrm{U}(1)$ | $2\times(\mathbf{adj},\mathbf{1}); 2\times(\mathbf{1},\mathbf{adj}); 4\times(\mathbf{2},\mathbf{2})_{+1}$ | 42 | 11 | 73 | 42 | 3 |
| $(1,0)^2(0,1)(0,1)$ | $\mathrm{SU}(2)\times\mathrm{U}(1)^2$ | $2\times\mathbf{adj}; 4\times\mathbf{2}_{(1,0)}; 4\times\mathbf{2}_{(0,1)}; 2\times\mathbf{1}_{(1,1)}$ | 38 | 7 | 73 | 42 | 3 |
| $(1,0)(1,0)$ $\cdot(0,1)(0,1)$ | $\mathrm{U}(1)^3$ | $2\times(1,1,0); 4\times(1,0,1); 4\times(0,1,1);$ $4\times(1,0,0); 4\times(0,1,0); 2\times(0,0,1)$ | 34 | 3 | 73 | 42 | 3 |
| $(2,0)(0,1)^2$ | $\mathrm{SU}(2)\times\mathrm{U}(1)$ | $2\times\mathbf{adj}; 8\times\mathbf{2}_{+1}$ | 36 | 6 | 73 | 43 | 2 |
| $(2,0)(0,1)(0,1)$ | $\mathrm{U}(1)^2$ | $8\times(1,0); 8\times(0,1); 2\times(1,1)$ | 32 | 2 | 73 | 43 | 2 |
| $(1,1)^2$ | $\mathrm{SU}(2)$ | $7\times\mathbf{adj}$ | 36 | 15 | 73 | 52 | 1 |
| $(1,1)(1,1)$ | $\mathrm{U}(1)$ | $12\times(+1)$ | 22 | 1 | 73 | 52 | 1 |
| $(2,0)(0,2)$ | $\mathrm{U}(1)$ | $16\times(+1)$ | 30 | 1 | 73 | 44 | 1 |
| $(2,1)(0,1)$ | $\mathrm{U}(1)$ | $10\times(+1)$ | 18 | 1 | 73 | 56 | 1 |

Table 4.8: The gauge theory branches of the $\mathrm{SU}(2)\times\mathrm{SU}(2)\times\mathrm{U}(1)$ gauge theory associated to the Fano threefold $W_6$ with Mori–Mukai label $\mathrm{MM48}_2$ [236]. Listed are the factors of the anti-canonical section $s_0$ with bi-degrees and multiplicities, the unbroken gauge subgroup, the $\mathcal{N}=2$ matter hypermultiplets, the complex dimensions $h^\flat$ and $c^\sharp$ of the Higgs and Coulomb branches, the reduced three-form Betti numbers $b_3^\flat$ and $b_3^\sharp$ of the twisted connected $G_2$-manifolds $Y^\flat$ and $Y^\sharp$, and the kernel $k^\sharp$ of the Coulomb phase building block $(Z^\sharp, S^\sharp)$.

**Further examples from toric semi-Fano threefolds**

Our last class of examples concerns $\mathcal{N} = 2$ gauge theory sectors from toric semi-Fano threefolds $P_\Sigma$, where the fan $\Sigma$ is obtained from a triangulation of a three-dimensional reflexive lattice polytope $\Delta$. In this toric setup, the anti-canonical divisor reads

$$-K_{P_\Sigma} = D_1 + \ldots + D_n \,, \tag{4.76}$$

where the toric divisors $D_i$, $i = 1, \ldots, n$, correspond to the one-dimensional cones of $\Sigma$, i.e., to the rays of the lattice polytope $\Delta$. For smooth toric varieties $P_\Sigma$, the toric divisors $D_i$ are smooth and intersect transversely [210]. As the anti-canonical divisor $-K_P$ is *base-point free*[11], we can apply Bertini's theorem [101] to argue that we can find a smooth global section $s_1$ of the anti-canonical divisor $-K_{P_\Sigma}$ and further generic global sections $s_{0,i}$ of $D_i$ such that the curves $C_i = \{s_{0,i} = 0\} \cap \{s_1 = 0\}$ are smooth and mutually intersect transversely. Hence, the toric semi-Fano threefold $P_\Sigma$ realizes indeed a $\mathrm{U}(1)^{n-1}$ gauge theory sector. The four-dimensional matter spectrum is then given by table 4.5, where the multiplicities $\chi_{ij}$ are the toric triple intersection numbers

$$\chi_{ij} = -K_{P_\Sigma}.D_i.D_j \,. \tag{4.77}$$

As proposed in section 4.2.1, we construct the building blocks $(Z^\sharp, S^\sharp)$ of the Coulomb branch $C^\sharp$ by the sequential blow-ups (4.27) along the curves $C_i$, while we determine the building block $(Z^\flat, S^\flat)$ of the Higgs branch $H^\flat$ by blow-up of a smooth curve $C^\flat = \{s_0 = 0\} \cap \{s_1 = 0\}$ obtained by deforming the singular section $s_{0,1} \cdots s_{0,n}$ to a generic anti-canonical section $s_0$. Therefore, we arrive at the twisted connected sum $G_2$-manifolds $Y^\sharp$ and $Y^\flat$ by orthogonally gluing these gauge theory building blocks with a right building block $(Z_R, S_R)$ in the usual way.[12]

Note that, due to linear equivalences among the toric divisors $D_i$ , the Abelian gauge theory can enhance to non-Abelian gauge groups as well. Namely, assume that the anti-canonical bundle $-K_{P_\Sigma}$ is linearly equivalent to

$$-K_{P_\Sigma} \sim k_1 \tilde{D}_1 + \ldots + k_s \tilde{D}_s \,, \tag{4.78}$$

where, for some divisors, there are some equivalences $\tilde{D}_\alpha \sim \sum_i a_{\alpha i} D_i$ with global sections $\tilde{s}_{0,\alpha}$. Furthermore, we require that the curves $\tilde{C}_\alpha$ are smooth and mutually intersect transversely. Following the prescription given in section 4.2.2, we arrive at the $\mathcal{N} = 2$ non-Abelian gauge theory sector with gauge group

$$G = \mathrm{SU}(k_1) \times \ldots \times \mathrm{SU}(k_s) \times \mathrm{U}(1)^{s-1} \,. \tag{4.79}$$

Note that rank of the gauge group $(k_1 + \ldots + k_s - 1)$ is a priori not correlated with the number $n$ of toric divisors. Instead, it depends on the precise nature of the linear equivalences among the toric divisors $D_i$, $i = 1, \ldots, n$, and the divisors $\tilde{D}_\alpha$, $\alpha = 1, \ldots, s$.

[11] For a given vector space of global sections, their locus of common zeros is called the base-locus or base-points.

[12] For toric semi-Fano threefolds $P_\Sigma$, some of the performed blow-ups discussed here and in the following can also be described with toric geometry techniques [234]. However, the use of the toric description is not an advantage to extract the relevant geometric data for us.

Let us give an example by analyzing the four-dimensional $\mathcal{N} = 2$ gauge theory sectors with the rank two toric semi-Fano threefold $P_\Sigma$ of reference number K32, which was already described in some detail in section 4.1. The linear equivalences among the toric divisors $D_1, \ldots, D_5$ leads to the anti-canonical divisor

$$-K_{P_\Sigma} \;=\; D_1 + \ldots + D_5 \;\sim\; 3D_1 \;\sim\; 3D_2 + 3D_4 \,. \tag{4.80}$$

With these linearly equivalent representations for $-K_{P_\Sigma}$, we arrive, for instance, at the gauge groups $\mathrm{U}(1)^4$ of rank four, $\mathrm{SU}(3)$ of rank three, or $\mathrm{SU}(3) \times \mathrm{SU}(3) \times \mathrm{U}(1)$ of rank five. Note that the phases of the lower rank gauge groups $\mathrm{U}(1)^4$ and $\mathrm{SU}(3)$ enjoy again the interpretation as mixed Higgs–Coulomb branches of the $\mathrm{SU}(3) \times \mathrm{SU}(3) \times \mathrm{U}(1)$ gauge theory of rank five which, by applying equation (4.77) and equation (4.30), yields the spectrum

$$1 \times (\mathbf{adj}, \mathbf{1}) \,; \quad 1 \times (\mathbf{1}, \mathbf{adj}) \,; \quad 3 \times (\mathbf{3}, \mathbf{3})_{+1} \,. \tag{4.81}$$

In table 4.9 we list the gauge theory sectors of a few toric semi-Fano threefolds $P_\Sigma$. This table does not display all mixed Higgs–Coulomb branches. Here, we focus on the resulting twisted connected sum $G_2$-manifolds $Y^\flat$ and $Y^\sharp$ associated to the Higgs $H^\flat$ and Coulomb branches $C^\sharp$ of the maximally enhanced gauge group of maximal rank, as obtained by the factorization of the anti-canonical bundle $-K_{P_\Sigma}$.

Notice the existence of an $\mathcal{N} = 2$ $\mathrm{SU}(3) \times \mathrm{SU}(2) \times \mathrm{U}(1)$ gauge theory with adjoint representations in both $\mathrm{SU}(3)$ and $\mathrm{SU}(2)$ as well as three generations of charged bi-fundamental matter $(\mathbf{3}, \mathbf{2})_{+1}$ — this is given in the first row of table 4.9. While this vaguely resembles the content of the Standard Model of Particle Physics, one still has to take care of supersymmetry breaking by allowing $\mathcal{N} = 2 \to \mathcal{N} = 1$.

### 4.2.4 Transitions among twisted connected sum $G_2$-manifolds

The proposed correspondence between phases of twisted connected sum $G_2$-manifolds and gauge theory branches of the described $\mathcal{N} = 2$ gauge theory sectors is essentially based upon the correspondence between extremal transitions in the asymptotically cylindrically Calabi–Yau threefolds $X_{L/R}$ and the Higgs–Coulomb phase structure of the associated $\mathcal{N} = 2$ gauge theories.

In the original type IIA string theory setting, the $\mathcal{N} = 2$ matter spectrum arises from solitons of massless D2-branes wrapping the vanishing cycles of the singular Calabi–Yau threefolds at the transition point [255, 256], which become membranes in the discussed context of M-theory. However, while in the type IIA setting these D2-branes furnish BPS states of the $\mathcal{N} = 2$ algebra, the corresponding interpretation of membrane states becomes more subtle in the context of M-theory on twisted connected sum $G_2$-manifolds because the corresponding membrane states do not admit a BPS interpretation due to minimal four-dimensional $\mathcal{N} = 1$ supersymmetry. Therefore, a natural question now is whether the described M-theory transitions are actually dynamically realized.

As discussed in chapter 3, the semi-classical moduli space $\mathcal{M}_\mathbb{C}$ of M-theory on $G_2$-manifolds has the geometric moduli space $\mathcal{M}$ of Ricci-flat $G_2$-manifolds as a real subspace. From the low-energy effective $\mathcal{N} = 1$ supergravity point of view, this is a consequence of the semi-classical

| No. | $\rho$ | Gauge Group | $\mathcal{N} = 2$ Hypermultiplet spectrum | $h^\flat$ | $c^\sharp$ | $b_3^\flat$ | $b_3^\sharp$ | $k^\sharp$ |
|---|---|---|---|---|---|---|---|---|
| K24, $MM34_2$ | 2 | $SU(3) \times SU(2) \times U(1)$ | $2 \times (\mathbf{adj}, \mathbf{1}); (\mathbf{1}, \mathbf{adj}); 3 \times (\mathbf{3}, \mathbf{2})_{+1}$ | 50 | 14 | 79 | 43 | 4 |
| K32 | 2 | $SU(3)^2 \times U(1)$ | $(\mathbf{adj}, \mathbf{1}); (\mathbf{1}, \mathbf{adj}); 3 \times (\mathbf{3}, \mathbf{3})_{+1}$ | 52 | 13 | 79 | 40 | 5 |
| K35, $MM36_2$ | 2 | $SU(5) \times SU(2) \times U(1)$ | $2 \times (\mathbf{adj}, \mathbf{1}); (\mathbf{5}, \mathbf{2})_{+1}$ | 60 | 22 | 87 | 49 | 6 |
| K36, $MM35_2$ | 2 | $SU(4) \times SU(2) \times U(1)$ | $2 \times (\mathbf{adj}, \mathbf{1}); 2 \times (\mathbf{4}, \mathbf{2})_{+1}$ | 54 | 17 | 81 | 44 | 5 |
| K37, $MM33_2$ | 2 | $SU(4) \times SU(3) \times U(1)$ | $(\mathbf{adj}, \mathbf{1}); 3 \times (\mathbf{4}, \mathbf{3})_{+1}$ | 54 | 12 | 79 | 37 | 6 |
| K62, $MM27_3$ | 3 | $SU(2)^3 \times U(1)^2$ | $(\mathbf{adj}, \mathbf{1}^2); (\mathbf{1}, \mathbf{adj}, \mathbf{1}); (\mathbf{1}^2, \mathbf{adj}); 2 \times (\mathbf{2}^2, \mathbf{1})_{(1,1)}$ $2 \times (\mathbf{2}, \mathbf{1}, \mathbf{2})_{(1,0)}; 2 \times (\mathbf{1}, \mathbf{2}^2)_{(0,1)}$ | 44 | 11 | 73 | 40 | 5 |
| K68, $MM25_3$ | 3 | $SU(3) \times SU(2) \times U(1)^2$ | $(\mathbf{adj}, \mathbf{1}); 3 \times (\mathbf{3}, \mathbf{2})_{(1,1)}; 2 \times (\mathbf{3}, \mathbf{1})_{(1,0)}; (\mathbf{1}, \mathbf{2})_{(0,1)}$ | 42 | 9 | 69 | 36 | 6 |
| K105, $MM31_3$ | 3 | $SU(3)^2 \times SU(2) \times U(1)^2$ | $(\mathbf{adj}, \mathbf{1}^2); (\mathbf{1}, \mathbf{adj}, \mathbf{1}); 2 \times (\mathbf{3}^2, \mathbf{1})_{(1,1)}; (\mathbf{3}, \mathbf{1}, \mathbf{2})_{(1,0)};$ $(\mathbf{1}, \mathbf{3}, \mathbf{2})_{(0,1)}$ | 50 | 15 | 77 | 42 | 7 |
| K124 | 3 | $SU(4) \times SU(2)^2 \times U(1)^2$ | $(\mathbf{adj}, \mathbf{1}, \mathbf{1}); 2 \times (\mathbf{4}, \mathbf{2}, \mathbf{1})_{(1,1)}; 2 \times (\mathbf{4}, \mathbf{1}, \mathbf{2})_{(1,0)}$ | 48 | 13 | 73 | 38 | 7 |
| K218, $MM12_4$ | 4 | $SU(4) \times SU(3) \times SU(2)^2 \times U(1)^3$ | $(\mathbf{adj}, \mathbf{1}^3); (\mathbf{4}, \mathbf{3}, \mathbf{1}^2)_{(1,1,0)}; (\mathbf{4}, \mathbf{1}, \mathbf{2}, \mathbf{1})_{(1,0,1)};$ $(\mathbf{4}, \mathbf{1}^2, \mathbf{2})_{(1,0,0)}; (\mathbf{1}, \mathbf{3}, \mathbf{2}, \mathbf{1})_{(0,1,1)}; (\mathbf{1}, \mathbf{3}, \mathbf{1}, \mathbf{2})_{(0,1,0)}$ | 46 | 16 | 71 | 41 | 10 |
| K266, $MM10_4$ | 4 | $SU(3) \times SU(2)^3 \times U(1)^3$ | $(\mathbf{1}, \mathbf{adj}, \mathbf{1}^2); (\mathbf{3}, \mathbf{2}, \mathbf{1}^2)_{(1,1,0)}; 2 \times (\mathbf{3}, \mathbf{1}, \mathbf{2}, \mathbf{1})_{(1,0,1)};$ $2 \times (\mathbf{3}, \mathbf{1}^2, \mathbf{2})_{(1,0,0)}; (\mathbf{1}, \mathbf{2}^2, \mathbf{1})_{(0,1,1)}; (\mathbf{1}, \mathbf{2}, \mathbf{1}, \mathbf{2})_{(0,1,0)}$ | 42 | 10 | 67 | 35 | 8 |
| K221 | 4 | $SU(3) \times SU(2)^2 \times U(1)^3$ | $2 \times (\mathbf{3}, \mathbf{2}, \mathbf{1})_{(1,1,0)}; 3 \times (\mathbf{3}, \mathbf{1}, \mathbf{2})_{(1,0,1)}; (\mathbf{3}, \mathbf{1}^2)_{(1,0,0)}$ $2 \times (\mathbf{1}, \mathbf{2}, \mathbf{1})_{(0,1,0)}$ | 40 | 7 | 63 | 30 | 7 |
| K232 | 4 | $SU(4) \times SU(2)^3 \times U(1)^3$ | $2 \times (\mathbf{4}, \mathbf{2}, \mathbf{1}^2)_{(1,1,0)}; 2 \times (\mathbf{4}, \mathbf{1}, \mathbf{2}, \mathbf{1})_{(1,0,1)};$ $2 \times (\mathbf{4}, \mathbf{1}^2, \mathbf{2})_{(1,0,0)}$ | 42 | 9 | 65 | 32 | 9 |
| K233 | 4 | $SU(3) \times SU(2)^2 \times U(1)^2$ | $3 \times (\mathbf{3}, \mathbf{2}, \mathbf{1})_{(1,1)}; 3 \times (\mathbf{3}, \mathbf{1}, \mathbf{2})_{(1,0)}$ | 40 | 6 | 63 | 29 | 6 |
| K247 | 4 | $SU(4) \times SU(3)^2 \times SU(2) \times U(1)^3$ | $2 \times (\mathbf{4}, \mathbf{3}, \mathbf{1}^2)_{(1,1,0)}; 2 \times (\mathbf{4}, \mathbf{1}, \mathbf{3}, \mathbf{1})_{(1,0,1)};$ $(\mathbf{1}, \mathbf{3}, \mathbf{1}, \mathbf{2})_{(0,1,0)}; (\mathbf{1}^2, \mathbf{3}, \mathbf{4})_{(0,0,1)}$ | 46 | 11 | 69 | 34 | 11 |
| K257 | 4 | $SU(5) \times SU(3)^2 \times SU(2) \times U(1)^3$ | $2 \times (\mathbf{5}, \mathbf{3}, \mathbf{1}^2)_{(1,1,0)}; 2 \times (\mathbf{5}, \mathbf{1}, \mathbf{3}, \mathbf{1})_{(1,0,1)};$ $(\mathbf{5}, \mathbf{1}^2, \mathbf{2})_{(1,0,0)}$ | 48 | 12 | 71 | 35 | 12 |

Table 4.9: The $\mathcal{N} = 2$ gauge theory sectors for some smooth toric semi-Fano threefolds $P_\Sigma$ of Picard rank two and higher. The columns display the number of the threefold $P_\Sigma$ in the Mori–Mukai [236] and/or Kasprzyk [238] classification, its Picard rank $\rho$, the maximally enhanced gauge group of maximal rank by factorizing the anti-canonical bundle, the $\mathcal{N} = 2$ matter hypermultiplets, the complex dimensions $h^\flat$ and $c^\sharp$ of the Higgs and Coulomb branches, the reduced three-form Betti numbers $b_3^\flat$ and $b_3^\sharp$, and the kernel $k^\sharp$ of the Coulomb branch.

shift symmetries with respect to the real parts of the chiral fields (3.57). However, due to arguments about the absence of global continuous symmetries in consistent theories of gravity, see e.g. reference [258], these shift symmetries should be broken non-perturbatively such that the flat directions of the chiral moduli fields are lifted. In the context of M-theory on $G_2$-manifolds, membrane instantons on suitable three-cycles generate non-perturbative superpotential terms that break these continuous shift symmetries [228]. As these non-perturbative corrections are exponentially suppressed in the volume of the wrapped three-cycles, the flat directions — as described by the semi-classical moduli space $\mathcal{M}_{\mathbb{C}}$ — are expected to be only realized in the large volume limit of the $G_2$-compactification. Hence, M-theory transitions among $G_2$-manifolds should only occur in the absence of such non-perturbative effects, as for instance in the case of the large volume limit.[13]

If we now take both the large volume limit and the Kovalev limit simultaneously, gravity decouples, and we arrive at a genuine four-dimensional $\mathcal{N} = 2$ gauge theory sector with eight unbroken supercharges. Then the lower energy dynamics is indeed described as in references [250, 251, 255, 256], and the gauge theory phases connect asymptotically cylindrical Calabi–Yau threefolds via extremal transitions. Thus, we claim that, in the large volume and in the large Kovalev limit, the transitions among the $\mathcal{N} = 2$ gauge theory sectors geometrically realize the anticipated transitions among twisted connected sum $G_2$-manifolds.

If we maintain the large volume limit but allow for finite Kovalevton, the situation becomes more subtle. While the massless spectrum is still $\mathcal{N} = 2$, we expect that the appearance of further interaction terms breaks $\mathcal{N} = 2$ supersymmetry to $\mathcal{N} = 1$. Then the $\mathcal{N} = 2$ gauge theory sector is partially broken to a $\mathcal{N} = 1$ gauge theory, whose supersymmetry breaking couplings are governed by the scale of the Kovalevton. In this $\mathcal{N} = 1$ language, the transition between non-Abelian $\mathcal{N} = 2$ Higgs and Coulomb branches essentially describes an enhancement to an Abelian gauge symmetry within the $\mathcal{N} = 1$ Higgs branches. Namely, in the $\mathcal{N} = 1$ language, the $\mathcal{N} = 2$ Coulomb phase corresponds to the partially higgsing of the non-Abelian group to its maximal Abelian subgroup. Thus, at low energies, the proposed (non-Abelian) $\mathcal{N} = 2$ Higgs–Coulomb phase transition describes the Higgs mechanism of a weakly-coupled Abelian $\mathcal{N} = 1$ gauge theory. These observations provide for some evidence that, in the large volume limit, the anticipated phase structure among the described twisted connected sum $G_2$-manifolds is still realized — even for finite Kovalevton.

Geometrically, we therefore propose that in the M-theory moduli space $\mathcal{M}_{\mathbb{C}}$ the presented transitions among twisted connected sum $G_2$-manifolds are indeed unobstructed. In other words, we conjecture that the construction of orthogonally gluing commutes with extremal transitions in the asymptotically cylindrical Calabi–Yau threefolds $X_{L/R}$. Furthermore, our proposal implies that the moduli space $\mathcal{M}$ of Ricci-flat $G_2$-metrics of the twisted connected sum type should exhibit a stratification structure as predicted by the phase structure of the analyzed $\mathcal{N} = 2$ gauge theories sectors. In the context of Abelian gauge theory sectors our proposal conforms with a similar conjecture put forward in reference [254].

[13] In the presence of small non-perturbative obstructions we can still have quantum-mechanical transitions among four-dimensional vacua. Then the transition probability is governed by the tunneling rate through the barrier of the non-perturbative scalar potential.

# Part II

# Dark matter in the KL moduli stabilization scenario

# Prelude

So far we have studied the formal aspects of a high-energy string/M-theory and obtained a low-energy effective description from a top-down approach. In part II we are now interested in more phenomenological/cosmological aspects of compactifications. In particular, we investigate a scenario in which neutralino dark matter is obtained from a string/M-theory framework.

In chapter 5 we introduce the Kallosh–Linde (KL) moduli stabilization scenario, adding an F-term dynamical supersymmetry breaking sector motivated by $\mathcal{N} = 1$ SUSY QCD to allow for an uplifting of the non-positive KL vacuum structure.

In chapter 6 we study the corresponding dynamics after the inflationary phase of the Universe and impose constraints from both late entropy production and the dark matter relic density. Firstly, we consider neutralino dark matter thermal production via gravitinos generated during the reheating phase of the inflaton. Secondly, we consider neutralino dark matter production via a mixture of thermal neutralino production and also non-thermal production from decays of the ISS fields.

The *novel results* presented in this part of the thesis are:

- the use of the Intriligator–Seiberg–Shih (ISS) from the low-energy effective theory of the magnetic dual of SU($N_c$) $\mathcal{N} = 1$ SUSY QCD as an F-term dynamical supersymmetry breaking sector to uplift the non-positive vacuum of the KL moduli stabilization scenario;
- the decay rates of the ISS fields into other ISS fields and into MSSM fields;
- the analysis of the dynamics after inflation within the context of KL-ISS-MSSM, obtaining constraints on late entropy production from the ISS fields and their decay products so that there is no dilution of products from the Big-Bang nucleosynthesis;
- the achievement of neutralino dark matter candidates compatible with the observed dark matter relic density (both from thermal and non-thermal processes).

CHAPTER 5

# The KL-ISS scenario

In the present chapter we introduce the background setup to investigate the possible emergence of dark matter candidates from a higher-dimensional string/M-theory perspective.

In section 5.1 we introduce the reader to the Kallosh–Linde (KL) moduli stabilization scenario. We comment on how it fits into the string/M-theory framework and also on how it deals with phenomenological issues of the previous semi-realistic moduli stabilization scenario for string cosmology, the Kachru–Kallosh–Linde–Trivedi (KKLT) scenario. Moreover, we present the AdS/Minkowski vacuum structure of the KL scenario.

In section 5.2 we introduce the reader to the Intriligator–Seiberg–Shih (ISS) model. We also comment on how it fits into the string/M-theory framework. After briefly commenting on the MSSM and the inflationary sectors in section 5.3, we show in section 5.4 how the ISS model serves as an F-term dynamical supersymmetry breaking sector useful to uplift the KL AdS/Minkowski vacuum structure to a dS vacuum with positive cosmological constant. Furthermore, in section 5.4, we see how the gravitino mass is related with parameters of both the KL moduli stabilization scenario and of the ISS sector.

Finally, in section 5.5 we present the masses of the fields in our general setup and the results for the relevant decay rates from interaction terms among these fields. These turn out to be relevant when the production of dark matter is analysed in chapter 6.

## 5.1 The Kallosh–Linde (KL) moduli stabilization scenario

In the original work of KKLT [153], it was shown that all moduli are stabilized in a controlable way in the context of compactifications of type IIB string theory on Calabi-Yau threefolds with the presence of fluxes. To be more precise, the starting point is F-theory compactified on an elliptically fibered Calabi-Yau fourfold $X$ — see e.g. Calabi-Yau fourfold constructions for F-theory in [105]. The manifold $M$ of the fibration encodes the data from the type IIB geometry whereas the type IIB axiodilaton $\tau$ is to be associated with deformations in the complex structure of the elliptic fiber.

In the absence of fluxes, this setup has a certain locus in the moduli space which is of type IIB compactified on an orientifolded Calabi-Yau threefold $M$ [259]. Moreover, the focus is on a

setup with only one[1] Kähler modulus $\rho$, from the Hodge number $h^{1,1}(M) = 1$ as in [260]. In the presence of fluxes, the superpotential takes the familiar form of the Gukov–Vafa–Witten superpotential [231]

$$W = \int_M G_3 \wedge \Omega \,, \tag{5.1}$$

where $\Omega$ is a holomorphic $(3,0)$-form on $M$, and $G_3 = F_3 - \tau H_3$ depends on the three-forms from RR and NS fluxes in type IIB — $F_3$ and $H_3$, respectively — and on the axiodilaton $\tau$. Furthermore, the tree-level Kähler potential reads

$$K = -3\ln(\rho + \bar{\rho}) - \ln(\tau + \bar{\tau}) - \ln\left(-i \int_M \Omega \wedge \bar{\Omega}\right) . \tag{5.2}$$

Let the covariant derivative be $D_i W = \partial_i W + (\partial_i K) W$ and the moduli space metric $K_{i\bar{j}} = \partial_i \partial_{\bar{j}} K$, with $i$ and $j$ running over all moduli fields. It follows that the four-dimensional effective $\mathcal{N} = 1$ supergravity scalar potential,

$$V = e^K (K^{i\bar{j}} D_i W \overline{D}_{\bar{j}} \overline{W} - 3|W|^2) \,, \tag{5.3}$$

leads to a positive semi-definite contribution. This is characteristic of no-scale models since the superpotential given in equation (5.1) is independent of the modulus $\rho$. Note that in part I of this thesis we obtained explicitly a scalar potential for M-theory compactifications on twisted connected sum $G_2$-manifolds with the same no-scale structure, see section 3.4.3 in chapter 3.4.

Furthermore, it was shown that all complex structure moduli from F-theory on an elliptically fibered Calabi-Yau fourfold are fixed at the mass scale $m \sim \alpha'/R^3$, where $\alpha' \sim T^{-1}$ with the string tension $T$, and $R$ is the radius of the orientifolded Calabi-Yau threefold $M$. However, the volume modulus $\rho$ was left unfixed. Therefore, in the following, we study the four-dimensional $\mathcal{N} = 1$ effective supergravity theory associated to this particular modulus only.

Notice that there can be non-perturbative corrections to the superpotential[2], either from Euclidean D3-branes or from gaugino condensation from stacks of D7-branes wrapping four-cycles in $M$. For both cases, the corrections follow a similar behaviour, namely, there are exponential corrections to the superpotential for $\rho$ at large volume [261].

Including these contributions, the analysis of the vacuum structure follows from the tree-level Kähler potential — now only for the volume modulus $\rho$ — and the superpotential with non-perturbative corrections, respectively given by

$$\begin{aligned} K_{\text{KKLT}} &= -3\ln(\rho + \bar{\rho}) \,, \\ W_{\text{KKLT}} &= W_0 + A e^{-a\rho} \,, \end{aligned} \tag{5.4}$$

where $W_0 < 0$ is a tree-level constant contribution from fluxes and $A, a > 0$ are coefficients determined by either of the two non-perturbative corrections mentioned in the previous para-

[1] The generalization to several Kähler moduli $\rho_i$ is also discussed in [260], but does not pose new aspects compared to what is presented here.

[2] Corrections to the Kähler potential have been neglected due to stabilization of $\rho$ at large values compared with the string scale, but there would still be an AdS supersymmetric vacuum [153].

graph. At a supersymmetric vacuum one requires $D_\rho W_{\rm KKLT} = 0$. Therefore, the scalar potential given in equation (5.3) has now a negative value. It is in this sense that the volume modulus $\rho$ is stabilized in an AdS supersymmetric vacuum.

The KKLT moduli stabilization scenario was very successful in its attempt to construct the first semi-realistic models for string cosmology. However, it had some issues [154]. Firstly, the gravitino mass is extremely large in this scenario, namely $m_{3/2} \sim 6 \times 10^{10}$ GeV. Secondly, the gravitino mass has to satisfy a relation $H \lesssim m_{3/2}$, due to the fact that the height of the potential stabilizing the modulus turns out to be related with the mass $m_{3/2}$, where $H$ is the Hubble parameter during inflation. In other words, we have two possible cases: either we have high-scale inflation with a large gravitino mass or low-scale inflation with a 'small' gravitino mass of $\mathcal{O}$(TeV). A large gravitino mass implies that supersymmetry is broken at very high-energy scales. This is not desired if we consider supersymmetry as a potential solution to the hierarchy problem. However, if this is not the case and other mechanisms are found to solve the hierarchy problem in the lines of, for example, reference [262], high-scale supersymmetry is still possible. Therefore, the first case is only a mild issue. However, the second case is a bit more severe as it indicates the necessity of string theory inspired models with stable extra dimensions for a very low-energy scale of inflation, $H \lesssim 10^{-15} M_{\rm P}$, which have proven to be very difficult to construct.

These issues were later dealt with in the new KL scenario for moduli stabilization [154]. The KL scenario is a consistent framework where the gravitino mass is small — in other words, supersymmetry breaking happens at low-scales — and inflation takes place at high-scales. This happens because the gravitino mass is no longer related to the height of the potential and, therefore, to the Hubble parameter during inflation. Compared to the original KKLT, the following modifications were performed in the KL scenario. Firstly, one now allows for stabilization of the volume modulus in a supersymmetric Minkowski vacuum and, secondly, the superpotential is modified to a racetrack expression, namely

$$W_{\rm KL} = W_0 + A e^{-a\rho} - B e^{-b\rho} \,, \tag{5.5}$$

where $W_0 < 0$ is a tree-level constant contribution from fluxes and $A, B, a, b > 0$ are coefficients determined by non-perturbative corrections. The Kähler potential is still the same as in the KKLT scenario, namely

$$K_{\rm KL} = -3 \ln(\rho + \bar{\rho}) \,. \tag{5.6}$$

At a supersymmetric Minkowski vacuum, both $W_{\rm KL} = 0$ and $D_\rho W_{\rm KL} = 0$ must be satisfied. This implies that the scalar potential in equation (5.3) vanishes, and we have a supersymmetric Minkowski minimum with a vanishing gravitino mass. Moreover, since the gravitino mass does not depend on the height of the potential, any possible uplifting of the Minkowski vacuum to de Sitter would not give a contribution depending on the Hubble parameter. Therefore, it would still be possible to have high-scale inflation without necessarily constraining the gravitino mass to be also large. Notice that it is also possible to find AdS vacuum with $W_{\rm KL} \neq 0$ and $D_\rho W_{\rm KL} = 0$. In this case it is also found that the gravitino mass does not depend on the Hubble parameter.

In both moduli stabilization scenarios, uplifting of the AdS/Minkowski vacuum can be per-

formed by explicitly breaking supersymmetry with non-perturbative terms from the addition of several anti-D3-branes that, however, do not add further moduli to the discussion. For a sufficient warped background, such anti-D3-branes give a small contribution to the AdS/Minkowski vacuum turning it to a small positive value without compromising the mechanisms that stabilized the moduli in the first place.

## 5.2 The Intriligator–Seiberg–Shih (ISS) sector

In contrast to the uplifting via explicit supersymmetry breaking from anti-D3-branes, in this thesis we perform the uplifting with a dynamical supersymmetry breaking sector provided by the so-called Intriligator–Seiberg–Shih (ISS) model [176]. In this section we present the details of the ISS model.

Sufficient conditions for the occurrence of dynamical supersymmetry breaking were suggested in [169, 170, 171, 172]. On the one hand, the theoretical requirement from the non-zero Witten index of $\mathcal{N} = 1$ Yang–Mills theory immediately implies that any $\mathcal{N} = 1$ supersymmetric gauge theory with massive vector-like matter has supersymmetric vacua. On the other hand, theories with no supersymmetric vacua must either be chiral or massless non-chiral. Satisfying the requirements for no supersymmetric vacua in a stable ground state from dynamical supersymmetry breaking have not only proven to be complicated but also posed various issues for phenomenology — see reviews [173, 174, 175]. In the original work of the ISS model [176], much simpler and phenomenologically viable models were constructed by allowing dynamical supersymmetry breaking to happen in metastable vacua. The background for metastable dynamical supersymmetry breaking in this thesis is provided by supersymmetric QCD, which allows for both supersymmetric vacua with massive vector-like matter as well as long-lived non-supersymmetric vacua.

Supersymmetric QCD is based on $\mathrm{SU}(N_c)$ $\mathcal{N} = 1$ with scale $\Lambda$ coupled with $N_f$ chiral multiplets (flavours) $Q^i$ in the $N_c$ representation and $\bar{N}_f$ chiral multiplets $\tilde{Q}_{\tilde{i}}$ in the $\bar{N}_c$ representation, where $i, \tilde{i} = 1, \ldots, N_f$ [263]. The anomaly free global symmetry of SUSY QCD is

$$\mathrm{SU}(N_f)_L \times \mathrm{SU}(N_f)_R \times \mathrm{U}(1)_B \times \mathrm{U}(1)_R \,. \tag{5.7}$$

The transformations for the quarks $Q$ and $\tilde{Q}$ are given by

$$\begin{array}{ll} Q & \left(N_f, 1, 1, 1\right) \,, \\ \tilde{Q} & \left(1, \bar{N}_f, -1, 1\right) \,. \end{array} \tag{5.8}$$

The original supersymmetric QCD theory has a non-Abelian Coulomb phase at the origin of its moduli space [264]. In the regime $3N_c/2 < N_f < 3N_c$, the non-Abelian Coulomb phase is a conformal field theory of interacting quarks and gluons which possesses two dual descriptions. The original description is in terms of *electric* variables, and it is an $\mathrm{SU}(N_c)$ gauge theory with $N_f$ chiral multiplets (flavours). The dual description is in terms of *magnetic* variables, and it is an $\mathrm{SU}(N)$ theory with $N_f$ flavours and $N_f^2$ massless fields. When one phase is weakly coupled, the other phase is strongly coupled in the sense of Seiberg S-duality [265]. For $N_f \geq 3N_c$,

the original theory is not asymptotically free. The electric variables are free in the IR and the magnetic ones are infinitely strongly coupled. Therefore, we call this the *free non-Abelian electric phase*. For $N_c + 1 \leq N_f < 3N_c/2$, the magnetic theory is not asymptotically free, the magnetic variables are free in the IR and the electric ones are infinitley strongly coupled. Therefore, we call this the *free non-Abelian magnetic phase*. While these two phases are dual to each other, the interacting theory in $3N_c/2 < N_f < 3N_c$ is self-dual.

Therefore, we define the ISS model to be the IR free, low-energy effective theory of the magnetic dual of SU($N_c$) $\mathcal{N} = 1$ supersymmetric QCD in the range $N_c + 1 \leq N_f < 3N_c/2$ with $N = N_f - N_c$. It consists of the ISS fields $\phi_{\rm ISS}$, which colectivelly denote the fields $q_i^a, \tilde{q}_b^j, S^i{}_j$, where $i, j = 1, \ldots, N_f$ are flavour indices, $a, b = 1, \ldots, N$, and $N_f > N = N_f - N_c$ [176]. With $L$ and $R$ standing for the left and right SU($N_f$) sectors, U(1)$_B$ for the baryon symmetry, and U(1)$_R$ standing for the R-symmetry, the anomaly free global symmetry group is

$$\mathrm{SU}(N) \times \mathrm{SU}(N_f)_L \times \mathrm{SU}(N_f)_R \times \mathrm{U}(1)_B \times \mathrm{U}(1)' \times \mathrm{U}(1)_R \,. \tag{5.9}$$

The transformations for the fields $q$, $\tilde{q}$ and $S$ are given by

$$\begin{aligned} S \quad & \left(1, N_f, \bar{N}_f, 0, -2, 2\right) , \\ q \quad & \left(N, \bar{N}_f, 1, 1, 1, 0\right) , \\ \tilde{q} \quad & \left(\bar{N}, 1, N_f, -1, 1, 0\right) . \end{aligned} \tag{5.10}$$

Following notation in [266], the Kähler potential and the tree-level superpotential — without gauging SU($N$) — are respectively given by

$$K_{\rm ISS} = |q|^2 + |\tilde{q}|^2 + |S|^2 = q_i^a \bar{q}_a^i + \tilde{q}_a^i \bar{\tilde{q}}_i^a + S^i{}_j \bar{S}^j{}_i \,, \tag{5.11}$$

$$W_{\rm ISS} = h(\mathrm{Tr}\tilde{q} S q - M^2 \mathrm{Tr} S) = h(\tilde{q}_a^i S^j{}_i q_j^a - M^2 S^i{}_j \delta_i^j) \,. \tag{5.12}$$

Here $h$ is a dimensionless coupling and $M \ll M_{\rm P}$ is the energy scale of the ISS model. Both parameters $h$ and $M$ will be constrained in our phenomenological and cosmological analysis in section 6.2 of chapter 6. The second term in equation (5.12) explicitly breaks the global symmetry group to SU($N$)× SU($N_f$)$_V$× U(1)$_B$× U(1)$_R$. Moreover, if the supergravity embedding is taken, U(1)$_R$ is explicitly broken.

## 5.3 The MSSM and the inflationary sectors

After introducing both the KL moduli stabilization scenario and the ISS model, we comment on the standard MSSM and the inflationary sectors.

We call the MSSM fields collectively by $\phi$ and adopt the canonical Kähler potential for them,

$$K_{\rm MSSM} = \phi\bar{\phi} \,. \tag{5.13}$$

Moreover, when mentioning the MSSM superpotential, we refer to the tree level superpotential

$W_{\rm MSSM} = W(\phi)$. We also consider the so-called *Giudice-Masiero term* [267]

$$K_{\rm GM} = c_H H_1 H_2 + \text{h.c.} \,, \tag{5.14}$$

where $H_1$ and $H_2$ are the Higgs superfields of the MSSM and $c_H$ is a constant with no mass dimension. This term is required in order to have acceptable phenomenology from both tan$\beta$ and the $\mu$-term in the four-dimensional low-energy effective theory context [266, 268, 269].

We adopt the following general behaviour for the Kähler and the superpotential for the inflaton field $\eta$, as in reference [270],

$$\begin{aligned} K_\eta &= K((\eta - \bar{\eta})^2, s\bar{s}) \,, \\ W_\eta &= s f(\eta) \,, \end{aligned} \tag{5.15}$$

where $s$ is a stabilizer field and $f(\eta)$ is an arbitrary holomorphic function. Since the explicit expressions in equation (5.15) are not used in this thesis, we only mention that the requirements are such that the field $\eta$ indeed accomplishes inflation and it does not decay into gravitinos. The last point will be made clear in section 6.1 when analysing the dynamics after the inflationary phase.

## 5.4 F-term uplifting in the KL-ISS scenario

Let us now discuss how the ISS sector is used to perform the uplifting of the vacuum in the KL scenario, from the most non-positive Minkowski solution, i.e., with a vanishing cosmological constant $\Lambda$, to a positive[3] de Sitter (dS),[4] with a positive cosmological constant. Furthermore, we comment on the dependence of the gravitino mass on the KL-ISS parameters.

Let us review the vacuum structure of the KL scenario. We give a vacuum expectation value (VEV) to the real part of the Kähler modulus only, i.e., we let Im$\rho = 0$ and Re$\rho = \sigma$ for simplicity [266]. Furthermore, let $\sigma_0$ be the value of $\rho$ at its minimum. The supersymmetric Minkowski vacuum $V_{\rm KL}(\sigma_0) = 0$ in the KL scenario must satisfy

$$\begin{aligned} D_\rho W_{\rm KL}|_{\sigma=\sigma_0} &= [\partial_\rho W_{\rm KL} + (\partial_\rho K_{\rm KL}) W_{\rm KL}]|_{\sigma=\sigma_0} = 0 \,, \\ W_{\rm KL}(\sigma_0) &= 0 \,. \end{aligned} \tag{5.16}$$

If we allow $W_{\rm KL}(\sigma_0) \equiv \Delta \neq 0$, the minimum now shifts to an anti-de Sitter (AdS) minimum

$$V_{\rm KL}(\sigma_0) \simeq -3 m_{3/2}^2 \simeq -\frac{3\Delta^2}{8\sigma_0^3} \,. \tag{5.17}$$

In order for the vacuum to stay supersymmetric, one requires $D_\rho W_{\rm KL}|_{\sigma=\sigma_0+\delta\sigma} = 0$, where $\delta\sigma \ll \sigma_0$ [272].

Let us now see how the ISS sector helps to uplift the non-positive vacuum structure of the

[3] Recall that the cosmological constant is measured to be $\Lambda \sim 10^{-120} M_{\rm P}^2$.

[4] For a systematic procedure of building locally stable dS vacua in $\mathcal{N} = 1$ supergravity models motivated by string theory see reference [271].

KL scenario. This uplifting is called an *F-term uplifting* [273, 274, 275, 276, 277, 278] as it is accomplished via F-terms in the scalar potential given by equation (5.3).

We start with a combination of the KL scenario and the ISS model, which means that we consider the following combination of Kähler potential and superpotential, respectively,

$$K_{\text{KL-ISS}} = -3\ln(\rho+\bar{\rho}) + |q|^2 + |\tilde{q}|^2 + |S|^2, \tag{5.18}$$

$$W_{\text{KL-ISS}} = W_0 + Ae^{-a\rho} - Be^{-b\rho} + h(\text{Tr}\tilde{q}Sq - M^2\text{Tr}S), \tag{5.19}$$

where $W_0 < 0$ and $A, B, a, b > 0$.

By working out the first derivative of the four-dimensional effective $\mathcal{N} = 1$ supergravity scalar potential (5.3), namely $\partial_{\phi_{\text{ISS}}} V_{\text{KL-ISS}} = 0$, the metastable ISS vacuum $(S_0, q_0, \tilde{q}_0)$ is given by

$$(S_0)^i_j = 0\,, \tag{5.20}$$

$$(q_0)^a_i = M\delta^a_i\,, \tag{5.21}$$

$$(\tilde{q}_0)^j_b = M\delta^j_b\,. \tag{5.22}$$

From a matrix viewpoint, $q_0$ and $\tilde{q}_0$ can be written as

$$\begin{aligned} q_0 &= \begin{pmatrix} M\mathbb{I}_{N\times N} \\ 0_{(N_f-N)\times N} \end{pmatrix}, \\ \tilde{q}_0 &= \begin{pmatrix} M\mathbb{I}_{N\times N} & 0_{N\times(N_f-N)} \end{pmatrix}. \end{aligned} \tag{5.23}$$

These are the VEVs responsible for the spontaneous symmetry breaking in the ISS model that allow for the uplifting of the non-positive vacuum in the KL scenario — given in equation (5.17). In fact, from terms $e^{K_{\text{KL-ISS}}}\partial_{\{q,\tilde{q},S\}}W_{\text{KL-ISS}}\partial_{\{\bar{q},\bar{\tilde{q}},\bar{S}\}}\overline{W}_{\text{KL-ISS}}$ in the four-dimensional scalar potential, these VEVs imply that the minimum of the KL-ISS potential is given by

$$V_{\text{min}} = \frac{e^{2NM^2/M_{\text{P}}^2}}{(2\sigma_0/M_{\text{P}})^3}\left\{\Delta^2\left(-3 + 2N\frac{M^2}{M_{\text{P}}^2}\right) + h^2\frac{M^4}{M_{\text{P}}^4}(N_f - N)\right\}. \tag{5.24}$$

Unless a huge $N = N_f - N_c$ of $O(10^{10})$ is taken — which is physically unlikely —, we neglect the term $2NM^2/M_{\text{P}}^2$ in the first parenthesis since $M \ll M_{\text{P}}$ due to the dynamical nature of the ISS sector. Together with the fact that the scalar potential minimum must equal the small but positive contribution from the cosmological constant $M_P^4\left(\frac{\Lambda}{M_P^2}\right) \sim 10^{-120}M_P^4 \simeq 0$, we obtain a constraint for the parameter $\Delta$, namely[5]

$$|\Delta| \simeq \sqrt{\frac{N_f - N}{3}}h\left(\frac{M}{M_{\text{P}}}\right)^2. \tag{5.25}$$

[5] The cosmological constant is set to approximately zero by positive values which, therefore, is in agreement with the fact that we have uplifted the KL vacua to positive values. We choose here the extreme case of a vanishing cosmological constant only to get a lower bound constraint for the superpotential $\Delta$ that is necessary to perform the uplifting.

Restoring the reduced Planck mass $M_{\rm P}$, the gravitino mass is given by

$$m_{3/2} \equiv \left\langle e^{K/2} W \right\rangle \simeq \frac{|\Delta|}{(2\sigma_0/M_{\rm P})^{3/2}} e^{NM^2/M_{\rm P}^2} \simeq \frac{1}{(2\sigma_0/M_{\rm P})^{3/2}} \sqrt{\frac{N_f - N}{3}} h \left(\frac{M}{M_{\rm P}}\right)^2 M_{\rm P} \,, \tag{5.26}$$

where in the last step we set $e^{NM^2/M_{\rm P}^2} = 1$ since $M \ll M_{\rm P}$. Notice that this is written in terms of the parameters $h$ and $M$ of the ISS sector as well as the VEV of the Kähler modulus $\rho$, which is given by $\sigma_0 = {\rm Re}\rho$. Furthermore, since $\sigma_0$ is obtained from $W_{\rm KL}$, which in turn depends on $a, b, A$ and $B$, the gravitino mass becomes a function of $a, b, A, B, h$ and $M$.

## 5.5 Properties of the KL-ISS-MSSM setup

In the previous section we focused on the direct consequences of F-term uplifting in the KL-ISS scenario. Now we focus in discussing the properties of the modulus $\rho$ and the ISS fields $\phi_{\rm ISS}$, such as their masses (section 5.5.1) and the relevant decay rates (section 5.5.2). These will be used in the phenomenological and cosmological analysis in chapter 6. From this section on, we write the ISS fields only with lowered indices for simplicity.

### 5.5.1 Masses

To obtain the masses for the ISS and the modulus fields, we diagonalize the $8 \times 8$ mass matrix for $\rho, \bar{\rho}, S, \bar{S}, q, \bar{q}, \tilde{q}, \bar{\tilde{q}}$ obtained from the scalar potential given in equation (5.3). Namely,

$$V = e^K (K^{i\bar{j}} D_i W \overline{D}_{\bar{j}} \overline{W} - 3|W|^2) \,, \tag{5.27}$$

with

$$\begin{aligned} K &\equiv K_{\text{KL-ISS}} + K_{\rm MSSM} + K_{\rm GM} \,, \\ W &\equiv W_{\text{KL-ISS}} + W_{\rm MSSM} \,. \end{aligned} \tag{5.28}$$

**The modulus field $\rho$**

We start the analysis with the modulus field $\rho$. After diagonalization of the mass matrix, we obtain its squared mass for both the real and imaginary components to be

$$m_\rho^2 = \frac{2}{9} AaBb\,(a-b) \left[\frac{aA}{bB}\right]^{\frac{-a-b}{a-b}} \ln\left(\frac{aA}{bB}\right) + O\left(M^2\right) \,. \tag{5.29}$$

This result was also obtained in reference [272]. A simple choice of parameters $a = 0.1$, $b = 0.05$, $A = B = 1$ gives $m_\rho \simeq 2.19 \times 10^{-3} M_P$. This value is much larger than the inflaton reference mass adopted here, namely $m_\eta = 10^{-5} M_P$ — for example, in the simplest chaotic inflation models, $m_\eta \sim 6 \times 10^{-6} M_P$. As shown in [270], this allows us to ignore the dynamics of the modulus field during inflation. The modulus and the inflaton decouple and can be studied separately. In particular, the modulus field potential does not receive contributions from the

inflaton during inflation. Therefore, the VEV of the modulus has the same value both during and after inflation, leading to a vanishing post-inflationary oscillation amplitude. We will return to this point in section 6.1. Recall that the $\rho$ value at the minimum of the potential is given by the VEV of its real part Re$\rho$, namely $\sigma_0$, which we compute to be $\sigma_0 = \frac{1}{a-b}\ln\left(\frac{aA}{bB}\right) + O\left(M^2\right)$. Again using $a = 0.1$, $b = 0.05$, $A = B = 1$, we obtain

$$\sigma_0 \simeq 13.86\, M_P\ . \tag{5.30}$$

**The ISS scalar fields**

For the ISS scalar fields, we replace the scalar components of the chiral superfields $q, \bar{q}, \tilde{q}, \bar{\tilde{q}}$ by linear combinations[6] $Q_1, Q_2, Q_3, Q_4$. For $i = 1, \ldots, N$ and $a = 1, \ldots, N$,

$$\text{Re, Im}\,[Q_1] = \frac{1}{2}(q_{ai} \pm \bar{q}_{ai} + \tilde{q}_{ia} \pm \bar{\tilde{q}}_{ia})\ , \tag{5.31}$$

$$\text{Re, Im}\,[Q_2] = \frac{1}{2}\left[q_{ai} \pm \bar{q}_{ai} - (\tilde{q}_{ia} \pm \bar{\tilde{q}}_{ia})\right]\ , \tag{5.32}$$

and, for $i = N+1, \ldots, N_f$ and $a = 1, \ldots, N$,

$$\text{Re, Im}\,[Q_3] = \frac{1}{2}(q_{ai} \pm \bar{q}_{ai} \pm \tilde{q}_{ia} + \bar{\tilde{q}}_{ia})\ , \tag{5.33}$$

$$\text{Re, Im}\,[Q_4] = \frac{1}{2}\left[q_{ai} \pm \bar{q}_{ai} - (\pm\tilde{q}_{ia} + \bar{\tilde{q}}_{ia})\right]\ . \tag{5.34}$$

In table 5.1 we show the number of real and imaginary components, as well as their mass eigenvalues, for each of the six kinds of mass eigenstates constructed from the ISS fields $S, \bar{S}, q, \bar{q}, \tilde{q}, \bar{\tilde{q}}$ after diagonalization of the mass matrix.

[6] Compare with the parameterizations given in reference [176]. Note our abuse of notation, as here $q, \bar{q}, \tilde{q}, \bar{\tilde{q}}$ are the scalar components of the chiral superfields represented by these same letters. We have also omitted the indices $i$ and $a$ in $Q$s.

| ISS scalar mass eingenstate | $\text{Number}_{\text{Re/Im}}$ | Mass |
|---|---|---|
| $S_1 \equiv S_{ij}\left(i \otimes j \in N^2\right)$ | $N^2$ | $\sqrt{\frac{6}{N_f - N}}\left(\frac{M_P}{M}\right) m_{3/2}$ |
| $S_2 \equiv S_{ij}\left(i \otimes j \in N_f^2 - N^2\right)$ | $\left(N_f + N\right)\left(N_f - N\right)$ | $O\left(m_{3/2}\right)$ |
| $Q_1 \equiv \text{Lc}\left[q_{ai}, \tilde{q}_{ia}\right]\left(i \otimes a \in N^2\right)$ | $N^2$ | $\sqrt{\frac{6}{N_f - N}}\left(\frac{M_P}{M}\right) m_{3/2}$ |
| $Q_2 \equiv \text{Lc}\left[q_{ai}, \tilde{q}_{ia}\right]\left(i \otimes a \in N^2\right)$ | $N^2$ | 0 |
| $Q_3 \equiv \text{Lc}\left[q_{ai}, \tilde{q}_{ia}\right]\left(i \otimes a \in N_f N - N^2\right)$ | $\left(N_f - N\right) N$ | $\sqrt{\frac{6}{N_f - N}}\left(\frac{M_P}{M}\right) m_{3/2}$ |
| $Q_4 \equiv \text{Lc}\left[q_{ai}, \tilde{q}_{ia}\right]\left(i \otimes a \in N_f N - N^2\right)$ | $\left(N_f - N\right) N$ | 0 |

Table 5.1: The ISS scalar mass eigenstates (first column), their corresponding number of real or imaginary components (second column) and their largest tree-level mass contributions (third column). The notation is such that $N_f N$ is the cartesian product $N_f \otimes N$ with $N = \{1, \ldots, N\}$ and $N_f = \{1, \ldots, N_f\}$, and similarly for $N^2$ and $N_f^2$. Lc stands for the linear combinations given in equations (5.31) to (5.34).

The fields $\text{Im}Q_2$, $\text{Re}Q_4$ and $\text{Im}Q_4$ are massless Goldstone modes [176], thereby accounting for $N^2 + 2(N_f - N)N = 2N_f N - N^2$ degrees of freedom. The field $\text{Re}Q_2$ is actually a pseudo-Goldstone, whose mass is given by higher order corrections, as we show in the next paragraph. The reason why the scalar mass spectrum yields $2N_f N - N^2$ massless bosons is that the VEVs of $(q, \tilde{q})$ break the original symmetry $\text{SU}(N) \times \text{SU}(N_f)_V \times \text{U}(1)_B$, with $N^2 + N_f^2 - 1$ generators, down to $\text{SU}(N)_V \times \text{SU}(N_f - N)_V \times \text{U}(1)_{B'}$, with $N^2 + (N_f - N)^2 - 1$ generators. $\text{SU}(N_f)_V$ breaks down to $\text{SU}(N)_V \times \text{SU}(N_f - N)_V \times \text{U}(1)_{B'}$ and the original $\text{SU}(N) \times \text{U}(1)_B$ is completely broken — since in the region $i \otimes a = N^2$, there exists $Q_2$ with null VEV. Furthermore, the $S$ field transforming as a singlet under $\text{SU}(N_f)_V$ gives no contribution to the massless Goldstone mode analysis.

Quantum corrections to the masses via one-loop calculations in [176] generate an additional mass of $O\left(m_{3/2}\frac{M_P}{M}\right)$ to $\text{Re}Q_2$ as well as to the real and imaginary parts of a subset of $S_2$, namely $S_{ij}$ with indices $i, j > N$, which we refer to as $S_2^{'}$. More precisely,

$$\begin{aligned} e^{K/2} m_{S_2^{'}}^{\text{1-loop}} &= e^{K/2}\left(\frac{\ln(4) - 1}{8\pi^2}\right)^{1/2} \sqrt{N} h^2 M \\ &= \left(\frac{3\left(\ln(4) - 1\right)}{8\pi^2}\right)^{1/2} \sqrt{\frac{N}{N_f - N}} h\left(\frac{M_P}{M}\right) m_{3/2}\,, \\ e^{K/2} m_{Q_2}^{\text{1-loop}} &= e^{K/2}\left(\frac{\ln(4) - 1}{8\pi^2}\right)^{1/2} \sqrt{N_f - N} h^2 M \\ &= \left(\frac{3\left(\ln(4) - 1\right)}{8\pi^2}\right)^{1/2} h\left(\frac{M_P}{M}\right) m_{3/2}\,. \end{aligned} \tag{5.35}$$

Since $M \ll M_P$, we can safely consider the one-loop contributions as the leading order masses of $\text{Re}S_2^{'}$, $\text{Im}S_2^{'}$ and $\text{Re}Q_2$.

The mass matrices for the ISS fields $S$ and $Q$ after diagonalization are diagramatically

displayed as, respectively,

$$S = \left( \begin{array}{c|c} (S_1)_{N\times N} & (S_2^{\rm nd})_{N\times(N_f-N)} \\ \hline (S_2^{\rm nd})_{(N_f-N)\times N} & (S_2')_{(N_f-N)\times(N_f-N)} \end{array} \right) , \tag{5.36}$$

$$Q = \left( \begin{array}{c|c} (Q_1 \,\&\, Q_2)_{N\times N} & (Q_3 \,\&\, Q_4)_{N\times(N_f-N)} \end{array} \right) . \tag{5.37}$$

Here we explicitly see the splitting of $S_2$ into the non-diagonal pieces $(S_2^{\rm nd})_{N\times(N_f-N)}$, $(S_2^{\rm nd})_{(N_f-N)\times N}$, and the subset $S_2'$ which receives mass through one-loop calculations beyond its tree-level mass of $O(m_{3/2})$, as presented above. Furthermore we see that $Q_1$ and $Q_2$ as well as $Q_3$ and $Q_4$ mix in the block forms sketched above. The indices here refer to the dimensionality of their corresponding blocks in terms of the cartesian product space.

Notice that when one considers the ISS model alone, the VEVs given in equations (5.20), (5.21) and (5.22) render $\partial V_{\rm ISS}/\partial\phi_{\rm ISS} = 0$. However, when the modulus field contribution is included, i.e., $W_\rho\big|_{\rm min} = \Delta$, the first derivatives of the combined potential with respect to the ISS fields change according to

$$\begin{aligned} \partial V_{\text{KL-ISS}}/\partial\left(q,\tilde{q}\right)_{ia} &= O\left(m_{3/2}^2 M_P \left\langle q,\tilde{q}\right\rangle_{ia}\right) , \\ \partial V_{\text{KL-ISS}}/\partial S_{ij} &= O\left(m_{3/2}^2 M_P\right)\delta_{ij} . \end{aligned} \tag{5.38}$$

If we still want to mantain $\partial V_{\text{KL-ISS}}/\partial_{\phi_{\rm ISS}} = 0$, assuming the VEVs of $q_{ia}$, $\tilde{q}_{ai}$, and $S_{ij}$ to be the diagonal ones, they should obtain the corrections

$$\begin{aligned} \langle q_{ia},\tilde{q}_{ai}\rangle &= \left(M - O\left(M^3 M_{\rm P}^{-2}\right)\right)\delta_{ia} , \\ \left\langle S_{ij}\right\rangle &= \left(\left(\frac{M}{M_{\rm P}}\right)^2 M_P + O\left(M^4 M_{\rm P}^{-3}\right)\right)\delta_{ij} \quad \text{for } i,j \le N , \\ \left\langle S_{ij}\right\rangle &= \left(\frac{16\pi^2\left(N_f-N\right)}{3\left(\ln 4-1\right)Nh^2}\left(\frac{M}{M_{\rm P}}\right)^2 M_{\rm P} + O\left(M^4 M_{\rm P}^{-3}\right)\right)\delta_{ij} \\ &\simeq \left(\frac{N_f-N}{3N}\frac{408.79}{h^2}\left(\frac{M}{M_{\rm P}}\right)^2 M_{\rm P} + O\left(M^4 M_{\rm P}^{-3}\right)\right)\delta_{ij} \quad \text{for } i,j > N . \end{aligned} \tag{5.39}$$

The last correction is dominated by one-loop contributions. Notice that equation (5.24) would not contain the term $2NM^2/M_{\rm P}^2$ for these modified VEVs.

An observation about the sign of $\Delta$ must be made. When we calculate the modified VEVs, written in equation (5.39), one must assume either that $h < 0$ or $\Delta < 0$ in order to obtain $\partial V_{\text{KL-ISS}}/\partial\phi_{\rm ISS} = 0$. We choose to restrain the sign freedom of $\Delta$ and take it to be negative, while opting for $h > 0$.

### The ISS fermion fields

We now present the masses and eigenstates of the ISS fermionic fields[7]. For $i \otimes a \in N^2$ and $i \otimes j \in N^2$, $i = a$ and $i = j$, the eigenstates are

$$\chi_{B1} = \frac{1}{\sqrt{5}}\left(\sqrt{2}q_{ai} + \sqrt{2}\tilde{q}_{ia} + S_{ij}\right) + O(M) \ , \tag{5.40}$$

$$\chi_{B2} = \frac{1}{\sqrt{5}}\left(\sqrt{2}q_{ai} + \sqrt{2}\tilde{q}_{ia} - S_{ij}\right) + O(M) \ , \tag{5.41}$$

$$\chi_{S1} = \frac{1}{\sqrt{2}}\left(q_{ai} - \tilde{q}_{ia}\right) \ . \tag{5.42}$$

For $i \neq a$ and $i \neq j$, one finds

$$\chi_{S3} = \frac{1}{2}\left(q_{i>a} + \tilde{q}_{a<i} - q_{i<a} - \tilde{q}_{a>i}\right) \ , \tag{5.43}$$

$$\chi_{S4} = \frac{1}{2}\left(q_{i>a} - \tilde{q}_{a<i} + q_{i<a} - \tilde{q}_{a>i}\right) \ , \tag{5.44}$$

$$\chi_{B3} = \frac{1}{2\sqrt{2}}\left(q_{i>a} - \tilde{q}_{a<i} - q_{i<a} + \tilde{q}_{a>i} - \sqrt{2}S_{i<j} + \sqrt{2}S_{i>j}\right) + O(M) \ , \tag{5.45}$$

$$\chi_{B4} = \frac{1}{2\sqrt{2}}\left(q_{i>a} + \tilde{q}_{a<i} + q_{i<a} + \tilde{q}_{a>i} - \sqrt{2}S_{i<j} - \sqrt{2}q_{i>j}\right) + O(M) \ , \tag{5.46}$$

$$\chi_{B5} = \frac{1}{2\sqrt{2}}\left(q_{i>a} - \tilde{q}_{a<i} - q_{i<a} + \tilde{q}_{a>i} + \sqrt{2}S_{i<j} - \sqrt{2}S_{i>j}\right) + O(M) \ , \tag{5.47}$$

$$\chi_{B6} = \frac{1}{2\sqrt{2}}\left(q_{i>a} + \tilde{q}_{a<i} + q_{i<a} + \tilde{q}_{a>i} + \sqrt{2}S_{i<j} + \sqrt{2}S_{i>j}\right) + O(M) \ . \tag{5.48}$$

For example, if $N = 2$, we have $(\chi_{S3})_{N=2} = \frac{1}{2}(q_{21} + \tilde{q}_{12} - q_{12} - \tilde{q}_{21})$, and similarly for the other states. For $i \otimes a \in N_f N - N^2$ and $i \otimes j \in N_f^2 - N^2$, we have

$$\chi_{M1} = \frac{1}{\sqrt{2}}\left(q_{ia} - \tilde{q}_{ai}\right) \ , \tag{5.49}$$

$$\chi_{M2} = \frac{1}{\sqrt{2}}\left(q_{ia} + \tilde{q}_{ai}\right) \ , \tag{5.50}$$

$$\chi_{S2} = \begin{cases} S_{ij} \ , \text{ for } i \neq j \ , \\ \frac{1}{\sqrt{2}}\left(S_{kk} - S_{ij}\right) \ , \text{ for } i = j \ , \end{cases} \tag{5.51}$$

where $k \equiv N + 1$. As an example, for $N = 2$ and $N_f = 5$ and $i = j$, we obtain the possibilities $\chi_{S2} = \{(S_{33} - S_{44})/\sqrt{2}, (S_{33} - S_{55})/\sqrt{2}\}$.

[7] Note our abuse of notation, as here $q, \bar{q}, \tilde{q}, \bar{\tilde{q}}, S_{ij}$ are the fermionic components of the chiral superfields represented by these same letters.

The Goldstino, which has been neglected in the above considerations, is given by

$$\chi_{\text{Goldstino}} = \frac{1}{\sqrt{N_f - N}} \sum_{i=N+1}^{N_f} S_{ii} + O\left(M^2\right) . \tag{5.52}$$

With $G = K + \ln(W\bar{W})$, the main contribution to the mass of the above eigenstates comes from the term $\left(e^{G/2}\frac{W_{ij}}{W}\right)\bar{\chi}_R\chi_L$ + h.c.. In tables 5.2 and 5.3 we collect the ISS fermion mass eigenstates as well as their corresponding quantity and leading order mass contributions.

| ISS fermion mass eigenstate | Number | Mass |
|---|---|---|
| $\chi_{B1} \equiv \text{Lc}\left[S_{ij}, q_{ai}, \tilde{q}_{ia}\right]\left(i \otimes a \in N^2\right)$ | $N$ | $\sqrt{\frac{6}{N_f - N}}\left(\frac{M_P}{M}\right) m_{3/2}$ |
| $\chi_{B2} \equiv \text{Lc}\left[S_{ij}, q_{ai}, \tilde{q}_{ia}\right]\left(i \otimes a \in N^2, i \otimes j \in N^2\right)$ | $N$ | $\sqrt{\frac{6}{N_f - N}}\left(\frac{M_P}{M}\right) m_{3/2}$ |
| $\chi_{S1} \equiv \text{Lc}\left[q_{ai}, \tilde{q}_{ia}\right]\left(i \otimes a \in N^2, i \otimes j \in N^2\right)$ | $N$ | $m_{3/2}$ |
| $\chi_{S3} \equiv \text{Lc}\left[q_{ai}, \tilde{q}_{ia}\right]\left(i \otimes a \in N^2\right)$ | $N(N-1)/2$ | $m_{3/2}$ |
| $\chi_{S4} \equiv \text{Lc}\left[q_{ai}, \tilde{q}_{ia}\right]\left(i \otimes a \in N^2\right)$ | $N(N-1)/2$ | $m_{3/2}$ |
| $\chi_{B3} \equiv \text{Lc}\left[S_{ij}, q_{ai}, \tilde{q}_{ia}\right]\left(i \otimes a \in N^2, i \otimes j \in N^2\right)$ | $N(N-1)/2$ | $\sqrt{\frac{6}{N_f - N}}\left(\frac{M_P}{M}\right) m_{3/2}$ |
| $\chi_{B4} \equiv \text{Lc}\left[S_{ij}, q_{ai}, \tilde{q}_{ia}\right]\left(i \otimes a \in N^2, i \otimes j \in N^2\right)$ | $N(N-1)/2$ | $\sqrt{\frac{6}{N_f - N}}\left(\frac{M_P}{M}\right) m_{3/2}$ |
| $\chi_{B5} \equiv \text{Lc}\left[S_{ij}, q_{ai}, \tilde{q}_{ia}\right]\left(i \otimes a \in N^2, i \otimes j \in N^2\right)$ | $N(N-1)/2$ | $\sqrt{\frac{6}{N_f - N}}\left(\frac{M_P}{M}\right) m_{3/2}$ |
| $\chi_{B6} \equiv \text{Lc}\left[S_{ij}, q_{ai}, \tilde{q}_{ia}\right]\left(i \otimes a \in N^2, i \otimes j \in N^2\right)$ | $N(N-1)/2$ | $\sqrt{\frac{6}{N_f - N}}\left(\frac{M_P}{M}\right) m_{3/2}$ |

Table 5.2: The ISS fermion eigenstates within the index spaces $i \otimes a \in N^2$ and $i \otimes j \in N^2$ (first column), their corresponding quantity (second column) and their leading order mass contributions (third column). The notations $i \otimes a$ and $i \otimes j$ are of the same type as the ones for the ISS scalar masses table 5.1. Lc stands for the linear combinations given from equations (5.40) to (5.48).

| ISS fermion mass eigenstate | Number | Mass |
|---|---|---|
| $\chi_{M1} \equiv \text{Lc}\left[q_{ai}, \tilde{q}_{ia}\right]\left(i \otimes a \in N_f N - N^2\right)$ | $N\left(N_f - N\right)$ | $\frac{16\pi^2}{(\ln[4]-1)h^2} m_{3/2}$ |
| $\chi_{M2} \equiv \text{Lc}\left[q_{ai}, \tilde{q}_{ia}\right]\left(i \otimes a \in N_f N - N^2\right)$ | $N\left(N_f - N\right)$ | $\frac{16\pi^2}{(\ln[4]-1)h^2} m_{3/2}$ |
| $\chi_{S2} \equiv \text{Lc}\left[S_{ij}\right]\left(i \otimes j \in N_f^2 - N^2\right)$ | $N_f^2 - N^2 - 1$ | 0 |

Table 5.3: The ISS fermion eigenstates within the index spaces $i \otimes a \in N_f N - N^2$ and $i \otimes j \in N_f^2 - N^2$ (first column), their corresponding quantity (second column) and their leading order mass contributions (third column). The notations $i \otimes a$ and $i \otimes j$ are of the same type as the ones for the ISS scalar masses table 5.1. Lc stands for the linear combinations given from equations (5.49) to (5.51).

### 5.5.2 Decay rates

Here we present the reader with the results of the largest decay rates needed in chapter 6. We refer the reader to the full publication [196] for a detailed account of all the interaction terms and

associated decay rates of the ISS and the MSSM fields. In appendix B we give the interaction terms as well as the computation of decay rates for those yielding the largest results, whereas only the interaction terms are given for those which do not lead to the largest decay rates.

In section 6.1 we will see that the imaginary components of the ISS scalar fields do not oscillate after inflation. Therefore they do not contribute significantly to the post-inflation dynamics. It is for this reason that, in the present section, we give the decay rates of only some of the real components of the ISS scalars. The largest decay rates, or the ones with non-vanishing oscillation amplitude, are obtained from $\mathrm{Re}Q_1$ and $\mathrm{Re}Q_2$ within the set of the $(q, \tilde{q})$ ISS fields, as well as from $\mathrm{Re}S_1$ and $\mathrm{Re}S_2$ within the set of the $S$ ISS fields. We use the short notation $Q_1$, $Q_2$, $S_1$ and $S_2$ for them. Despite the oscillation amplitude of $\mathrm{Re}Q_2$ being zero, its decay rate is important since it is a decay product of $\mathrm{Re}Q_1$ itself.

To compute the decay rates, we consider both two-body decays ($\phi_{\mathrm{ISS}} \to 1+2$) and three-body decays ($\phi_{\mathrm{ISS}} \to 1+2+3$), and use

$$\frac{d\overline{\Gamma}^{12}_{\phi_{\mathrm{ISS}}}}{d\Omega_{\mathrm{CM}}} = \frac{\left|\overline{\mathcal{M}}^{12}_{\phi_{\mathrm{ISS}}}\right|^2}{64\pi^2}\frac{S_{12}}{m^3_{\phi_{\mathrm{ISS}}}}s\,, \tag{5.53}$$

$$\overline{\Gamma}^{123}_{\phi_{\mathrm{ISS}}} = \frac{1}{m_{\phi_{\mathrm{ISS}}}64\pi^3}\int_0^{\frac{m_{\phi_{\mathrm{ISS}}}}{2}} dE_2 \int_{\frac{m_{\phi_{\mathrm{ISS}}}}{2}-E_2}^{\frac{m_{\phi_{\mathrm{ISS}}}}{2}} dE_1 \left|\overline{\mathcal{M}}^{123}_{\phi_{\mathrm{ISS}}}\right|^2\,, \tag{5.54}$$

where $\mathrm{d}\Omega_{\mathrm{CM}}$ is the phase space differential element, $\overline{\mathcal{M}}^{12}_{\phi_{\mathrm{ISS}}}$ ($\overline{\mathcal{M}}^{123}_{\phi_{\mathrm{ISS}}}$) is the amplitude of the two(three)-body decay, $S_{12} = \left[m^2_{\phi_{\mathrm{ISS}}} - (m_1-m_2)^2\right]^{1/2}\left[m^2_{\phi_{\mathrm{ISS}}} - (m_1+m_2)^2\right]^{1/2}$, $m_{\phi_{\mathrm{ISS}}}$ is the mass of the decaying ISS particle, and $s$ is the symmetry factor for indistinguishable final states. Here we denote decay rates where helicities were summed over by the overline above $\Gamma$. Since the ISS fields are much heavier[8] than the gravitino, the MSSM fields, and the ISS products, we consider all final particles to be massless for simplicity.

Assuming[9] $N = 1$ and $N_f = 4$, the largest contributions to the total decay rates of the ISS fields originate from their decays

- to gravitinos via $(S_2,\ Q_1,\ Q_2) \to \bar{\psi}_{3/2}\psi_{3/2}$ ;
- to two ISS fermions via $S_1 \to \bar{\chi}_{S1} + \chi_{S1}$ ;
- and to two ISS fermions plus one ISS scalar via both $Q_1 \to \chi_{S1} + \bar{\chi}_{S1} + Q_2$ and $Q_2 \to \chi_{S1} + \bar{\chi}_{S1} + \mathrm{Im}Q_2$ .

[8] Exceptions are the fields $\mathrm{Im}Q_2$ and $Q_4$. However these fields do not oscillate after inflation, thus they do not yield important contributions to the energy content of the Universe and would be neglected after all.

[9] Remember that this is the minimal choice for $N_f > 3N$ — equivalent to $N_f < \frac{3}{2}N_c$ —, which is required for the ISS model to be infrared free in the magnetic range.

In other words,

$$\Gamma_{S_1}^{\text{total}} \simeq \overline{\Gamma}_{S_1}^{\chi\chi} , \tag{5.55}$$

$$\Gamma_{S_2}^{\text{total}} \simeq \overline{\Gamma}_{S_2}^{2\psi_{3/2}} , \tag{5.56}$$

$$\Gamma_{Q_1}^{\text{total}} \simeq \overline{\Gamma}_{Q_1}^{2\psi_{3/2}} + \overline{\Gamma}_{Q_1}^{\chi\chi\text{Re}Q_2} + \overline{\Gamma}_{Q_1}^{\chi\chi\text{Im}Q_2} , \tag{5.57}$$

$$\Gamma_{Q_2}^{\text{total}} \simeq \overline{\Gamma}_{Q_2}^{2\psi_{3/2}} + \overline{\Gamma}_{Q_2}^{\chi\chi\text{Im}Q_2} . \tag{5.58}$$

Notice the short notation $Q_1, Q_2, S_1, S_2$ for $\text{Re}Q_1$, $\text{Re}Q_2$, $\text{Re}S_1$, $\text{Re}S_2$ for the initial states. Furthermore, $\chi_{S_1}$ and $\bar{\chi}_{S_1}$ are represented by[10] $\chi\chi$. Each of the partial decay rates are computed to be

$$\overline{\Gamma}_{S_1}^{\chi\chi} \simeq 5.63 \times 10^{-2} \frac{m_{3/2}^3}{M_{\text{P}}^2} \left(\frac{M_{\text{P}}}{M}\right)^5 , \tag{5.59}$$

$$\overline{\Gamma}_{S_2}^{\psi_{3/2}} \simeq 2.31 \times 10^{-9} \frac{m_{3/2}^3 h^5}{M_{\text{P}}^2} \left(\frac{M_{\text{P}}}{M}\right)^5 , \tag{5.60}$$

$$\overline{\Gamma}_{Q_1}^{2\psi_{3/2}} \simeq 3.13 \times 10^{-3} \frac{m_{3/2}^3}{M_{\text{P}}^2} \left(\frac{M_{\text{P}}}{M}\right)^3 , \tag{5.61}$$

$$\overline{\Gamma}_{Q_1}^{\chi\chi\text{Re}Q_2} = \Gamma_{Q_1}^{\chi\chi\text{Im}Q_2} \simeq 4.90 \times 10^{-11} \frac{m_{3/2}^3 h^2}{M_{\text{P}}^2} \left(\frac{M_{\text{P}}}{M}\right)^5 , \tag{5.62}$$

$$\overline{\Gamma}_{Q_2}^{2\psi_{3/2}} \simeq 1.44 \times 10^{-8} \frac{m_{3/2}^3 h^5}{M_{\text{P}}^2} \left(\frac{M_{\text{P}}}{M}\right)^3 , \tag{5.63}$$

$$\overline{\Gamma}_{Q_2}^{\chi\chi\text{Im}Q_2} \simeq 2.57 \times 10^{-14} \frac{m_{3/2}^3 h^5}{M_{\text{P}}^2} \left(\frac{M_{\text{P}}}{M}\right)^5 . \tag{5.64}$$

Let us now present the decay rates of the remaining subsequent products in the decays of the ISS fields, namely the gravitino $\psi_{3/2}$ and the ISS fermion $\chi_{S_1}$. We assume $m_{3/2} \gg m_{\text{MSSM}}$ with $m_{\text{MSSM}}$ being the mass of any MSSM particle. The gravitino decay rate is given by [279]

$$\overline{\Gamma}_{3/2}\left(\psi_{3/2} \to \text{MSSM}\right) = \frac{193}{384\pi} \frac{m_{3/2}^3}{M_P^2} . \tag{5.65}$$

The gravitino decays predominantly into an R-parity even MSSM particle and its supersymmetric

[10] They should not be confused with the neutralino, which will appear later in this thesis.

partner[11], since it possesses $R = -1$ [280]. The $\chi_{S1}$ decay rate is

$$\begin{aligned}\overline{\Gamma}_{\chi_{S1}}(\chi_{S1} \to \mathrm{Im}Q_2 + \chi_{\mathrm{MSSM}} + \phi_{\mathrm{MSSM}}) &= 2.38 \times 10^{-4} \frac{m_{3/2}^5}{M_P^4} \\ &\simeq 1.12 \times 10^{-8} \frac{m_{3/2}^3}{M_P^2} h^2 \left(\frac{M}{M_P}\right)^4 ,\end{aligned} \tag{5.66}$$

which is obtained from the term $e^{G/2}\left(\frac{1}{3}\left(K_{q_{ia}} + K_{\tilde{q}_{ia}}\right) K_{\mathrm{MSSM}}\right) \bar{\chi}_R^{ia} \chi_L^{\mathrm{MSSM}}$ in the scalar potential with $c_H = 1$ from the Giudice-Masiero term.

Let us now make some general comments regarding these decay rates and their impact on the thermal history of the Universe. These will be relevant for the phenomenological and cosmological analysis in chapter 6.

First of all, for late decay rates of the ISS fields into other ISS fields or into MSSM fields — i.e., for small values of the decay rates — the ISS fields will decay after the inflaton in a Universe with low temperature and will, therefore, generate some reheating. If these decays happen after Big-Bang nucleosynthesis (BBN), when the temperature of the Universe is $T \sim 1$ MeV, they can lead to unacceptable production of entropy, which would dilute the BBN products. Furthermore, these decays can give rise to a large number of unstable gravitinos or lighter ISS fields, which can then decay into lightest supersymmetric particle (LSP) in the MSSM, with a corresponding large dark matter relic density overclosing the Universe. These are the so-called *moduli*[12] and *gravitino problems* [144, 145, 146, 147, 148, 149]. In order to avoid these issues, we must guarantee that the ISS fields and their decay products decay before BBN.

In the scenario of decays before BBN, one could generate the observed baryon asymmetry $(n_B - n_{\bar{B}})/s_0 \sim 10^{-10}$ via the Affleck–Dine baryogenesis mechanisms [281, 282] only if the entropy production from ISS sources is sufficiently large, thus compensating the large entropy dilution necessary in this mechanism. Alternatively, baryogenesis can also be accomplished for a small ISS entropy production through other mechanisms, such as electroweak baryogenesis [283, 284].

In the next chapter 6, we obtain constraints in order to avoid the moduli and the gravitino problems, and — assuming some non-Affleck–Dine baryogenesis mechanism — to have entropy production from the ISS fields smaller than the entropy from the inflaton $\eta$. Furthermore, we investigate whether an acceptable dark matter relic density can still be obtained within this scenario.

[11] The decay channels are given by $\psi_{3/2} \to \lambda + A_m$, $\psi_{3/2} \to \phi_m + \bar{\chi}_m$ and $\psi_{3/2} \to \phi_m^* + \chi_m$, where $\lambda$ are gauginos, $A_m$ are gauge bosons, $\phi_m$ are scalars, and $\chi_m$ are left-handed fermions.

[12] Notice that the term moduli here refers to all the scalar fields acquiring mass after supersymmetry breaking, that is, the modulus field $\rho$ and the ISS scalar fields in our scenario.

CHAPTER 6

# Dark matter in the KL-ISS-MSSM scenario

In this chapter we study the post-inflationary dynamics of the Universe in the KL-ISS-MSSM scenario, imposing constraints from late entropy production in section 6.1 and from the dark matter relic density in section 6.2. We also show that neutralinos are good dark matter candidates in this setup, both from thermal and non-thermal processes.

## 6.1 Post-inflation dynamics

### 6.1.1 Oscillations and decays

We begin with a study of oscillations from the modulus $\rho$, the ISS fields and from the inflaton field $\eta$. Let $\varphi$ be some generic field and $H$ the Hubble parameter $H := \dot{R}/R$, where $R$ denotes the cosmological scale factor in the FLRW metric and $\dot{R}$ its derivative with respect to time $t$. The field $\varphi$ starts oscillating at $m_\varphi \sim H$ when it possesses a non-vanishing difference between its VEV during inflation, $\langle\varphi\rangle_{\rm ins}$, and its VEV at the offset of inflation, $\langle\varphi\rangle_{\rm min}$, i.e.,

$$|\langle\varphi\rangle|_{\rm amp} = |\langle\varphi\rangle_{\rm ins} - \langle\varphi\rangle_{\rm min}| \neq 0 \,. \tag{6.1}$$

First of all, recall from section 5.5 that the modulus $\rho$ is much heavier than the inflaton, implying that they decouple from each other. Therefore, the modulus will have the same VEV both during and after inflation, leading to a vanishing post-inflationary oscillation amplitude. Hence, it is justified to neglect the evolution of the modulus $\rho$ after inflation.

As for the inflaton field $\eta$, after the end of inflation it starts to oscillate about its true minimum when $m_\eta \sim H$ [285, 286, 287]. At the end of inflation we have $\langle\eta\rangle_{\rm amp} = \langle\eta\rangle_{\rm ins} = \sqrt{8/3}M_P$ because $\langle\eta\rangle_{\rm min} = 0$ at the offset of inflation. Let $R_\eta$ denotes the cosmological scale factor at the onset of the $\eta$ oscillations. The energy density of the inflaton $\eta$ and the Hubble parameter after

inflation are given by

$$\rho_\eta = \frac{1}{2}m_\eta^2\eta^2 = \frac{1}{2}m_\eta^2\langle\eta\rangle_{\rm amp}^2\left(\frac{R_\eta}{R}\right)^3 = \frac{4}{3}m_\eta^2 M_P^2\left(\frac{R_\eta}{R}\right)^3 , \tag{6.2}$$

$$H = \sqrt{\frac{1}{M_P^2}\frac{\Omega}{3}} = \frac{2}{3}m_\eta\left(\frac{R_\eta}{R}\right)^{3/2} , \tag{6.3}$$

where $\Omega$ is the density parameter $\Omega = \rho/\rho_c = 8\pi G\rho/3H^2 = \rho/3H^2M_P^2$ defined as the ratio between the actual density $\rho$ and the critical density (closure) $\rho_c$ of the FLRW Universe. Since the energy density of the inflaton $\eta$ dominates the energy density of the Universe after inflation, we enter into a matter-dominated period — actually, the so-called *reheating phase*.

Let us now determine which of the ISS fields start to oscillate after inflation. To do so, we need to add the inflaton contributions to the ISS model, which so far have been neglected in our analysis.

Recall the VEVs of the ISS fields without contributions from the inflaton $\eta$,

$$\begin{aligned}
&\langle q_{ia}, \tilde{q}_{ai}\rangle \simeq M\delta_{ia} ,\\
&\left\langle S_{ij}\right\rangle \simeq \left(\frac{M}{M_P}\right)^2 M_P\,\delta_{ij} \quad \text{for } i,j \le N ,\\
&\left\langle S_{ij}\right\rangle \simeq \frac{N_f - N}{3N}\frac{408.79}{h^2}\left(\frac{M}{M_P}\right)^2 M_P\,\delta_{ij} \quad \text{for } i,j > N .
\end{aligned} \tag{6.4}$$

The contributions from the inflaton $\eta$ modify the ISS scalar potential by addition of a term[1] [147, 281, 285]

$$\Delta V(\phi_{\rm ISS}, \bar{\phi}_{\rm ISS}) \sim e^{K(\phi_{\rm ISS},\bar{\phi}_{\rm ISS})}V(\eta) = cH^2\phi_{\rm ISS}\bar{\phi}_{\rm ISS} + \cdots , \tag{6.5}$$

where $H$ is the Hubble parameter, and generically $c = 3$ for $K_{\rm ISS} = \phi_{\rm ISS}\bar{\phi}_{\rm ISS}$ [285], which is the case for the ISS fields $\phi_{\rm ISS} = \{S_{ij}, q_{ia}, \tilde{q}_{ai}\}$ — recall equation (5.11). The effect of $\Delta V(\phi_{\rm ISS}, \bar{\phi}_{\rm ISS})$ is to make the VEVs during inflation, $\left\langle S_{ij}\right\rangle_{\rm ins}$ and $\langle q_{ia}, \tilde{q}_{ai}\rangle_{\rm ins}$, assume smaller values compared with their true minima given in equation (6.4), which we call from now on $\left\langle S_{ij}\right\rangle_{\rm min}$ and $\langle q_{ia}, \tilde{q}_{ai}\rangle_{\rm min}$ . Indeed, assuming high-scale inflation, i.e., $H \gg M$, one has for $S$,

$$\left\langle S_{ij}\right\rangle_{\rm ins} \simeq \left\langle S_{ij}\right\rangle_{\rm min}\left(1 + \frac{cH^2}{2h^2M^2}\right)^{-1} \simeq \frac{2h^2M^4}{cH^2M_{\rm P}} \ll \left\langle S_{ij}\right\rangle_{\rm min} \text{ for } i,j \le N , \tag{6.6}$$

$$\left\langle S_{ij}\right\rangle_{\rm ins} \simeq \left\langle S_{ij}\right\rangle_{\rm min}\left(1 + \frac{8\pi^2cH^2}{(\ln(4)-1)\,h^4M^2}\right)^{-1} \simeq \frac{2h^2M^4}{cH^2M_{\rm P}} \ll \left\langle S_{ij}\right\rangle_{\rm min} \text{ for } i,j > N . \tag{6.7}$$

[1] The inflaton potential introduces a mass contribution $\sim \sqrt{c}H$ to all ISS fields during inflation with $H \gg M$, including the mass of the Goldstone modes $\mathrm{Im}Q_2$, $\mathrm{Re}Q_4$ and $\mathrm{Im}Q_4$. Although the $S_{ij}$ retain a small VEV, the Goldstone particles cannot be prevented from becoming massive.

Furthemore, for $q_{ia}$ and $\tilde{q}_{ai}$, one has

$$\langle q_{ia}, \tilde{q}_{ai} \rangle_{\text{ins}} \simeq \begin{cases} \frac{1}{h}\sqrt{h^2M^2 - cH^2} & \text{for } cH^2 \leq h^2M^2 \,, \\ 0 & \text{for } cH^2 > h^2M^2 \,. \end{cases} \tag{6.8}$$

The $\left\langle S_{ij} \right\rangle_{\text{ins}}$ and $\langle q_{ia}, \tilde{q}_{ai} \rangle_{\text{ins}}$ now evolve into the direction of the minima $\left\langle S_{ij} \right\rangle_{\text{min}}$ and $\langle q_{ia}, \tilde{q}_{ai} \rangle_{\text{min}}$. Therefore, from equation (6.1), we notice that there are $N_f$ oscillating fields in the $S_{ij}$ sector, $N$ for $i, j \leq N$ and $(N_f - N)$ for $i, j > N$. The linear combinations responsible for their oscillations are $\text{Re}S_1$ and $\text{Re}S_2$. Furthermore, since $q$ and $\tilde{q}$ must have the same VEV due to the symmetry of the superpotential, there are no oscillations for $Q_2$ as can be seen from its definition in equation (5.32). Since $Q_3$ and $Q_4$ are defined in the region $i \leq N$ and $N < a \leq N_f$, by the first equation in (6.4) and their definition in equations (5.33) and (5.34), they also do not contribute with any oscillation. Therefore, there are only $N$ oscillating fields from $q$ and $\tilde{q}$, corresponding to the mass eigenstate $\text{Re}Q_1$. In summary, the ISS fields that start oscillations after inflation are given in table 6.1.

| Oscillating ISS fields | $\text{Re}S_1$ | $\text{Re}S_2$ | $\text{Re}Q_1$ |
|---|---|---|---|
| Quantity | $N$ | $N_f - N$ | $N$ |

Table 6.1: The ISS fields responsible for oscillations after inflation as well as the number of oscillating fields for each type.

Within the period after inflation with dominant oscillations from $\eta$, the ISS fields adiabatically track their instantaneous minimum given by equations (6.6) and (6.8). This happens until they reach the point $H = \frac{2}{3}m_{\phi_{\text{ISS}}}$, where they start damped oscillations about their true minimum[2] given in equation (6.4) [285, 286, 287].

The cosmological scale factor at the onset of $\phi_{\text{ISS}}$ oscillations is given by

$$R_{\phi_{\text{ISS}}} = \left(\frac{m_\eta}{m_{\phi_{\text{ISS}}}}\right)^{2/3} R_\eta \,. \tag{6.9}$$

For $\text{Re}Q_1$, $\text{Re}S_1$ and $\text{Re}S_2$, this becomes

$$R_{Q_1} = \left(\frac{N_f - N}{6}\right)^{1/3} \left(\frac{M}{M_P}\frac{m_\eta}{m_{3/2}}\right)^{2/3} R_\eta \,, \tag{6.10}$$

$$R_{S_1} = \left(\frac{N_f - N}{6}\right)^{1/3} \left(\frac{M}{M_P}\frac{m_\eta}{m_{3/2}}\right)^{2/3} R_\eta \,, \tag{6.11}$$

$$R_{S_2} = \left(\frac{N_f - N}{3N}\right)^{1/3} \left(\frac{8\pi^2}{(\ln(4) - 1)\, h^2}\right)^{1/3} \left(\frac{M}{M_P}\frac{m_\eta}{m_{3/2}}\right)^{2/3} R_\eta \,. \tag{6.12}$$

[2] The condition $h^2M^2 \gtrsim c\, H^2\big|_{H=2m_{q_{ia}}/3}$ implies that $\langle q_{ia}, \tilde{q}_{ai} \rangle_{\text{ins}} > 0$ and consequently $q$ and $\tilde{q}$ can indeed start to oscillate. This condition is satisfied for any $h$ and $M$, with the generic $c = 3$.

Plugging in the oscillation amplitudes from equations (6.4), (6.6) and (6.8), as well as their corresponding masses as given in chapter 5, the energy densities for the $N$ oscillating fields $\mathrm{Re}Q_1$, and the $N_f$ oscillating $\mathrm{Re}S_1$ and $\mathrm{Re}S_2$ are given by

$$\rho_{Q_1} = \frac{N}{2} m_{Q_1}^2 \langle Q_1 \rangle_{\mathrm{amp}}^2 \left(\frac{R_{Q_1}}{R}\right)^3 = \frac{12N}{N_f - N} \left(\frac{m_{3/2}}{M_{\mathrm{P}}}\right)^2 M_{\mathrm{P}}^4 \left(\frac{R_{Q_1}}{R}\right)^3 , \tag{6.13}$$

$$\rho_{S_1} = \frac{N}{2} m_{S_1}^2 \langle S_1 \rangle_{\mathrm{amp}}^2 \left(\frac{R_{S_1}}{R}\right)^3 = \frac{12N}{N_f - N} \left(\frac{m_{3/2}}{M_{\mathrm{P}}}\right)^2 M_{\mathrm{P}}^4 \left(\frac{R_{Q_1}}{R}\right)^3 , \tag{6.14}$$

$$\rho_{S_2} = \frac{N_f - N}{2} m_{S_2}^2 \langle S_2 \rangle_{\mathrm{amp}}^2 \left(\frac{R_{S_2}}{R}\right)^3 \tag{6.15}$$

$$= \frac{\left(N_f - N\right)^2}{N} \left(\frac{16\pi^2}{3\left(\ln(4) - 1\right) h^2}\right) \left(\frac{m_{3/2}}{M_{\mathrm{P}}}\right)^2 \left(\frac{M}{M_{\mathrm{P}}}\right)^2 M_{\mathrm{P}}^4 \left(\frac{R_{S_2}}{R}\right)^3 . \tag{6.16}$$

Notice that the start of oscillations from the ISS fields after inflation may happen before or after the inflaton oscillations have decayed.

Furthermore, reheating after inflation leads to coupling of the inflaton $\eta$ with matter via gravitational interactions. Under the conditions that the gauge kinetic function depends linearly on the inflaton [270], the latter couples to two MSSM gauge bosons with coupling $d_\eta$, yielding a decay rate

$$\Gamma_\eta = \frac{3}{64\pi} d_\eta^2 \frac{m_\eta^3}{M_P^2} \sim 10^{-2} d_\eta^2 \frac{m_\eta^3}{M_P^2} = a_\eta^2 \frac{m_\eta^3}{M_P^2} . \tag{6.17}$$

Here the coupling $a_\eta$ is defined as

$$a_\eta \equiv 10^{-1} d_\eta . \tag{6.18}$$

This decay rate is extremely small [270], a reminiscent of no-scale supergravity models [288]. When presenting the constraints from late entropy production (section 6.1.2) and from dark matter relic density (section 6.2 ), we give them for two realistic values of the coupling $a_\eta$, namely for $a_\eta = 10^{-3}$ and $a_\eta = 10^{-1}$.

### 6.1.2 Evolution of the Universe and entropy production

We now turn to the evolution of the oscillations presented in the previous section and to entropy production from the decays of the inflaton, the oscillating ISS fields and the gravitinos. For this purpose, we remind the reader of equation (6.17) for the decay of the inflaton, equations (5.59) to (5.64) for the relevant decay rates of the ISS fields $\mathrm{Re}Q_1$, $\mathrm{Re}S_1$ and $\mathrm{Re}S_2$ as well as equations (5.65) and (5.66) for their subsequent decay products — into the gravitino $\psi_{3/2}$ and the ISS fermion $\chi_{S1}$.

The list below summarizes the assumptions necessary for the ISS fields not to drastically alter the thermal history of the Universe. We will then work out the corresponding constraints, indicating the regions in the parameter space where they hold.

(i) We assume that the energy of the Universe after the end of inflation is dominated by $\eta$ oscillations and by the decay products of $\eta$.

(ii) If the ISS fields decay after the inflaton, the entropy they generate should not dominate over the entropy from reheating, in order not to spoil successful production of later relics.

(iii) It is also possible that the relativistic decay products of the ISS fields may turn non-relativistic as the Universe cools down, thereby changing the evolution of their energy densities according to $\rho_{\rm rad}/\rho_{\rm non} \sim R^{-1}$. This would have an impact on the results for item (ii) above, which we also take into account.

Furthermore, the following experimental constraints must also be satisfied.

(iv) Massless particles from decays of the ISS fields must be in agreement with observable relativistic degrees of freedom $N_{\rm eff} = 3.15 \pm 0.23$ as measured by the Planck collaboration [16].

(v) Decay products with small decay rates must not decay after the BBN epoch — this will be treated in section 6.2.

Let us start by working out the constraints coming from the first (i) and the second (ii) points. The energy density from oscillations of the ISS fields are given by the combination

$$\begin{aligned}\rho_{\phi_{\rm ISS}} &= \rho_{Q_1} + \rho_{S_1} + \rho_{S_2} \\ &= \left(\frac{m_{3/2}}{M_P}\right)^2 M_P^4 \left\{ \frac{12N}{N_f - N}\left(\frac{R_{Q_1}}{R}\right)^3 + N\left(\frac{M}{M_P}\right)^2\left(\frac{R_{S_1}}{R}\right)^3 \right. \\ &\quad \left. + \frac{\left(N_f - N\right)^2}{3N}\left(\frac{16\pi^2}{3\left(\ln(4) - 1\right)}\right)\left(\frac{M}{M_P}\right)^2\left(\frac{R_{S_2}}{R}\right)^3 \right\} .\end{aligned} \tag{6.19}$$

In order to compare $\rho_{\phi_{\rm ISS}}$ and $\rho_\eta$, we rearrange the above expression in terms of quantities for the inflaton. With the use of $N_f = 4$ and $N = 1$ — as already adopted to compute the decay rates — we find

$$\rho_{\phi_{\rm ISS}} = m_\eta^2 M_P^2 \left\{ 2\left(\frac{M}{M_P}\right)^2 + \frac{1}{2}\left(\frac{M}{M_P}\right)^4 + \frac{2.51\times 10^5}{h^4}\left(\frac{M}{M_P}\right)^4 \right\}\left(\frac{R_\eta}{R}\right)^3 . \tag{6.20}$$

We compare this expression with the energy density from oscillations of $\eta$ given in equation (6.2), which yields $\rho_\eta > \rho_{\phi_{\rm ISS}}$ at the end of inflation only if

$$M < 4.80\times 10^{-2} h M_{\rm P} . \tag{6.21}$$

This requirement will be displayed in figures 6.3 and 6.4 where the parameter space $(h, M)$ is also constrained by entropy production from ISS decays and the subsequent decays of their products.

Now, let $R_{{\rm d}\phi_{\rm ISS}}$ be the scale factor at decay of $\phi_{\rm ISS}$ and $R_{{\rm d}\eta}$ be the scale factor at decay of $\eta$. Depending on whether the $\phi_{\rm ISS}$ decays before or after decays of $\eta$, these scale factors satisfy,

respectively,

$$\frac{R_{\mathrm{d}\phi_{\mathrm{ISS}}}}{R_{\mathrm{d}\eta}} = a_\eta^{4/3}\left(\frac{M_P}{\Gamma_{\phi_{\mathrm{ISS}}}}\right)^{2/3}\left(\frac{m_\eta}{M_P}\right)^2 , \tag{6.22}$$

$$\frac{R_{\mathrm{d}\phi_{\mathrm{ISS}}}}{R_{\mathrm{d}\eta}} = \frac{2}{\sqrt{3}}a_\eta\left(\frac{M_P}{\Gamma_{\phi_{\mathrm{ISS}}}}\right)^{1/2}\left(\frac{m_\eta}{M_P}\right)^{3/2} . \tag{6.23}$$

To obtain the decay epochs we used $H = k\Gamma_{\phi_{\mathrm{ISS}}}$ with $k = 2/3$ for matter domination (before reheating) and $k = 1/2$ for radiation domination (during reheating). Furthermore, we have also used the following relation, with $H = (2/3)\Gamma_\eta$,

$$R_\eta/R_{\mathrm{d}\eta} = a_\eta^{4/3}\left(\frac{m_\eta}{M_P}\right)^{4/3} . \tag{6.24}$$

On the one hand, if $R_{\mathrm{d}\phi_{\mathrm{ISS}}}/R_{\mathrm{d}\eta} < 1$, $\phi_{\mathrm{ISS}}$ decays before the inflaton — otherwise it decays after. In figure 6.1 we show how the parameters $M$ and $h$ of the ISS model, which are implicit in $\Gamma_{\phi_{\mathrm{ISS}}}$, determine the time of ISS decays. We should now analyse how this information on the time of

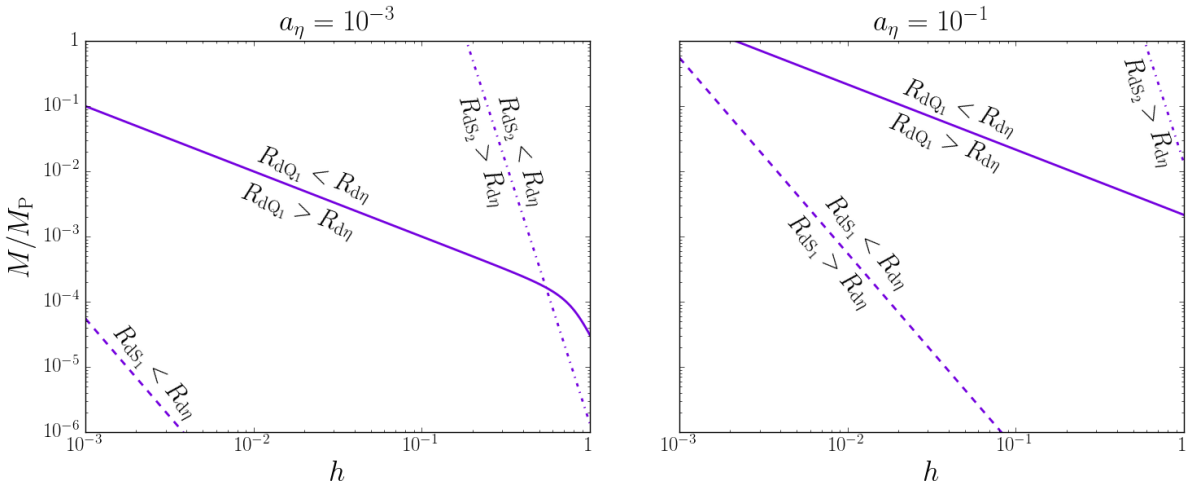


Figure 6.1: The curves of $\Gamma^i_{\phi_{\mathrm{ISS}}} = \Gamma_\eta$, where $i = S_1, S_2, Q_1$, for small (large) coupling $a_\eta = 10^{-3}$ ($a_\eta = 10^{-1}$). Above these curves, the ISS decay rates $\Gamma^i_{\phi_{\mathrm{ISS}}}$ become larger, implying a smaller scale factor at the time of their decays. In other words, each of the ISS fields decays before (after) the inflaton above (below) their curves.

ISS decays translate into energy density and entropy production. Since we want $\eta$ oscillations or decay products of $\eta$ to dominate the energy of the Universe after inflation — see point (i) —, production of entropy from $\phi_{\mathrm{ISS}}$ will only be problematic if one or more of them decays after $\eta$ has already decayed, as this can wash out the contributions from $\eta$. Let $\rho_{\mathrm{d}\eta}$ be the energy density at the moment of $\eta$ decay. The energy density of the decay products of $\eta$ is given by

$$\rho^r_\eta(R) = \rho_{\mathrm{d}\eta}\left(\frac{R_{\mathrm{d}\eta}}{R}\right)^4 = \frac{4}{3}a_\eta^4 M_P^4\left(\frac{m_\eta}{M_P}\right)^6\left(\frac{R_{\mathrm{d}\eta}}{R}\right)^4 . \tag{6.25}$$

Furthermore, $\rho^r_{\phi_{\rm ISS}}$ is the energy density of the decay products of $S_1$, $S_2$ and $Q_1$, given by

$$\rho^r_{\phi_{\rm ISS}}(R) = \rho_{{\rm d}Q_1}\left(\frac{R_{{\rm d}Q_1}}{R}\right)^4 + \rho_{{\rm d}S_1}\left(\frac{R_{{\rm d}S_2}}{R}\right)^4 + \rho_{{\rm d}S_2}\left(\frac{R_{{\rm d}S_2}}{R}\right)^4 . \tag{6.26}$$

We can define a scale factor $R_1$ where $\rho^r_\eta(R_1) = \rho^r_{\phi_{\rm ISS}}(R_1)$. Since for any field $i$ the relation $s_i/s_j \sim \left(\rho^r_i/\rho^r_j\right)^{3/4}$ holds, finding an $R_1$ means that there exists a limit on the entropy produced by the ISS fields $s_\eta > s_{\phi_{\rm ISS}}$ such that this production is not problematic for any time after $R_1$. In other words, if $\rho^r_\eta(R_1) > \rho^r_{\phi_{\rm ISS}}(R_1)$, then most entropy comes from $\eta$ decays. Otherwise, the ISS decays would provide the most entropy. When $\rho^r_{\phi_{\rm ISS}}$ is evaluated at $R_1$, $R_1$ is necessarily equal to the scale factor of the last decaying field. This happens because $\rho_{\rm rad}/\rho_{\rm matter} \sim R^{-1}$ in a mixture of radiation from decays and matter and, if we look into an ISS field decaying before $R_1$, this would mean that the associated energy density $\rho_r$ and entropy would become larger.

In our scenario, $S_2$ is the last decaying particle. Therefore,

$$\rho^r_{\phi_{\rm ISS}}(R_1) = \rho_{{\rm d}Q_1}\left(\frac{R_{{\rm d}Q_1}}{R_1}\right)^4 + \rho_{{\rm d}S_1}\left(\frac{R_{{\rm d}S_2}}{R_1}\right)^4 + \rho_{{\rm d}S_2} . \tag{6.27}$$

In figure 6.2, we use $\rho^r_\eta(R_1) > \rho^r_{\phi_{\rm ISS}}$ to plot numerically the bound for entropy production from decays of the ISS fields, i.e., $s_\eta > s_{\phi_{\rm ISS}}$. For the region at which the curve is drawn, $S_2$ dominates the energy density compared to either $Q_1$ or $S_1$ because its VEV is the largest of them. Both $Q_1$ and $S_1$ become important only for smaller $M$ and larger $h$, i.e., in the lower right corner of both figures. In addition to that, there is a noticeable dip at the right upper corner for both cases $a_\eta = 10^{-1}$ and $a_\eta = 10^{-3}$. They form at the point at which $S_2$ turns from decaying after $\eta$ to decaying before $\eta$. This introduces a steep in the energy density function. The dip is quite steep only because our analysis assumes instantaneous decays.

Let us now discuss point (iii) in the above list, that is, we must add the behaviour of the decay products of $Q_1$, $S_1$ and $S_2$. These decay products can turn from relativistic to non-relativistic at some point, which could render their energy density larger than $\rho^r_\eta$. Below we find constraints such that their energy densities do not surpass $\rho^r_\eta$. We start by displaying the decay products of each ISS field,

$$\begin{aligned}
{\rm Re}S_1 &: (\chi_{S1} + \bar{\chi}_{S1}) , && (6.28)\\
{\rm Re}S_2 &: (\psi_{3/2} + \psi_{3/2}) , && (6.29)\\
{\rm Re}Q_1 &: (\psi_{3/2} + \psi_{3/2}, \chi_{S1} + \bar{\chi}_{S1} + {\rm Im}Q_2, \chi_{S1} + \bar{\chi}_{S1} + {\rm Re}Q_2) , && (6.30)\\
{\rm Re}Q_2 &: (\psi_{3/2} + \psi_{3/2}, \chi_{S1} + \bar{\chi}_{S1} + {\rm Im}Q_2) . && (6.31)
\end{aligned}$$

Furthermore, recall the masses of the final particles

$$\begin{aligned}
m_{\chi_{S1}} &= m_{3/2} ,\\
m_{{\rm Re}Q_2} &= \sqrt{\frac{3\left(\ln(4) - 1\right)}{8\pi^2}} h \left(\frac{M_P}{M}\right) m_{3/2} ,\\
m_{{\rm Im}Q_2} &= 0 .
\end{aligned} \tag{6.32}$$

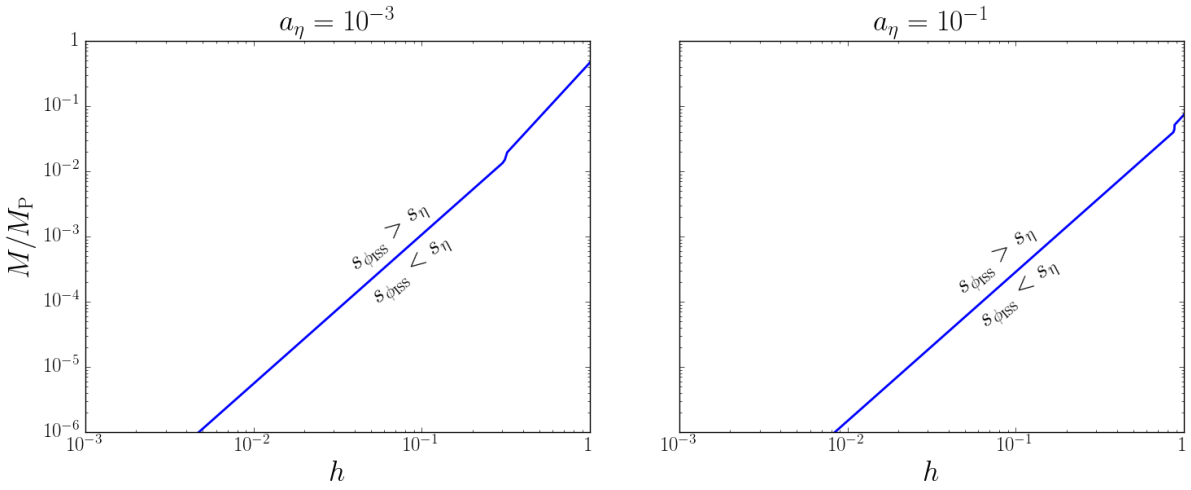


Figure 6.2: The curve of $s_{\phi_{\rm ISS}} = s_\eta$ numerically obtained from equations (6.25) and (6.27) at the decay epoch of the last decaying ISS particle $S_2$, for small (large) coupling $a_\eta = 10^{-3}$ ($a_\eta = 10^{-1}$). Above the curve, the energy density $\rho^r_{\phi_{\rm ISS}}$ becomes larger than $\rho^r_\eta$, implying also a larger entropy production at the decay time of $S_2$ than the entropy from decay products of $\eta$.

Since $m_{{\rm Im}Q_2} = 0$, it can never become non-relativistic. For massive particles, the scale factor at which they become non-relativistic $R_{\rm non}$ is related to the scale factor at the decay of the initial particle. We have the following relations[3]

$$
\begin{aligned}
{\rm Re}S_1 \;:&\; \frac{R_{{\rm d}S_1}}{R^{\chi_{S1}}_{\rm non}} = \frac{2m_{\chi_{S1}}}{m_{{\rm Re}S_1}}\,, \\
{\rm Re}S_2 \;:&\; \frac{R_{{\rm d}S_2}}{R^{\psi_{3/2}}_{\rm non}} = \frac{2m_{\psi_{3/2}}}{m_{{\rm Re}S_2}}\,, \\
{\rm Re}Q_1 \;:&\; \frac{R_{{\rm d}Q_1}}{R^{\psi_{3/2}}_{\rm non}} = \frac{2m_{\psi_{3/2}}}{m_{{\rm Re}Q_1}}\,, \quad \frac{R_{{\rm d}Q_1}}{R^{\chi_{S1}}_{\rm non}} = \frac{3m_{\chi_{S1}}}{m_{{\rm Re}Q_1}}\,, \quad \frac{R_{{\rm d}Q_1}}{R^{{\rm Re}Q_2}_{\rm non}} = \frac{3m_{{\rm Re}Q_2}}{m_{{\rm Re}Q_1}}\,, \\
{\rm Re}Q_2 \;:&\; \frac{R_{{\rm d}Q_2}}{R^{\psi_{3/2}}_{\rm non}} = \frac{2m_{\psi_{3/2}}}{m_{{\rm Re}Q_2}}\,, \quad \frac{R_{{\rm d}Q_2}}{R^{\chi_{S1}}_{\rm non}} = \frac{3m_{\chi_{S1}}}{m_{{\rm Re}Q_2}}\,.
\end{aligned}
\tag{6.33}
$$

On the one hand, if the decay rate of a particle is sufficiently large, it decays before it can turn non-relativistic. In that case, there would be no change to the curve presented in figure 6.2. On the other hand, if its decay rate is small, the energy density equations must change accordingly,

$$
\rho^{\rm non}_i = \sum_j \rho_{{\rm d}i} \left(\frac{R_{{\rm d}i}}{R^j_{\rm non}}\right)^4 \left(\frac{R^j_{\rm non}}{R}\right)^3 = \sum_j \rho_{{\rm d}i} \left(\frac{R_{{\rm d}i}}{R^j_{\rm non}}\right)\left(\frac{R_{{\rm d}i}}{R}\right)^3\,, \tag{6.34}
$$

[3] These were computed via $f^{\varphi_i}_\Phi \cdot \rho_{{\rm d}\Phi} \left(R_{{\rm d}\Phi}/R^{\varphi_i}_{\rm non}\right)^4 = \rho_{\varphi_i}|_{T=m_{\varphi_i}}$, where $\Phi$ is the mother-particle which decays into $\varphi_i + \varphi_j\,(+\varphi_k)$, and $f^{\varphi_i}_\Phi$ is the share of the energy of each $\Phi$ particle given to a product-particle $\varphi_i$. For example, $f^{\varphi_i}_\Phi = 1$ for $\Phi = {\rm Re}Q_2$ and $\varphi_i = \psi_{3/2}$. We have also considered that the masses of the products are much smaller than the masses of the decaying particles, which leads to the numerical factors in these expressions.

where $i$ stands for any of the ISS decaying particles. Notice that the decay rate of the product $\mathrm{Re}Q_2$ — from the decay of $\mathrm{Re}Q_1$ — has already been obtained in equation (5.58).

We calculate again the entropy production bound, now taking into account the non-relativistic behaviour of the products $\chi_{S1}$, $\psi_{3/2}$, and $\mathrm{Re}Q_2$. This is shown in the red curve of figure 6.3. It was obtained numerically from equations (6.25) and (6.34). As one can notice, the deviation from the blue curve becomes more pronounced for lower values of $M$ and $h$. This is because the products from ISS decays become non-relativistic earlier in this case. At $h \gtrsim 0.1$ and for $a_\eta = 10^{-3}$, the ISS products decay when they are still relativistic and, therefore, there is an agreement between the blue and the red curves. The same happens for $h \gtrsim 0.4$ in the case $a_\eta = 10^{-1}$. Since the red curve constrains more the parameter space, we consider it for later analysis.

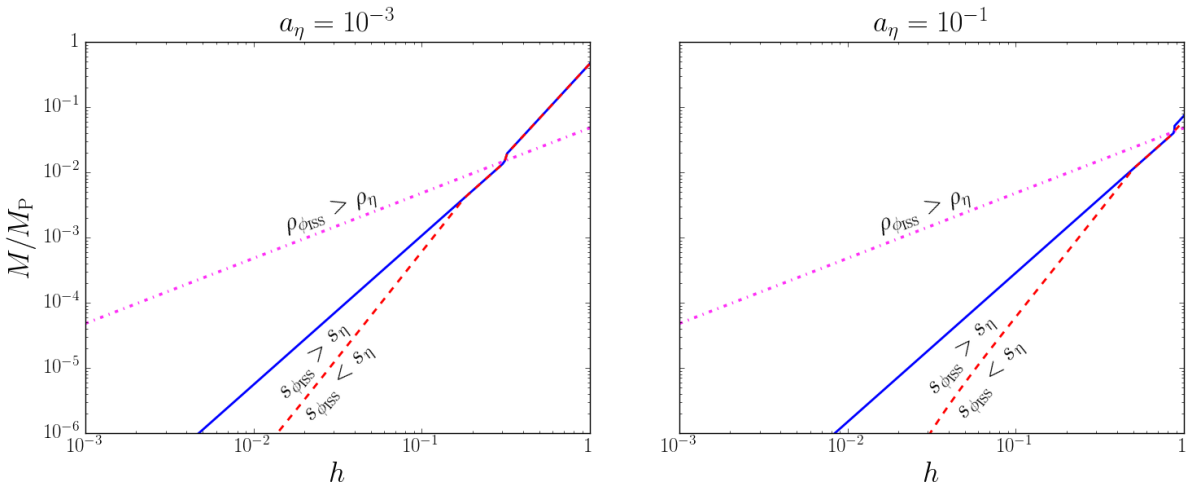


Figure 6.3: The curves of $s_{\phi_{\mathrm{ISS}}} = s_\eta$ (red-dashed and solid blue) and $\rho_{\phi_{\mathrm{ISS}}} = \rho_\eta$ (magenta dot-dashed) for small (large) coupling $a_\eta = 10^{-3}$ ($a_\eta = 10^{-1}$). The blue curve is evaluated at the decay epoch of $S_2$, the last decaying ISS particle, as already seen in figure 6.2. The red curve is evaluated at the decay time of $\chi_{S1}$, which is the last product to decay. Legends are shown only for the latter because for the blue curve it is the same as in figure 6.2.

Now we address point (iv), considering that the only massless product from ISS decays is $\mathrm{Im}Q_2$. First of all, its energy density is given by

$$\begin{aligned}
\rho_{\mathrm{Im}Q_2} &= \frac{\Gamma^{\chi\chi\,\mathrm{Re}Q_2}_{Q_1}}{\Gamma^{\mathrm{total}}_{Q_1}}\left[\frac{1}{3}\left(\frac{R_{\mathrm{d}Q_1}}{R}\right)^4 + \frac{1}{3}\cdot\frac{1}{3}\frac{\Gamma^{\chi\chi\,\mathrm{Im}Q_2}_{Q_2}}{\Gamma^{\mathrm{total}}_{Q_2}}\left(\frac{R_{\mathrm{d}Q_1}}{R^{\mathrm{Re}Q_2}_{\mathrm{non}}}\right)^4\left(\frac{R^{\mathrm{Re}Q_2}_{\mathrm{non}}}{R_{\mathrm{d}Q_2}}\right)^3\left(\frac{R_{\mathrm{d}Q_2}}{R}\right)^4\right]\rho_{\mathrm{d}Q_1} \\
&= \frac{\Gamma^{\chi\chi\,\mathrm{Re}Q_2}_{Q_1}}{\Gamma^{\mathrm{total}}_{Q_1}}\left[\frac{1}{3} + \frac{1}{9}\frac{\Gamma^{\chi\chi\,\mathrm{Im}Q_2}_{Q_2}}{\Gamma^{\mathrm{total}}_{Q_2}}\left(\frac{R_{\mathrm{d}Q_2}}{R^{\mathrm{Re}Q_2}_{\mathrm{non}}}\right)\right]\rho_{\mathrm{d}Q_1}\left(\frac{R_{\mathrm{d}Q_1}}{R}\right)^4 \\
&\simeq \frac{\Gamma^{\chi\chi\,\mathrm{Re}Q_2}_{Q_1}}{\Gamma^{\mathrm{total}}_{Q_1}}\left[\frac{1}{9}\frac{\Gamma^{\chi\chi\,\mathrm{Im}Q_2}_{Q_2}}{\Gamma^{\mathrm{total}}_{Q_2}}\left(\frac{R_{\mathrm{d}Q_2}}{R^{\mathrm{Re}Q_2}_{\mathrm{non}}}\right)\right]\rho_{\mathrm{d}Q_1}\left(\frac{R_{\mathrm{d}Q_1}}{R}\right)^4 \\
&\leq \frac{1}{18}\left(\frac{R_{\mathrm{d}Q_2}}{R^{\mathrm{Re}Q_2}_{\mathrm{non}}}\right)\rho_{\mathrm{d}Q_1}\left(\frac{R_{\mathrm{d}Q_1}}{R}\right)^4 .
\end{aligned} \tag{6.35}$$

Here the ratios $1/3$ and $1/3 \cdot 1/3$ correspond to the energy share carried by $\mathrm{Im}Q_2$ from its two respective sources, $Q_1 \to \bar{\chi}_{S1} + \chi_{S1} + \mathrm{Im}Q_2$ and $Q_1 \to \bar{\chi}_{S1} + \chi_{S1} + \mathrm{Re}Q_2$ followed by $\mathrm{Re}Q_2 \to \bar{\chi}_{S1} + \chi_{S1} + \mathrm{Im}Q_2$, where we assumed massless products when compared to $\mathrm{Re}Q_1$. From the second to the third line, we used[4] $R_{\mathrm{d}Q_2}/R_{\mathrm{non}}^{\mathrm{Re}Q_2} > 100$. From the third to the fourth line, we used the maximum values for the branching ratios for simplicity, i.e., $\Gamma_{Q_1}^{\chi\chi\mathrm{Re}Q_2}/\Gamma_{Q_1}^{\mathrm{total}} = 1/2$ and $\Gamma_{Q_2}^{\chi\chi\mathrm{Im}Q_2}/\Gamma_{Q_2}^{\mathrm{total}} = 1$.

Dark radiation energy density accounts for the total relativistic energy density in neutrinos plus other unknown degrees of freedom, and is parametrized by the effective degrees of freedom $N_{\mathrm{eff}}$. Let $\rho_\gamma$ be the photon energy density. For times much earlier than BBN, i.e., for $T \ll 1\,\mathrm{MeV}$, the energy density for dark radiation is given by

$$\rho_{\mathrm{dark}} = N_{\mathrm{eff}} \frac{7}{8} \left(\frac{4}{11}\right)^{4/3} \rho_\gamma \quad , \tag{6.36}$$

The contribution from the three SM neutrinos to this radiation density leads to $N_\nu \simeq 3.046$ [289]. On the other hand, the observational parameter $N_{\mathrm{eff}} = 3.15 \pm 0.23$ [16] allows for some additional radiation density. We check that $\rho_{\mathrm{Im}Q_2} < \rho_{\mathrm{dark}} - \rho_{\mathrm{SM}\,\nu}$ is indeed satisfied in the parameter space we consider, i.e., $M/M_P \in (10^{-6},\, 1)$ and $h \in (10^{-3},\, 1)$.

The constraints regarding entropy production obtained in this section, which are relevant for section 6.2, are collected in table 6.2. They are depicted in figure 6.4.

| | Constraint | Meaning | Legend |
|---|---|---|---|
| Eq. (6.21) | $M < 4.80 \times 10^{-2} h M_{\mathrm{P}}$ | $\rho_\eta > \rho_{\phi_{\mathrm{ISS}}}$ at the end of inflation | magenta curve |
| Eq. (6.27) | Numerical | $s_\eta > s_{\phi_{\mathrm{ISS}}}$ at decay epoch of last decaying particle $S_2$ | blue curve |
| Eq. (6.27) | Numerical | $s_\eta > s_{\phi_{\mathrm{ISS}}}$ at decay epoch of last decaying product $\chi_{S1}$ | red curve |

Table 6.2: The constraints on the ISS parameters $M$ and $h$ obtained in this section 6.1.2, their location in the text, their meaning, and their depiction in the figures of this section.

For the figures in the next section we will present the combined red and magenta curves in figure 6.4 as a new red curve, which we will label as *entropy*.

## 6.2 Dark matter production

After finding a protocol for constraining the parameter space of solutions such that ISS entropy production is negligible, in this section we turn to the production of dark matter.

[4] This can be proven for the parameter space we consider, i.e., $M/M_P \in (10^{-6},\, 1)$ and $h \in (10^{-3},\, 1)$.

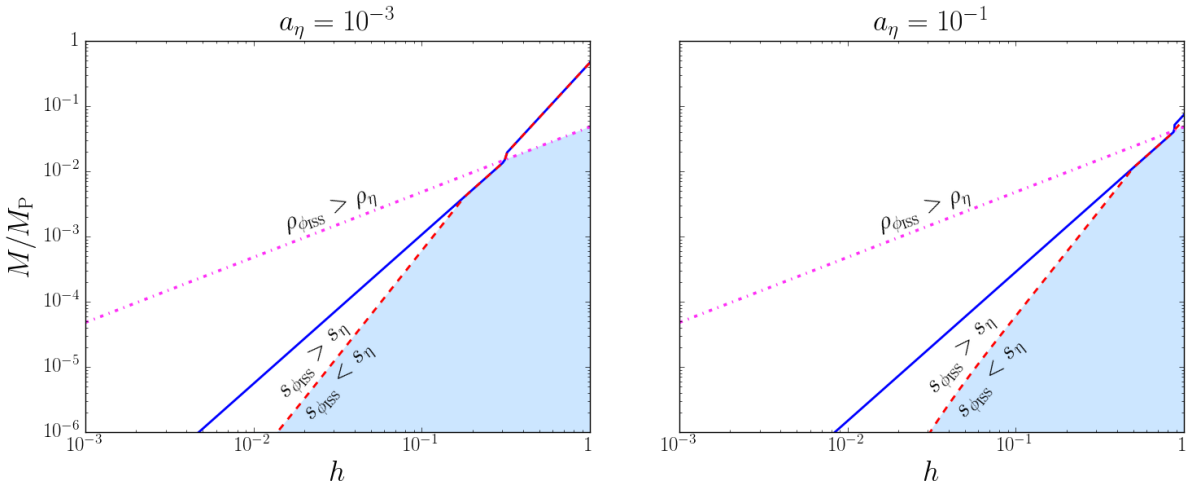


Figure 6.4: The curves $s_{\phi_{ISS}} = s_\eta$ summarizing the constraints obtained in this section — see table 6.2 — for small (large) coupling $a_\eta = 10^{-3}$ ($a_\eta = 10^{-1}$). The allowed region is shaded in blue.

We consider both thermal and non-thermal production [290] of dark matter, adopting the natural candidates for dark matter in supersymmetric scenarios, namely the stable[5] lightest supersymmetric particles (LSPs), the neutralinos referred to in this thesis as $\chi$ [53].

In the first case we consider gravitinos thermally produced in the reheating phase[6] of the inflaton $\eta$ to be the source for neutralinos. They can constitute dark matter when decaying at freeze-out, i.e., when the energy density for the gravitinos evolves constantly after their decoupling from the thermal bath at $H \sim \overline{\Gamma}_{3/2}$. Notice that, in principle, there can also be gravitinos produced from direct decays of the inflaton. However, we show in section 6.2.1 that this is negligible.

In the second case we consider the chain of decays from the ISS fields $\mathrm{Re}S_1$, $\mathrm{Re}S_2$ and $\mathrm{Re}Q_1$ into gravitinos $\psi_{3/2}$, and small massive fermions $\chi_{S1}$ and $\mathrm{Re}Q_2$. For $\mathrm{Re}Q_2$, it subsequently decays into gravitinos, and small massive fermions $\chi_{S1}$ and $\mathrm{Im}Q_2$. We recall here the decay channels from equations (6.28) to (6.31),

$$\begin{aligned}
\mathrm{Re}S_1 &: (\chi_{S1} + \bar{\chi}_{S1}) \ , \\
\mathrm{Re}S_2 &: (\psi_{3/2} + \psi_{3/2}) \ , \\
\mathrm{Re}Q_1 &: (\psi_{3/2} + \psi_{3/2}, \chi_{S1} + \bar{\chi}_{S1} + \mathrm{Im}Q_2, \chi_{S1} + \bar{\chi}_{S1} + \mathrm{Re}Q_2) \ , \\
\mathrm{Re}Q_2 &: (\psi_{3/2} + \psi_{3/2}, \chi_{S1} + \bar{\chi}_{S1} + \mathrm{Im}Q_2) \ .
\end{aligned}$$

Therefore, $\psi_{3/2}$ and $\chi_{S1}$ products can then decay into neutralinos. We have the following relation between the number density of ISS particles $n^i_{\phi_{ISS}}$ and the number density of the final gravitinos,

[5] These are guaranteed to be stable in conserved R-parity models [48, 57, 58, 59, 60, 61].

[6] When the ISS fields decay, they could generate a thermal bath with temperature $T_R^{ISS}$, which would produce gravitinos. Therefore, in principle, an exact treatment should also consider the reheating phase of ISS fields besides the reheating phase of $\eta$. However, since we constrain the entropy production from ISS decays and from the subsequent decays of their products to be smaller than the entropy production from decays of $\eta$ (see section 6.1.2), we do not have to be concerned with gravitino production within a reheating phase of ISS fields.

$n^i_{\phi_{\rm ISS}} = (n_{3/2})/2$. Each $\psi_{3/2}$ in turn contributes to the production of one neutralino at the epoch $H \sim \overline{\Gamma}_{3/2}$. Furthermore, we have distinct relations between the number density of ISS particles and the number density of $\chi_{S1}$. For decays from $S_1$ we have $n_{\chi_{S1}}/2$. For decays from $Q_1$ we have $n_{\chi_{S1}}/2$ or $n_{\chi_{S1}}/4$, where the last case occurs when there is a subsequent decay from its product Re$Q_2$. Finally, for decays from $Q_2$ we have $n_{\chi_{S1}}/2$. Each $\chi_{S1}$ in turn contributes to the production of one neutralino at the epoch $H \sim \overline{\Gamma}_{\chi_{S1}}$. Within this second case of non-thermal production of neutralinos, we also study the possible late thermalization of neutralinos.

Since the overproduction of dark matter is a delicate issue within the scenario of non-thermal production, as already mentioned at the end of chapter 5, we discuss how to take care of this issue within our context.

### 6.2.1 Thermal gravitino production

Let us start the analysis of dark matter production via its thermal gravitino source, from the thermal plasma created by the decay of the inflaton[7] [291]. This production depends on the reheating temperature[8] of the universe dominated by the inflaton after its decay. Let $g_\eta$ be the number of thermal relativistic degrees of freedom from decays of $\eta$. The reheating temperature is given by

$$T_R = \left(\frac{40}{\pi^2 g_\eta}\right)^{1/4} a_\eta \left(\frac{m_\eta}{M_P}\right)^{3/2} M_P \,. \tag{6.37}$$

Assuming that the gaugino masses $m_{1/2}$ satisfy $m_{1/2} \ll m_{3/2}$, the ratio of the gravitino number density to the entropy density in the reheating phase is given by [292]

$$\left(\frac{n_{3/2}}{s}\right)_{\rm rh} = 2.3 \times 10^{-12} \left(\frac{T_R}{10^{10}\ {\rm GeV}}\right) = 2.5 \times 10^{-11} a_\eta g_\eta^{-1/4} \left(\frac{m_\eta}{10^{-5} M_P}\right)^{3/2} \,. \tag{6.38}$$

For high values of $T_R$, this ratio may potentially overclose the universe.

Today's density of photons is related to today's entropy density via $7n_\gamma \simeq s_0$. Let $h_{\rm d} = H_0/\left(100\ {\rm km\ s^{-1} Mpc^{-1}}\right)$ be today's dimensionless Hubble parameter. If one assumes that the number density of neutralinos $\chi$ is given by[9] $n_\chi \simeq n_{3/2}$, its energy density ratio will be given by

$$\Omega^{\rm rh}_\chi h^2_{\rm d} \simeq \frac{7 n_\gamma}{s} \frac{m_\chi n_{3/2}}{\rho_c} h^2_{\rm d} \simeq 2.78 \times 10^{10} \left(\frac{m_\chi}{100\ {\rm GeV}}\right) \left(\frac{n_{3/2}}{s}\right)_{\rm rh} \,. \tag{6.39}$$

[7] We assume the inflaton to decay mainly into MSSM particles.

[8] Notice that the ISS and the MSSM sectors do not have sizeable interactions with each other. If this were the case, this would mean the ISS fields could thermalize with a temperature $T_R^{\rm ISS}$ and we should consider thermal production of gravitinos within this reheating phase as well. Furthermore, if $T_R > M_{\rm P}$, the condensate ISS sector would melt — recall that the ISS sector is a description of SQCD at low temperatures — and the description should be in terms of quarks, squarks, gauge bosons and gauginos. Moreover, also notice that $T_R \lesssim 10^{-9} M_{\rm P}$ for $a_\eta \leq 10^{-1}$, $g_\eta = 100$ and $m_\eta = 10^{-5} M_{\rm P}$. Therefore, $T_R$ is below the energy scale of $M/M_{\rm P}$ considered in our parameter range $M/M_{\rm P} \in (10^{-6}, 1)$.

[9] This assumption is feasible. Since R-parity of the gravitino is odd, its largest decay rates are into channels $\phi_i^{\rm odd} + \phi_j^{\rm even}$, $\phi_i^{\rm odd} + \phi_j^{\rm even} + \phi_k^{\rm even}$, $\phi_i^{\rm odd} + \phi_j^{\rm odd} + \phi_k^{\rm odd}$. Given a number $n$ of final particles, $(2n-3)$ final particles can be fermions since $\psi_{3/2}$ has mass dimension 3/2. The lowest order process is $\psi_{3/2} \to \phi_i^{\rm odd} + \phi_j^{\rm even}$, which leads to $n_{\rm odd} = n_{3/2}$.

Therefore, to have an acceptable dark matter relic density — i.e., $\Omega_\chi^{\rm rh} h_{\rm d}^2 \lesssim 0.12$ —, the allowed gravitino to entropy ratio must be

$$\left(\frac{n_{3/2}}{s}\right)_{\rm rh} \lesssim 4.32 \times 10^{-12} \left(\frac{100\ {\rm GeV}}{m_\chi}\right) . \tag{6.40}$$

By combining equations (6.38) and (6.40), we have the lower bound

$$a_\eta g_\eta^{-1/4} \left(\frac{m_\eta}{10^{-5} M_p}\right)^{3/2} \left(\frac{m_\chi}{100\ {\rm GeV}}\right) \lesssim 0.17 . \tag{6.41}$$

This bound can be evaded in the following three distinct situations.

- When the inflaton decays into a gravitino plus an inflatino. However, this channel may be kinematically forbidden if $\left|m_\eta - m_{\tilde\eta}\right| < m_{3/2}$, where $\tilde\eta$ is the inflatino, or kinematically suppressed if the inflaton(ino) scale is much higher than the gravitino scale, $O\left(m_{3/2}\right) \ll O\left(m_\eta, m_{\tilde\eta}\right)$ [293].

- When the inflaton decays into a pair of gravitinos through the interaction term

$$\begin{aligned} \mathcal{L}_\eta^{3/2} = -\frac{i}{8} \epsilon^{\mu\nu\rho\sigma} \bar\psi_\mu \gamma_\nu \psi_\rho \left(G_\eta \partial_\sigma \eta - G_{\eta^*} \partial_\sigma \eta^*\right) \\ + \frac{i}{4} \left(1 + K\left(\eta, \bar\eta\right)\right) m_{3/2} \left(2 + \frac{W\left(\eta\right)}{W}\right) M_P \bar\psi_\mu \sigma^{\mu\nu} \psi_\nu , \end{aligned} \tag{6.42}$$

  where $W = W_{\text{KL-ISS}} + W_{\rm MSSM} + W(\eta)$ is the total superpotential, $G_\eta$ is the derivative of $G = K + \ln(W\overline{W})$ with respect to $\eta$ and $K = K\left(\eta, \bar\eta\right) + K_{\text{KL-ISS}} + K_{\rm MSSM}$ is the total Kähler potential. We have already mentioned earlier in section 5.3 that our choice for the Kähler potential and the superpotential in the inflationary sector are such that there are no interaction terms in (6.42) between the inflaton and the gravitinos, thereby yielding a null decay rate for $\eta \to 2\psi_{3/2}$ [270].

- When gravitinos decay at a higher temperature than the freeze-out temperature for neutralinos, $T_\chi^f \sim m_\chi/20$.

Equation (6.41), which has to be satisfied in order to have acceptable dark matter relic density without overclosing the universe, is valid if none of the conditions discussed above applies. As we have already seen, the first two points are satisfied with the considerations of this thesis. We will see in section 6.2.2 how we can also satisfy the third point above. We will also discuss the same issue for the ISS fermion $\chi_{S1}$ which constitutes another candidate to decay to neutralinos. Therefore, thermal gravitinos can give rise to an acceptable dark matter relic density.

### 6.2.2 Mixture of thermal and non-thermal production

Let us now analyze dark matter production via a mixture of thermal and non-thermal processes, from neutralinos produced during the reheating phase of $\eta$ and from $\phi_{\rm ISS}$ decays, respectively.

First of all, consider the production of neutralinos from decays of $\psi_{3/2}$ or $\chi_{S1}$. The number density of neutralinos $\chi$ differs whether $R_{\mathrm{d}\phi_{\mathrm{ISS}}} > R_{\mathrm{d}\eta}$ or $R_{\mathrm{d}\phi_{\mathrm{ISS}}} < R_{\mathrm{d}\eta}$, since in the former scenario these decays happen within the $\eta$-reheated universe, and in the latter case the universe is dominated by matter from $\eta$ oscillations. However, the same ratios of number densities for $\psi_{3/2}$ or $\chi_{S1}$ to entropy density $s$ are produced in the end. These are given by, respectively,

$$\begin{aligned}\frac{n_{3/2}}{s} &= a_\eta g_\eta^{-1/4}\left(\frac{m_\eta}{M_P}\right)^{3/2}\left(\frac{M_P}{m_{3/2}}\right)\left(\frac{M}{M_P}\right)^3 \\ &\quad\times\left\{2.26\left(\frac{\Gamma_{Q_1}^{2\psi_{3/2}}}{\Gamma_{Q_1}^{\mathrm{total}}}+\frac{\Gamma_{Q_1}^{\chi\chi\mathrm{Re}Q_2}}{\Gamma_{Q_1}^{\mathrm{total}}}\frac{\Gamma_{Q_2}^{2\psi_{3/2}}}{\Gamma_{Q_2}^{\mathrm{total}}}\right)+\frac{5.72\times10^6}{h^5}\left(\frac{M}{M_P}\right)^2\frac{\Gamma_{S_2}^{2\psi_{3/2}}}{\Gamma_{S_2}^{\mathrm{total}}}\right\}\,,\end{aligned} \tag{6.43}$$

$$\begin{aligned}\frac{n_{\chi_{S1}}}{s} &= a_\eta g_\eta^{-1/4}\left(\frac{m_\eta}{M_P}\right)^{3/2}\left(\frac{M_P}{m_{3/2}}\right)\left(\frac{M}{M_P}\right)^3 \\ &\quad\times\left\{2.26\frac{\Gamma_{Q_1}^{\chi\chi\mathrm{Re}Q_2}}{\Gamma_{Q_1}^{\mathrm{total}}}\left(\frac{\Gamma_{Q_2}^{2\psi_{3/2}}}{\Gamma_{Q_2}^{\mathrm{total}}}+2\frac{\Gamma_{Q_2}^{\chi\chi\mathrm{Im}Q_2}}{\Gamma_{Q_2}^{\mathrm{total}}}+1\right)+0.56\left(\frac{M}{M_P}\right)^2\frac{\Gamma_{S_1}^{\chi\chi}}{\Gamma_{S_1}^{\mathrm{total}}}\right\}\,.\end{aligned} \tag{6.44}$$

To obtain these expressions we used

$$n_{3/2} \simeq 2\left(\Gamma_{\phi_{\mathrm{ISS}}}^{2\psi_{3/2}}/\Gamma_{\phi_{\mathrm{ISS}}}^{\mathrm{total}}\right)n_{\phi_{\mathrm{ISS}}}, \tag{6.45}$$

$$n_{\chi_{S1}} \simeq 2\left(\Gamma_{\phi_{\mathrm{ISS}}}^{\chi\chi}/\Gamma_{\phi_{\mathrm{ISS}}}^{\mathrm{total}}\right)n_{\phi_{\mathrm{ISS}}}\,, \tag{6.46}$$

where $n_{\phi_{\mathrm{ISS}}} = \rho_{\phi_{\mathrm{ISS}}}/m_{\phi_{\mathrm{ISS}}}$. Furthermore, we have assumed that $\Gamma_{Q_1}^{\mathrm{Im}Q_2} \simeq \Gamma_{Q_1}^{\mathrm{Re}Q_2}$, and we have also taken into account the possibility that $\mathrm{Re}Q_2$ also decays to $\chi_{S1}$, thereby generating the following term in equation (6.43),

$$\frac{\Gamma_{Q_1}^{\chi\chi\mathrm{Re}Q_2}}{\Gamma_{Q_1}^{\mathrm{total}}}\frac{\Gamma_{Q_2}^{2\psi_{3/2}}}{\Gamma_{Q_2}^{\mathrm{total}}}\,. \tag{6.47}$$

Now, with $n_\chi \simeq n_{3/2}$ and $n_\chi \simeq n_{\chi_{S1}}$ applied, respectively, in (6.43) and (6.44), the neutralino relic densities from both $\psi_{3/2}$ and $\chi_{S1}$ sources are given by

$$\begin{aligned}\Omega_\chi^{3/2}h_{\mathrm{d}}^2 &\simeq \frac{7n_\gamma}{s}\frac{m_\chi n_{3/2}}{\rho_c}h_{\mathrm{d}}^2 \\ &\simeq 0.12\times\left(\frac{a_\eta}{10^{-2}}\right)\left(\frac{100}{g_\eta}\right)^{1/4}\left(\frac{m_\eta}{10^{-5}M_P}\right)^{3/2}\left(\frac{m_\chi}{100\ \mathrm{GeV}}\right)f_{\psi_{3/2}}(h,M)\,,\end{aligned} \tag{6.48}$$

$$\begin{aligned}\Omega_\chi^{\chi_{S1}}h_{\mathrm{d}}^2 &\simeq \frac{7n_\gamma}{s}\frac{m_\chi n_{\chi_{S1}}}{\rho_c}h_{\mathrm{d}}^2 \\ &\simeq 0.12\times\left(\frac{a_\eta}{10^{-2}}\right)\left(\frac{100}{g_\eta}\right)^{1/4}\left(\frac{m_\eta}{10^{-5}M_P}\right)^{3/2}\left(\frac{m_\chi}{100\ \mathrm{GeV}}\right)f_{\chi_{S1}}(h,M)\,,\end{aligned} \tag{6.49}$$

where the functions $f_i$ for $i = \{\psi_{3/2}, \chi_{S1}\}$ are defined as

$$f_{\psi_{3/2}}(h, M) = 406.56 \left(\frac{1}{h}\right)\left(\frac{M}{M_P}\right)\times \left\{2.26\left(\frac{\Gamma_{Q_1}^{2\psi_{3/2}}}{\Gamma_{Q_1}^{\text{total}}} + \frac{\Gamma_{Q_1}^{\chi\chi\text{Re}Q_2}}{\Gamma_{Q_1}^{\text{total}}}\frac{\Gamma_{Q_2}^{2\psi_{3/2}}}{\Gamma_{Q_2}^{\text{total}}}\right) + \frac{5.72\times 10^6}{h^5}\left(\frac{M}{M_P}\right)^2\right\} , \tag{6.50}$$

$$f_{\chi_{S1}}(h, M) = 406.56 \left(\frac{1}{h}\right)\left(\frac{M}{M_P}\right)\times \left\{2.26\frac{\Gamma_{Q_1}^{\chi\chi\text{Re}Q_2}}{\Gamma_{Q_1}^{\text{total}}}\left(\frac{\Gamma_{Q_2}^{2\psi_{3/2}}}{\Gamma_{Q_2}^{\text{total}}} + 2\frac{\Gamma_{Q_2}^{\chi\chi\text{Im}Q_2}}{\Gamma_{Q_2}^{\text{total}}} + 1\right) + 0.56\left(\frac{M}{M_P}\right)^2\right\} . \tag{6.51}$$

From these equations and with the use of $g_\eta = 100$, $m_\eta = 10^{-5}M_P$ and $m_\chi = 100$ GeV, we obtain the curves $\Omega_\chi^i h_{\text{d}}^2 = 0.12$ in terms of the parameters $h$ and $M$. Notice that we also replaced $m_{3/2} = m_{3/2}(h, M)$ via equation (5.26). We plot these curves later in figures 6.5 and 6.6 when all the constraints from entropy production and possible subsequent annihilations are considered — they are labelled as $\text{DM}_{\text{dec}}^{3/2}$ and $\text{DM}_{\text{dec}}^{\chi_{S1}}$ and the arrows indicate the allowed regions for acceptable dark matter relic density satisfying $\Omega_\chi^i h_{\text{d}}^2 \lesssim 0.12$. In appendix C we present a solution for these equations in order to obtain $\Omega_\chi^i h_{\text{d}}^2 = 0.12$ as a matter of illustration. There, we also explain why there are three distinct possible curves of $\Omega_\chi^i h_{\text{d}}^2 = 0.12$ in the case of $\chi_{S1}$ when $a_\eta = 10^{-1}$.

Let us now obtain constraints such that both decays from $\psi_{3/2}$ and $\chi_{S1}$ happen before BBN, i.e., when $\overline{\Gamma}_{3/2} > t_{\text{BBN}}^{-1}$ and $\overline{\Gamma}_{\chi_{S1}} > t_{\text{BBN}}^{-1}$ where $t_{\text{BBN}}$ is the time associated with the occurrence of BBN at a temperature of $T \sim 1$ MeV. For $\psi_{3/2}$ we have

$$\frac{M}{M_P} \gtrsim 3.82\times 10^{-6} h^{-1/2} M_P , \tag{6.52}$$

whereas for $\chi_{S1}$ we have

$$\frac{M}{M_P} \gtrsim 1.75\times 10^{-3} h^{-1/2} . \tag{6.53}$$

Notice that equation (6.53) implies a quite heavy gravitino mass — recall equation (5.26). If $\chi_{S1}$ is allowed to decay after the present time, a dark matter relic density from $\chi_{S1}$ that does not close the universe can only be obtained for $M/M_P$ values which do not satisfy equation (6.52) within the parameter range we consider. Therefore, we neglect this scenario in the following and use the constraints given by equations (6.52) and (6.53) such that both $\psi_{3/2}$ and $\chi_{S1}$ can only decay before BBN.

Let us now check whether neutralinos are mainly produced from thermal gravitinos $\psi_{3/2}$ within the reheating phase of $\eta$ or from decays of gravitinos $\psi_{3/2}$ and ISS fermions $\chi_{S1}$. To do

so we compare the number densities for each of these processes, which gives

$$\frac{\left(n_\chi/s\right)_{\phi_{\rm ISS}\ \rm decays}}{\left(n_\chi/s\right)_{\eta\ \rm reheating}} \simeq 1.83\times 10^5 \left(\frac{1}{h}\right)\left(\frac{M}{M_P}\right)\left\{2.26\left(1+\frac{\Gamma_{Q_1}^{\chi\chi \mathrm{Re}Q_2}}{\Gamma_{Q_1}^{\rm total}}\right)+\frac{5.72\cdot 10^6}{h^5}\left(\frac{M}{M_P}\right)^2\right\}\,, \tag{6.54}$$

Here we have replaced $\Gamma_{Q_1}^{2\psi_{3/2}} = \Gamma_{Q_1}^{\rm total} - 2\Gamma_{Q_1}^{\chi\chi \mathrm{Re}Q_2}$ and neglected the last term in equation (6.44) when compared to equation (6.43). It turns out that, unless $M$ assumes very small values violating the bound from equation (6.52), $\left(n_\chi/s\right)_{\phi_{\rm ISS}\ \rm decays}$ is dominant over thermal gravitinos. Therefore, we assume the neutralino number density to be given by decays of $\psi_{3/2}$ and $\chi_{S1}$ from now on.

An important issue we have to tackle now is the annihilation of neutralinos after their production [147]. If the number density of neutralinos produced from $\psi_{3/2}$ or $\chi_{S1}$ decays is large enough, they can mutually annihilate, thus decreasing their number density. Technically stated, the neutralino number density is governed by the Boltzmann equation

$$\frac{dn_\chi}{dt} + 3Hn_\chi = -\left\langle\sigma_{\rm ann}v_{\rm M\o l}\right\rangle n_\chi^2\,, \tag{6.55}$$

where $\left\langle\sigma_{\rm ann}v_{\rm M\o l}\right\rangle$ is the thermally averaged annihilation cross section of the neutralinos with $v_{\rm M\o l}$ being the Møller velocity involving the initial particles. A possible equilibrium number density $n_{\chi,\rm eq}$ of neutralinos in this expression was neglected since we look at the epoch soon after they decouple, for which $n_\chi > n_{\chi,\rm eq}$ is satisfied.

For $n_\chi > H/\left\langle\sigma_{\rm ann}v_{\rm M\o l}\right\rangle$, the neutralino annihilates after $\psi_{3/2}$ or $\chi_{S1}$ decays, and eventually freezes-out when $n_\chi \sim H/\left\langle\sigma_{\rm ann}v_{\rm M\o l}\right\rangle$, where the Hubble term $3Hn_\chi$ and the annihilation term $\left\langle\sigma_{\rm ann}v_{\rm M\o l}\right\rangle n_\chi^2$ are of the same order of magnitude. On the other hand, for $n_\chi < H/\left\langle\sigma_{\rm ann}v_{\rm M\o l}\right\rangle$, the neutralino density is given at the time of decay of the $\psi_{3/2}$ or the $\chi_{S1}$.

Let us study the approximate expression for the relic density abundance of the neutralino given by [294, 295, 296]

$$\left(\frac{n_\chi}{s}\right)^{-1} \simeq \left(\frac{n_\chi}{s}\right)_{\rm decay}^{-1} + \left(\frac{H}{s\left\langle\sigma_{\rm ann}v_{\rm M\o l}\right\rangle}\right)_{\rm decay}^{-1}\,. \tag{6.56}$$

Here the lower index *decay* means evaluation at the time of $\psi_{3/2}$ or $\chi_{S1}$ decay. Therefore, we have an upper limit on $n_\chi/s$, i.e., $n_\chi/s \lesssim H\left\langle\sigma_{\rm ann}v_{\rm M\o l}\right\rangle^{-1}/s$. The following ratio compares both quantities on the right-hand side of equation (6.56), both for the gravitino $\psi_{3/2}$ and for $\chi_{S1}$,

$$\left(\frac{H\left\langle\sigma v\right\rangle^{-1}/s}{n_{3/2}/s}\right)_{\psi_{3/2}} \simeq \left(\frac{10^{-2}}{a_\eta}\right)\left(\frac{10^{-5}M_P}{m_\eta}\right)^{3/2}\left(\frac{10^{-7}\mathrm{GeV}^{-2}}{\left\langle\sigma v\right\rangle}\right) w_{\psi_{3/2}}^{-1}(h,M)\,, \tag{6.57}$$

$$\left(\frac{H\left\langle\sigma v\right\rangle^{-1}/s}{n_{\chi_{S1}}/s}\right)_{\chi_{S1}} \simeq \left(\frac{10^{-2}}{a_\eta}\right)\left(\frac{10^{-5}M_P}{m_\eta}\right)^{3/2}\left(\frac{10^{-7}\mathrm{GeV}^{-2}}{\left\langle\sigma v\right\rangle}\right) w_{\chi_{S1}}^{-1}(h,M)\,, \tag{6.58}$$

with the definitions

$$w_{\psi_{3/2}}(h,M) = 6.64 \times 10^{12}\, h^{3/2}\left(\frac{M}{M_{\rm P}}\right)^3 f_{\psi_{3/2}}(h,M)\ , \tag{6.59}$$

$$w_{\chi_{S1}}(h,M) = 2.49 \times 10^{16}\, h^{5/2}\left(\frac{M}{M_{\rm P}}\right)^5 f_{\chi_{S1}}(h,M)\ . \tag{6.60}$$

For $\langle\sigma_{\rm ann}v_{\rm M\o l}\rangle = 10^{-7}{\rm GeV}^{-2}$ and $m_\eta = 10^{-5}M_P$, the curves $(n_{3/2}/s = H\langle\sigma v\rangle^{-1}/s)_{\psi_{3/2}}$ and $(n_{\chi_{S1}}/s = H\langle\sigma v\rangle^{-1}/s)_{\chi_{S1}}$ are obtained in terms of the parameters $h$ and $M$. Notice that we also replaced $m_{3/2}$ by its function depending on both $h$ and $M$ via equation (5.26). For $(n_{3/2}/s < H\langle\sigma v\rangle^{-1}/s)_{\psi_{3/2}}$ and $(n_{\chi_{S1}}/s < H\langle\sigma v\rangle^{-1}/s)_{\chi_{S1}}$, the neutralinos do not annihilate and $(n_\chi/s)_{\rm decay}$ stays constant. In this case equations (6.48) and (6.49) are valid for obtaining the neutralino relic density $\Omega^i_\chi h^2_d$. For $(n_{3/2}/s > H\langle\sigma v\rangle^{-1}/s)_{\psi_{3/2}}$ and $(n_{\chi_{S1}}/s > H\langle\sigma v\rangle^{-1}/s)_{\chi_{S1}}$, the neutralinos annihilate until they reach $n_\chi/s \sim H\langle\sigma v\rangle^{-1}/s$. In this case, the neutralino relic density $\Omega^i_\chi h^2_d$ must satisfy a different equation, namely

$$\begin{aligned}\Omega^i_\chi h^2_{\rm d} &= \frac{7n_\gamma}{s}\frac{m_\chi n^i_\chi}{\rho_c}h^2_{\rm d}\\ &\simeq 0.12\left(\frac{100}{g_\eta}\right)^{1/4}\left(\frac{\alpha_h}{h}\right)^{c_i/2}\left(\frac{\varepsilon^i_M M_P}{M}\right)^{c_i}\left(\frac{m_\chi}{100\ {\rm GeV}}\right)\left(\frac{10^{-7}{\rm GeV}^{-2}}{\langle\sigma v\rangle}\right),\end{aligned} \tag{6.61}$$

where $c_i$ stands for the exponents associated with $\psi_{3/2}$ or $\chi_{S1}$ and assumes the values $c_{\psi_{3/2}} = 3$ or $c_{\chi_{S1}} = 5$. The parameters $\varepsilon^i$ respect the equations

$$3.33 \times 10^{-16}\left(\alpha_h^{1/2}\varepsilon_M^{\psi_{3/2}}\right)^{-3} = 1\ , \tag{6.62}$$

$$7.25 \times 10^{-8}\left(\alpha_h^{1/2}\varepsilon_M^{\chi_{S1}}\right)^{-5} = 1\ . \tag{6.63}$$

The curves labelled as $n_{3/2}$ and $n_{\chi_{S1}}$ in figures 6.5 and 6.6, when all the constraints are considered, separate the regions of validity of equations (6.48) and (6.49) or equation (6.61). Each region represents different processes for dark matter production. Moreover, with the use of $g_\eta = 100$, $m_\chi = 100$ GeV and $\langle\sigma_{\rm ann}v_{\rm M\o l}\rangle = 10^{-7}{\rm GeV}^{-2}$, we obtain the curves $\Omega^i_\chi h^2_{\rm d} = 0.12$ in terms of the parameters $h$ and $M$ for processes considering possible annihilations of neutralinos, i.e., those for which equation (6.61) should be satisfied. Notice that we also replaced $m_{3/2}$ by its function depending on both $h$ and $M$ via equation (5.26). We plot the curves $\Omega^i_\chi h^2_{\rm d} = 0.12$ for processes with annihilation of neutralinos in figures 6.5 and 6.6 when all the constraints are considered — they are labelled as $\rm DM^{3/2}_{ann}$ and $\rm DM^{\chi_{S1}}_{ann}$ and the arrows there indicate the allowed regions for acceptable dark matter relic density satisfying $\Omega^i_\chi h^2_{\rm d} \lesssim 0.12$.

Recalling the third point in section 6.2.1, we now discuss how to make both the gravitinos $\psi_{3/2}$ and the ISS fermions $\chi_{S1}$ decay after neutralino freeze-out. To do so, let us consider the fact that there are four types of neutralinos, namely Winos, Binos and two neutral Higgsinos. Wino pairs annihilate into $W^\pm$ pairs through the mediation of charged Winos[10]. Bino pairs annihilate into

[10] We disregard coannihilations. If one does consider them, they end up increasing $\langle\sigma_{\rm ann}v_{\rm M\o l}\rangle$ — though not

lepton pairs via right-handed slepton mediation[11]. Finally, Higgsinos pairs annihilate mainly into $W^{\pm}$ and $Z$ pairs. These possess the thermally averaged annihilation cross sections[12]

$$\langle \sigma_{\rm ann} v_{\rm M\o l} \rangle_{\rm Wino} \simeq \frac{g_2^4}{2\pi} \frac{1}{m_\chi^2} \frac{\left(1 - x_W^2\right)^{3/2}}{\left(2 - x_W^2\right)^2} \overset{m_\chi = 100\ \rm GeV}{\longrightarrow} 3.33 \times 10^{-7} \rm GeV^{-2} \,, \tag{6.64}$$

$$\langle \sigma_{\rm ann} v_{\rm M\o l} \rangle_{\rm Bino} \simeq \frac{g_1^4}{16\pi} \frac{1}{m_\chi^2} \left(\frac{6 T_\chi}{m_\chi}\right) \overset{m_\chi = 100\ \rm GeV}{\longrightarrow} 1.79 \times 10^{-9}\, T_\chi\ \rm GeV^{-3} \,, \tag{6.65}$$

$$\langle \sigma_{\rm ann} v_{\rm M\o l} \rangle_{\rm Higgsino} \simeq \frac{g_2^4}{32\pi} \frac{1}{m_\chi^2} \frac{\left(1 - x_W^2\right)^{3/2}}{\left(2 - x_W^2\right)^2} \overset{m_\chi = 100\ \rm GeV}{\longrightarrow} 2.08 \times 10^{-8}\ \rm GeV^{-2} \,, \tag{6.66}$$

where $x_W \equiv m_W / m_\chi$, and $g_1$ and $g_2$ are the couplings of the $U(1)_Y$ and $SU(2)_L$.

For the thermal cross sections of the Wino, Bino and Higgsinos, we know that they freeze-out at the values $T_\chi^f \simeq (3.69, 4.27, 4.10)$ GeV, respectively [298]. With a typical reference value $\langle \sigma_{\rm ann} v_{\rm M\o l} \rangle = 10^{-7}\ \rm GeV^{-2}$, one finds $T_\chi^f = 3.86$ GeV. Therefore, for both $\psi_{3/2}$ and $\chi_{S1}$ to decay after the neutralino freeze-out, $M$ must assume the values, respectively[13],

$$M \lesssim 2.56 \times 10^{-5} h^{-1/2} M_{\rm P} \,, \tag{6.67}$$

$$M \lesssim 9.12 \times 10^{-3} h^{-1/2} M_{\rm P} \,. \tag{6.68}$$

These two constraints for $\psi_{3/2}$ and $\chi_{S1}$ to decay after neutralino freeze-out, together with the bounds from equations (6.52) and (6.53) for $\psi_{3/2}$ and $\chi_{S1}$ to decay before BBN, form a range in which the particle decay is non-negligible and safe. They are given by yellow bands in the figures of this section.

In table 6.3 we collect all constraints on the parameter space obtained in section 6.1 and in the current section. We take them into account for the figures we present momentarily in this section.

In figures 6.5 and 6.6, we draw the following curves:

- $\rm DM_{dec}^{3/2}$ and $\rm DM_{dec}^{\chi_{S1}}$ when $\Omega_\chi^i h_d^2 = 0.12$ without further annihilations of neutralinos, obtained from equations (6.48) and (6.49) — these are represented by black solid lines;

- $\rm DM_{ann}^{3/2}$ and $\rm DM_{ann}^{\chi_{S1}}$ when $\Omega_\chi^i h_d^2 = 0.12$ with further annihilations of neutralinos, obtained from equation (6.61) — these are represented by green solid lines;

necessarily for Winos —, which in turn decreases their relic density.

[11] We defined the right-handed slepton mass $m_{\tilde{l}_R}$ to be equal to $m_\chi$. Considering a greater $m_{\tilde{l}_R}$ decreases its $\langle \sigma_{\rm ann} v_{\rm M\o l} \rangle$, which in turn increases its relic density.

[12] The Wino thermal cross section can be found from anomaly mediated SUSY breaking [296], while the Bino and the Higgsinos cross sections have been given in [297].

[13] These results come from $\rho_\eta^r(R_{{\rm d}\psi_{3/2}} \text{ or } R_{{\rm d}\chi_{S1}}) = \frac{\pi}{30} g_\eta (T_\chi^f)^4$. One should replace the left-hand side by either $\rho_\eta \left(R_{{\rm d}\eta} / R_{{\rm d}\psi_{3/2}}\right)^4$ or $\rho_\eta \left(R_{{\rm d}\eta} / R_{{\rm d}\psi_{\chi_{S1}}}\right)^4$, and the $M$ dependence will show up once we replace $R_{{\rm d}\eta}/R_{{\rm d}\psi_{3/2}} \propto (\Gamma^{3/2}/\Gamma_\eta)^{1/2}$ or, similarly, $R_{{\rm d}\eta}/R_{{\rm d}\chi_{S1}} \propto (\Gamma^{\chi_{S1}}/\Gamma_\eta)^{1/2}$.

| | Constraint | Meaning | Legend |
|---|---|---|---|
| Fig. 6.4 | Numerical and $M < 4.80 \times 10^{-2} h M_{\rm P}$ | $s_\eta > s_{\phi_{\rm ISS}}$ and $\rho_\eta > \rho_{\phi_{\rm ISS}}$ | blue shaded region |
| Eq. (6.52) and eq. (6.67) | $M \gtrsim 3.82 \times 10^{-6} h^{-1/2} M_{\rm P}$ and $M \lesssim 2.56 \times 10^{-5} h^{-1/2} M_{\rm P}$ | $\psi_{3/2}$ decays before BBN and $\psi_{3/2}$ decays after neutralino freezeout | lower yellow band |
| Eq. (6.53) and eq. (6.68) | $M \gtrsim 1.75 \times 10^{-3} h^{-1/2} M_{\rm P}$ and $M \lesssim 9.12 \times 10^{-3} h^{-1/2} M_{\rm P}$ | $\chi_{S1}$ decays before BBN and $\chi_{S1}$ decays after neutralino freezeout | upper yellow band |

Table 6.3: All constraints on the ISS parameters $M$ and $h$. Their location in the text, their meaning, and their depiction in the figures of this section are also given. Notice that the blue shaded region enlarges for the figures corresponding to $\chi_{S1}$, when the entropy production from $\psi_{3/2}$ should not be considered, so that the red curve obtained in section 6.1 must be replaced by the orange curve labelled *entropy w/o* $\psi_{3/2}$.

- $n_{3/2}$ and $n_{\chi_{S1}}$ separating the parameter space into a region where the neutralinos do and do not annihilate. Above $n_{3/2}$ and $n_{\chi_{S1}}$ we should consider $\mathrm{DM}^{3/2}_{\rm ann}$ and $\mathrm{DM}^{\chi_{S1}}_{\rm ann}$, respectively, whereas below $n_{3/2}$ and $n_{\chi_{S1}}$ we should consider $\mathrm{DM}^{3/2}_{\rm dec}$ and $\mathrm{DM}^{\chi_{S1}}_{\rm dec}$, respectively. These are represented by blue dashed lines.

Apart from these curves, we also depict the constraints summarized in table 6.3, some of which must be taken into account for avoiding cosmological issues such as the gravitino or the moduli problems. In figure 6.5 we adopt $\langle \sigma_{\rm ann} v_{\rm M\o l} \rangle = 10^{-7} \mathrm{GeV}^{-2}$, and in figure 6.6 we adopt a lower thermal cross section for annihilations of the neutralinos given by $\langle \sigma_{\rm ann} v_{\rm M\o l} \rangle = 10^{-10} \mathrm{GeV}^{-2}$ for comparison. The upper plots in both figures are for $\chi_{S1}$ and the lower plots in both figures are for $\psi_{3/2}$.

First of all, notice that when the blue region and the yellow bands intersect they yield a *green region*, which highlights the allowed parameter region for acceptable dark matter production. Notice that the yellow band for $\chi_{S1}$ does not appear separately from the green region, but is essentially hidden behind the green region. For $\psi_{3/2}$ one can still see part of its yellow band because the red curve which applies for $\psi_{3/2}$ is more constrained than the orange curve for $\chi_{S1}$.

Let us start by discussing the meaning of the *yellow bands*. They stand for the region where $\psi_{3/2}$ or $\chi_{S1}$ decay before BBN and after neutralino freeze-out. While the former condition must be respected, the latter is somewhat a weaker condition, since its violation does not pose problems to cosmological evolution. In fact, if $\psi_{3/2}$ or $\chi_{S1}$ decays before neutralino freeze-out, the neutralino relic density is given by standard thermal production. Notice that the yellow band for $\psi_{3/2}$ is located well below the yellow band for $\chi_{S1}$, therefore in a region where $\chi_{S1}$ decays after BBN. Since $\chi_{S1}$ decaying after BBN could dilute the BBN products, sufficient dark matter production from $\psi_{3/2}$ decays can never be achieved. Inverting the perspective, the yellow band for $\chi_{S1}$ is located well above the yellow band for $\psi_{3/2}$ in a region where $\psi_{3/2}$ decays before neutralino freeze-out, thereby neutralino production from $\psi_{3/2}$ decays is negligible. This implies that we should replace the red curve, which considers the entropy production from decays of $\psi_{3/2}$, by a curve without this contribution. This is the orange curve labelled by *entropy w/o* $\psi_{3/2}$ in the upper plots for $a_\eta = 10^{-1}$. A similar curve would also appear in the figure for $\chi_{S1}$

at $a_\eta = 10^{-3}$, however it shows up at even larger values of $M/M_{\rm P}$ and lower values of $h$ and is therefore beyond the bounds of the figure.

Now that there is an allowed parameter region in green from the constraints in table 6.3, let us see how the curves $\mathrm{DM}^{3/2}_{\rm dec}$, $\mathrm{DM}^{\chi_{S1}}_{\rm dec}$, $\mathrm{DM}^{3/2}_{\rm ann}$, $\mathrm{DM}^{\chi_{S1}}_{\rm ann}$, $n_{3/2}$ and $n_{\chi_{S1}}$ enter into this discussion.

As already stated, in the region above $n_{3/2}$ and $n_{\chi_{S1}}$, we should consider processes from ISS fields decay followed by annihilation of their products, i.e., the green lines $\mathrm{DM}^{3/2}_{\rm ann}$ and $\mathrm{DM}^{\chi_{S1}}_{\rm ann}$, respectively. In the region below $n_{3/2}$ and $n_{\chi_{S1}}$, we should consider processes without further annihilation but from ISS decays only, i.e., the black lines $\mathrm{DM}^{3/2}_{\rm dec}$ and $\mathrm{DM}^{\chi_{S1}}_{\rm dec}$, respectively. Once the region of validity is selected from $n_{3/2}$ and $n_{\chi_{S1}}$, we should further look into the arrows for the selected DM curves, which single out the *dark green regions* where an acceptable dark matter relic density of $\Omega^i_\chi h^2_{\rm d} \leq 0.12$ is possible. Notice that we hatch differently the regions where $\Omega_\chi h^2_{\rm d} \leq 0.12$ can be achieved from either the first or the second type of processes. In the first case we use diagonal lines inclined to the right and in the second case we use diagonal lines inclined to the left.

Summarizing our results, we find that a correct dark matter relic density of $\Omega_\chi h^2_{\rm d} \leq 0.12$ from non-thermal processes can be obtained in the following cases:

- from decays of $\chi_{S1}$ for both $a_\eta = 10^{-3}$ and $a_\eta = 10^{-1}$, for a thermal cross section $\langle \sigma_{\rm ann} v_{\rm Møl} \rangle = 10^{-7}\mathrm{GeV}^{-2}$;
- from decays of $\chi_{S1}$ followed by annihilations for both $a_\eta = 10^{-3}$ and $a_\eta = 10^{-1}$, for a thermal cross section $\langle \sigma_{\rm ann} v_{\rm Møl} \rangle = 10^{-7}\mathrm{GeV}^{-2}$.
- from decays of $\chi_{S1}$ for both $a_\eta = 10^{-3}$ and $a_\eta = 10^{-1}$, for a thermal cross section $\langle \sigma_{\rm ann} v_{\rm Møl} \rangle = 10^{-10}\mathrm{GeV}^{-2}$;

In the first case, the allowed region for $a_\eta = 10^{-3}$ is below the blue line of $n_{\chi_{S1}}$ and below the black lines. For $a_\eta = 10^{-1}$, this region is below the blue line of $n_{\chi_{S1}}$, below the upper black line and above the middle black line.

In the second case, the allowed region for $a_\eta = 10^{-3}$ is above the blue line of $n_{\chi_{S1}}$ and above the green line. For $a_\eta = 10^{-1}$, this region is above the blue line of $n_{\chi_{S1}}$ and above the green line.

In the third case, the allowed region for $a_\eta = 10^{-3}$ is below the blue line of $n_{\chi_{S1}}$ and below the black lines. For $a_\eta = 10^{-1}$, this regions is below the blue line of $n_{\chi_{S1}}$ and below the upper black line and on/above the middle black line.

Notice that, if we consider the two lower plots alone, we could have dark matter production from $\psi_{3/2}$ decays either followed by annihilations or not. These happen because parts of the black and green lines and their corresponding arrows are within the allowed green shaded region. However, we recall that this green region is below the yellow band for $\chi_{S1}$, for which it would decay after BBN. Since this can pose issues for BBN, we neglect production of dark matter from $\psi_{3/2}$ decays and subsequent annihilations and we, therefore, do not hatch any dark green region as done for the upper plots considering $\chi_{S1}$.

Along with non-thermal production of neutralinos, it remains to discuss their thermal production from freeze-out. The contributions, due to purely thermal neutralino freeze-out from the $\eta$

plasma, assumes the values for Wino, Bino and Higgsino [298, 299]

$$\Omega_{\text{Wino}}^{\text{freeze-out}} h_{\text{d}}^2 \simeq 7.03 \times 10^{-4} , \tag{6.69}$$

$$\Omega_{\text{Bino}}^{\text{freeze-out}} h_{\text{d}}^2 \simeq 0.0261 , \tag{6.70}$$

$$\Omega_{\text{Higgsino}}^{\text{freeze-out}} h_{\text{d}}^2 \simeq 0.010 . \tag{6.71}$$

For $m_\chi = 100$ GeV, each of the Bino and Higgsino relic densities yields $\sim 10\%$ of the required $\Omega_{\text{CDM}} h_{\text{d}}^2 \simeq 0.12$. Therefore, in these cases, in order to obtain $\Omega_\chi h_{\text{d}}^2 \simeq 0.12$ for $m_\chi = 100$ GeV, one has to consider $(h, M)$ points that are slightly off the black and green lines such that $\Omega_\chi^{\chi_{S1}} h_{\text{d}}^2 \sim 0.9 \cdot \Omega_{\text{CDM}} h_{\text{d}}^2$. In the end, summing up both non-thermal processes and thermal processes from freeze-out must lead to $\Omega_\chi^{\text{freeze-out}} h_{\text{d}}^2 + \Omega_\chi^{\chi_{S1}} h_{\text{d}}^2 \simeq \Omega_{\text{CDM}} h_{\text{d}}^2$.

For the case when $\chi_{S1}$ decays above its green band, all dark matter density should come from its thermal freeze-out, i.e., $\Omega_\chi^{\text{freeze-out}} h_{\text{d}}^2 \simeq 0.12$. This can be accomplished considering for example a Bino LSP with a right handed slepton mass $m_{\tilde{l}_R} \simeq 220$ GeV if we take $m_{\tilde{l}_R} = m_\chi$.

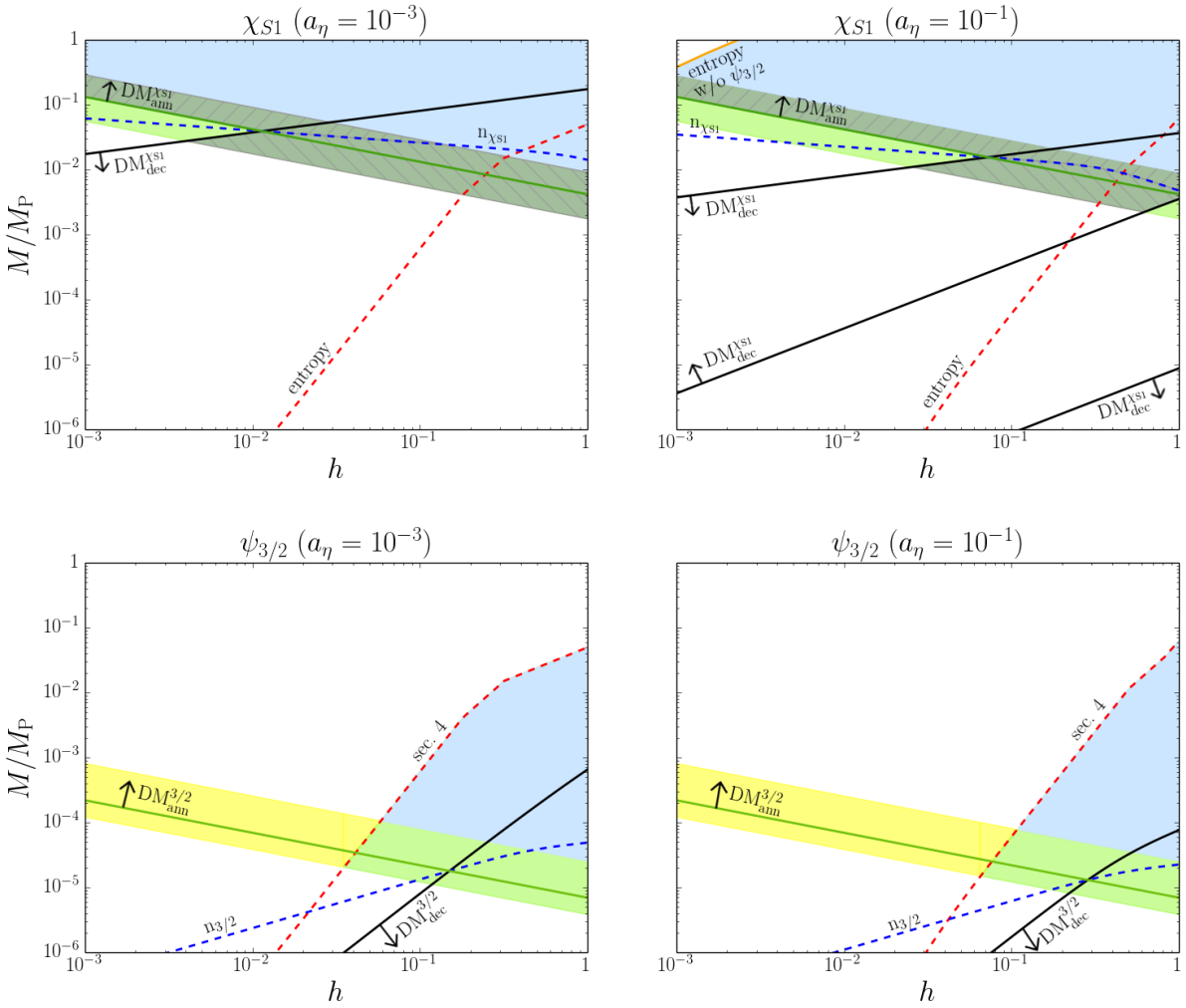


Figure 6.5: All constraints on the ISS parameters $M$ and $h$ for dark matter production from either direct decays $DM_{dec}$ or decays followed by annihilations $DM_{ann}$ for $\chi_{S1}$ and $\psi_{3/2}$. A thermal cross section $\langle \sigma_{ann} v_{M\text{øl}} \rangle = 10^{-7}\text{GeV}^{-2}$ and a small (large) coupling $a_\eta = 10^{-3}$ ($a_\eta = 10^{-1}$) are used. The arrows for the green and black lines point in the directions where $\Omega_\chi h_d^2 < 0.12$. The dark green regions highlight the areas where $\Omega_\chi h_d^2 \leq 0.12$ for decays before BBN, thereby not posing any cosmological issues.

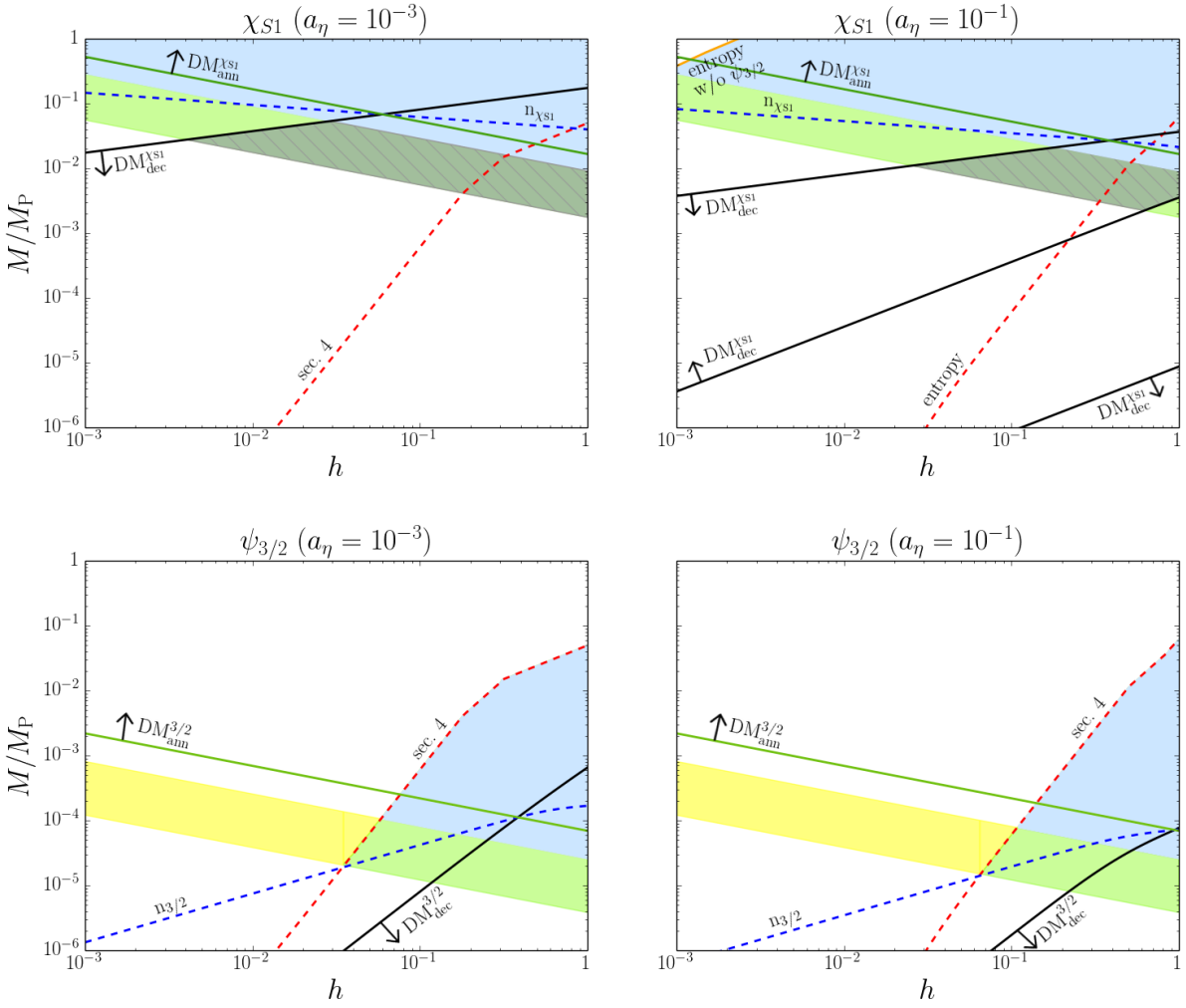


Figure 6.6: The same as in figure 6.5 for a thermal cross section $\langle \sigma_{\text{ann}} v_{\text{Møl}} \rangle = 10^{-10}\text{GeV}^{-2}$.

CHAPTER 7

# Conclusions and Outlook

In this thesis we studied effective actions in the general context of compactifications of higher-dimensional string/M-theory with a two-fold perspective. In the first part we adopted a more formal approach to obtain an $\mathcal{N} = 1$ effective supergravity description from compactifications of M-theory on $G_2$-manifolds. In the second part, we adopted a more phenomenological approach, in which we already start with an $\mathcal{N} = 1$ effective supergravity theory from compactifications of type IIB on orientifold Calabi–Yau threefolds, and analyse the viability of obtaining neutralino dark matter candidates in a combined framework with the MSSM and an F-term SUSY breaking sector, the latter responsible for uplifting the AdS supergravity vacuum.

In the first part we delved into the mathematical machinery of general $G_2$-manifolds and, especially, of the Kovalev's twisted connected sum type, built from suitably gluing together a pair of non-compact asymptotically cylindrical Calabi–Yau threefolds $X_{L/R}$ in their asymptotic regions. There were for a long time only about a hundred examples for compact $G_2$-manifolds from resolutions of special orbifolds of the seven-dimensional torus. The importance of Kovalev's construction is that it realizes a large class of about $O(10^8 n_g)$ compact $G_2$-manifolds [141, 234, 254], where $n_g \geq 1$ is the multiplicity due to the possible gluings. Our identification of the Kovalev limit, in which the $G_2$-metric was approximated in terms of the metrics of the constituents of this construction, allowed for the identification of two neutral universal $\mathcal{N} = 1$ chiral moduli fields associated to a complexified overall volume modulus $\nu$ and a gluing modulus — called the Kovalevton $\varkappa$. The latter parametrizes the Kovalev limit via $\mathrm{Re}(\varkappa) \to \infty$. Furthermore, this limit allowed for a decomposition of the fields of the $\mathcal{N} = 1$ effective supergravity theory into $\mathcal{N} = 1$ neutral chiral moduli multiplets, into two $\mathcal{N} = 2$ gauge theory sectors coming from the two asymptotic regions $Y_{L/R}$, and into one $\mathcal{N} = 4$ gauge sector that comes from the trivial K3 fibration with fibre $S$ in the gluing region $T^2 \times S \times (0, 1)$, cf. table 3.2.

This decomposition becomes exact in a controllable way in the Kovalev limit, and yields a scheme in which the four-dimensional low-energy effective theory can be approximated in terms of these sectors with small corrections. In particular, we worked out the dependence of the effective action on these two universal chiral moduli fields, and obtained a phenomenologically motivated Kähler potential with an intrinsic no-scale structure — therefore, with a non-AdS

supergravity vacuum. Moreover, the two scales thus obtained also control the behavior of M-theory corrections.

Due to this decomposition, we could identify Abelian and non-Abelian gauge theory sectors with various matter content, arising from singularities in the asymptotic cylindrical Calabi–Yau threefolds $X_{L/R}$ in codimension four and six that occur in the twisted connected sum $Y$ away from the gluing region. These led to transitions in the threefolds $X_{L/R}$, whose deformations and resolutions can be described by methods of algebraic geometry familiar in the context of $\mathcal{N} = 2$ theories. These transitions commute with the Kovalev limit and the gluing construction and, therefore, connect $G_2$-manifolds whose change in the cohomology groups corresponds exactly to the change in the spectrum of $\mathcal{N} = 1$ vector and chiral superfields as predicted by the geometrical transitions. This suggests that, in a suitably compactified moduli space of the Ricci-flat $G_2$-metrics, there are many new types of singular loci through which it is possible to reach topological inequivalent $G_2$-manifolds.

Another interesting physical consequence of the decomposition and the Kovalev limit is that the more advanced $\mathcal{N} = 2$ techniques — for example, computations of exact gauge couplings and exact BPS masses from the periods of the holomorphic three-form — serve as a zeroth order approximation with inverse power laws or exponential corrections in the Kovalevton $\varkappa$ and the volume modulus $\nu$, similarly as the calculations carried out in the context of local $G_2$-manifolds [243, 244]. Those corrections leading to holomorphic terms in the four-dimensional $\mathcal{N} = 1$ effective theory are expected to be accessible by techniques similar to the ones used to calculate four-dimensional $\mathcal{N} = 1$ F-terms in flux and/or brane compactifications of type II theories.

An attractive feature of the twisted connected sum compactification is that we have algebraic methods to geometrically engineer gauge groups, spectra and interactions in the two individual $\mathcal{N} = 2$ gauge theory sectors from $X_{L/R}$. The examples presented in table 4.9 yield small rank gauge groups such as the Standard Model group and possible Grand Unification scenarios. The matter content could in principle be broken into phenomenologically more suitable massless $\mathcal{N} = 1$ chiral matter multiplets. In fact, the computed $\mathcal{N} = 2$ spectra can be broken to $\mathcal{N} = 1$ multiplets by various non-local effects, for example via the introduction of a flux-induced superpotential (3.70), which also potentially introduces chirality [231]. Due to the absence of tadpole constraints for four-form fluxes on $G_2$-manifolds, the local scenario for fluxes in type II string theories proposed in reference [300] is readily realized on the level of the non-compact asymptotically cylindrical Calabi–Yaus $X_{L/R}$. We expect that non-trivial background four-form fluxes provides for a much more intricate and genuine $\mathcal{N} = 1$ gauge theory branch structure, similarly as in references [257, 301]. All these effects would come with different scales — partially exponentially suppressed — which exhibit potentially attractive hierarchies. While in type II Calabi–Yau threefold compactifications we arrive at four-dimensional $\mathcal{N} = 2$ effective supergravity theories with two massless gravitinos realizing extended supersymmetry, breaking the $\mathcal{N} = 2$ gravity multiplet down to the $\mathcal{N} = 1$ is rather non-trivial, see for instance the discussion in reference [302]. In our case, however, the obtained four-dimensional supergravity theory has already minimal supersymmetry. It is only the gauge theory sectors in the Kovalev limit that approximately exhibit extended global supersymmetries. Therefore, introducing background fluxes to break supersymmetry in the gauge theory sectors is much simpler than in the type II Calabi–Yau threefold compactifications. In particular, turning on background fluxes

resembles to a great extent the type II scenario of reference [300], in which, however, gravity is decoupled.

Let us point out a further potentially phenomenologically attractive possibility. The separation of the two sectors $X_L$ and $X_R$ in figure 2.1 is controlled by the real part of the Kovalevton $\kappa$. Together with the local construction of the spectra on $X_{L/R}$ described in chapter 4, this offers the possibility to consider a hidden and a visible sector and to employ the mechanism of mediation of supersymmetry breaking only in the gravitational sector with a controllable scale set by Kovalevton $\kappa$. Or alternatively, as there is an anomaly inflow mechanism in the local theories [253, 240], one could use the anomaly mediation of supersymmetry breaking as proposed in [303].

Finally, we comment on the possible relation of the twisted connected sum construction to other non-perturbative descriptions of $\mathcal{N} = 1$ theories. In lower dimensions, the algebraic-geometrical approach towards the Hořava–Witten setup describes a duality with F-theory [304]. Namely, certain Calabi–Yau compactifications of the heterotic string are dual to F-theory on elliptically fibered Calabi–Yau fourfolds in a particular stable degeneration limit [305]. To obtain four-dimensional $\mathcal{N} = 1$ supergravity theory, this heterotic/F-theory correspondence is realized on the level of elliptically-fibered Calabi–Yau fourfolds. It is intriguing to observe that such Calabi–Yau fourfolds in the stable degeneration limit are obtained by gluing a pair of suitably chosen Fano fourfolds along their mutual anti-canonical Calabi–Yau threefold divisor [306, 307]. This construction of Calabi–Yau fourfolds in the stable degeneration limit shows a resemblance — yet in one real dimension higher — to twisted connected sum $G_2$-manifolds in the Kovalev limit. It would be interesting to see if such a speculation could be made precise, namely establishing a duality between M-theory on $G_2$-manifolds in the Kovalev limit and F-theory on elliptically-fibered Calabi–Yau fourfolds in a certain degeneration limit.

In the second part of this thesis we investigated the emergence of dark matter candidates from effective actions. Here we already started with a four-dimensional effective action motivated from F-theory/type IIB string theory on Calabi-Yau manifolds. More specifically, we analyzed the production of dark matter neutralino candidates (Wino, Bino, and Higgsino) within a setup mixing the Minimal Supersymmetric Standard Model (MSSM) with the KL moduli stabilization scenario. The vacuum in the KL scenario is uplifted via the so-called ISS sector, which is based on the free magnetic dual of $\mathcal{N} = 1$ supersymmetric QCD.

We performed a careful analysis of the interactions between the KL-ISS and the MSSM sectors. We found that the largest decay rates are related to decays of the ISS fields to gravitinos via $(Q_1, Q_2, S_2) \to \psi_{3/2} + \psi_{3/2}$, to $\chi_{S1}$ pairs via $S_1 \to \bar{\chi}_{S1} + \chi_{S1}$, and to three ISS fields via $Q_1 \to \bar{\chi}_{S1} + \chi_{S1} + \mathrm{Re}Q_2$ and $Q_1 \to \bar{\chi}_{S1} + \chi_{S1} + \mathrm{Im}Q_2$, and $Q_2 \to \bar{\chi}_{S1} + \chi_{S1} + \mathrm{Im}Q_2$.

A detailed study of oscillations from the inflaton $\eta$ and the ISS fields was then performed, and we discussed the epochs of the decays of the inflaton $\eta$ and these ISS fields. We obtain constraints on the parameter space of the model by requiring the entropy density of the inflaton to dominate over that of the ISS fields. This enables mainstream baryogenesis mechanisms to work, besides avoiding possible dilution of Big-Bang nucleosynthesis products. In this calculation, we also take into account the possible non-relativistic behaviour of the final products from ISS decays.

Finally, we tackled the production of neutralino dark matter. We provided expressions for

dark matter production via thermal gravitino production, or via a mixture of thermal production from neutralino freeze-out and decays of products from ISS decays, followed by annihilations or not. We set these expressions against the constraints for negligible entropy production, as well as constraints on the decay epochs of $\psi_{3/2}$ and $\chi_{S1}$. The parameter space can accomodate an acceptable dark matter relic density compatible with observations. While the gravitino could generate enough neutralinos, the constraint that the ISS fermion $\chi_{S1}$ must decay before BBN forbids this solution. For $\chi_{S1}$, sufficient dark matter can be generated, either through direct decays of $\chi_{S1}$ or through their subsequent annihilation. We concluded that, for $m_\chi = 100$ GeV, the standard thermal scenario yields at most 10% of the required dark matter relic density, while the non-thermal scenario can provide the remaining 90% dark matter content, in a consistent framework without moduli and gravitino problems.

APPENDIX A

# Higher dimensional gamma matrices

In this appendix we spell out definitions and properties of the eleven-, seven- and four-dimensional gamma matrices, following reference [138]. The eleven-dimensional gamma matrices are represented by 32-dimensional matrices, which satisfy the usual Clifford algebra

$$\{\hat{\Gamma}_M, \hat{\Gamma}_N\} = 2g_{MN} \,, \tag{A.1}$$

with the eleven-dimensional Lorentzian metric $g_{MN}$. Furthermore, in the chosen 32-dimensional Majorana representation, the gamma matrices obey

$$\hat{\Gamma}_0 \cdots \hat{\Gamma}_{10} = \mathbb{I} \,, \tag{A.2}$$

in terms of the 32-dimesional identity matrix $\mathbb{I}$. With the compactification ansatz $M^{1,10} = \mathbb{R}^{1,3} \times Y$, the eleven-dimensional gamma matrices split into two sets of commuting gamma matrices,

$$\hat{\Gamma}_M = (\hat{\Gamma}_\mu, \hat{\Gamma}_m) \,, \quad \hat{\Gamma}_\mu = \gamma_\mu \otimes \mathbb{I} \,, \quad \hat{\Gamma}_m = \gamma \otimes \gamma_m \,, \tag{A.3}$$

where $\mathbb{I}$ is the seven-dimensional identity matrix, $\gamma_\mu$, $\mu = 0, 1, 2, 3$, are the four-dimensional imaginary gamma matrices, $\gamma_m$, $m = 4, \ldots, 10$, are purely imaginary seven-dimensional gamma matrices satisfying $\gamma_4 \cdots \gamma_{10} = i$. Furthermore, we define $\gamma = (i/4!)\epsilon_{\mu\nu\rho\sigma}\gamma^\mu\gamma^\nu\gamma^\rho\gamma^\sigma$ as the four-dimensional chirality matrix, which is purely imaginary and satisfies $\gamma^2 = 1$.

The four- and seven-dimensional gamma matrices satisfy the Clifford algebra in their corresponding dimensions

$$\{\gamma_\mu, \gamma_\nu\} = 2\eta_{\mu\nu} \,, \qquad \{\gamma_m, \gamma_n\} = 2g_{mn} \,. \tag{A.4}$$

Here we use the Minkowski metric $\eta_{\mu\nu}$ with signature $(-1, +1, +1, +1)$ and $g_{mn}$ denotes the Riemannian metric of the seven-dimensional compactification space $Y$.

We define the anti-symmetrized product of eleven-dimensional gamma matrices as

$$\hat{\Gamma}^{M_1 \cdots M_n} = \hat{\Gamma}^{[M_1} \cdots \hat{\Gamma}^{M_n]} \,, \tag{A.5}$$

and we use the same notation for the anti-symmetrized products of four- and seven-dimensional

gamma matrices, i.e., $\gamma^{\mu_1\cdots\mu_n} = \gamma^{[\mu_1}\cdots\gamma^{\mu_n]}$ and $\gamma^{m_1\cdots m_n} = \gamma^{[m_1}\cdots\gamma^{m_n]}$. For the decomposition of $\hat{\Gamma}^{MNP}$ into lower-dimensional gamma matrices we arrive at the useful relation

$$\begin{aligned}\hat{\Gamma}^{MNP} &= (\gamma^{\mu\nu\rho}\otimes\mathbb{I}) + (\gamma^{\mu\nu-}\otimes\gamma^{p}) + (\gamma^{\mu-\rho}\otimes\gamma^{n}) + (\gamma^{-\nu\rho}\otimes\gamma^{m}) \\ &\quad +\frac{1}{3}(\gamma^{\rho}\otimes\gamma^{mn} + \gamma^{\nu}\otimes\gamma^{pm} + \gamma^{\mu}\otimes\gamma^{np}) \\ &\quad +\gamma\otimes\gamma^{mnp}\,,\end{aligned} \tag{A.6}$$

where the index '$-$' refers to the four-dimensional chirality matrix $\gamma$.

For the zero mode analysis we record here a few useful identities among products of anti-symmetrized gamma matrices

$$\begin{aligned}\gamma^{mnp}\gamma^{q} &= \gamma^{mnpq} + 3g^{q[m}\gamma^{np]}\,, \\ \gamma^{mnp}\gamma^{qr} &= \gamma^{mnpqr} + 3\left(g^{q[m}\gamma^{np]r} - g^{r[m}\gamma^{np]q}\right) + 6g^{q[m}\gamma^{n}g^{p]r}\,.\end{aligned} \tag{A.7}$$

# APPENDIX B

# Relevant decay rates

Here we present the interaction terms associated with the largest decay rates that appear in section 5.5.2 and give their full result. As explained there, recall that only decays of ISS scalars turn out to be relevant. Furthermore, for irrelevant decay rates, we list here only their origin for completeness, referring the reader to the full publication [196] for the full results.

Instead of using the supergravity Lagrangian density that appears in [225], we chose to use the form in [53] — also found in [308, 309] — because it is expressed easily in terms of the combination $G = K + \ln\left(W\overline{W}\right)$, where the Kähler potential $K$ and the superpotential $W$ are given in equation (5.28) with respect to the whole KL-ISS-MSSM setup.

In the following, we use the indices

$$\begin{aligned} i, j, a, b &\quad \text{for ISS fields ,} \\ m, n, p, q, r, s &\quad \text{for MSSM fields ,} \\ \alpha, \beta &\quad \text{for both ISS and MSSM fields without distinction ,} \\ \mu, \nu, \rho, \sigma &\quad \text{for spacetime indices ,} \end{aligned} \tag{B.1}$$

and similarly for the same indices with an overbar for ISS and MSSM fields, e.g., $\bar{i}$, $\bar{m}$ and $\bar{\alpha}$. Recall that $\delta_{ij} = \mathrm{diag}(1, \ldots, 1)$ with $N_f$ entries. We further define

$$\delta'_{ij} = \mathrm{diag}(\underbrace{1, \ldots, 1}_{N}, \underbrace{0, \ldots, 0}_{N_f - N}) \,. \tag{B.2}$$

The couplings of the ISS fields to the MSSM fields are derived with the simplifications $K_m, W_m \ll 1$ for the MSSM fields. This can be done because the VEVs of the MSSM fields are either zero or at most of the weak scale.

- **Decays to MSSM gravitinos**

  Here we consider the interaction Lagrangian between the ISS scalars and the MSSM

gravitinos $\psi_\mu \equiv \psi_{3/2}$ [53, 308]

$$\mathcal{L}^{3/2}_{\phi_{\rm ISS}} = -\frac{i}{8}\epsilon^{\mu\nu\rho\sigma}\bar{\psi}_\mu\gamma_\nu\psi_\rho G_i D_\sigma \phi^i_{\rm ISS} + \frac{i}{2}e^{G/2}\bar{\psi}_{\mu L}\sigma^{\mu\nu}\psi_{\nu R} + \text{h.c.} \equiv X + Y\,, \tag{B.3}$$

where $\sigma^{\mu\nu} = \frac{i}{2}\left[\gamma^\mu, \gamma^\nu\right]$, and $\gamma^\mu$ are the usual four-dimensional gamma matrices. Working out the contributions from the $X$ terms in equation (B.3), we obtain

$$X_{S_{ij}} = \frac{i\left(\delta'_{ij} - \delta_{ij}\right)}{8M_{\rm P}}\sqrt{\frac{3}{N_f - N}}\epsilon^{\mu\nu\rho\sigma}\bar{\psi}_\mu\gamma_\nu\psi_\rho\partial_\sigma S_{ij}\,, \tag{B.4}$$

$$X_{(q_{ia},\tilde{q}_{ai})} \propto \left(\frac{M}{M_{\rm P}}\right)^3 \frac{i\delta_{ia}}{8M_{\rm P}}\epsilon^{\mu\nu\rho\sigma}\bar{\psi}_\mu\gamma_\nu\psi_\rho\partial_\sigma\left(q_{ia}, \tilde{q}_{ai}\right)\,, \tag{B.5}$$

where the term $O\left(M^3\right)$ stems from the function $G_{(q_{ia},\tilde{q}_{ai})} = \left(\frac{K_{(q_{ia},\tilde{q}_{ai})}}{M_{\rm P}^2} + \frac{W_{(q_{ia},\tilde{q}_{ai})}}{W}\right)M_{\rm P}$. Working out the contributions from the $Y$ terms in equation (B.3), we obtain

$$Y_{S_{ij}} = \frac{\left(\delta_{ij} - \delta'_{ij}\right)}{8}\sqrt{\frac{3}{N_f - N}}\frac{m_{3/2}}{M_{\rm P}}S_{ij}\bar{\psi}_\mu\left[\gamma^\mu, \gamma^\nu\right]\psi_\nu\,, \tag{B.6}$$

$$Y_{(q_{ia},\tilde{q}_{ai})} = \frac{\delta_{ia}}{8}\frac{m_{3/2}M}{M_{\rm P}^2}\left(q_{ia}, \tilde{q}_{ai}\right)\bar{\psi}_\mu\left[\gamma^\mu, \gamma^\nu\right]\psi_\nu\,. \tag{B.7}$$

Since both $X$ and $Y$ terms yield similar contributions, they both must be taken into account to obtain the decay rate for each of the particles. The largest decay rates are from $S_2$, $Q_1$ and $Q_3$, which are given by

$$\overline{\Gamma}^{2\psi_{3/2}}_{S_{2ij}} = \frac{5\left(\delta_{ij} - \delta'_{ij}\right)}{18\times 2^6\pi}\frac{3}{N_f - N}\left(\frac{3\left(\ln(4) - 1\right)N}{8\pi^2\left(N_f - N\right)}\right)^{5/2} h^5\frac{m^3_{3/2}}{M^2_{\rm P}}\left(\frac{M_{\rm P}}{M}\right)^5\,, \tag{B.8}$$

$$\overline{\Gamma}^{2\psi_{3/2}}_{Q_{1ia}} = \frac{\sqrt{2}\delta_{ia}}{9\times 2^4\pi}\left(\frac{3}{N_f - N}\right)^{5/2}\frac{m^3_{3/2}}{M^2_{\rm P}}\left(\frac{M_{\rm P}}{M}\right)^3\,, \tag{B.9}$$

$$\overline{\Gamma}^{2\psi_{3/2}}_{Q_{2ia}} = \frac{\delta_{ia}}{9\times 2^6\pi}\left(\frac{3\left(\ln(4) - 1\right)}{8\pi^2}\right)^{5/2} h^5\frac{m^3_{3/2}}{M^2_{\rm P}}\left(\frac{M_{\rm P}}{M}\right)^3\,. \tag{B.10}$$

- **Decays to ISS fermions**

  Here we consider the interaction Lagrangian between the ISS scalars and fermions. The decay rate for $S_1$ is calculated from $e^{G/2}\left(\frac{W_{ij}}{W}\right)\bar{\chi}^i_R\chi^j_L + \text{h.c.} \supset \sqrt{\frac{3}{N_f - N}}\frac{m_{3/2}}{hM^2}W_{ij}\bar{\chi}^i_R\chi^j_L + \text{h.c.}$, whereas the decay rates for $S_2$, $Q_1$ and $Q_2$ come fom $e^{G/2}\left(K_iK_j\right)\bar{\chi}^i_R\chi^j_L + \text{h.c.} \supset m_{3/2}K_iK_j\bar{\chi}^i_R\chi^j_L + \text{h.c.}$ . The largest decay rate is from $S_1 \to \chi_{S1} + \bar{\chi}_{S1}$, which is given by

$$\overline{\Gamma}\left(S_1 \to \chi_{S1} + \bar{\chi}_{S1}\right) = \frac{3\sqrt{3}}{4\sqrt{2}}\frac{1}{\pi}\frac{1}{\left(N_f - N\right)^{3/2}}\frac{m^3_{3/2}}{M^2_{\rm P}}\left(\frac{M_{\rm P}}{M}\right)^5\,, \tag{B.11}$$

where $\chi_{S1}$ is one of the ISS fermions given in table 5.2.

- **Decays to two ISS fermions and one ISS scalar**

  Here we consider the interaction Lagrangian between the ISS scalars with two ISS fermions and one ISS complex scalar. Two contributions for this kind of process can take place, namely the contribution from four-point vertices and the contribution with an intermediate fermion propagator. The largest decay rates are from decays of $Q_1$ and $Q_2$, with dominant contribution via fermion exchange. These are given by

$$\begin{aligned}\overline{\Gamma}(Q_1 \to \chi_{S1} + \bar{\chi}_{S1} + Q_2) &= \frac{27\sqrt{3}}{2^{15}\sqrt{2}}\frac{1}{\pi^3}\frac{1}{(N_f-N)^{5/2}}\frac{m_{3/2}^5}{M^9}M_{\rm P}^5 \\ &\simeq 5.09\times 10^{-10}\frac{1}{(N_f-N)^{3/2}}\frac{m_{3/2}^3 h^2}{M_{\rm P}^2}\left(\frac{M_{\rm P}}{M}\right)^5 ,\end{aligned} \tag{B.12}$$

$$\begin{aligned}\overline{\Gamma}(Q_2 \to \chi_{S1} + \bar{\chi}_{S1} + {\rm Im}Q_2) &= \frac{45\sqrt{3}}{2^{24}\sqrt{2}}\frac{[\ln(4)-1]^{3/2}}{\pi^6}\frac{1}{N_f-N}\frac{m_{3/2}^5 h^3}{M^9}M_{\rm P}^5 \\ &\simeq 2.57\times 10^{-14}\frac{m_{3/2}^3 h^5}{M_{\rm P}^2}\left(\frac{M_{\rm P}}{M}\right)^5 .\end{aligned} \tag{B.13}$$

  Here we use the notation $\overline{\Gamma}(Q_1 \to \chi_{S1} + \bar{\chi}_{S1} + Q_2)$ to denote the process with an ISS complex scalar $Q_2$ in the products. In other words, this notation denotes two decays, namely $\overline{\Gamma}(Q_1 \to \chi_{S1} + \bar{\chi}_{S1} + {\rm Re}Q_2)$ and $\overline{\Gamma}(Q_1 \to \chi_{S1} + \bar{\chi}_{S1} + {\rm Im}Q_2)$.

- **Other decays**

  The computation of the decay rates of the ISS scalars into fields other than the ones presented above are given in detail in the full publication [196]. Below we list their origin only.

  — Decays to MSSM scalars $\phi^m$: these originated from the Lagrangian

$$\mathcal{L}_{\phi_{\rm ISS}}^{\rm scalars} = G_{m\bar{n}} D_\mu \phi^m D^\mu \bar{\phi}^{\bar{n}} - e^G\left(G_\alpha G^{\alpha\bar{\beta}} G_{\bar{\beta}} - 3\right) . \tag{B.14}$$

  — Decays to MSSM fermions $\bar{\chi}^m$ and $\chi^n$: these originated from the Lagrangian

$$\begin{aligned}\mathcal{L}_{\phi_{\rm ISS}}^{\rm fermions} &= iG_{m\bar{n}}\bar{\chi}_R^m\gamma^\mu D_\mu \chi_R^n + \left(-G_{mi\bar{n}} + \frac{1}{2}G_{m\bar{n}}G_i\right)\bar{\chi}_R^m\gamma^\mu D_\mu \phi_{\rm ISS}^i \chi_R^{\bar{n}} \\ &\quad + e^{G/2}\left(-G_{mn} - G_m G_n + G_{mn\bar{i}}G^{j\bar{i}}G_j\right)\bar{\chi}_R^m \chi_L^n + {\rm h.c.} .\end{aligned} \tag{B.15}$$

  — Decays to two MSSM fermions $\bar{\chi}^m$ and $\chi^n$ and an MSSM scalar $\phi^p$: the effective

Lagrangian for this interaction is given by

$$\begin{aligned}\mathcal{L}_{\text{ISS}}^{2f+1s} &\simeq \left(\frac{1}{2}W_{mnp}\right)\left(\frac{i\gamma_\nu p^\nu_{\chi_m}+m_{\chi_m}}{\left(p^\nu_{\chi_m}\right)^2-m^2_{\chi_m}}\right)\left[\frac{1}{2}\left(\frac{K_{\phi_{\text{ISS}}}}{M_{\text{P}}}+M_{\text{P}}\frac{W_{\phi_{\text{ISS}}}}{W}\right)\gamma^\mu\right]\partial_\mu\phi_{\text{ISS}}\bar{\chi}_m\chi_n\phi_p \\ &\simeq \frac{i}{4}\left(\frac{K_{\phi_{\text{ISS}}}}{M_{\text{P}}}+M_{\text{P}}\frac{W_{\phi_{\text{ISS}}}}{W}\right)\left(W_{mnp}\right)\left(\frac{p^{\chi_m}_\nu}{\left(p^{\chi_m}_\nu\right)^2}\right)\gamma^\nu\gamma^\mu\partial_\mu\phi_{\text{ISS}}\bar{\chi}_m\chi_n\phi_p\ .\end{aligned} \tag{B.16}$$

— Decays to the MSSM gauge sector: it is possible for $\phi_{\text{ISS}}$ to decay into two gauge bosons $g$ or two gauginos $\tilde{g}$ at the quantum level due to anomaly effects [310]. The corresponding decay rate is given by

$$\Gamma\left(\phi_{\text{ISS}}\to gg,\tilde{g}\tilde{g}\right) \sim \frac{N_g\alpha_g^2}{2^8\pi^3}\frac{\left|K_{\phi_{\text{ISS}}}\right|^2 m^3_{\phi_{\text{ISS}}}}{M^4_{\text{P}}}\ , \tag{B.17}$$

where $N_g$ is the number of generators of the relevant gauge group and $\alpha_g$ is its corresponding fine structure constant.

— Decays to ISS scalars: the decay rates for $S_1$ are calculated from the Lagrangian term $e^G\left(K_{\bar{S}_{ij}}K_{S_{ij}}\right)\supset\frac{m^2_{3/2}}{h}W_{\phi_{\text{ISS}}}S_{ij}\delta'_{ij}$. For $S_2$, they stem from

$$e^G\left(K_{\bar{S}_{ij}}\frac{W_{S_{ij}}}{W}\right)\supset\frac{3}{N_f-N}\frac{m^2_{3/2}}{hM^2}W_{\phi_{\text{ISS}}}S_{ij}\left(\delta'_{ij}-\delta_{ij}\right)\ .$$

For $Q_i$, they are obtained from

$$e^G\left(K_{(\bar{q},\bar{\tilde{q}})_{ia}}K_{(q,\tilde{q})_{ia}}\right)\supset\sqrt{\frac{3}{N_f-N}}\frac{m^2_{3/2}}{hM}W_{\phi_{\text{ISS}}}q_{ia}\delta_{ia}\ .$$

# APPENDIX C

# Neutralino dark matter solution

In this appendix we show a possible solution to the neutralino relic densities presented in section 6.2.

For some specific values of the parameters $\alpha_h$, $\lambda_M$ and $\alpha_M$, these yield $f_{\psi_{3/2}}(\alpha_h, \alpha_M M_{\rm P}) = 1$ and $f_{\chi_{S1}}(\alpha_h, \lambda_M M_{\rm P}) = 1$, where the parameters satisfy the following relations

$$406.56\,\alpha_h^{-1}\alpha_M\left\{2.26\left[\frac{\Gamma_{Q_1}^{2\psi_{3/2}}}{\Gamma_{Q_1}^{\rm total}}+\frac{\Gamma_{Q_1}^{\chi\chi{\rm Re}Q_2}}{\Gamma_{Q_1}^{\rm total}}\frac{\Gamma_{Q_2}^{2\psi_{3/2}}}{\Gamma_{Q_2}^{\rm total}}\right]_{h=\alpha_h,\ M=\alpha_M M_{\rm P}}+5.72\times10^6\,\frac{\alpha_M^2}{\alpha_h^5}\right\}=1\,, \quad \text{(C.1)}$$

$$406.56\,\alpha_h^{-1}\lambda_M\left\{2.26\left[\frac{\Gamma_{Q_1}^{\chi\chi{\rm Re}Q_2}}{\Gamma_{Q_1}^{\rm total}}\left(\frac{\Gamma_{Q_2}^{2\psi_{3/2}}}{\Gamma_{Q_2}^{\rm total}}+2\frac{\Gamma_{Q_2}^{\chi\chi{\rm Im}Q_2}}{\Gamma_{Q_2}^{\rm total}}+1\right)\right]_{h=\alpha_h,\ M=\lambda_M M_{\rm P}}+0.56\,\lambda_M^2\right\}=1\,. \quad \text{(C.2)}$$

Numerically, for $\alpha_h = 10^{-2}$ we obtain $\alpha_M = 3.72\times10^{-8}$ and three possible solutions of $\lambda_M = \left(1.74\times10^{-2},\ 1.48\times10^{-6},\ 2.12\times10^{-6}\right)$. Also, for $\alpha_h = 1$, we obtain $\alpha_M = 1.99\times10^{-4}$ as well as three possible solutions of $\lambda_M = \left(8.05\times10^{-2},\ 1.48\times10^{-4},\ 2.12\times10^{-4}\right)$. Furthermore, one should use $h = \alpha_h$ and $M = (\alpha_M;\ \lambda_M)\,M_{\rm P}$ to obtain $\Omega_\chi^i h_{\rm d}^2 \simeq 0.12$, which is already assumed when writing the relations (6.48) and (6.49). Since there are three distinct values $\lambda_M$ can assume, together with a value for $\alpha_M$ and $\alpha_h$, this leads to three distinct solutions for neutralinos from $\chi_{S1}$ with $\Omega_\chi^i h_{\rm d}^2 \simeq 0.12$. In all the equations above we replaced $m_{3/2}$ by its function depending on both $h$ and $M$ via equation (5.26).

# List of Figures

# List of Tables

# Bibliography


[1] S. Weinberg, *Gravitation and Cosmology: Principles and Applications of the General Theory of Relativity*, John Wiley & Sons, Inc (1972).

[2] E. Hubble, *A relation between distance and radial velocity among extra-galactic nebulae*, Proc. Nat. Acad. Sci. **15** (1929) 168-173.

[3] E. Hubble and M. L. Humason, *The Velocity-Distance Relation among Extra-Galactic Nebulae*, Astrophys. J. **74** (1931) 43-80.

[4] G. Lemaître, *Un Univers homogène de masse constante et de rayon croissant rendant compte de la vitesse radiale des nébuleuses extra-galactiques*, Annales de la Société Scientifique de Bruxelles **47** (1927) 49-59.

[5] E. W. Kolb and M. S. Turner, *The Early Universe*, Addison-Wesley Publishing Company (1990).

[6] V. Mukhanov, *Physical Foundations of Cosmology*, Cambridge University Press (2005).

[7] D. H. Lyth and A. R. Liddle, *The primordial density perturbation: Cosmology, inflation and the origin of structure*, Cambridge University Press (2009).

[8] T. Padmanabhan, *Gravitation: Foundations and Frontiers*, Cambridge University Press (2010).

[9] R. A. Alpher, H. Bethe and G. Gamow, *The Origin of Chemical Elements*, Phys. Rev. **73** (1948) 803.

[10] G. Gamow, *The evolution of the Universe*, Nature **162** (1948) 680-682.

[11] R. A. Alpher and R. Herman, *Evolution of the Universe*, Nature **162** (1948) 774-775.

[12] R. A. Alpher, J. W. Follin and R. C. Herman, *Physical Conditions in the Initial Stages of the Expanding Universe*, Phys. Rev. **92** (1953) 1347-1361.

[13] A. A. Penzias and R. W. Wilson, *A Measurement of excess antenna temperature at 4080-Mc/s*, Astrophys. J. **142** (1965) 419.

[14] R. Dicke, P. Peebles, P. Roll and D. Wilkinson, *Cosmic blackbody radiation*, Astrophys. J. **142** (1965) 414-419.

[15] D. J. Fixsen, *The Temperature of the Cosmic Microwave Background*, Astrophys. J. **707** (2009) 916-920 [arXiv:0911.1955 [astro-ph.CO]].

[16] P. A. R. Ade *et al.*, *Planck 2015 results. XIII. Cosmological parameters*, Astron. Astrophys. **594** (2016) A13 [arXiv:1502.01589 [astro-ph]].

[17] D. Baumann, *TASI Lectures on Inflation*, [arXiv:0907.5424 [hep-th]].

[18] A. D. Linde, *Eternally Existing Selfreproducing Chaotic Inflationary Universe*, Phys. Lett. B **175** (1986) 395.

[19] A. Starobinsky, *Spectrum Of Relict Gravitational Radiation And The Early State Of The Universe*, ZhETF Pisma Redaktsiiu, **30** (1979) 719-723. Translation in Soviet Journal of Experimental and Theoretical Physics Letters, **30** (1979) 682-685.

[20] A. Y. Kamenshchik, U. Moschella and V. Pasquier, *An Alternative to quintessence* Phys. Lett. B **511** (2001) 265 [arXiv:0103004 [gr-qc]].

[21] M. C. Bento, O. Bertolami and A. A. Sen, *Generalized Chaplygin gas, accelerated expansion and dark energy matter unification*, Phys. Rev. D **66** (2002) 043507 [arXiv:0202064 [gr-qc]].

[22] J. C. Fabris, T. C. da C. Guio, M. Hamani Daouda and O. F. Piattella, *Scalar models for the generalized Chaplygin gas and the structure formation constraints*, Grav. Cosmol. **17** (2011) 259 [arXiv:1011.0286 [astro-ph.CO]].

[23] A. G. Riess *et al.* [Supernova Search Team], *Observational evidence from supernovae for an accelerating universe and a cosmological constant*, Astron. J. **116** (1998) 1009 [arXiv:9805201 [astro-ph]].

[24] S. Perlmutter *et al.* [Supernova Cosmology Project Collaboration], *Measurements of Omega and Lambda from 42 high redshift supernovae*, Astrophys. J. **517** (1999) 565 [arXiv:9812133 [astro-ph]].

[25] C. L. Bennet *et al.*, *Nine-Year Wilkinson Microwave Anisotropy Probe (WMAP) Observations: Final Maps and Results*, The Astrophysical Journal Supplement **208** (2013) Issue 2 [arXiv:1212.5225 [astro-ph.CO]].

[26] C. Contreras *et al.* [WiggleZ Collaboration], *The WiggleZ Dark Energy Survey: measuring the cosmic growth rate with the two-point galaxy correlation function*, Mon. Not. Roy. Astron. Soc. **430** (2013) 924 [arXiv:1302.5178 [astro-ph.CO]].

[27] V. C. Rubin, N. Thonnard and W. K. Ford Jr., *Rotational properties of 21 SC galaxies with a large range of luminosities and radii, from NGC 4605 /R = 4kpc/ to UGC 2885 /R = 122 kpc/*, The Astrophysical Journal **238** (1980) 471.

[28] A. N. Taylor, S. Dye, T. J. Broadhurst, N. Benítez and E. van Kampen, *Gravitational Lens Magnification and the Mass of Abell 1689*, Astrophys. J. **501** (1998) 539 [arXiv:9801158 [astro-ph]].

[29] S. Glashow, *The renormalizability of vector meson interactions*, Nucl. Phys. **10** (1959) 107.

[30] A. Salam, J. C. Ward, *Weak and electromagnetic interactions*, Nuovo Cimento **11** (1959) 568-577.

[31] S. Glashow, *Partial-symmetries of weak interactions*, Nuclear Physics **22** (1961) 579-588.

[32] S. Weinberg, *A Model of Leptons*, Phys. Rev. Lett. **19** (1967) (21) 1264-1266.

[33] F. Englert, R. Brout, *Broken Symmetry and the Mass of Gauge Vector Mesons*, Phys. Rev. Lett. **13** (1964) (9) 321-323.

[34] P. Higgs, *Broken Symmetries and the Masses of Gauge Bosons*, Phys. Rev. Lett. **13** (1964) (16) 508-509.

[35] G. Guralnik, C. Hagen, T. Kibble, *Global Conservation Laws and Massless Particles*, Phys. Rev. Lett. **13** (20) (1964) 585-587.

[36] D. Gross, F. Wilczek, *Ultraviolet behavior of non-abelian gauge theories*, Phys. Rev. Lett. **30** (26) (1973) 1343-1346.

[37] H. Politzer, *Reliable perturbative results for strong interactions*, Phys. Rev. Lett. **30** (26) (1973) 1346-1349.

[38] ATLAS Collaboration, G. Aad *et al.*, *Observation of a new particle in the search for the Standard Model Higgs boson with the ATLAS detector at the LHC*, Phys. Lett. B **716** (2012) 1-29, [arXiv:1207.7214 [hep-ex]].

[39] V. A. Kuzmin, V. A. Rubakov and M. E. Shaposhnikov, *On the Anomalous Electroweak Baryon Number Nonconservation in the Early Universe*, Phys. Lett. B **155** (1985) 36.

[40] M. D'Onofrio, K. Rummukainen, and A. Tranberg, *The Sphaleron Rate in the Minimal Standard Model*, Phys. Rev. Lett. **113** (2014) 141602, [arXiv:1404.3565].

[41] M. B. Gavela, P. Hernandez, J. Orloff, O. Pene and C. Quimbay, *Standard model CP violation and baryon asymmetry. Part 2: Finite temperature*, Nucl. Phys. B **430** (1994) 382.

[42] B. Pontecorvo, *Mesonium and anti-mesonium*, Sov. Phys. JETP **6** (1957) 429 [Zh. Eksp. Teor. Fiz. **33** (1957) 549].

[43] B. Pontecorvo, *Inverse beta processes and nonconservation of lepton charge*, Sov. Phys. JETP **7** (1958) 172 [Zh. Eksp. Teor. Fiz. **34** (1957) 247].

[44] Y. Fukuda *et al.* [Super-Kamiokande Collaboration], Phys. Rev. Lett. **82** (1999) 2644 [arXiv:9812014 [hep-ex]].

[45] Q. R. Ahmad *et al.* [SNO Collaboration], Phys. Rev. Lett. **89** (2002) 011301 [arXiv:0204008 [nucl-ex]].

[46] K. Eguchi *et al.* [KamLAND Collaboration], Phys. Rev. Lett. **90** (2003) 021802 [arXiv:0212021 [hep-ex]].

[47] A. A. Aguilar-Arevalo *et al.* [MiniBooNE Collaboration], *Observation of a Significant Excess of Electron-Like Events in the MiniBooNE Short-Baseline Neutrino Experiment* [arXiv:1805.12028 [hep-ex]].

[48] S. Dimopoulos and H. Georgi, *Softly Broken Supersymmetry and SU(5)*, Nucl. Phys. B **193** (1981) 150.

[49] J. Wess and B. Zumino, *Supergauge Transformations in Four-Dimensions*, Nucl. Phys. B **70** (1974) 39-50.

[50] H. P. Nilles, *Supersymmetry, Supergravity and Particle Physics*, Phys. Rept. **110** (1984) 1.

[51] J. Wess and J. Bagger, *Supersymmetry and supergravity*, Princeton University Press (1992).

[52] M. Drees, *An Introduction to supersymmetry*, Lectures at Seoul summer symposium on field theory (1996) [arXiv:9611409 [hep-ph]].

[53] M. Drees, R. Godbole and P. Roy, *Theory and phenomenology of sparticles: An account of four-dimensional $N = 1$ supersymmetry in high energy physics*, World Scientific, Hackensack, USA (2004).

[54] S. P. Martin, *A Supersymmetry primer*, Adv. Ser. Direct. High Energy Phys. **18** 1 (1997) [arXiv:9709356 [hep-ph]].

[55] P. West, *Introduction to supersymmetry and supergravity*, World Scientific (1990).

[56] H. Georgi and S. L. Glashow, *Unity of All Elementary Particle Forces*, Phys. Rev. Lett. **32** (1974) (8) 438-41.

[57] G. R. Farrar and P. Fayet, *Phenomenology of the Production, Decay, and Detection of New Hadronic States Associated with Supersymmetry*, Phys. Lett. B **76** (1978) 575.

[58] P. Fayet, *Supergauge Invariant Extension of the Higgs Mechanism and a Model for the electron and Its Neutrino*, Nucl. Phys. B **90** (1975) 104.

[59] P. Fayet, *Spontaneously Broken Supersymmetric Theories of Weak, Electromagnetic and Strong Interactions*, Phys. Lett. B **69** (1977) 489.

[60] A. Salam and J. A. Strathdee, *Supersymmetry and Fermion Number Conservation*, Nucl. Phys. B **87** (1975) 85.

[61] H. Pagels and J. R. Primack, *Supersymmetry, Cosmology and New TeV Physics*, Phys. Rev. Lett. **48** (1982) 223.

[62] K. A. Intriligator and N. Seiberg, *Lectures on Supersymmetry Breaking*, Class. Quant. Grav. **24** (2007) S741 [Les Houches **87** (2008) 125] [arXiv:0702069 [hep-ph]].

[63] M. A. Luty, *2004 TASI lectures on supersymmetry breaking*, [arXiv:0509029 [hep-th]].

[64] W. Nahm, *Supersymmetries and their representations* Nuclear Physics B. **135** (1978) (1) 149-166.

[65] E. Witten, *Search for a realistic Kaluza-Klein theory*, Nuclear Physics B. 186 (1981) (3) 412-428.

[66] B. de Wit, *Supergravity*, Lecture notes in the Les Houches Summerschool (2001) [arXiv:0212245 [hep-th]].

[67] P. Van Nieuwenhuizen, *Supergravity*, P. Phys.Rept. 68 (1981) 189-398.

[68] H. Nastase, *Introduction to Supergravity*, [arXiv:1112.3502 [hep-th]].

[69] S. Deser, J. H. Kay and K. S. Stelle, *Renormalizability Properties of Supergravity*, Phys. Rev. Lett. **38** (1977) 527 [arXiv:1506.03757 [hep-th]].

[70] E. Cremmer, B. Julia and J. Scherk, *Supergravity Theory in Eleven-Dimensions*, Phys. Lett. B **76** (1978) 409.

[71] R. Blumenagen, D. Lüst and S. Theisen, *Basic Concepts of String Theory*, Springer (2013).

[72] K. Becker, M. Becker and J. Schwarz, *String Theory and M-Theory: A Modern Introduction*, Cambridge University Press (2006).

[73] M. Green, J. Schwarz and E. Witten, *Superstring Theory - Volume 1: Introduction, Volume 2: Loop Amplitudes, Anomalies and Phenomenology*, Cambridge University Press (1987).

[74] J. Polchinski, *String Theory - Volume 1: An Introduction to the Bosonic String, Volume 2: Superstring Theory and Beyond*, Cambridge University Press (1998).

[75] E. Kiritsis, *Introduction to superstring theory*, [arXiv:9709062 [hep-th]].

[76] T. Kaluza, *Zum Unitätsproblem in der Physik*, Sitzungsber. Preuss. Akad. Wiss. Berlin. (Math. Phys.) (1921) 966-972.

[77] O. Klein, *Quantentheorie und fünfdimensionale Relativitätstheorie*, Zeitschrift für Physik A. 37 (12) (1926) 895–906.

[78] O. Klein, *The Atomicity of Electricity as a Quantum Theory Law* Nature **118** (1926) 516.

[79] A. Giveon, M. Porrati and E. Rabinovici, *Target space duality in string theory*, Phys. Rept. **244** (1994) 77 [arXiv:9401139 [hep-th]].

[80] E. Alvarez, L. Alvarez-Gaume and Y. Lozano, *An Introduction to T duality in string theory*, Nucl. Phys. Proc. Suppl. **41** (1995) 1 [arXiv:9410237 [hep-th]].

[81] A. Sen, *Strong-weak coupling duality in four-dimensional string theory*, Int. J. Mod. Phys. A **9** (1994) 3707 [arXiv:9402002 [hep-th]].

[82] J. Polchinski, *Dirichlet Branes and Ramond-Ramond charges*, Phys. Rev. Lett. **75** (1995) 4724 [arXiv:9510017 [hep-th]].

[83] C. Johnson, *D-branes*, Cambridge University Press (2003).

[84] S. Förste, *Strings, branes and extra dimensions*, Fortsch. Phys. **50** (2002) 221 [arXiv:0110055 [hep-th]].

[85] E. Witten, *Solutions Of Four-Dimensional Field Theories Via M Theory*, Nucl. Phys. B **500** (1997) 3-42 [arXiv:9703166 [hep-th]].

[86] E. Witten, *String theory dynamics in various dimensions*, Nucl. Phys. B **443** (1995) 85 [arXiv:9503124 [hep-th]].

[87] P. K. Townsend, *The eleven-dimensional supermembrane revisited*, Phys. Lett. B **350** (1995) 184 [arXiv:9501068 [hep-th]].

[88] C. M. Hull and P. K. Townsend, *Unity of superstring dualities*, Nucl. Phys. B **438** (1995) 109 [arXiv:9410167 [hep-th]].

[89] J. H. Schwarz, *Lectures on superstring and M theory dualities*, ICTP Spring School and TASI Summer School, Nucl. Phys. Proc. Suppl. **55B** (1997) 1 [arXiv:9607201 [hep-th]].

[90] S. Förste and J. Louis, *Duality in string theory*, Nucl. Phys. Proc. Suppl. **61A** (1998) 3 [arXiv:9612192 [hep-th]].

[91] C. Vafa, *Lectures on strings and dualities* (1997) [arXiv:9702201 [hep-th]].

[92] R. Dijkgraaf, *Les Houches lectures on fields, strings and duality* (1997) [arXiv:9703136 [hep-th]].

[93] P. S. Aspinwall, *String theory and duality*, Doc. Math. J. DMV **2** (1998) 229 [arXiv:9809004 [math.AG]].

[94] J. Polchinski, *Dualities of Fields and Strings*, Stud. Hist. Philos. Mod. Phys. **59** (2017) 6 [arXiv:1412.5704 [hep-th]].

[95] H. B. Lawson and M.-L. Michelsohn, *Spin Geometry*, Princeton University Press (1989).

[96] M. Berger, *Sur les groupes d'holonomie homogène des variétés à connexion affines et des variétés riemannienes*, Bulletin de la Société Mathématique de France **83** (1955) 279-330.

[97] D. Joyce, *Compact manifolds with special holonomy*, Oxford University Press (2000).

[98] E. Calabi, *On Kähler manifolds with vanishing canonical class*, in Ralph H. Fox, D. C. Spencer and A. W. Tucker (ed.): Algebraic geometry and topology. A symposium in honor of S. Lefschetz, volume **12** of Princeton Mathematical Series, pages 78-89, Princeton University Press (1957).

[99] S.-T. Yau, *Calabi's conjecture and some new results in algebraic geometry*, Proc. Natl. Acad. Sci. **74** (1977) no. 5, 1798-1799.

[100] S.-T. Yau, *On the Ricci curvature of a compact Kähler manifold and the complex Monge-Ampère equation. I*, Communications on Pure and Applied Mathematics **31** (1978) 339-411.

[101] P. Griffiths and J. Harris, *Principles of algebraic geometry*, John Wiley & Sons, Inc., New York (1994).

[102] P. Candelas and X. de la Ossa, *Moduli Space of Calabi-Yau Manifolds*, Nucl. Phys. B **355** (1991) 455.

[103] P. Candelas, *Lectures on complex manifolds*, Proceedings of Superstrings 87, p.1 (1987).

[104] B. R. Greene, *String theory on Calabi-Yau manifolds*, Fields, strings and duality in Proceedings, Summer School, Theoretical Advanced Study Institute in Elementary Particle Physics, TASI 96 (1996) [arXiv:9702155 [hep-th]].

[105] A. Klemm, B. Lian, S. S. Roan and S.-T. Yau, *Calabi-Yau fourfolds for M theory and F theory compactifications*, Nucl. Phys. B **518** (1998) 515 [arXiv:9701023 [hep-th]].

[106] M. Kreuzer and H. Skarke, *Calabi-Yau four folds and toric fibrations*, J. Geom. Phys. **26** (1998) 272 [arXiv:9701175 [hep-th]].

[107] N. Hitchin, *Generalized Calabi-Yau manifolds*, The Quarterly Journal of Mathematics **54** (2003) (3) 281-308 [arXiv:0209099 [math.DG]].

[108] N. J. Hitchin, A. Karlhede, U. Lindstrom and M. Rocek, *Hyperkähler Metrics and Supersymmetry*, Commun. Math. Phys. **108** (1987) 535.

[109] P. S. Aspinwall, B. R. Greene and D. R. Morrison, *Calabi-Yau moduli space, mirror manifolds and space-time topology change in string theory*, Nucl. Phys. B **416** (1994) 414 [arXiv:9309097 [hep-th]].

[110] T. Hübsch, *Calabi-Yau manifolds: a bestiary for physicists*, World Scientific Publishing (1992).

[111] M. Gross, D. Huybrechts and D. Joyce, *Calabi-Yau manifolds and related geometries*, Universitext, Springer (2003).

[112] D. Joyce, *Lectures on Calabi-Yau and special Lagrangian geometry* (2001) [arXiv:0108088 [math.DG]].

[113] V. Bouchard, *Lectures on complex geometry, Calabi-Yau manifolds and toric geometry* (2007) [arXiv:0702063 [hep-th]].

[114] P. Candelas, G. Horowitz, A. Strominger and E. Witten, *Vacuum configurations for superstrings*, Nucl. Phys. B **258** (1985) 46-74.

[115] B. Greene, K. H. Kirklin, P. J. Miron and G. G. Ross, *A Superstring Inspired Standard Model*, Phys. Lett. B **180** (1986) 69; *A Three Generation Superstring Model. 1. Compactification and Discrete Symmetries*, Nucl. Phys. B **278** (1986) 667; *A Three Generation Superstring Model. 2. Symmetry Breaking and the Low-Energy Theory*, Nucl. Phys. B **292** (1987) 602.

[116] V. Braun, Y. H. He, B. A. Ovrut and T. Pantev, *A heterotic standard model*, Phys. Lett. B **618** (2005) 252 [arXiv:0501070 [hep-th]].

[117] V. Braun, Y. H. He, B. A. Ovrut and T. Pantev, *A standard model from the $E(8) \times E(8)$ heterotic superstring*, JHEP **0506** (2005) 039 [arXiv:0502155 [hep-th]].

[118] V. Braun, Y. H. He, B. A. Ovrut and T. Pantev, *The exact MSSM spectrum from string theory*, JHEP **0605** (2006) 043 [arXiv:0512177 [hep-th]].

[119] V. Braun, Y. H. He, B. A. Ovrut and T. Pantev, *Vector bundle extensions, sheaf cohomology, and the heterotic standard model*, Adv. Theor. Math. Phys. **10** (2006) no.4, 525 [arXiv:0505041 [hep-th]].

[120] V. Bouchard and R. Donagi, *An SU(5) heterotic standard model*, Phys. Lett. B **633** (2006) 783 [arXiv:0512149 [hep-th]].

[121] R. Donagi, Y. H. He, B. A. Ovrut and R. Reinbacher, *The particle spectrum of heterotic compactifications*, JHEP **0412** (2004) 054 [arXiv:405014 [hep-th]].

[122] R. Donagi, Y. H. He, B. A. Ovrut and R. Reinbacher, *Higgs doublets, split multiplets and heterotic SU(3)(C) x SU(2)(L) x U(1)(Y) spectra*, Phys. Lett. B **618** (2005) 259 [arXiv:0409291 [hep-th]].

[123] R. Donagi, Y. H. He, B. A. Ovrut and R. Reinbacher, *The spectra of heterotic standard model vacua*, JHEP **0506** (2005) 070 [arXiv:0411156 [hep-th]].

[124] P. Candelas, M. Lynker, R. Schimmrigk, *Calabi-Yau manifolds in weighted $\mathbb{P}^*_4$*, Nucl. Phys. B **341** (1990) 383.

[125] K. Hori, S. Katz, A. Klemm, R. Phandharipande, R. Thomas, C. Vafa, R. Vakil, E. Zaslow, *Mirror Symmetry*, Clay Mathematics Monographs (2003).

[126] D. Cox and S. Katz, *Mirror Symmetry and Algebraic Geometry*, Mathematical Surveys and Monographs, American Mathematical Society (1999).

[127] S. Hosono, A. Klemm and S. Theisen, *Lectures on mirror symmetry*, Lect. Notes Phys. **436** (1994) 235 [arXiv:9403096 [hep-th]].

[128] E. Witten, *On the Structure of the Topological Phase of Two-dimensional Gravity*, Nucl. Phys. B **340** (1990) 281.

[129] E. Witten, *Topological Sigma Models*, Commun. Math. Phys. 118 (1988) 411.

[130] M. Vonk, *A Mini-course on topological strings* (2005) [arXiv:0504147 [hep-th]].

[131] M. Alim, *Lectures on Mirror Symmetry and Topological String Theory* (2005) [arXiv:1207.0496 [hep-th]].

[132] P. Candelas and D. J. Raine, *Spontaneous Compactification and Supersymmetry in $d = 11$ Supergravity*, Nucl. Phys. B248 (1984) 415.

[133] B. de Wit, D. J. Smit and N. D. H. Dass, *Residual Supersymmetry of Compactified $D = 10$ Supergravity*, Nucl. Phys. B283 (1987) 165.

[134] B. S. Acharya and B. J. Spence, *Flux, supersymmetry and M theory on seven manifolds*, [arXiv:0007213 [hep-th]].

[135] C. Beasley and E. Witten, *A Note on fluxes and superpotentials in M theory compactifications on manifolds of $G_2$ holonomy*, JHEP **0207** (2002) 046 [arXiv:0203061 [hep-th]].

[136] A. Lukas and S. Morris, *Kähler potential for M-theory on a $G_2$ manifold*, Phys. Rev. D **69** (2004) 066003 [arXiv:0305078 [hep-th]].

[137] A. Lukas and S. Morris, *Rolling $G_2$ moduli*, JHEP **01** (2004) 045 [arXiv:0308195 [hep-th]].

[138] T. House and A. Micu, *M-Theory compactifications on manifolds with $G_2$ structure*, Class. Quant. Grav. **22** (2005) 1709 [arXiv:0412006 [hep-th]].

[139] D. Joyce, *Compact Riemannian 7-manifolds with holonomy $G_2$ I, II*. J. Diff. Geom. **43** 291-328, 329-365 (1996).

[140] A. Kovalev, *Twisted connected sums and special Riemannian holonomy*, J. Reine Angew. Math. **565** (2003) 125-160 [arXiv:0012189 [math.DG]].

[141] A. Corti, M. Haskins, J. Nordström and T. Pacini, *$G_2$-manifolds and associative submanifolds via semi-Fano 3-folds*, Duke Math. J. **164** (2015) 1971-2092 [arXiv:1207.4470 [math.DG]].

[142] A. Corti, M. Haskins, J. Nordström and T. Pacini, *Asymptotically cylindrical Calabi-Yau 3-folds from weak Fano 3-folds*, Geom. Topol. **17** (2013) 1955-2059 [arXiv:1206.2277 [math.AG]].

[143] D. Baumann and L. McAllister, *Inflation and String Theory*, Cambridge University Press, Cambridge U.K. (2015) [arXiv:1404.2601 [hep-th]].

[144] J. Polonyi, Budapest preprint KFKI-1977-93.

[145] G. D. Coughlan, W. Fischler, E. W. Kolb, S. Raby and G. G. Ross, *Cosmological problems for the polonyi potential*, Phys. Lett. B **131** (1983) 59.

[146] S. Nakamura and M. Yamaguchi, *A note on Polonyi problem*, Phys. Lett. B **655** (2007) 167 [arXiv:0707.4538 [hep-ph]].

[147] J. L. Evans, M. A. G. Garcia and K. A. Olive, *The moduli and gravitino (non)-problems in models with strongly stabilized moduli*, Journal of Cosmology and Astroparticle Physics **2014** (2014) no. 3, 22 [arXiv:1311.0052 [hep-ph]].

[148] G. Kane, K. Sinha and S. Watson, *Cosmological Moduli and the Post-Inflationary Universe: A Critical Review*, Int. J. Mod. Phys. D **24** (2015) no.08, 1530022 [arXiv:1502.07746 [hep-th]].

[149] B. S. Acharya, G. Kane and P. Kumar, *Compactified String Theories – Generic Predictions for Particle Physics*, Int. J. Mod. Phys. A **27** (2012) 1230012 [arXiv:1204.2795 [hep-ph]].

[150] M. Dine and N. Seiberg, *Is the Superstring Weakly Coupled?*, Phys. Lett. **162B** (1985) 299.

[151] F. Denef, *Les Houches Lectures on Constructing String Vacua*, Les Houches **87** (2008) 483 [arXiv:0803.1194 [hep-th]].

[152] V. Balasubramanian, P. Berglund, J. P. Conlon and F. Quevedo, *Systematics of moduli stabilisation in Calabi-Yau flux compactifications*, JHEP **3** (2005) 7 [arXiv:0502058 [hep-th]].

[153] S. Kachru, R. Kallosh, A. D. Linde and S. P. Trivedi, *De Sitter vacua in string theory*, Phys. Rev. D **68** (2003) 046005 [arXiv:0301240 [hep-th]].

[154] R. Kallosh and A. D. Linde, *Landscape, the scale of SUSY breaking, and inflation*, JHEP **12** (2004) 4 [arXiv:0411011 [hep-th]].

[155] C. P. Burgess, R. Kallosh and F. Quevedo, *De Sitter string vacua from supersymmetric D terms*, JHEP **0310** (2003) 056 [arXiv:0309187 [hep-th]].

[156] E. Dudas and S. K. Vempati, *Large D-terms, hierarchical soft spectra and moduli stabilisation*, Nucl. Phys. B **727** (2005) 139 [arXiv:0506172 [hep-th]].

[157] H. Jockers and J. Louis, *D-terms and F-terms from D7-brane fluxes*, Nucl. Phys. B **718** (2005) 203 [arXiv:0502059 [hep-th]].

[158] M. Haack, D. Krefl, D. Lust, A. Van Proeyen and M. Zagermann, *Gaugino Condensates and D-terms from D7-branes*, JHEP **0701** (2007) 078 [arXiv:0609211 [hep-th]].

[159] A. Achucarro, B. de Carlos, J. A. Casas and L. Doplicher, *De Sitter vacua from uplifting D-terms in effective supergravities from realistic strings*, JHEP **0606** (2006) 014 [arXiv:0601190 [hep-th]].

[160] E. Dudas and Y. Mambrini, *Moduli stabilization with positive vacuum energy*, JHEP **0610** (2006) 044 [arXiv:0607077 [hep-th]].

[161] G. Villadoro and F. Zwirner, *De-Sitter vacua via consistent D-terms*, Phys. Rev. Lett. **95** (2005) 231602 [arXiv:0508167 [hep-th]].

[162] K. Choi and K. S. Jeong, *Supersymmetry breaking and moduli stabilization with anomalous $U(1)$ gauge symmetry*, JHEP **0608** (2006) 007 [arXiv:0605108 [hep-th]].

[163] K. Choi, A. Falkowski, H. P. Nilles and M. Olechowski, *Soft supersymmetry breaking in KKLT flux compactification*, Nucl. Phys. B **718** (2005) 113 [arXiv:0605108 [hep-th]].

[164] A. Saltman and E. Silverstein, [*The Scaling of the no scale potential and de Sitter model building*, JHEP **0411** (2004) 066 [arXiv:0402135 [hep-th]].

[165] M. Gomez-Reino and C. A. Scrucca, *Constraints for the existence of flat and stable non-supersymmetric vacua in supergravity*, JHEP **0609** (2006) 008 [arXiv:0606273 [hep-th]].

[166] O. Lebedev, H. P. Nilles and M. Ratz, *De Sitter vacua from matter superpotentials*, Phys. Lett. B **636** (2006) 126 [arXiv:0603047 [hep-th]].

[167] E. Witten, *Dynamical Breaking of Supersymmetry*, Nucl. Phys. B **188** (1981) 513.

[168] E. Witten, *Constraints on Supersymmetry Breaking*, Nucl. Phys. B **202** (1982) 253.

[169] I. Affleck, M. Dine and N. Seiberg, *Dynamical Supersymmetry Breaking in Chiral Theories*, Phys. Lett. B **137** (1984) 187.

[170] I. Affleck, M. Dine and N. Seiberg, *Dynamical Supersymmetry Breaking in Supersymmetric QCD*, Nucl. Phys. B **241** (1984) 493.

[171] I. Affleck, M. Dine and N. Seiberg, *Exponential Hierarchy From Dynamical Supersymmetry Breaking*, Phys. Lett. B **140** (1984) 59.

[172] I. Affleck, M. Dine and N. Seiberg, *Dynamical Supersymmetry Breaking in Four-Dimensions and Its Phenomenological Implications*, Nucl. Phys. B **256** (1985) 557.

[173] Y. Shadmi and Y. Shirman, *Dynamical supersymmetry breaking*, Rev. Mod. Phys. **72** (2000) 25 [arXiv:9907225 [hep-th]].

[174] G. F. Giudice and R. Rattazzi, *Theories with gauge mediated supersymmetry breaking*, Phys. Rept. **322** (1999) 419 [arXiv:9801271 [hep-ph]].

[175] J. Terning, *TASI 2002 lectures: Nonperturbative supersymmetry*, in *Particle physics and cosmology: The quest for physics beyond the standard model(s). Proceedings, Theoretical Advanced Study Institute, TASI 2002*, Boulder, USA, June 3-28 (2002) [arXiv:0306119 [hep-th]].

[176] K. Intriligator, N. Seiberg and D. Shih, *Dynamical SUSY breaking in meta-stable vacua*, Journal of High Energy Physics **2006** (2006) 21 [arXiv:0602239 [hep-ph]].

[177] A. Giveon and D. Kutasov, *Gauge Symmetry and Supersymmetry Breaking From Intersecting Branes*, Nucl.Phys. B **778** (2007) 129-158 [arXiv:0703135 [hep-th]].

[178] A. Giveon and D. Kutasov, *Brane dynamics and gauge theory*, Rev. Mod. Phys. **71** (1999) 983 [arXiv:9802067 [hep-th]].

[179] A. Giveon, D. Kutasov, J. McOrist and A. B. Royston, *D-Terms and supersymmetry breaking from Branes*, Nucl. Phys. B **822** (2009) 106 [arXiv:0904.0459 [hep-th]].

[180] H. Ooguri and Y. Ookouchi, *Meta-Stable Supersymmetry Breaking Vacua on Intersecting Branes*, Phys. Lett. B **641** (2006) 323 [arXiv:0607183 [hep-th]].

[181] S. Elitzur, A. Giveon and D. Kutasov, *Branes and N=1 Duality in String Theory*, Phys. Lett. B **400** (1997) 269-274 [arXiv:9702014 [hep-th]].

[182] K. Hori, H. Ooguri and Y. Oz, *Strong Coupling Dynamics of Four-Dimensional N=1 Gauge Theories from M Theory Fivebrane*, Adv. Theor. Math.Phys. **1** (1998) 1-52 [arXiv:9706082 [hep-th]].

[183] A. Brandhuber, N. Itzhaki, V. Kaplunovsky, J. Sonnenschein and S. Yankielowicz, *Comments on the M Theory Approach to N=1 SQCD and Brane Dynamics*, Phys. Lett. B **410** (1997) 27-35 [arXiv:9706127 [hep-th]].

[184] E. Witten, *Branes And The Dynamics Of QCD*, Nucl. Phys. B **507** (1997) 658-690 [arXiv:9706109 [hep-th]].

[185] S. Nam, K. Oh and S.-J. Sin, *Superpotentials of N=1 Supersymmetric Gauge Theories from M-theory*, Phys.Lett. B **416** (1998) 319-326 [arXiv:9707247 [hep-th]].

[186] I. Bena, E. Gorbatov, S.Hellerman, N. Seiberg and D. Shih, *A Note on (Meta)stable Brane Configurations in MQCD*, JHEP 0611 (2006) 088 [arXiv:0608157 [hep-th]].

[187] R. D. Peccei and H. R. Quinn, *Constraints imposed by* CP *conservation in the presence of pseudoparticles*, Phys. Rev. D **16** (1977) 1791.

[188] R. D. Peccei and H. R. Quinn, *CP Conservation in the Presence of Pseudoparticles*, Phys. Rev. Lett. **38** (1977) 1440.

[189] L. D. Duffy and K. van Bibber, *Axions as Dark Matter Particles*, New J. Phys. **11** (2009) 105008 [arXiv:0904.3346 [hep-ph]].

[190] D. J. E. Marsh, *Axion Cosmology*, Phys. Rept. **643** (2016) 1 [arXiv:1510.07633 [astro-ph.CO]].

[191] G. Jungman, M. Kamionkowski and K. Griest, *Supersymmetric dark matter*, Phys. Rept. **267** (1996) 195 [arXiv:9506380 [hep-ph]].

[192] N. Bernal, C. Garcia-Cely and R. Rosenfeld, *WIMP and SIMP Dark Matter from the Spontaneous Breaking of a Global Group*, JCAP **1504** (2015) 4 [arXiv:1501.01973 [hep-ph].

[193] B. L. Sánchez-Vega, J. C. Montero and E. R. Schmitz, *Complex Scalar DM in a B-L Model*, Phys. Rev. D **90** (2014) 5 [arXiv:1404.5973 [hep-ph]].

[194] B. L. Sánchez-Vega and E. R. Schmitz, E. R., *Fermionic dark matter and neutrino masses in a B-L model*, Phys. Rev. D **92** (2015) 53007 [arXiv:1505.03595 [hep-ph]].

[195] T. C. da C. Guio, H. Jockers, A. Klemm, H.-Y. Yeh, *Effective action from M-theory on twisted connected sum $G_2$-manifolds*, Commun. Math. Phys. 359 (2018), no. 2, 535-601, [arXiv:1702.05435 [hep-th]].

[196] T. C. da C. Guio and E. R. Schmitz, *Dark matter in the KL moduli stabilization scenario with SUSY breaking sector from $\mathcal{N} = 1$ SQCD*, submitted to Journal of High Energy Physics (JHEP), [arXiv:1805.01521 [hep-ph]].

[197] R. L. Bryant, *Metrics with exceptional holonomy*, Ann. of Math. (2) **126** (1987) 525–576.

[198] N. J. Hitchin, *The geometry of three-forms in six and seven dimensions*, J.Diff.Geom. **55** (2000), no. 3, 547-576 [arXiv:0010054 [math.DG]].

[199] M. Fernández and A. Gray, *Riemannian manifolds with structure group $G_2$*, Ann. Mat. Pura Appl. (4) **132** (1982) 19–45.

[200] S. Salamon, *Riemannian geometry and holonomy groups*, Longman Scientific & Technical (1989).

[201] R. L. Bryant, *Some remarks on the geometry of manifolds with exceptional holonomy*, unpublished (1994).

[202] R. L. Bryant, *Some remarks on $G_2$-structures*, Proceedings of Gokova Geometry-Topology Conference (2005) [arXiv:0305124 [math.DG]].

[203] H.-Yu Yeh, *Period, Central Charge and Effective Action on Ricci-Flat Manifolds with Special Holonomy*, PhD thesis, University of Bonn (2016).

[204] M. Haskins, H.-J. Hein, and J. Nordström, *Asymptotically cylindrical Calabi-Yau manifolds*, J. Differential Geom. **101** (2015) 213-265 [arXiv:1212.6929 [math.DG]].

[205] E. R. Van Kampen, *On the Connection between the Fundamental Groups of Some Related Spaces*, American J. of Mathematics **55** (1933), no. 1, 261-267.

[206] D. Huybrechts, *Lectures on K3 Surfaces*, Cambridge University Press (2015).

[207] A. Kovalev and N.-H. Lee, *K3 surfaces with non-symplectic involution and compact irreducible $G_2$-manifolds*, Math. Proc. Cambridge Philos. Soc. **151** (2011) 193-218, [arXiv:0810.0957 [math.DG]].

[208] P. S. Aspinwall, *K3 surfaces and string duality*, in S. T. Yau (ed.): Differential geometry inspired by string theory 1-95, [arXiv:9611137 [hep-th]].

[209] W. Fulton, *Introduction to toric varieties*, Annals of Mathematics Studies, The William H. Roever Lectures in Geometry **131**, Princeton University Press (1993).

[210] D. A. Cox, J. B. Little and H. K. Schenck, *Toric Varieties*, Graduate Studies in Mathematics **124** American Mathematical Society (2011).

[211] D. Crowley and J. Nordström, *Exotic $G_2$-manifolds* (2014) [arXiv:1411.0656 [math.AG]].

[212] A. Beauville, *Fano threefolds and K3 surfaces*, The Fano Conference, University of Turin (2002) 175-184[arXiv:0211313 [math.AG]].

[213] V. V. Batyrev, *Dual Polyhedra and Mirror Symmetry for Calabi-Yau Hypersurfaces in Toric Varieties* (1993) [arXiv:9310003 [alg-geom]].

[214] M. Kreuzer and H. Skarke, *Classification of reflexive polyhedra in three-dimensions*, Adv. Theor. Math. Phys. **2** (1998) 847-864 [arXiv:9805190 [hep-th]].

[215] M. Kreuzer and H. Skarke, *PALP: A Package for analyzing lattice polytopes with applications to toric geometry*, Comput. Phys. Commun. **157** (2004) 87-106 [arXiv:0204356 [math.NA]].

[216] A. Klemm, J. Manschot and T. Wotschke, *Quantum geometry of elliptic Calabi-Yau manifolds*, Comm. Number Theor. Phys. 6 (2012) 849-917 [arXiv:1205.1795 [hep-th]].

[217] J. Kollár and S. Mori, *Birational geometry of algebraic varieties*, Cambridge University Press (1998).

[218] V. V. Nikulin, *Integer symmetric bilinear forms and some of their geometric applications*, Izv. Akad. Nauk SSSR Ser. Mat. 43 (1979) 111–177.

[219] E. Witten, *On flux quantization in M theory and the effective action*, J. Geom. Phys. **22** (1997) 1–13 [arXiv:9609122 [hep-th]].

[220] B. S. Acharya, $N = 1$ *heterotic/M theory duality and Joyce manifolds*, Nucl. Phys. B **475** (1996) 579–596 [arXiv:9603033 [hep-th]].

[221] B. S. Acharya, *M theory, Joyce orbifolds and superYang-Mills*, Adv. Theor. Math. Phys. 3 (1999) 227–248 [arXiv:9812205 [hep-th]].

[222] S. Grigorian, *Moduli spaces of G(2) manifolds* Rev. Math. Phys. **22** (2010) 1061 [arXiv:0911.2185 [math.DG]].

[223] S. Karigiannis, *Flows of $G_2$ Structures, I*, Quarterly Journal of Mathematics **60** (2009) 487-522 [arXiv:0702077].

[224] S. Karigiannis, *Deformations of $G_2$ and Spin(7) Structures on Manifolds*, Canadian Journal of Mathematics **57** (2005) 1012-1055 [arXiv:0301218 [math.DG]].

[225] J. Wess and J. Bagger, *Supersymmetry and supergravity*, Princeton University Press, Princeton, New Jersey, USA (1992).

[226] K. Becker, M. Becker, W. D. Linch and D. Robbins, *Abelian tensor hierarchy in 4D, N = 1 superspace*, JHEP **1603** (2016) 052 [arXiv:1601.03066 [hep-th]].

[227] K. Becker, M. Becker, S. Guha, W. D. Linch and D. Robbins, *M-theory potential from the $G_2$ Hitchin functional in superspace*, JHEP **1612** (2016) 085 [arXiv:1611.03098 [hep-th]].

[228] J. A. Harvey and G. W. Moore, *Superpotentials and membrane instantons*, [arXiv:9907026 [hep-th]].

[229] K. Becker, D. Robbins and E. Witten, *The $\alpha'$ expansion on a compact manifold of exceptional holonomy*, JHEP **1406** (2014) 051 [arXiv:1404.2460 [hep-th]].

[230] S. Gurrieri, A. Lukas and A. Micu, *Heterotic on half-flat*, Phys. Rev. D **70** (2004) 126009 [arXiv:0408121 [hep-th]].

[231] S. Gukov, C. Vafa and E. Witten, *CFT's from Calabi-Yau four-folds*, Nucl. Phys. B **584** (2000) 69 [arXiv:9906070 [hep-th]], *Erratum-op.cit.* S. Gukov, C. Vafa and E. Witten, *CFT's from Calabi-Yau four-folds*, Nucl. Phys. B **608** (2001) 477-478 [arXiv:9906070 [hep-th]].

[232] S. Gukov, *Solitons, superpotentials and calibrations*, Nucl. Phys. B **574** (2000) 169 [arXiv:9911011 [hep-th]].

[233] N. Hitchin, *Stable forms and special metrics*, Global differential geometry: the mathematical legacy of Alfred Gray (Bilbao, 2000), Contemp. Math **288** (2001) 70 [arXiv:0107101 [math.DG]].

[234] A. P. Braun, *Tops as Building Blocks for $G_2$ Manifolds*, JHEP **10** (2017) 083 [arXiv:1602.03521 [hep-th]].

[235] M. Krämer, *Bestimmung von No-Scale Kähler Potentialen*, Master's thesis, II. Institut für Theoretische Physik der Universität Hamburg, September (2005).

[236] S. Mori and S. Mukai, *Classification of Fano* 3*-folds with* $B_2 \geq 2$, Manuscr. Math. **36** (1981) 147-162. *Erratum-op.cit.* S. Mori and S. Mukai *Classification of Fano* 3*-folds with* $B_2 \geq 2$ *— Erratum*, Manuscr. Math. **110** (2003) 407.

[237] A. Kasprzyk, *Toric Fano 3-folds with terminal singularities*, Tohoku Math. J. **58** (2006) no. 1, 101-121 [arXiv:0311284].

[238] A. M. Kasprzyk, *Graded Ring Database — Toric terminal Fano 3-folds*, (2006), http://www.grdb.co.uk/Index.

[239] J. Borwein and K.-K. Choi, *On the representations of* $xy + yz + zx$, Experiment. Math. **9**, Issue 1 (2000) 153-158.

[240] B. S. Acharya and E. Witten, *Chiral fermions from manifolds of* $G_2$ *holonomy* [arXiv:0109152 [hep-th]].

[241] A. Strominger, S. T. Yau and E. Zaslow, *Mirror symmetry is T duality*, Nucl. Phys. B **479** (1996) 243 [arXiv:9606040 [hep-th]].

[242] M. Atiyah and E. Witten, *M theory dynamics on a manifold of* $G_2$ *holonomy*, Adv. Theor. Math. Phys. **6** (2003) 1 [arXiv:0107177 [hep-th]].

[243] M. Atiyah, J. M. Maldacena and C. Vafa, *An M theory flop as a large N duality*, J. Math. Phys. **42** (2001) 3209 [arXiv:0011256 [hep-th]].

[244] M. Aganagic and C. Vafa, $G_2$ *manifolds, mirror symmetry and geometric engineering* [arXiv:0110171 [hep-th]].

[245] S. Gukov, S. T. Yau and E. Zaslow, *Duality and fibrations on* $G_2$ *manifolds* [arXiv:0203217 [hep-th]].

[246] A. P. Braun and M. Del Zotto, *Mirror Symmetry for* $G_2$*-Manifolds: Twisted Connected Sums and Dual Tops*, JHEP **1705** (2017) 080 [arXiv:1701.05202 [hep-th]].

[247] S. Kachru and C. Vafa, *Exact results for N=2 compactifications of heterotic strings*, Nucl. Phys. B **450** (1995) 69 [arXiv:9505105 [hep-th]].

[248] A. Klemm, W. Lerche and P. Mayr, *K3 Fibrations and heterotic type II string duality*, Phys. Lett. B **357** (1995) 313 [arXiv:9506112 [hep-th]].

[249] J. Halverson and D. R. Morrison, *On gauge enhancement and singular limits in* $G_2$ *compactifications of M-theory*, JHEP **1604** (2016) 100 [arXiv:1507.05965 [hep-th]].

[250] A. Klemm and P. Mayr, *Strong coupling singularities and non-Abelian gauge symmetries in* $N = 2$ *string theory*, Nucl. Phys. B **469** (1996) 37 [arXiv:9601014 [hep-th]].

[251] S. H. Katz, D. R. Morrison and M. R. Plesser, *Enhanced gauge symmetry in type II string theory*, Nucl. Phys. B **477** (1996) 105 [arXiv:9601108 [hep-th]].

[252] S. H. Katz and C. Vafa, *Matter from geometry*, Nucl. Phys. B **497** (1997) 146 [arXiv:9606086 [hep-th]].

[253] E. Witten, *Anomaly cancellation on manifolds of $G_2$ holonomy* (2001) [arXiv:0108165 [hep-th]].

[254] J. Halverson and D. R. Morrison, *The landscape of M-theory compactifications on seven-manifolds with $G_2$ holonomy*, JHEP **1504** (2015) 047 [arXiv:1412.4123 [hep-th]].

[255] A. Strominger, *Massless black holes and conifolds in string theory*, Nucl. Phys. B **451** (1995) 96 [arXiv:9504090 [hep-th]].

[256] B. R. Greene, D. R. Morrison and A. Strominger, *Black hole condensation and the unification of string vacua*, Nucl. Phys. B **451** (1995) 109 [arXiv:9504145 [hep-th]].

[257] K. Intriligator, H. Jockers, P. Mayr, D. R. Morrison and M. R. Plesser, *Conifold Transitions in M-theory on Calabi-Yau Fourfolds with Background Fluxes*, Adv. Theor. Math. Phys. **17** (2013) no. 3, 601 [arXiv:1203.6662 [hep-th]].

[258] T. Banks and N. Seiberg, *Symmetries and Strings in Field Theory and Gravity*, Phys. Rev. D **83** (2011) 084019 [arXiv:1011.5120 [hep-th]].

[259] A. Sen, *Orientifold limit of F theory vacua*, Phys. Rev. D **55** (1997) 7345 [arXiv:9702165 [hep-th]].

[260] S. B. Giddings, S. Kachru and J. Polchinski, *Hierarchies from fluxes in string compactifications*, Phys. Rev. D **66** (2002) 106006 [arXiv:0105097 [hep-th]].

[261] E. Witten, *Non-Perturbative Superpotentials In String Theory*, Nucl. Phys. B **474** (1996) 343 [arXiv:9604030 [hep-th]].

[262] N. Arkani-Hamed and S. Dimopoulos, *Supersymmetric Unification Without Low Energy Supersymmetry And Signatures for Fine-Tuning at the LHC*, JHEP 0506 (2005) 073 [arXiv:0405159 [hep-th]].

[263] K. A. Intriligator and N. Seiberg, *Lectures on supersymmetric gauge theories and electric-magnetic duality*, Nucl. Phys. Proc. Suppl. **45BC** (1996) 1 [arXiv:9509066 [hep-th]].

[264] N. Seiberg, *Exact results on the space of vacua of four-dimensional SUSY gauge theories*, Phys. Rev. D **49** (1994) 6857 [arXiv:9402044 [hep-th]].

[265] N. Seiberg, *Electric-magnetic duality in supersymmetric non-Abelian gauge theories*, Nucl. Phys. B **435** (1995) 129 [arXiv:9411149 [hep-th]].

[266] E. Dudas, A. D. Linde, Y. Mambrini, A. Mustafayev and K. A. Olive, *Strong moduli stabilization and phenomenology*, The European Physical Journal C **73** (2013) 2268 [arXiv:1209.0499 [hep-ph]].

[267] G. F. Giudice and A. Masiero, *A natural solution to the μ-problem in supergravity theories*, Phys. Lett. B **206** (1988) 480.

[268] J. L. Evans, M. Ibe, K. A. Olive and T. T. Yanagida, *Universality in pure gravity mediation*, The European Physical Journal C **73** (2013), no. 7, 2468 [arXiv:1302.5346 [hep-ph]].

[269] J. L. Evans, M. Ibe, K. A. Olive and T. T. Yanagida, *Non-universalities in pure gravity mediation*, The European Physical Journal C **73** (2013), no.10, 2611 [arXiv:1305.7461 [hep-ph]].

[270] R. Kallosh, A. D. Linde, K. A. Olive and T. Rube, *Chaotic inflation and supersymmetry breaking*, Phys. Rev. D **84** (2011) 083519 [arXiv:1106.6025 [hep-th]].

[271] R. Kallosh, A. Linde, B. Vercnocke and T. Wrase, *Analytic Classes of Metastable de Sitter Vacua*, JHEP 1410 (2014) 011 [arXiv:1406.4866 [hep-th]].

[272] A. D. Linde, Y. Mambrini and K. A. Olive, *Supersymmetry Breaking due to Moduli Stabilization in String Theory*, Phys. Rev. D **85** (2012) 066005 [arXiv:1111.1465 [hep-th]].

[273] A. Saltman and E. Silverstein, *The Scaling of the No Scale Potential and de Sitter Model Building*, JHEP **0411** (2004) 066 [arXiv:0402135 [hep-th]].

[274] E. Dudas, C. Papineau and S. Pokorski, *Moduli stabilization and uplifting with dynamically generated F-terms*, JHEP **0702** (2007) 028 [arXiv:0610297 [hep-th]].

[275] R. Kallosh and A. Linde, *O'KKLT*, JHEP **0702** (2007) 002 [arXiv:0611183 [hep-th]].

[276] H. Abe, T. Higaki, T. Kobayashi and Y. Omura, *Moduli stabilization, F-term uplifting and soft supersymmetry breaking terms*, Phys. Rev. D **75** (2007) 025019 [arXiv:0611024 [hep-th]].

[277] H. Abe, T. Higaki and T. Kobayashi, *More about F-term uplifting*, Phys. Rev. D **76** (2007) 105003 [arXiv:0707.2671 [hep-th]].

[278] O. Lebedev, V. Lowen, Y. Mambrini, H. P. Nilles and M. Ratz, *Metastable Vacua in Flux Compactifications and Their Phenomenology*, JHEP **0702** (2007) 063 [arXiv:0612035 [hep-ph]].

[279] T. Moroi, *Effects of the gravitino on the inflationary universe*, PhD Thesis, University of Tohoku (1995) [arXiv:9503210 [hep-ph]].

[280] R. Barbier *et al.*, *R-Parity-violating supersymmetry*, Phys. Rep. **420** (2005) 1 [arXiv:0406039 [hep-ph]].

[281] M. A. G. Garcia and K. A. Olive, *Affleck-Dine baryogenesis and inflation in supergravity with strongly stabilized moduli*, Journal of Cosmology and Astroparticle Physics **2013** (2013), no. 9, 7 [arXiv:1306.6119 [hep-ph]].

[282] I. Affleck and M. Dine, *A new mechanism for baryogenesis*, Nucl. Phys. B **249** (1985), no. 2, 361.

[283] T. Konstandin, *Quantum Transport and Electroweak Baryogenesis*, Phys. Usp. **56** (2013) 747 [arXiv:1302.6713 [hep-ph]].

[284] D. E. Morrissey and M. J. Ramsey-Musolf, *Electroweak baryogenesis*, New J. Phys. **14** (2012) 125003 [arXiv:1206.2942 [hep-ph]].

[285] M. Dine, L. Randall and S. Thomas, *Baryogenesis from flat directions of the supersymmetric standard model*, Nucl. Phys. B **458** (1996), no.1, 291 [arXiv:9507453 [hep-ph]].

[286] A. D. Linde, *Relaxing the cosmological moduli problem*, Phys. Rev. D **53** (1996) R4129 [arXiv:9601083 [hep-th]].

[287] K. Nakayama, F. Takahashi and T. T. Yanagida, *Adiabatic solution to the Polonyi/moduli problem*, Phys. Rev. D **84** (2011) 123523 [arXiv:1109.2073 [hep-th]].

[288] M. Endo, K. Kadota, K. A. Olive, F. Takahashi and T. T. Yanagida, *The decay of the inflaton in no-scale supergravity*, JCAP **0702** (2007) 018 [arXiv:0612263 [hep-ph]].

[289] G. Mangano *et al.*, *Relic neutrino decoupling including flavour oscillations*, Nucl. Phys. B **729** (2005) 221 [arXiv:0506164 [hep-ph]].

[290] G. Kane, P. Kumar, B. D. Nelson and B. Zheng, *Dark Matter Production Mechanisms with a Non-Thermal Cosmological History - A Classification*, Phys.Rev. D **93** (2016) no. 6, 063527 [arXiv:1502.05406 [hep-ph]].

[291] M. Bolz, A. Brandenburg and W. Buchmüller, *Thermal production of gravitinos*, Nucl. Phys. B **606** (2001) 518 [arXiv:0012052 [hep-ph]].

[292] M. Kawasaki, K. Kohri, T. Moroi and A. Yotsuyanagi, *Big-bang nucleosynthesis and gravitinos*, Phys. Rev. D **78** (2008) 065011 [arXiv:0804.3745 [hep-ph]].

[293] H. P. Nilles, K. A. Olive and M. Peloso, *The inflatino problem in supergravity inflationary models*, Phys. Lett. B **522** (2001), no.3, 304 [arXiv:0107212 [hep-ph]].

[294] M. Endo, K. Hamaguchi and F. Takahashi, *Moduli/inflaton mixing with supersymmetry-breaking field*, Phys. Rev. D **74** (2006) 023531 [arXiv:0605091 [hep-ph]].

[295] K. S. Jeong and F. Takahashi, *A gravitino-rich universe*, Journal of High Energy Physics **2013** (2013) 173 [arXiv:1210.4077 [hep-ph]].

[296] T. Moroi and L. Randall, *Wino cold dark matter from anomaly mediated SUSY breaking*, Nucl. Phys. B **570** (2000) 455 [arXiv:9906527 [hep-ph]].

[297] T. Moroi, M. Yamaguchi and T. Yanagida, *On the solution to the Polonyi problem with O(10 TeV) gravitino mass in supergravity*, Phys. Lett. B **342** (1995) 105 [arXiv:9409367 [hep-ph]].

[298] K. Griest and D. Seckel, *Three exceptions in the calculation of relic abundances*, Phys. Rev. D **43** (1991) 3191.

[299] M. Drees and M. M. Nojiri, *Neutralino relic density in minimal $N = 1$ supergravity*, Phys. Rev. D **47** (1992) 376 [arXiv:9207234 [hep-ph]].

[300] T. R. Taylor and C. Vafa, *RR flux on Calabi-Yau and partial supersymmetry breaking*, Phys. Lett. B **474** (2000) 130 [arXiv:9912152 [hep-th]].

[301] H. Jockers, S. Katz, D. R. Morrison and M. R. Plesser, *SU(N) Transitions in M-Theory on Calabi-Yau Fourfolds and Background Fluxes*, Commun. Math. Phys. **351** (2017) no. 2, 837 [arXiv:1602.07693 [hep-th]].

[302] J. Louis, *Aspects of spontaneous $N = 2 \to N = 1$ breaking in supergravity* (2002) [arXiv:0203138 [hep-th]].

[303] L. Randall and R. Sundrum, *Out of this world supersymmetry breaking*, Nucl. Phys. B **557** (1999) 79 [arXiv:9810155 [hep-th]].

[304] P. S. Aspinwall, *M theory versus F theory pictures of the heterotic string*, Adv. Theor. Math. Phys. **1** (1998) 127 [arXiv:9707014 [hep-th]].

[305] R. Friedman, J. Morgan and E. Witten, *Vector bundles and F theory*, Commun. Math. Phys. **187** (1997) 679 [arXiv:9701162 [hep-th]].

[306] R. P. Thomas, *A Holomorphic Casson invariant for Calabi-Yau three folds, and bundles on K3 fibrations*, J. Diff. Geom. **54** (2000) no. 2, 367 [arXiv:9806111 [math-ag]].

[307] H. Jockers, P. Mayr and J. Walcher, *On N=1 4d Effective Couplings for F-theory and Heterotic Vacua*, Adv. Theor. Math. Phys. **14** (2010) no. 5, 1433 [arXiv:0912.3265 [hep-th]].

[308] E. Cremmer, S. Ferrara, L. Girardell and A. Van Proeyen, *Yang-Mills theories with local supersymmetry: Lagrangian, transformation laws and super-Higgs effect*, Nucl. Phys. B **212** (1983) 413.

[309] E. Cremmer, B. Julia, J. Scherk, S. Ferrara, L. Girardello and P. van Nieuwenhuizen, *Spontaneous symmetry breaking and Higgs effect in supergravity without cosmological constant*, Nucl. Phys. B **147** (1979) 105.

[310] M. Endo, F. Takahashi and T. T. Yanagida, *Inflaton decay in supergravity*, Phys. Rev. D **76** (2007) 083509 [arXiv:0706.0986 [hep-ph]].